SBIR

(2)

USAAVSCOM TR 89-D-13B

US ARMY
AVIATION
SYSTEMS COMMAND

ADVANCED TECHNOLOGY LANDING GEAR

Volume II -Test

J.K. Sen

McDonnell Douglas Helicopter Company
5000 East McDowell Road
Mesa, AZ 85205

August 1990

Final Report for Period September 1985 - December 1989

Prepared for

AVIATION APPLIED TECHNOLOGY DIRECTORATE
US ARMY AVIATION SYSTEMS COMMAND
FORT EUSTIS, VA 23604-5577

AVIATION APPLIED TECHNOLOGY DIRECTORATE POSITION STATEMENT

The objective of the Advanced Technology Landing Gear (ATLG) Program was to design, fabricate, and test a crashworthy retractable main landing gear system suitable for an 8500-pound utility helicopter. Among the technical issues addressed and resolved as a result of the ATLG development effort were landing gear system integration and structural compatibility in a limited space airframe, MIL-STD-1290 crashworthiness for a compact landing gear configuration, hydraulic/electrical support systems redundancy, and extention/retraction reliability and fail-safety. Landing gear testing was accomplished using conventional platform drop tests, as well as "iron bird" drop tests. Test results were compared with KRASH analytical predictions to evaluate landing gear performance and characterize system dynamic behavior. The results of the ATLG demonstration effort will be used to guide the development of future Army helicopter landing gear systems.

Mr. Ned Chase of the Aeronautical Technology Division served as Project Engineer for this effort.

REPORT DOCUMENTATION PAGE

Form Approved
OMB No. 0704-0188

1. AGENCY USE ONLY *(Leave blank)*	2. REPORT DATE	3. REPORT TYPE AND DATES COVERED
	August 1990	Final September 1985 - December 1989

4. TITLE AND SUBTITLE
Advanced Technology Landing Gear
Volume II - Test

5. FUNDING NUMBERS
(C) DAAJ02-85-C-0049

6. AUTHOR(S)
J.K. Sen

7. PERFORMING ORGANIZATION NAME(S) AND ADDRESS(ES)
McDonnell Douglas Helicopter Company
5000 East McDowell Road
Mesa, AZ 85205

8. PERFORMING ORGANIZATION REPORT NUMBER
MDHC 89-17

9. SPONSORING/MONITORING AGENCY NAME(S) AND ADDRESS(ES)
Aviation Applied Technology Directorate
U.S. Army Aviation Systems Command
Fort Eustis, VA 23604-5577

10. SPONSORING/MONITORING AGENCY REPORT NUMBER
USAAVSCOM TR 89-D-13B

11. SUPPLEMENTARY NOTES
Volume II of a two-volume report

12a. DISTRIBUTION/AVAILABILITY STATEMENT
Approved for public release; distribution is unlimited.

12b. DISTRIBUTION CODE

13. ABSTRACT *(Maximum 200 words)*

This report describes the development of a retractable, crashworthy, main landing gear system for an LHX-size utility helicopter. The landing gear is of a tricycle configuration and is designed to absorb 60 percent of the energy from a 42 fps level impact condition. The landing gear extends automatically in less than two seconds in an emergency. In the event that the hydraulic and electrical systems fail, the gear is extended with the hydraulic accumulator that primarily supports the helicopter APU. Five sets of landing gears were fabricated in the program. The tests included single-gear platform drop tests with level and simulated roll and pitch conditions, and combined pitch (+15°) and roll (10°) conditions with an iron-bird fixture simulating a helicopter. The tests were conducted for five impact velocities from 10 to 42 fps. The crashworthiness analyses were conducted using program KRASH. The correlation between test and crashworthiness analysis results was very good and demonstrated how analyses can be used to predict the response of landing gears without utilizing expensive tests. The cost of 5000 shipsets over a 13-year production cycle has been projected from the cost of landing gears fabricated in this program.

14. SUBJECT TERMS	15. NUMBER OF PAGES
Landing gear, Helicopter, Crashworthiness, Drop tests, Energy absorption	137
	16. PRICE CODE

17. SECURITY CLASSIFICATION OF REPORT	18. SECURITY CLASSIFICATION OF THIS PAGE	19. SECURITY CLASSIFICATION OF ABSTRACT	20. LIMITATION OF ABSTRACT
UNCLASSIFIED	UNCLASSIFIED	UNCLASSIFIED	

FOREWORD

This report is Volume II of the final report of the Advanced Technology Landing Gear Program. The report covers the work performed under Contract DAAJ02-85-C-0049 from 20 September 1985 to 31 May 1989. This contract with McDonnell Douglas Helicopter Company was conducted for the Aviation Applied Technology Directorate, U.S. Army Aviation Research and Technology Activity (AVSCOM), Fort Eustis, Virginia. The program was under the direction of Mr. Ned Chase.

The program was accomplished by the Structures Department of McDonnell Douglas Helicopter Company, Mesa, Arizona, with Dr. J. K. Sen as Program Manager and Project Engineer. Subcontracting to McDonnell Douglas Helicopter Company was Menasco California Division, Burbank, California. The Program Manager at Menasco was Mr. R. J. Hernandez.

The key personnel associated with the program and their areas of responsibility were:

McDonnell Douglas Helicopter Company

J. K. Sen	Project Engineer
L. Bohorquez	Design
M. Jones	Structures
A. Bolukbasi	Crashworthiness
R. March	Weights
L. Richmond	Operations Research
E. Murgia	Maintainability
J. Williams	Reliability

Menasco California Division

D. Martin	Project Engineer and Design
H. Kawada	Stress Analysis
C. Wilson	Test

The performance was under the general direction of Mr. F. J. Widmann, Manager, Research Projects.

This program was undertaken to develop a retractable, crashworthy landing gear system for an LHX-size utility helicopter with extensive energy absorption trade-off study and crashworthiness analysis to verify the design concepts. The design and crashworthiness analysis have been verified by single-gear platform drop tests, and by tests for combined roll and pitch impact attitude with an iron-bird test fixture simulating a helicopter. This program has demonstrated the differences in the behavior of landing gears in platform and iron-bird drop tests, and the close correlation that can be achieved between crashworthiness analysis and impact tests of helicopters.

TABLE OF CONTENTS

TABLE OF CONTENTS - Continued

TABLE OF CONTENTS - Continued

LIST OF FIGURES

LIST OF FIGURES - Continued

LIST OF FIGURES - Continued

LIST OF TABLES

LIST OF GRAPHS

LIST OF GRAPHS - Continued

LIST OF GRAPHS - Continued

1.0 INTRODUCTION

The Advanced Technology Landing Gear (ATLG) was subjected to all the qualification tests of a production landing gear in addition to impact drop tests with an iron-bird fixture simulating the utility helicopter for which the landing gear was designed. The results of the drop tests were correlated with results from analysis of crash-impact conditions conducted with program KRASH.

Presented in this report are the results of the acceptance tests, single-gear platform drop tests, iron-bird drop tests, and correlation of iron-bird drop test data with results predicted by program KRASH. The single-gear platform drop tests were conducted for level impact, and simulated roll and pitch impacts separately. Each impact attitude was tested for four impact velocities at two representative helicopter gross weights. The iron-bird drop tests were conducted with combined roll and pitch impacts at five impact velocities and two helicopter gross weights.

Five landing gear systems were fabricated and tested to complete twelve single-gear platform drop tests and six iron-bird drop tests. The iron-bird drop tests required the use of two landing gear systems per test. The tests were planned such that lightly loaded gears from previous tests could be used in subsequent tests. Though the total number of planned single-gear platform tests was only twelve, additional preliminary tests, up to impact velocities not exceeding 20 fps, were conducted to calibrate the fixture. Similarly, preliminary tests in excess of the planned five iron-bird tests were conducted to assure that the test conditions were being satisfied.

The test results were correlated with analytical results using program KRASH. The correlation for the iron-bird tests was made with a KRASH model of the iron-bird fixture with the same center of gravity, gross weight, and moments of inertia.

All the tests were conducted at and by Menasco in Burbank, California. The acceptance tests were conducted in Menasco's Central Laboratory and the drop tests in Menasco's drop test tower.

The acceptance and extension-retraction tests are described in Section 2.0. The drop test tower, the instrumentation and the data analysis procedures are described in Section 3.0. The results of the level-impact and the inclined-impact (with roll or pitch) platform drop tests are described in Section 4.0. The results of the iron-bird drop tests, given in Section 5.0, are followed by the correlation of the test results with those of KRASH in Section 6.0.

2.0 DEVELOPMENT TESTS

2.1 OBJECTIVES

The objectives of the development tests were to verify the design parameters and the function of the ATLG before any of the drop tests were conducted. The development tests consisted of the following:

1. Acceptance tests of the shock strut.
2. Acceptance tests of the retraction actuator.
3. Verification of the performance of the fused orifice in the shock strut.
4. Compression tests of the shock strut to verify the shock strut spring curves.
5. Extension-retraction tests of the ATLG through 50 cycles.
6. Verification of the designed time of a maximum of 2.5 seconds to extend the gear.

2.2 FUNCTION DESCRIPTION

2.2.1 Shock Strut

The ATLG absorbs impact energy using the shock strut, P/N 1252100, with an oil chamber separating the two gas chambers. Each of the two gas chambers contains floating pistons to separate the hydraulic fluid from the gas chambers. Under normal landing conditions for impact velocities up to 10 fps, the impact energy is absorbed by the fluid flowing through the first stage orifice.

For hard landings up to 20 fps, hydraulic fluid flow is through the first and second stage orifices. During crash landings in excess of 20 fps but below 42 fps, the fuse orifice will rupture to increase the area of the second stage orifice and allow additional fluid to flow. This design also reduces the possibility of load spiking in a 42 fps impact.

The second stage air chamber includes a static stop onto which the helicopter "kneels" during loading and unloading, and when transported. The kneeling stop is designed to buckle under compression loads of 22,400 psi. This additional feature further reduces the possibility of load spiking at impacts of 42 fps when the second stage piston has completed its full stroke. The shock strut and the static stop are schematically shown in Figure 1.

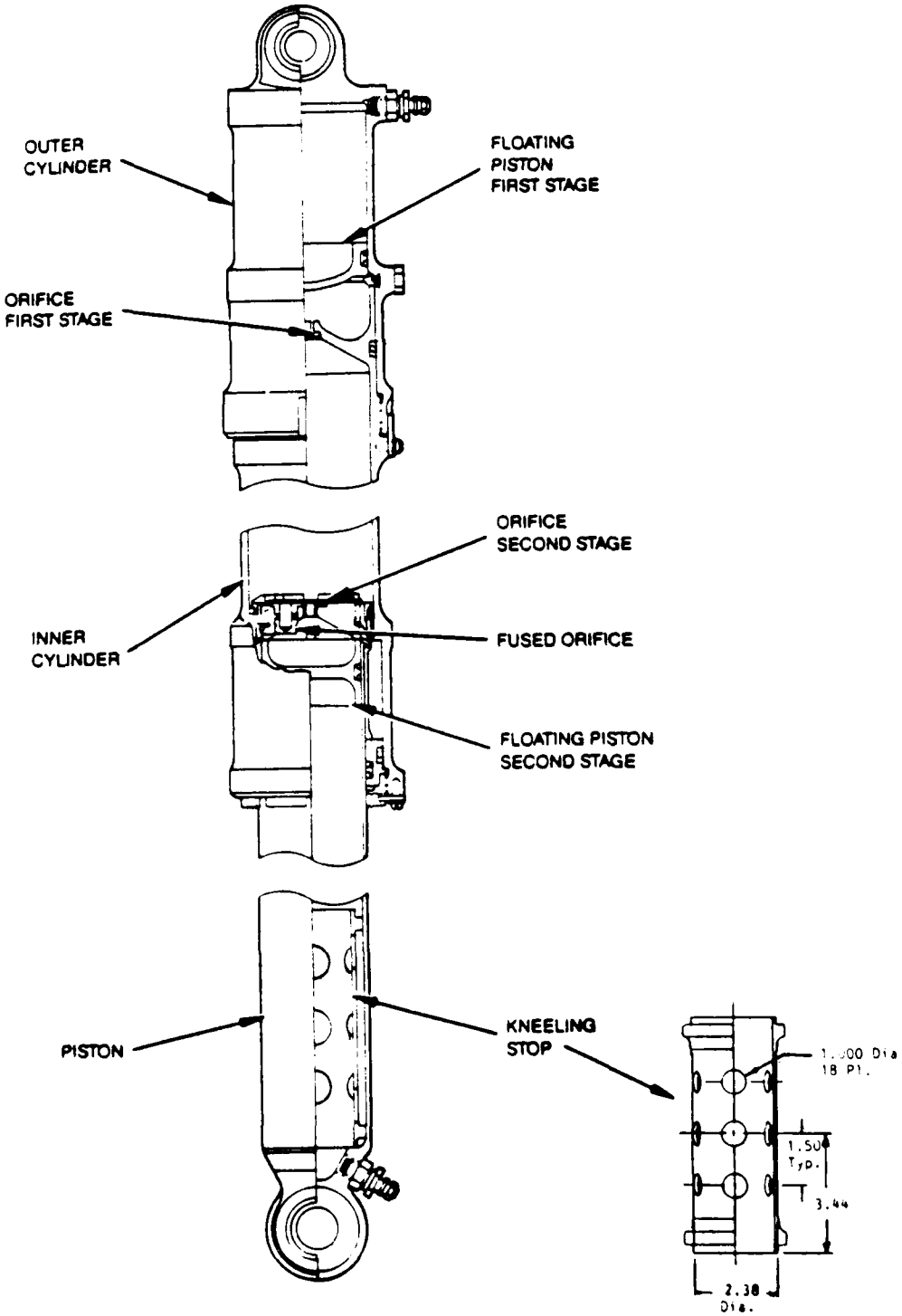

Figure 1. Schematic view of shock strut with kneeling stop.

2.2.2 Retraction Actuator

An ordinary two-port hydraulic actuator is used to retract and extend the landing gear. The retraction actuator, P/N 1252400, is attached to a linkage assembly, P/N 1252300, which reacts all the load and which locks in both the retracted and extended positions by an overcenter linkage.

2.3 ACCEPTANCE TESTS

2.3.1 Shock Strut

Each of the five ATLG shock struts, P/N 1252100, was tested on a bench using a hydraulic motor pump, a hydraulic hand pump, a 10-micron hydraulic filter, MIL-H-5606 hydraulic fluid, dry nitrogen conforming to MIL-P-27401B, and pressure gages. The test conditions were the prevailing ambient temperature, humidity and atmospheric pressure. The shock struts completed the tests successfully. The tests and the sequence in which they were conducted are given below.

1. Each shock strut assembly was inspected and certified before initiating any mechanical testing.

2. Highly stressed areas of the strut assembly were inspected by X-ray and ultrasonic methods for internal defects.

3. Critical parts were inspected for surface defects by magnetic particle, nital-etch and/or penetrant inspection methods.

4. Each shock strut was dimensionally inspected and weighed.

5. The shock struts were serviced for proof pressure before proof pressure testing. The servicing test qualified the first and second stage gas chambers, and the oil chamber. The proof pressure test was conducted by slowly applying 6,760 psig to the shock strut and holding the pressure for 15 minutes. Following the test, the shock struts were disassembled and examined for leakage, yielding or permanent deformation.

6. The hand-cycle test checked for functionality of the shock strut. Before the test, a servicing test was conducted to identify irregularities. The hand-cycle test, repeated six times, checked the piston action and measured the length of the retracted and fully extended positions of the shock strut.

7. The last test was the vertical leak test where the shock strut was suspended vertically for 6 hours and the gas pressures measured and compared with those initially recorded.

2.3.2 Retraction Actuator

Each of the retraction actuators and the linkage assemblies, P/N 1252400 and 1252300, were subjected to five acceptance tests. The retraction actuators completed the tests successfully. The order of the tests is given below.

1. Each retraction actuator assembly was inspected and certified before initiating any mechanical testing.

2. Each critical part was inspected for internal defects by magnetic particle, nital-etch and/or penetrant inspection methods.

3. The retraction actuators were dimensionally inspected and weighed.

4. Tests on the retraction actuators were performed at 4000±100 psig and the pressure was maintained for 5 minutes to check for external leakages from the gland-nut/piston area. Internal leakages were also checked from evidences of fluid draining from the open extending port.

5. The proof pressure tests were conducted by first conducting a test to retract and extend the actuator ten times. Proof pressure was then applied and maintained for 3 minutes. Inspection for internal and external leakages and permanent deformation were made.

2.4 FUSED ORIFICE VERIFICATION TEST

The test of the fused orifice of the shock strut was conducted on a bench provided with a hand pump and a pressure transducer. The fused orifice was designed to rupture at 3,500 psi. The original design of the fuse, P/N 1252114-1, withstood loads up to 5,000 psi. The fuse assembly was then redesigned, P/N 1252123-101, using a shear pin-type fuse assembly, P/N 1252126-1. The orifice was retested and the pin sheared at 3,500 psi. The redesigned fuse assembly is also less expensive to manufacture and more reliable in operation.

2.5 STATIC COMPRESSION TEST OF SHOCK STRUT

The static compression test of the shock strut, P/N 1252100, was conducted to develop the load-stroke curve in both extension and compression. The strut was tested in a specially designed drop-test machine. The strut was compressed in increments of 0.5 inch from the fully extended to 29 inches of vertical axle stroke. The stroke was measured on the strut piston and vertically at the axle. The pressure was recorded by a pressure gage. The pressure and strokes were also recorded in 0.5 inch increments when the strut was extended. The strut load-stroke curve is shown in Figure 2 and the strut load versus axle travel curve in Figure 3.

The compression and extension curves are shown on both figures. Also shown on the figures are the predicted curves. The experimental curves agree very well with the predicted curves.

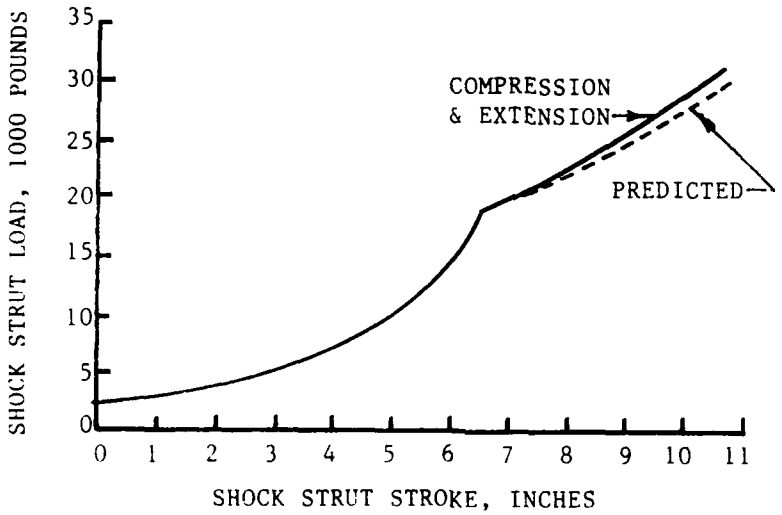

Figure 2. Load-stroke curve of ATLG shock strut.

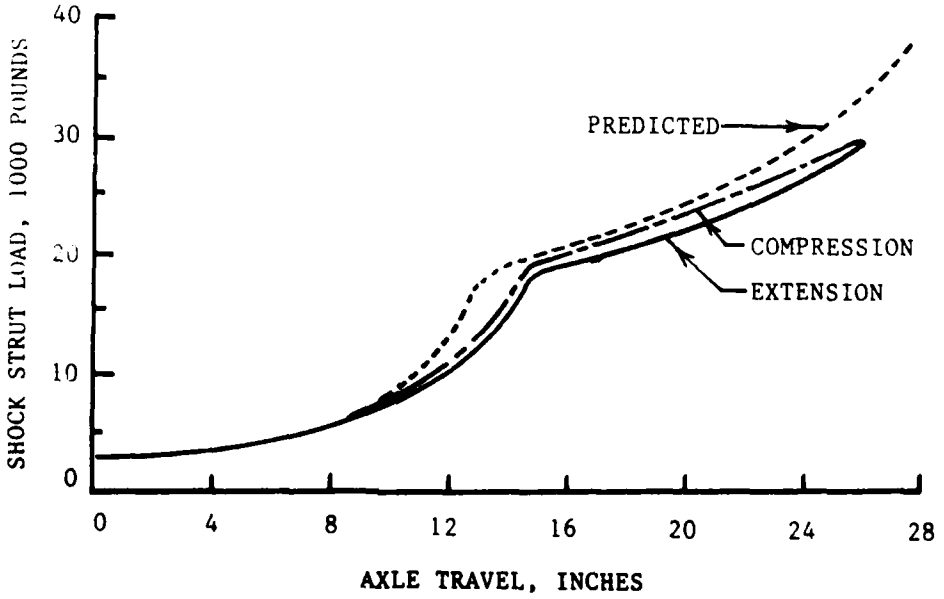

Figure 3. Load in ATLG shock strut in terms of axle travel.

2.6 EXTENSION-RETRACTION TEST

The extension-retraction test of the landing gear was also conducted in the specially designed drop-test machine. The test was conducted with the landing gear wheel slightly off the ground. The test setup is shown in Figure 4. A total of 51 test cycles were applied. An additional 35 cycles were applied to record the test in motion pictures. During the test, both up and down operations of the overcenter lock mechanisms were monitored. Following the test, the shock strut was inspected and no damage was evident. The data recorded for both retraction and extension were the maximum operating pressures, the flow rate and the operating time. The average of 51 readings are given below.

	Retraction	Extension
Max. Operating Pressure	2,800 psig	850 psig
Operating Time	4.5 sec	1.5 sec
Flow Rate	0.8 gpm	0.87 gpm

The minimum pressures required to release the overcenter locks were also experimentally determined. A pressure of 950 psig was required to release the overcenter lock to extend the landing gear, and 2,250 psig was required in retraction to lock up the gear.

2.7 SUMMARY

The test results showed that the shock strut and the retraction actuator have been designed and manufactured to meet the design specifications. The orifice of the shock strut was redesigned and tuned to the desired specifications. Subsequent tests showed that the response of the shock strut was very close to that predicted. The extension and retraction curves for the shock strut closely matched the predicted curve.

The requirements for emergency operation were also met by the retraction actuator. An extension time of 1.5 seconds betters the requirement of less than 2.5 seconds in an emergency. In the case of hydraulic and electrical failures, the 4,000 psig pressure from the helicopter's accumulator (to power the APU) will easily unlock the gear for emergency extension. The pressures for up-lock and down-lock positions were well below 4,000 psig.

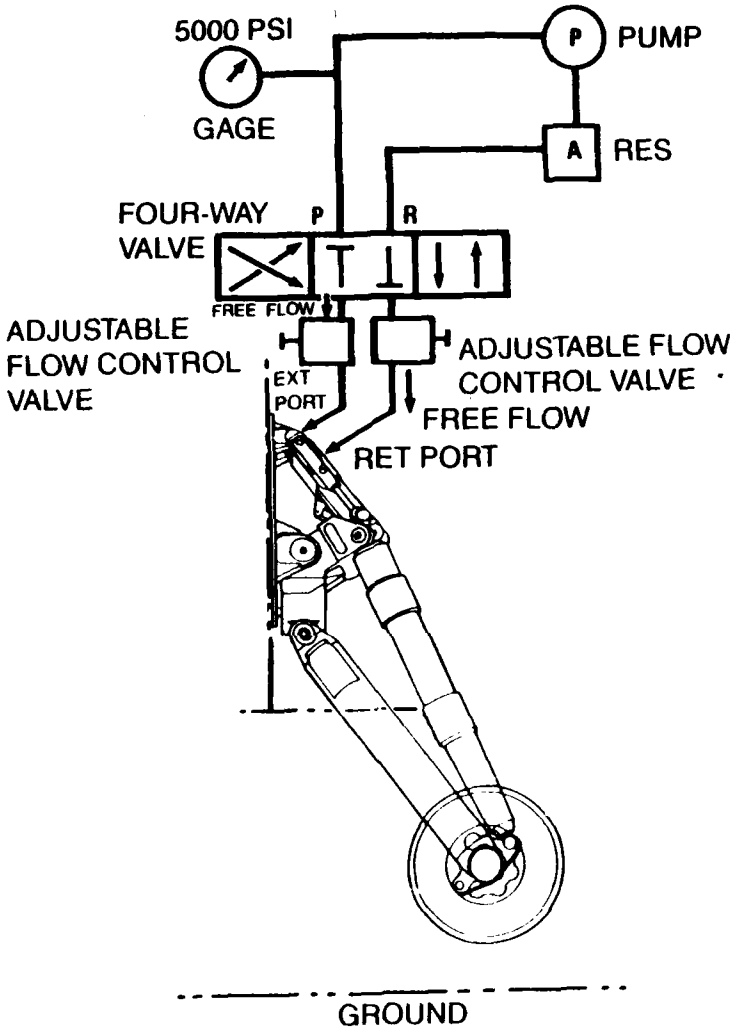

Figure 4. Setup for the extension-retraction test.

3.0 DROP TEST TOWER AND FIXTURES

3.1 GENERAL

The drop test tower was used for all the single-gear level-impact and inclined-impact platform drop tests, and the iron-bird drop tests. Two special fixtures were designed and fabricated to operate with the crosshead in the drop test tower. The fixtures simulated the mounting of the landing gear in the helicopter exactly. The single-gear fixture was used for the platform drop tests. The iron-bird fixture simulated the utility helicopter and was used for the combined roll and pitch tests. The fixtures were designed to react the loads from the repeated drop tests without failure. The drop tower, the special landing gear fixtures, and the instrumentation are described in this section.

3.2 DROP TEST TOWER

The drop test tower consists of two vertical columns over 70 feet high. The crosshead to which the drop test fixtures are mounted rides on guide rails mounted on the inside surfaces of the columns. Two landing gear drop test fixtures were used for the tests: the single-gear and the iron-bird fixture. The entire drop test fixture with the gear assembly can be weighed by mounting a load cell between the crosshead and the fixture. The fixture weight can then be adjusted to meet the test requirements. A schematic view of the tower is given in Figure 5, and a photograph in Figure 6.

Canisters of specially designed Hexcel aluminum crushable material were used to absorb the energy from high impact velocities after the landing gear stroked above the fuselage. This prevented the fixtures from impacting the ground as the stroking landing gear strokes above the lowest fuselage waterline. This design also prevented the landing gear from being crushed between the oncoming fixture and the ground. The high impact velocities at which the canisters were required to absorb the energy were for velocities above 20 fps. The canisters, positioned at the bottom of the inner sides of the columns, would absorb the energy of the stroking fixture after the landing gear had stroked above the lowest fuselage waterline. Two additional canisters of Hexcel crushable material were positioned in series with the first pair of canisters in case the landing gear failed. For tests at 20 fps and greater, the canisters were inspected, and the deformation measured and replaced if sufficient damage had occurred. These canisters will henceforth be referred to as "catchers" and are so identified in the data plots whenever they come into play in the tests.

The rotor-lift of 0.67g was simulated mechanically by two interconnected gas-operated cylinders. The cylinders, mounted to the test floor, reacted against the fixtures at specially designed locations. The gas cylinder reservoirs were sufficiently large to permit the rotor-lift force to be nearly constant during the entire test sequence. For the level-impact test at 42 fps and all subsequent tests, a contact switch was installed on one of the canisters to record the time of contact with the fixture. Valves in the rotor-lift cylinders were designed to relieve the built-up pressure during the test in order to prevent the cylinder pistons from rebounding after they were compressed during the test. The pistons did rebound during the level-impact test at 42 fps causing extensive damage to the cylinders and their load cells.

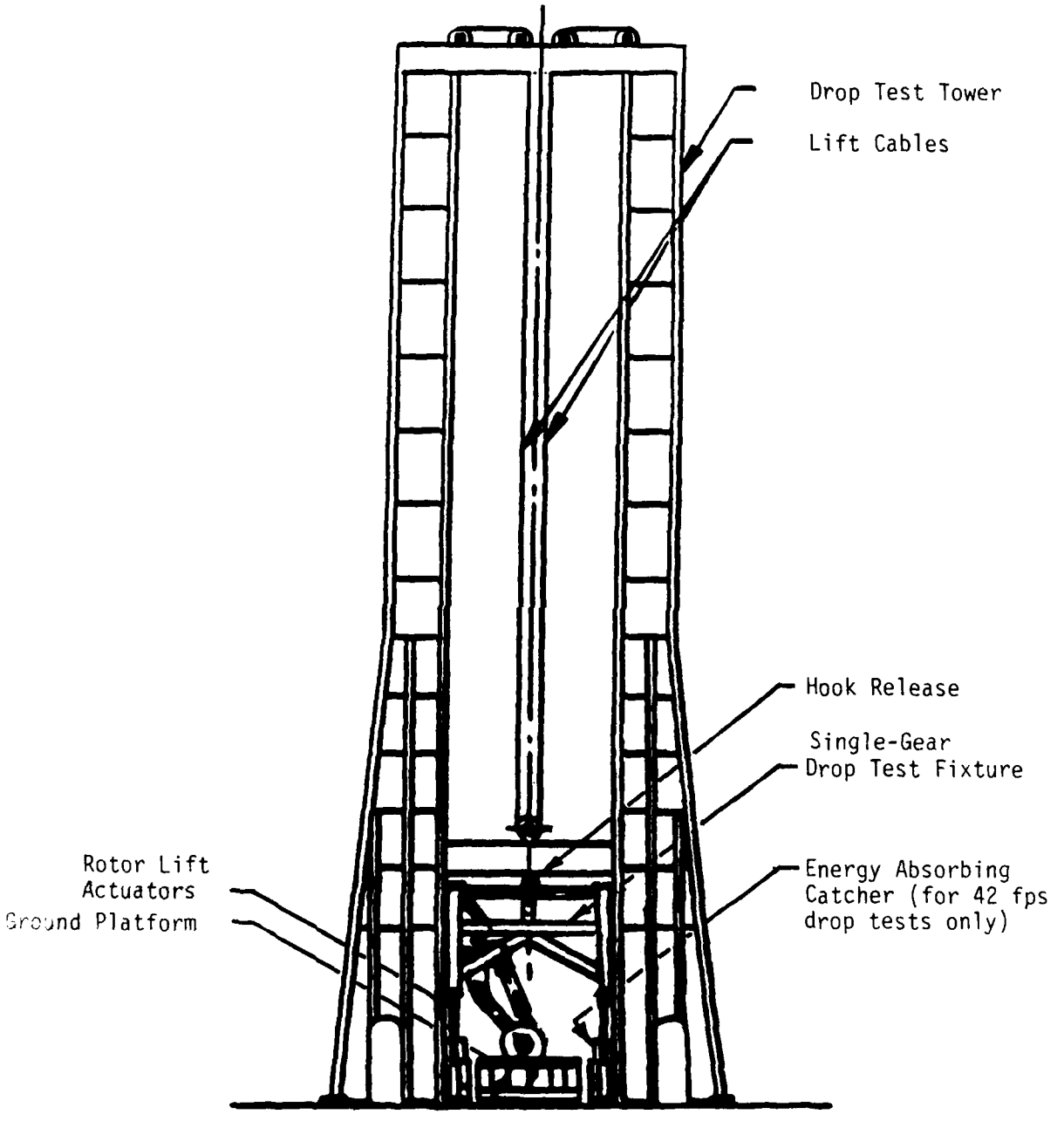

Figure 5. Schematic view of the drop test tower.

OVERALL VIEW OF DROP TEST TOWER

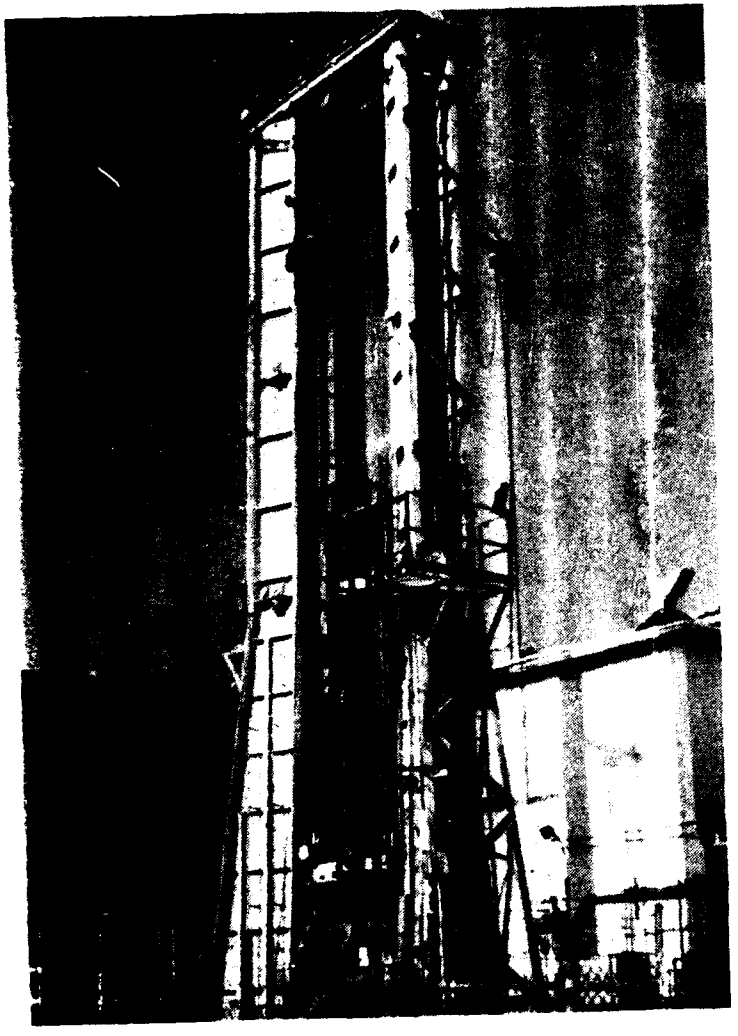

DETAILS OF PLATFORM DROP FIXTURE IN DROP TEST TOWER

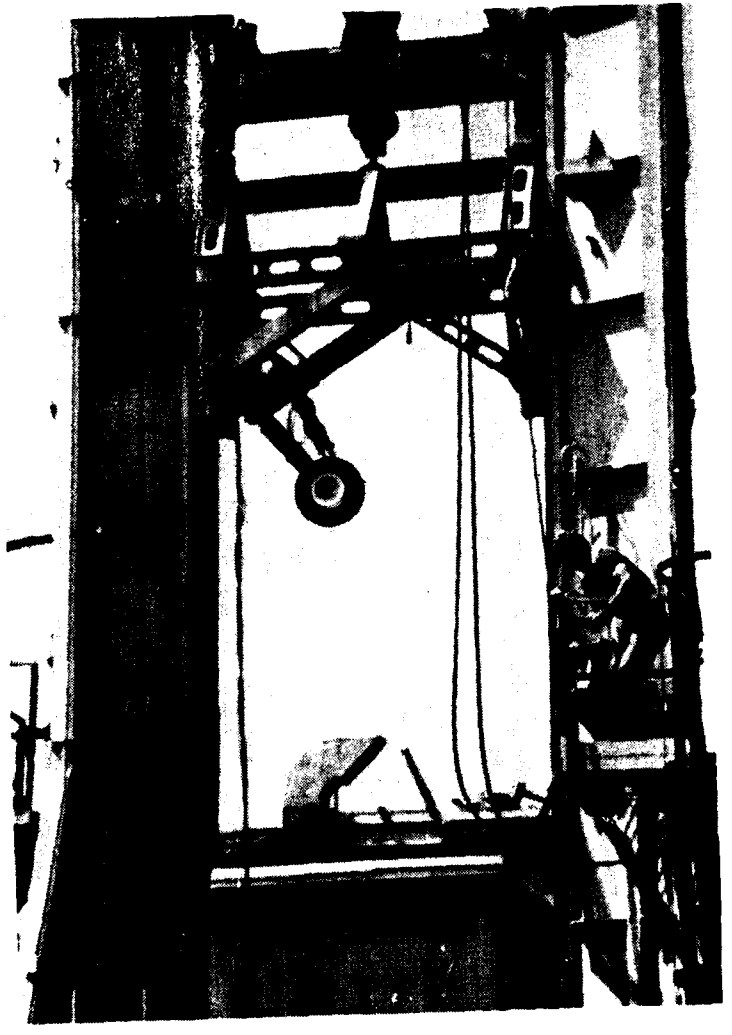

8811449-1

Figure 6. Drop test tower with single-gear fixture for platform drop tests.

The ground was a perfectly rigid surface simulated by steel plates. Each of the steel plates was supported on four ring-type load cells to measure the vertical ground reaction load. For the level-impact platform tests, a flat plate was used. For the inclined-impact platform tests, the steel plate was mounted on a platform inclined at +15° pitch or at 10° roll. The setup of the +15° pitch test is shown in Figure 7 and for the 10° roll in Figure 8. For the iron-bird drop tests, additional load cells were first used to measure the drag load and then reconfigured to measure the side-to-side lateral loads. Thus, the drag load was measured in the 17 fps iron-bird drop test and the lateral load in all other tests (10, 20, 30 and 42 fps).

To perform the drop tests, the drop weight was adjusted and the shock strut, tire and rotor-lift cylinder pressures were checked. The attitude of the fixture was checked with a level protractor. The fixture was then raised above the platform by a hook to the height required to attain the desired impact velocity. The safety pin in the hook was released by actuating a remote solenoid, and the hook was opened by hydraulic action to allow the fixture to drop freely.

3.3 SINGLE-GEAR TEST FIXTURE

The single-gear fixture used for the platform drop tests was a simple design of structural steel members. The fixture was designed to the constraints of the drop test tower and for reacting loads from repeated drop tests. The fixture is seen in Figures 6, 7 and 8. The hook to raise the fixture is seen in the top center of Figure 7. Also clearly seen in the middle of the figure is one of the rotor-lift cylinders and the specially designed bracket on the fixture to react the load from the cylinder piston. The pair of canisters of Hexcel crushable material is visible on the ground at either side of the figure against the columns of the tower. The assembled landing gear in this test fixture is shown in Figure 9.

The weight of the single-gear fixture was adjusted for each of the three cases of impact tests: level, 10° roll and +15° pitch. Each of the main landing gears was designed to react 34.5 percent of the helicopter's gross weight. However, the minimum weight of the single-gear fixture was 3,115 pounds, which is greater than 2,932 pounds, the lowest weight desirable for the platform drop tests. The lowest weight was computed as 34.5 percent of the basic structural design gross weight (BSDGW) of 8,500 pounds. Therefore, for level-impact tests at the BSDGW, the fixture weight was 3,115 pounds, or 6.2 percent greater than that required.

For the roll and pitch platform drop tests, the weights were computed from the static distribution of the inclined helicopter in these two respective planes. The required weights for the single-gear fixture and the rotor lift forces for the BSDGW and the alternate design gross weight (ADGW) of 10,625 pounds are given in Table 1.

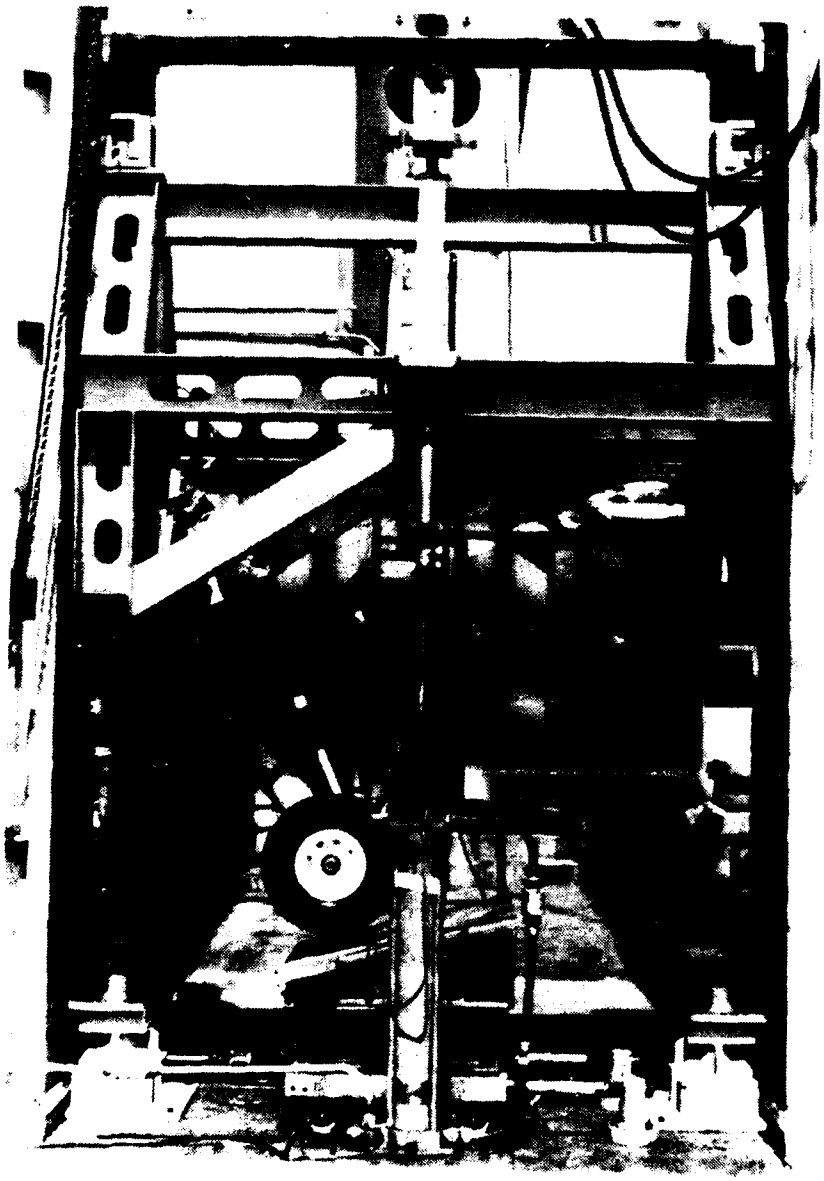

Figure 7. Test setup for +15° pitch platform tests.

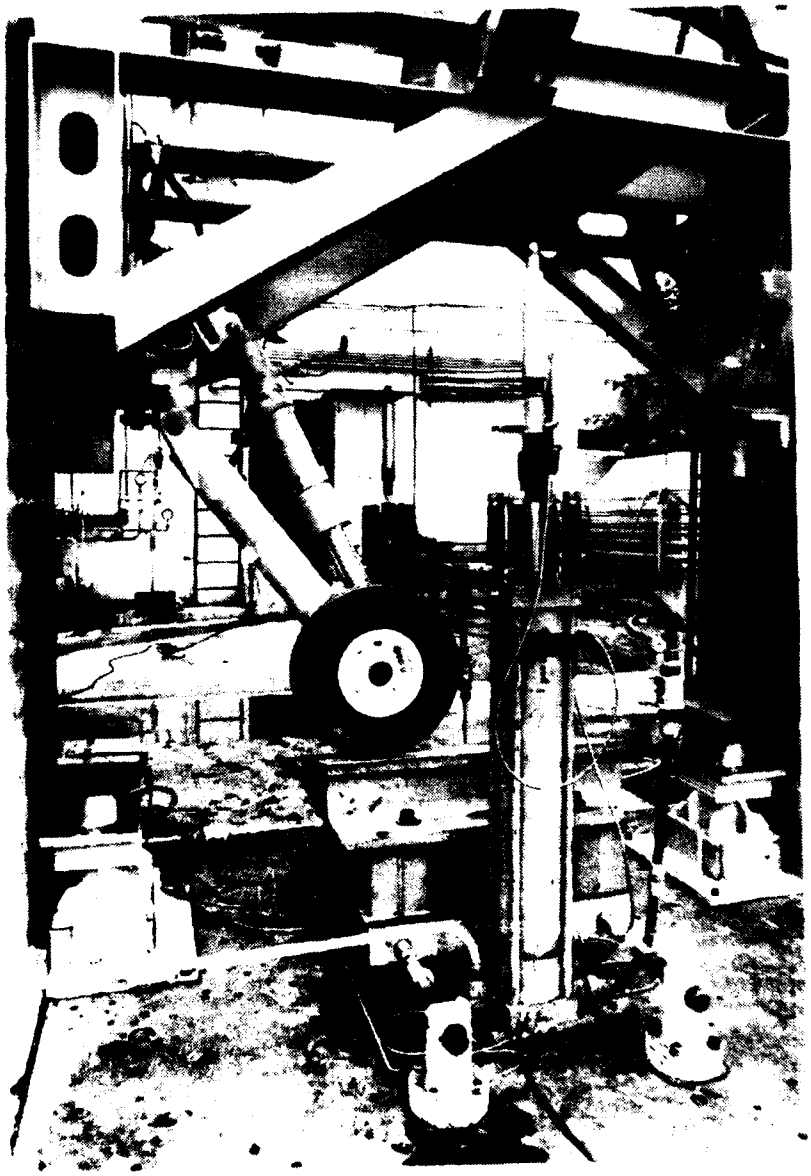

Figure 8. Test setup for 10° roll platform tests.

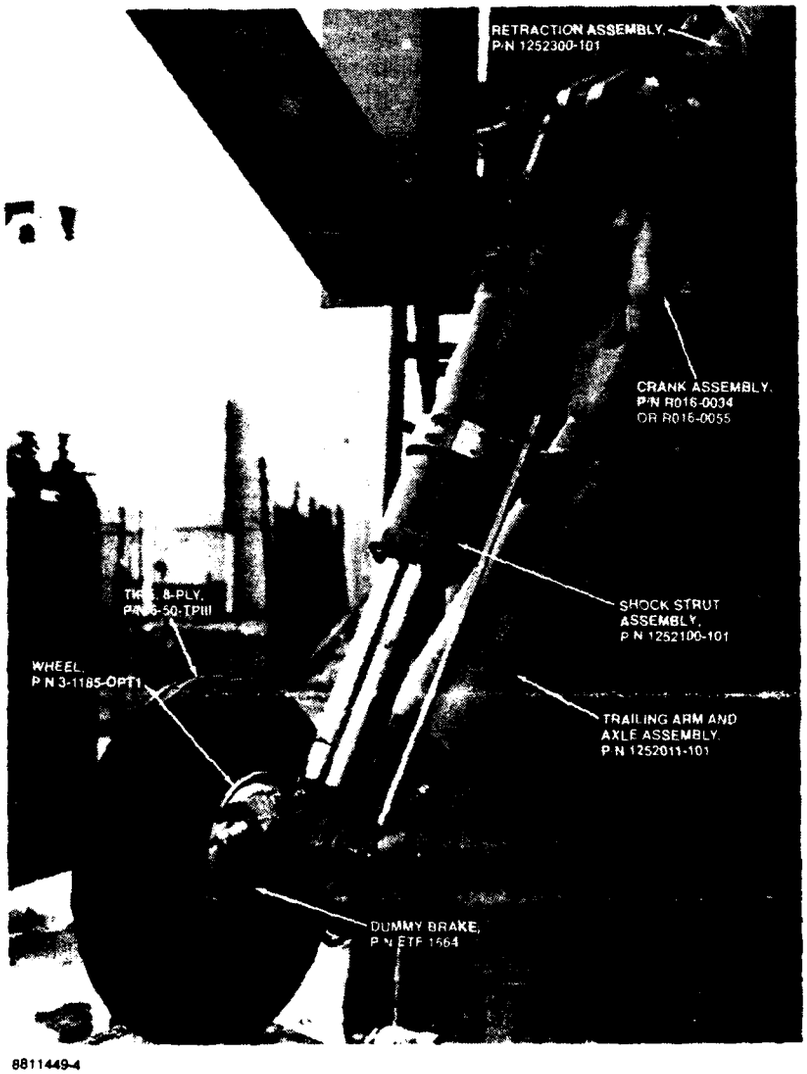

Figure 9. Assembled landing gear in single-gear test fixture.

TABLE 1. REQUIRED WEIGHTS AND ROTOR-LIFT FORCES FOR SINGLE-GEAR PLATFORM DROP TESTS

Impact Attitude	Single-gear fixture weight		Rotor-lift force	
	for BSDGW	for ADGW	for BSDGW	for ADGW
Level	2,932 lb*	3,665 lb	1,955 lb**	2,440 lb
10° Roll	3,300 lb	4,124 lb	2,200 lb	2,749 lb
15° Pitch	3,270 lb	4,088 lb	2,180 lb	2,725 lb

*The actual weight was 3,115 pounds because the weight of the drop test fixture exceeds this value.

**The actual rotor-lift force was 2,080 pounds, i.e., 0.67 percent of the actual fixture weight of 3,115 pounds

3.4 IRON-BIRD TEST FIXTURE

The iron-bird fixture was designed with structural steel members to simulate the utility helicopter for which the landing gears were designed. The fixture was designed to be subjected to repeated drop tests. The locations of the main and nose landing gears are exactly as in the helicopter with respect to the center of gravity. The main landing gear was mounted exactly as in the helicopter, except that the pivot crank, P/N R016-0055, was replaced by a plate with clevises in position and orientation exactly the same as in the crank. This was done because the cranks had been tested previously in the platform drop tests and the manufacturing lead time for the cranks was very long. The nose landing gear was simulated by an energy absorbing structure with a shoe simulating the tire. The iron-bird fixture simulated exactly the gross weights and the location of the center of gravity of the helicopter. The center of gravity was located at

fuselage station = 198.4
butt line = 0.0
water line = 128.9

Since the iron-bird fixture was designed within the constraints of the available dimensions of the drop test tower and the area available around it, the iron-bird fixture was restrained in the yaw direction to prevent it from damaging itself and the drop test tower. The moments of inertia were therefore not exactly duplicated. The moments of inertia of the iron-bird fixture for the BSDGW of 8,500 pounds and the ADGW of 10,625 pounds are compared with those of the helicopter in Table 2.

To prevent the iron-bird fixture from striking the ground in drop tests at high impact velocities, a stack of styrofoam sheets, instead of the canisters of Hexcel crushable material, was used to absorb the kinetic energy not absorbed by the landing gear. The styrofoam sheets were contoured to the planform shape of the iron-bird fixture and positioned on the ground below it.

TABLE 2. MOMENTS OF INERTIA OF THE HELICOPTER AND THE IRON-BIRD FIXTURE

Direction	Moments of Inertia (in-lb-sec**2)			
	BSDGW of 8,500 lb		ADGW of 10,625 lb	
	Helicopter	Iron-Bird	Helicopter	Iron-Bird
Roll	52,086	18,430	52,086	31,190
Yaw	236,864	85,320	249,600	144,250
Pitch	248,402	92,380	256,800	156,230

The iron-bird fixture rode vertically down the guide rails supported by the crosshead. The crosshead supported the fixture at its center of gravity through a gimbal. The gimbal permitted free movement along the roll and pitch axes but restrained movement in the yaw direction. The gimbal was mounted on two highly polished rods on the crosshead which permitted the fixture to translate laterally when the fixture rolled after impact to correct its attitude. The rotor-lift force was simulated by two gas cylinders. A schematic view of the iron-bird fixture is shown in Figure 10. Photographs of the aft and front view are shown in Figure 11.

Prior to a drop test, weights simulating the BSDGW of 8,500 pounds or the ADGW of 10,625 pounds were mounted and strapped in at preassigned positions on the iron-bird fixture. To position the fixture in the desired attitude, the fixture was first moved laterally on the crosshead in the direction of the landing gear which would first impact the ground, i.e., the down-side gear. The 10° roll and +15° pitch attitude was achieved by rotating the fixture at the gimbal and securing it in position by shear cables. The cables were designed to shear when the fixture impacts the ground, thus allowing the fixture to act as a free body in the roll and pitch planes. The required weights and rotor-lift forces for the iron-bird drop tests are as follows:

Iron-bird fixture weight		Rotor-lift force	
for BSDGW	for ADGW	for BSDGW	for ADGW
8,500 lb	10,625 lb	5,667lb	7,083 lb

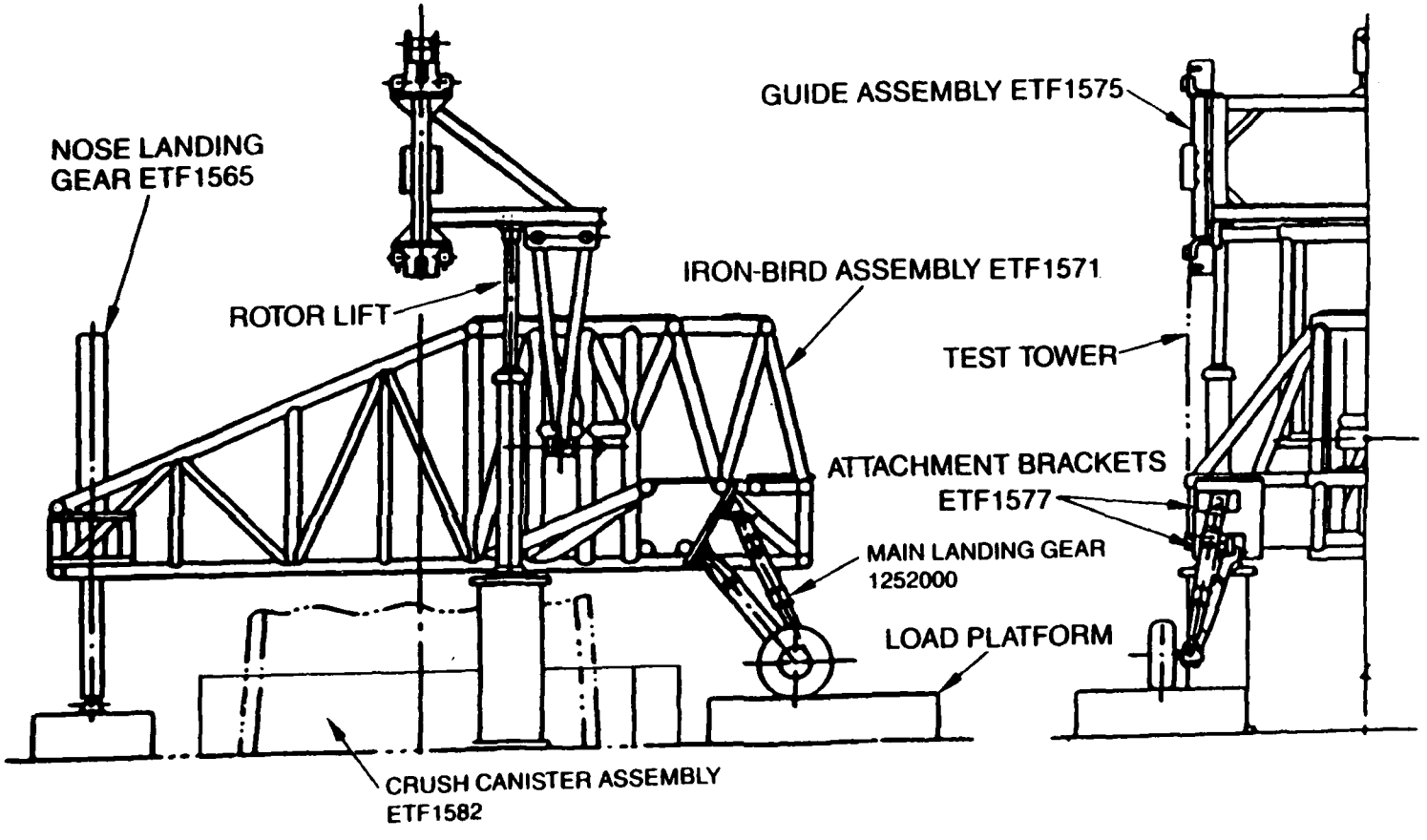

Figure 10. Schematic view of the iron-bird fixture.

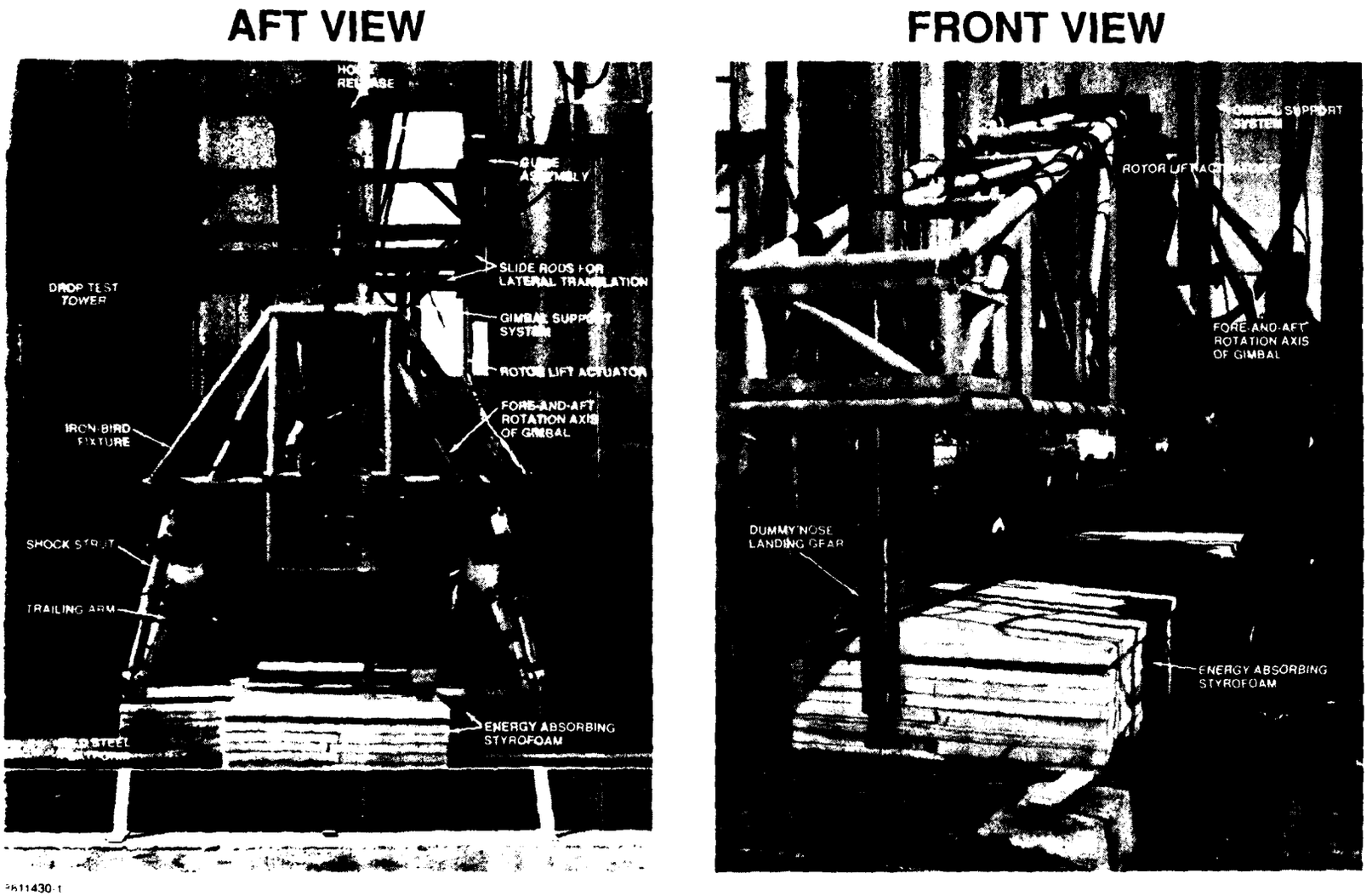

Figure 11. Aft and front views of the iron-bird fixture showing the various components.

3.5 TEST INSTRUMENTATION

Sixteen channels of data were recorded from the data acquisition system for the drop test tower. The data signals recorded by the sixteen channels were from load cells, displacement transducers, accelerometers, velocity pick-ups and pressure transducers. The data was recorded by a PDP-11 computer system at the rate of 1000 events per second. The data was then plotted on a graphics terminal for viewing and evaluation. In order to assure that the channels were recording as planned, several preliminary tests at low impact velocities were conducted before the initiation of the test program.

In addition to the sixteen transducer signals, high-speed motion pictures were recorded. The locations of the motion pictures for the iron-bird drop tests are shown in Figure 12. The left camera was located to record the behavior of the left (down-side) gear. For the single-gear drop tests, three motion picture cameras were also located to record the behavior from both sides of the fixture.

3.5.1 Platform Drop Tests

For the single-gear drop tests, ten channels of data were recorded as functions of time. The data was then reduced and plotted from the time of impact. The data channels were:

1. Vertical ground reaction load
2. Fixture acceleration
3. Shock strut axial load
4. Shock strut piston stroke
5. Fixture velocity
6. Fixture displacement normal to the ground
7. Rotor-lift force
8. First-stage gas pressure
9. Second-stage gas pressure
10. Oil pressure

3.5.2 Iron-Bird Drop Tests

For the iron-bird drop tests, sixteen channels of data were recorded as functions of time. The data was then reduced and plotted from the time of impact of the down-side gear. The data channels were:

1.	Vertical ground reaction load, both gears	2 channels
2.	Lateral or drag ground reaction load, both gears	2 channels
3.	Load on nose landing gear	1 channel
4.	Acceleration at fixture center of gravity	1 channel
5.	Acceleration of landing gear, both gears	2 channels
6.	Shock strut axial load, both gears	2 channels
7.	Shock strut piston stroke, both gears	2 channels
8.	Acceleration of nose landing gear	1 channel
9.	Fixture velocity	1 channel
10.	Fixture displacement normal to the ground	1 channel
11.	Rotor-lift force	1 channel

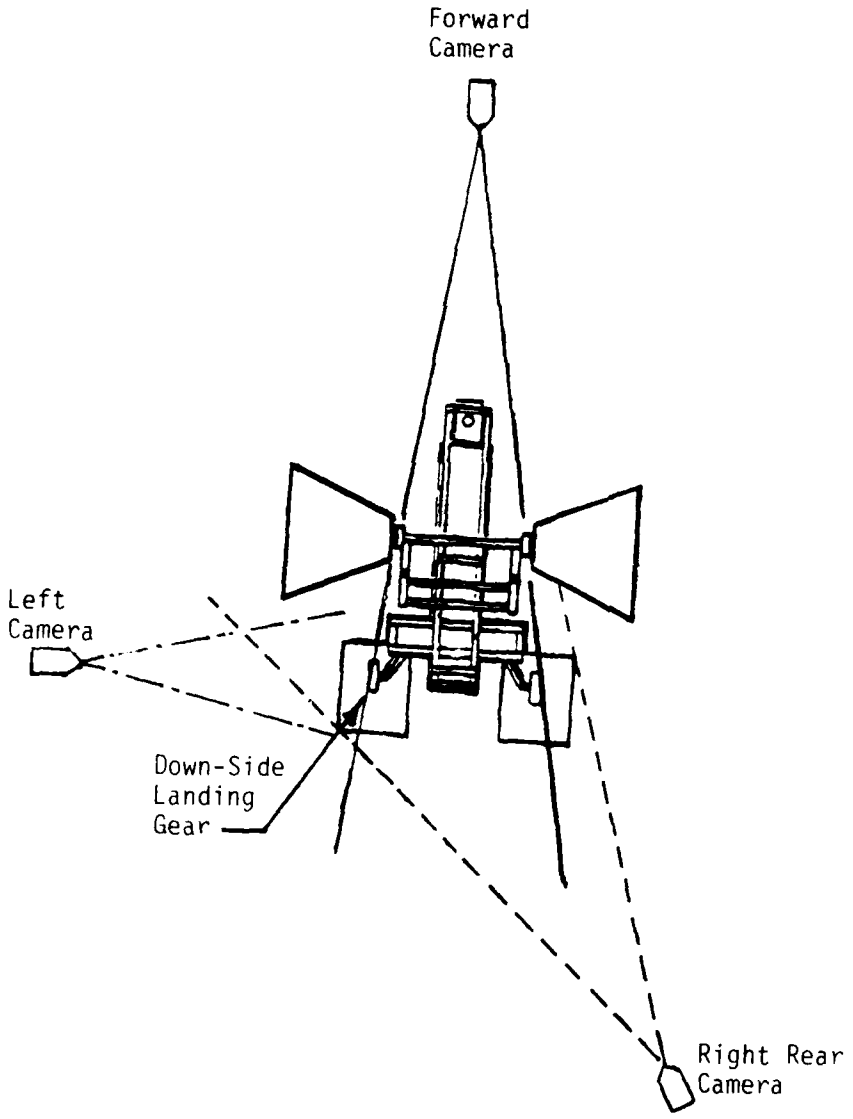

Figure 12. Location of motion picture cameras for the iron-bird drop tests.

3.5.3 Data Reduction

With the acquisition of 1000 events/second per channel, the data was reduced using a PDP-11 computer system. The data was filtered before being plotted. The filtering frequency for each channel was chosen to get correspondence between related data channels. All the filters were single-pole Butterworth-type. The filtering frequency bands used for the data channels are given below:

Data Channel	Filter Frequency Band
Sink velocity	20 Hz
Fixture displacement	20 Hz
Strut axial load	1 KHz
Strut stroke	30 Hz
Vertical ground load	1 KHz
Horizontal/Lateral ground load	1 KHz
Rotor lift load	20 Hz
1st Stage gas pressure	1 KHz
2nd Stage gas pressure	1 KHz
Oil pressure	1 KHz
Accelerometers	100 Hz

4.0 PLATFORM DROP TESTS

4.1 GENERAL

The platform drop tests were divided into single-gear level-impact and inclined-impact tests. Four level-impact tests were conducted at impact velocities of 10, 17, 20 and 42 fps. Eight inclined-impact tests were conducted, four each at 10° roll and +15° pitch for the same velocities. The fixture weight was designed for 34.5 percent of the helicopter gross weight. The tests at 10, 17 and 42 fps were conducted for the BSDGW of 8,500 pounds. However, for level-impact tests, the fixture weight was 6.2 percent greater than that desired. The tests at 20 fps were conducted for the ADGW of 10,625 pounds. The rotor-lift forces were proportional to 0.67 percent of the fixture weight.

4.2 LEVEL-IMPACT TESTS

4.2.1 Test Specimen

One landing gear assembly was used for all the four tests. The landing gear represented the left-hand gear of the helicopter. The landing gear assembly consisted of one trailing arm, P/N 1252001; one shock strut, P/N 1252100; one retraction actuator, P/N 1252400; one retraction linkage assembly, P/N 1252300; one pivot crank, P/N R01C [illegible]4; and one running gear assembly. The brake for the running gear was replaced by a simulated brake.

The tire was pressurized to 113±8 psig under no load. The shock strut gas chambers were precharged with dry nitrogen in the fully extended position. The precharge of the first stage chamber was 325+10/-0 psig and that of the second stage chamber was 2,292+25/-0 psig.

4.2.2 Test Results

All the tests were successfully conducted. The results are presented in Table 3. The plots of the shock strut load-stroke curves for the four tests are shown in Figure 13. The curves of the vertical ground reaction load in terms of the test fixture displacements are given in Figure 14.

In the first three tests at 10 and 17 fps at the BSDGW and at 20 fps at the ADGW, the landing gear absorbed all of the kinetic energy and the catchers were untouched. In the test at 42 fps, the absorption of the kinetic energy was shared by the landing gear and the catchers. The landing gear absorbed 58 percent of the kinetic energy from a level impact at 42 fps, while the catchers, representing the helicopter fuselage, absorbed 42 percent of the energy. The energies absorbed by the landing gear in the tests and their respective efficiencies are shown in Table 4. The difference in the system and calculated energies represents the energy lost due to friction.

In the last test at 42 fps, both pistons of the rotor-lift cylinders rebounded under built-up pressure to damage their retention nuts and load cells. In all subsequent tests, the rotor-lift cylinders were connected to an accumulator to reduce the pressure buildup. Detail inspection of the landing gear components did not show evidence of damage or failure.

TABLE 3. RESULTS OF LEVEL-IMPACT PLATFORM DROP TESTS

Data Measured	Test for			
	10 fps	17 fps	20 fps	42 fps
Ambient Temp. (°F)	94	87	98	84
Drop Weight (lb) Req'd/Actual	2932/3115	2932/3115	3665/3665	2932/3115
Rotor-Lift (lb) Req'd/Actual	1955/1990	1955/2080	2440/2400	1955/2080
Impact Velocity (fps) Req'd/Actual	10.0/10.2	17.0/17.1	19,9/19.8	42.0/42.1*
Fixture Displ. (in.)	12.50	19.78	26.30	31.80
Strut Stroke (in.)	4.90	7.10	9.20	11.20
Vert. Grnd. Load (lb)	8,075	12,211	14.126	27,596
Strut Load (lb)	19,166	28,335	35,777	65,077
Gas Press. #1 (psig)	1,560	2,870	3,305	3,305
Gas Press. #2 (psig)	2,300	2,795	3,840	6,505
Oil Press. (psig)	1,625	2,935	4,092	5,537
Fixture Accel. (g's)	3.20	4.90	4.20	9.00

* The impact velocity was calculated because the velocity channel had failed.

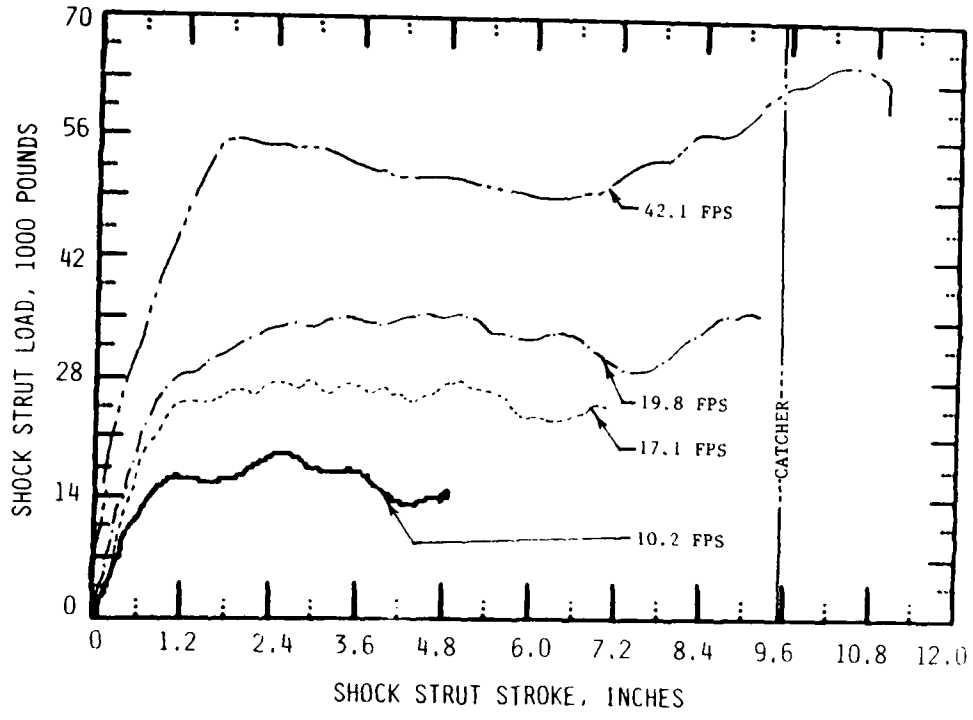

Figure 13. Load-stroke curves of ATLG shock strut in level platform drop tests.

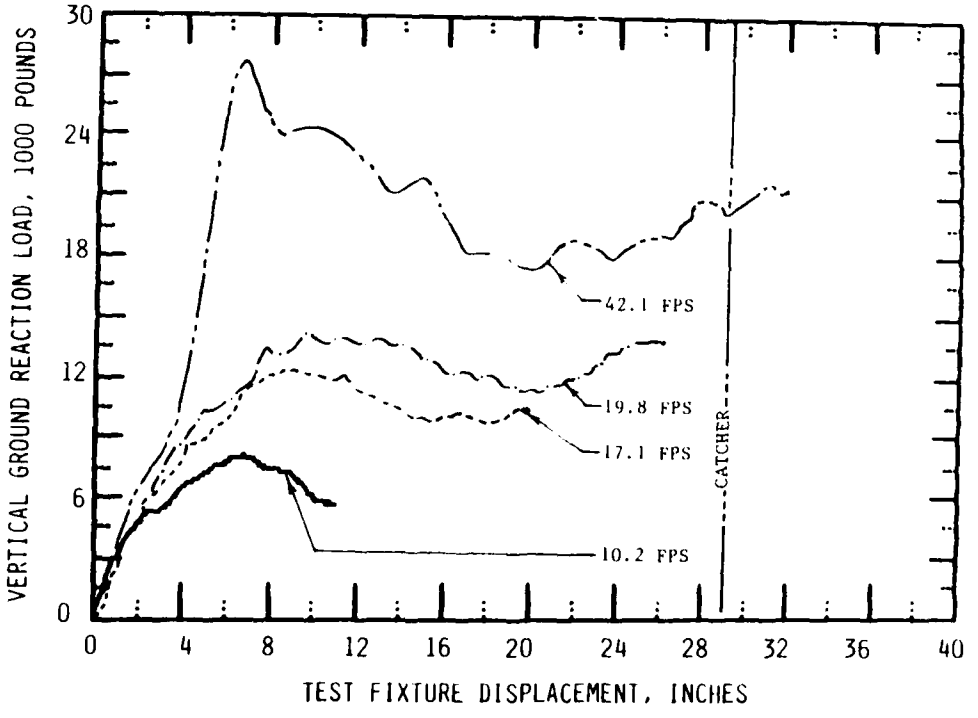

Figure 14. Vertical ground reaction load in terms of test fixture displacement in level platform drop tests.

TABLE 4. ENERGIES ABSORBED BY THE LANDING GEAR IN LEVEL-IMPACT PLATFORM TESTS

Contact Velocity (fps)	System Energy (in-lb)	Calculated Energy (in-lb)	Differences in Energies (%)	Gear Efficiency* (%)
10.2	74,650	73,850	1.1	73.2
17.1	190,430	187,700	1.4	77.7
19.8	315,200	310,030	1.6	83.4
42.1	1,061,790	1,039,270	2.2	**

* Gear Efficiency = $\frac{\text{Area under the curve in Figure 14}}{\text{(Max. load) (Max. displacement)}}$

** The efficiency of the gear in this test was not calculated because part of the energy was absorbed by the catchers.

The R016-0034 pivot crank was visually inspected. The same crank would be used for the roll-impact tests but with new bushings. When the old bushings had been removed, it was found that the wall of the housing through which the pivot crank is mounted on to the fuselage bulkhead was slightly out of round. This housing wall was reworked and new bushings, manufactured to the reworked dimensions, were used in this housing.

4.2.3 Discussion

The level-impact tests demonstrated the initial design parameters to be valid and met the requirements of the landing gear. The only difference from the design parameter was the high vertical ground load at 42 fps impact velocity. The design vertical ground load was 22,400 pounds. The test load was 27,596 pounds. From the data, the following observations can be made:

1. The load-stroke curves of the shock strut, shown in Figure 13, are reasonably flat at all the impact velocities tested.

2. The ratio of the kinetic energies absorbed by the landing gear and the fuselage for a 42 fps level impact was 58 percent to 42 percent, which is very close to the design requirement.

3. The frictional energy (as shown by the differences in the energies in Table 5) increases with impact velocity.

4. The gear efficiency increases with the impact velocity at level-impact conditions.

4.3 INCLINED-IMPACT TESTS

4.3.1 Test Specimens

Two sets of landing gear assemblies were used for the inclined-impact tests. One set was for the four 10° roll tests and a second set for the +15° pitch tests. The number of specimens and their part numbers are given below.

1. Trailing arm, P/N 1252001, one each for roll and pitch tests
2. Shock strut, P/N 1252100, one each for roll and pitch tests
3. Retraction actuator, P/N 1252400, one each for roll and pitch tests
4. Retraction linkage assembly, P/N 1252300, one each for roll and pitch tests
5. Pivot crank, P/N R016-0034, for the roll tests; this is the same crank that was used in the single-gear level-impact tests but with the bushing housing areas reworked and new bushings
6. Pivot crank, P/N R016-0055, for the pitch tests
7. Running gear with simulated brake, one each for roll and pitch tests.

The -0034 crank was replaced by the -0055 crank in the pitch-impact tests. The -0055 crank was a design improvement for a low-cost crank. The tire was pressurized to 113±8 psig under no load. The shock strut gas chambers were precharged with dry nitrogen in the fully extended position: 325+10/-0 psig and 2,310+25/-0 psig for the first and second stage chambers, respectively.

4.3.2 Results for 10° Roll Tests

The first three tests at the lower impact velocities were completed successfully. In the last test at an impact velocity of 42 fps, the R016-0034 pivot crank failed. At impact the tire was ruptured and the wheel rim was damaged. Therefore, the 42 fps test was not completed. The test results are summarized in Table 5. The plots of the shock strut load-stroke curves for the three tests are shown in Figure 15. The curves of the vertical ground reaction load in terms of the test fixture displacements are given in Figure 16.

All the energy in the first three roll-impact tests was absorbed by the landing gear. The results of the energy analysis are given in Table 6.

Inspection of the landing gear components of the 42 fps test revealed damage to the following parts:

1. Failure of the -0034 crank at the attachment area to the fuselage bulkhead.
2. Damage to the wheel rim and the tire.
3. Kneeling stop, P/N 1252122, of the shock strut: slight deformation.
4. Piston assembly, P/N 1252101, of the shock strut: the bearing lug was bent 3 degrees.
5. Outer cylinder, P/N 1252103, of the shock strut: out of round.

TABLE 5. RESULTS OF ROLL-IMPACT PLATFORM DROP TESTS

Data Measured	Test for			
	10 fps	17 fps	20 fps	42 fps
Ambient Temp. (°F)	74	52	65	60
Drop Weight (lb) Req'd/Actual	3300/3275	3300/3275	4124/4125	3300/3275
Rotor-Lift (lb) Req'd/Actual	2200/2186	2200/2000	2749/2614	2200/*
Impact Velocity (fps) Req'd/Actual	10.0/ 9.9	17.0/16.8	20.0/19.8	42.0/41.7
Fixture Displ. (in.)	11.90	19.74	27.85	(16.80)*
Strut Stroke (in.)	4.68	7.60	10.22	(2.18)*
Vert. Grnd. Load (lb)	7,731	12,313	15,043	34,172
Horiz. Grnd. Load (lb)	1,295	882	1,701	4,200
Strut Load (lb)	18,563	29,136	37,726	55,219
Gas Press. #1 (psig)	1,542	2,942	4,458	(568)*
Gas Press. #2 (psig)	2,300	3,340	4,322	*
Oil Press. (psig)	1,462	2,849	4,338	(408)*
Fixture Accel. (g's)	3.90	4.80	5.80	(18.80)*

* These magnitudes were not recorded or were improperly recorded when the -0034 crank failed.

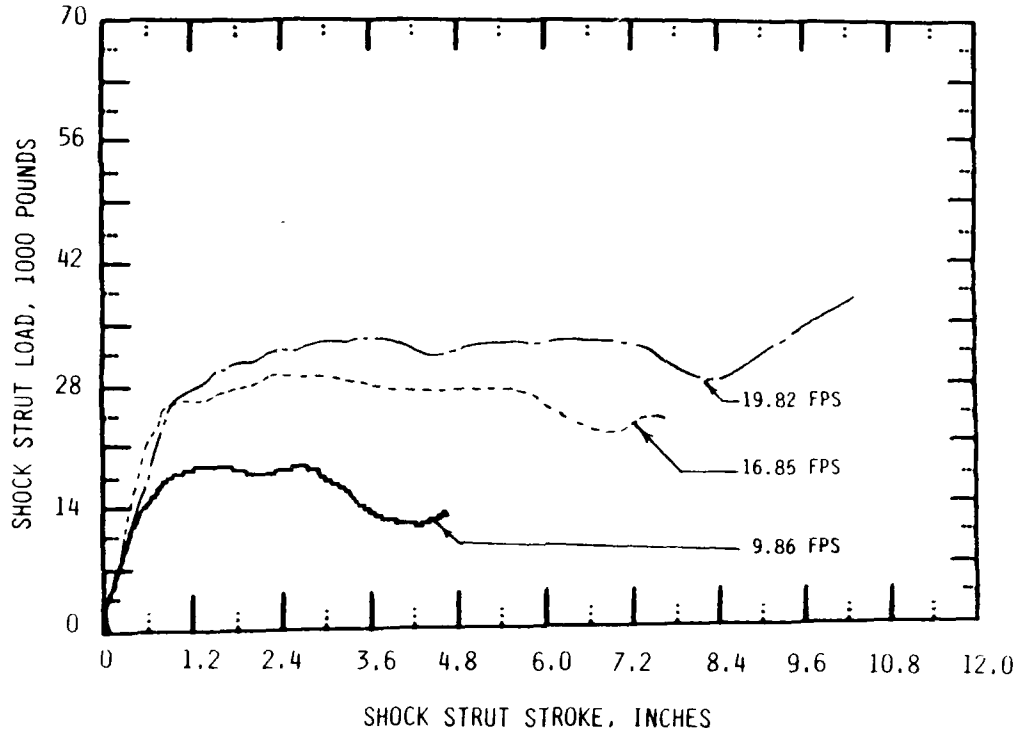

Figure 15. Load-stroke curves of ATLG shock strut in 10° roll platform drop tests.

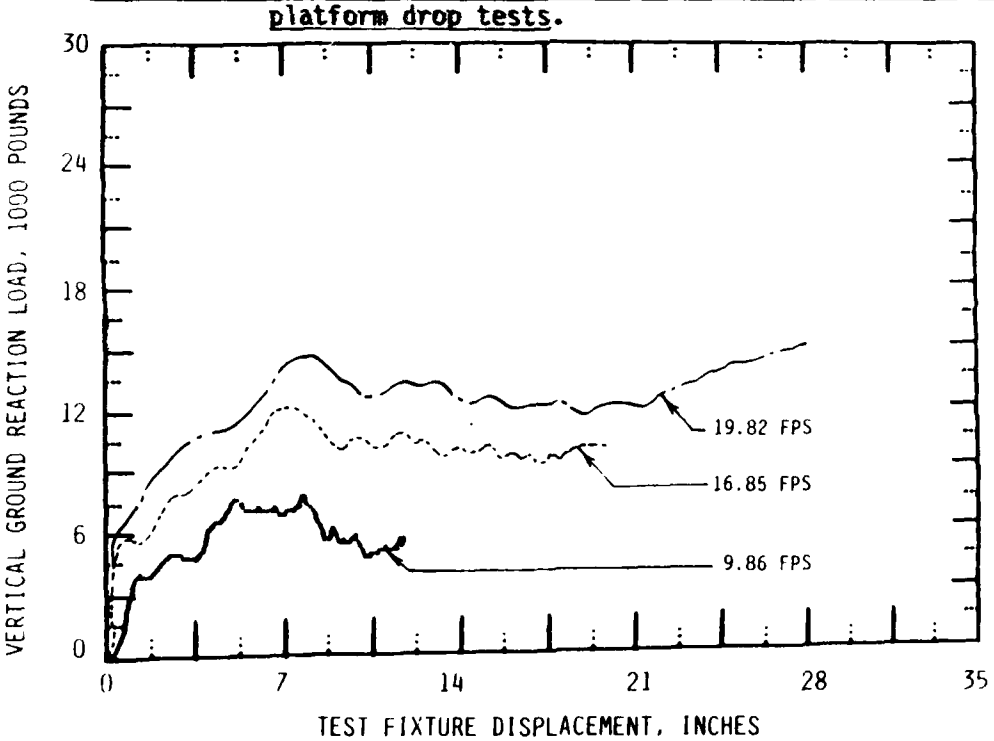

Figure 16. Vertical ground reaction load in terms of test fixture displacement in 10° roll platform drop tests.

TABLE 6. ENERGIES ABSORBED BY THE LANDING GEAR IN ROLL-IMPACT PLATFORM TESTS

Contact Velocity (fps)	System Energy (in-lb)	Calculated Energy (in-lb)	Differences in Energies (%)	Gear Efficiency* (%)
9.86	72,398	70,229	3.0	76.3
16.85	198,755	196,487	1.1	80.8
19.82	344,589	343,136	0.4	81.9
41.67	*	*	*	**

* Gear Efficiency = $\frac{\text{Area under the curve in Figure 16}}{\text{(Max. load) (Max. displacement)}}$

** The data for the 41.67 fps impact test is not included because of the failure of the R016-0034 pivot crank.

4.3.3 Failure Analysis of -0034 Pivot Crank

The R016-0034 pivot crank, during the roll-impact test at 42 fps, failed in several pieces in the area where the crank is attached to the bulkhead, i.e., the area where the crank had been reworked following the level-impact test. The failure is shown in Figure 17. This crank had been used in several preliminary drop tests, all the level-impact tests and all the roll-impact tests. The failure occurred in the fortieth drop test with this pivot crank. The number of drop tests, and the respective drop weights, impact velocities and vertical ground reaction loads to which this crank was subjected are listed in Table 7.

The failure analysis identified it as a ductile overload-type failure with minor yielding. Fractographs revealed eutectic melting and/or high temperature oxidation resulted in weaker grain boundaries where the failure had occurred. An elliptical shaped impression of the bushing near the origin and the material yielding indicated an impact-type loading. Dimensional analysis indicated the wall thickness of the housing near the origin was 0.418 to 0.450 inch. The rest of the wall measured 0.455 to 0.470 inch. The design thickness of the wall is 0.500 inch.

Thus, the failure appeared to be due to improper rework of this area following the level-impact tests. The reduced wall thickness is in the section of the housing subject to tensile loading under impact. Any clearance between the housing and the bushing in this region will introduce an impact load proportional to the clearance and a stress 10 to 16 percent higher than that for which the crank was designed.

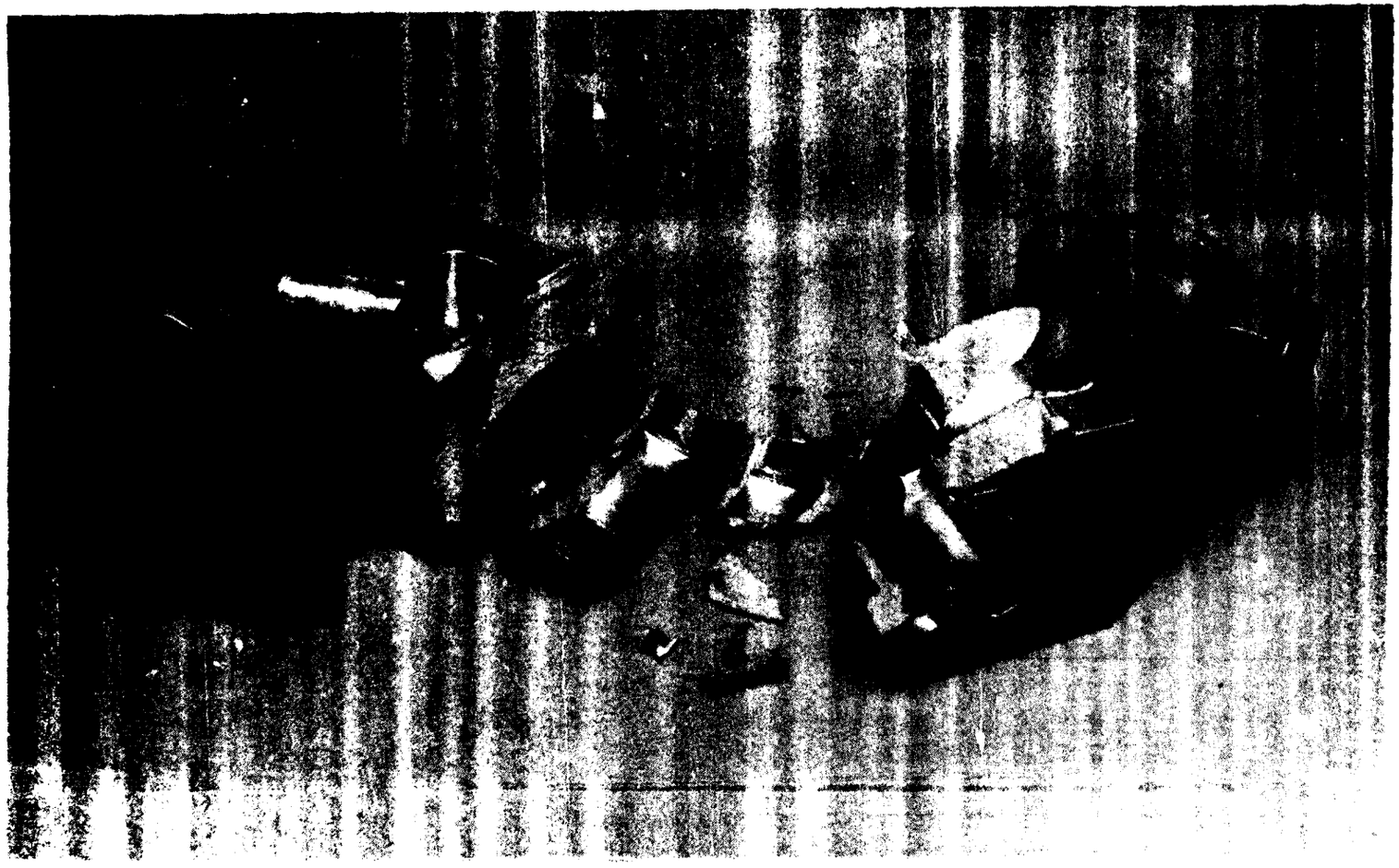

Figure 17. Overall view of the R016-0034 crank failure.

Note: The arrow 'O' points to the origin. The failure started in this region and quickly propagated around and along the wall of the bolt hole. The direction of this fracture was counter-clockwise and upward as viewed from the inboard size of the ship.

TABLE 7. IMPACT DROP TESTS OF R016-0034 PIVOT CRANK

Drop Condition	Drop Weights (lb)	Range of Impact Velocity (fps)	Range of Vertical Ground Load (kips)	No. of Tests
Level	3115	9.9 - 10.2	7.8 - 8.0	3
Level	3115	16.8 - 17.0	12.0 - 12.2	2
Level	3115	19.8	14.2	1
Level	3115	42.1	27.6	1
Level	3275	6.0 - 12.0	5.0 - 10.0	7
Level	3275	13.0 - 17.5	12.0 - 13.0	3
Level	3275	18.0 - 20.0	13.5 - 15.0	2
Level	3665	16.0 - 17.0	12.4 - 12.7	2
Level	3665	18.0 - 20.0	13.5 - 14.6	3
Roll	3275	8.0 - 10.0	6.0 - 8.0	8
Roll	3275	16.0 - 17.0	12.0 - 13.0	5
Roll	3275	41.7	34.2	1*
Roll	4125	20.0 - 22.0	15.0 - 16.0	2

* The -0034 crank failed in this test.

4.3.4 Discussion of Roll-Impact Tests

The results of the roll-impact tests further validate the design parameters even though the pivot crank failed at the highest impact velocity. Further observations on the roll-impact tests are given below.

1. The load-stroke curves of the shock strut continue the flat-top trend from the level-impact tests.

2. The gear efficiencies continue to be in excess of 75 percent and indicate the same trend as for level-impact tests, i.e., the efficiencies increase with increased impact velocity.

3. The failure of the -0034 pivot crank was expected to have no effect on the integrity of the original design because

   a. the critical area was improperly reworked,and

   b. the weaker grain boundaries occurred when such a large billet, 16 inches cube and weighing 500 pounds, was heat treated before being machined down to 33.1 pounds.

   In production, a much lighter forged member would be used to manufacture the crank. It was felt that the design would be qualified if subsequent tests with a second crank were successfully conducted.

4.3.5 Results for +15° Pitch Tests

All the tests were successfully completed. During the test at 42 fps, the tire burst and a section of the wheel rim sheared off. Also in this test, the redundant lugs of the trailing arm struck the ground and sheared off. The test results are summarized in Table 8. The plots of the shock strut load-stroke curves are given in Figure 18. The curves in Figure 18 are a composite of the original test data on the load-time and stroke-time curves for the struts. The discontinuity in the load-stroke curve for 42.93 fps occurs in the load-time curve. To determine the reason for this discontinuity, the original time-dependent curves for the strut load, strut stroke, ground load and fixture displacement were evaluated and the video of the test reviewed. It was determined that the discontinuity immediately follows the shearing off of the redundant lugs. It was concluded that the high g-loads occurring during the failure of the redundant lugs temporarily interrupted the signal from the load cell measuring the strut axial load.

The vertical ground reaction loads in terms of the test fixture displacements are given in Figure 19. All the energies in the first three pitch-impact tests were absorbed by the landing gear (see Table 9). The energy from the 42 fps test was absorbed by the landing gear and the catcher, representing the fuselage in the ratio of 59.8 percent to 27.3 percent. The remaining 12.9 percent was dissipated by friction, rupture of the tire, and shearing of the wheel rim and trailing arm lugs. The results of the energy analysis are summarized in Table 9.

4.3.6 Discussion of Pitch-Impact Tests

The results from the single-gear platform pitch-impact tests, given in Table 8, show that the strut is less efficient in pitch-impact than in the roll-impact tests. Under pitch-impact conditions, the vertical and horizontal ground loads are higher than under roll-impact conditions. However, the strut loads under pitch-impact conditions are 20 percent to 40 percent lower than under roll-impact conditions. As the system energies for the roll- and pitch-impact cases are almost identical, the lower shock strut load was compensated for by the higher strut stroke. The overall efficiencies of the shock struts are about 20 percent lower than for roll-impact for the intermediate impact velocities. These trends are less obvious for the 42 fps impact condition than for the other three. The results for the 42 fps condition are lower because the rotor lift force was 95.2 percent greater than that desired, or 130 percent of the "helicopter" weight.

In the platform tests, the largest amount of energy dissipated by friction was only 3.0 percent in the 10 fps pitch-impact test. The failures of the wheel rim and the redundant lug of the trailing arm absorbed considerable energy. If friction accounts, conservatively, for 3.0 percent of the energy, almost 10 percent is accounted for by these failures and the bursting of the tire. The failure of the wheel rim and the redundant lugs of the trailing arm can be seen in Figure 20. The R016-0055 pivot crank did not fail in the pitch-impact tests.

TABLE 8. RESULTS OF PITCH-IMPACT PLATFORM DROP TESTS

Data Measured	Test for			
	10 fps	17 fps	20 fps	42 fps
Ambient Temp. (°F)	87	79	77	70
Drop Weight (lb) Req'd/Actual	3270/3280	3270/3280	4088/4080	3270/3280
Rotor-Lift (lb) Req'd/Actual	2180/2335	2180/2127	2725/2687	2180/4255
Impact Velocity (fps) Req'd/Actual	10.0/ 9.90	17.0/16.95	20.0/19.82	42.0/42.93
Fixture Displ. (in.)	8.00	14.30	20.70	25.40
Strut Stroke (in.)	4.00	6.14	8.63	10.76
Vert. Grnd. Load (lb)	10,378	22,679	26,042	38,977
Horiz. Grnd. Load (lb)	2,192	4,676	6,811	11,359
Strut Load (lb)	11,071	21,077	30,375	42,953
Gas Press. #1 (psig)	1,160	2,564	3,548	4,662
Gas Press. #2 (psig)	2,300	2,766	3,470	6,203
Oil Press. (psig)	1,023	2,361	3,473	4,572
Fixture Accel. (g's)	6.10	10.00	7.40	25.40

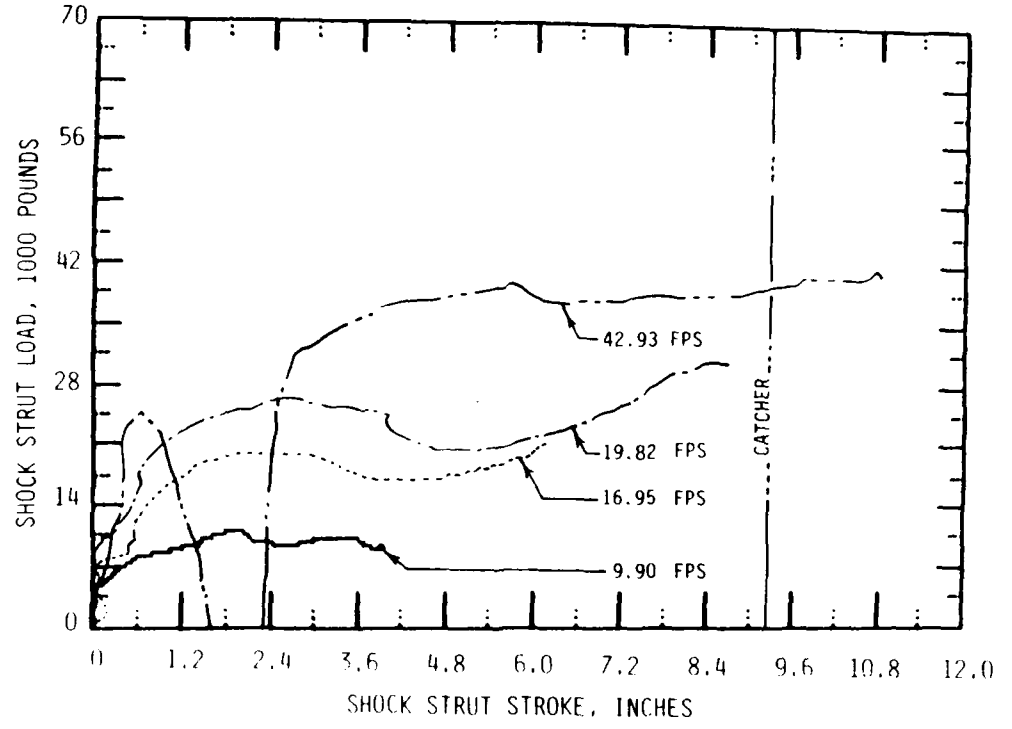

Figure 18. Load-stroke curve of ATLG shock strut in +15° pitch platform drop tests.

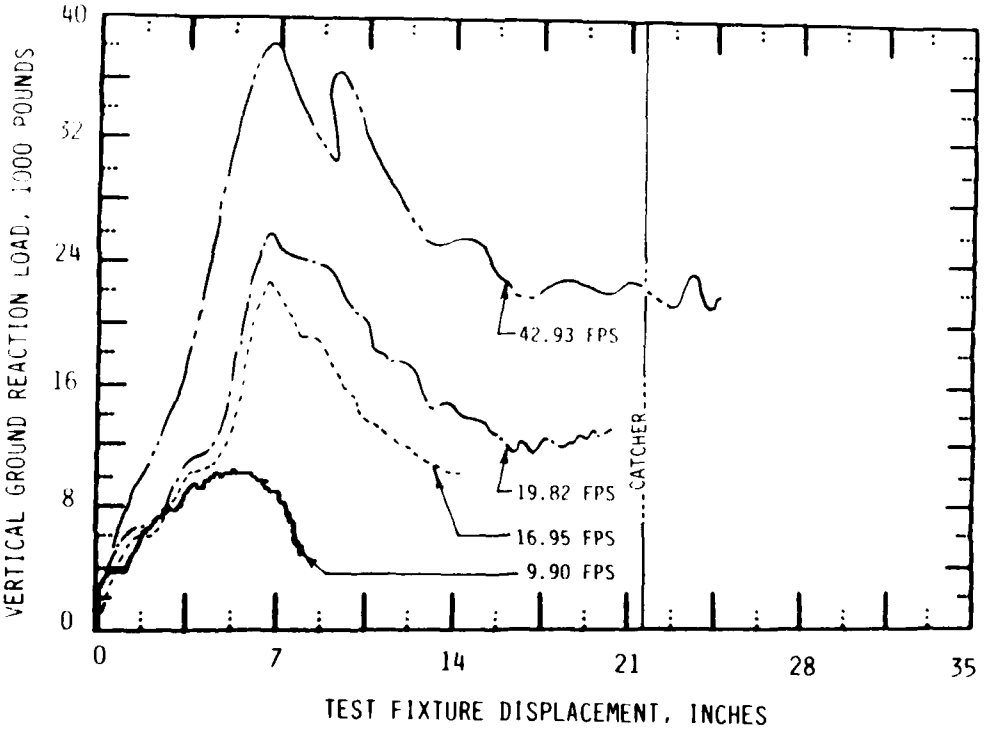

Figure 19. Vertical ground reaction load in terms of test fixture displacement in +15° pitch platform drop tests.

TABLE 9. ENERGIES ABSORBED BY THE LANDING GEAR IN PITCH-IMPACT PLATFORM TESTS

Contact Velocity (fps)	System Energy (in-lb)	Calculated Energy (in-lb)	Differences in Energies (%)	Gear Efficiency* (%)
9.90	67,774	66,614	1.7	80.2
16.95	192,409	190,470	1.0	58.7
19.82	325,787	321,470	1.3	59.6
42.93	1,105,140	962,528	12.9	**

* Gear Efficiency = $\frac{\text{Area under the curve in Figure 19}}{\text{(Max. load) (Max. displacement)}}$

** The data for the 42.93 fps impact test is not included because of the failure of the R016-0034 pivot crank.

Figure 20. Failure of wheel rim and redundant lugs of the trailing arm in the 42 fps pitch-impact test.

5.0 IRON-BIRD DROP TESTS

5.1 GENERAL

Six tests were conducted in the drop test tower using the iron-bird fixture. The tests at 10, 17, 30 and 42 fps were conducted at the BSDGW of 8,500 pounds. The test at 20 fps was conducted at the ADGW of 10,625 pounds. The test at 20 fps was conducted twice. The tests were conducted in two groups. The tests in the first group were at 10, 17, 20 and 30 fps. In the second group, tests were conducted only at 20 and 42 fps.

The drop test tower and the iron-bird fixture are described in Section 3.0. The attitude of the iron-bird fixture for all tests was combined 10° roll and +15° pitch. This attitude when viewed in the drop test tower is shown in Figure 21. Two sets of landing gear systems were used for each of the tests. Typical views of the iron-bird fixture in the drop test tower just before the start of the test at impact velocities of 20, 30 and 42 fps are shown in Figure 22.

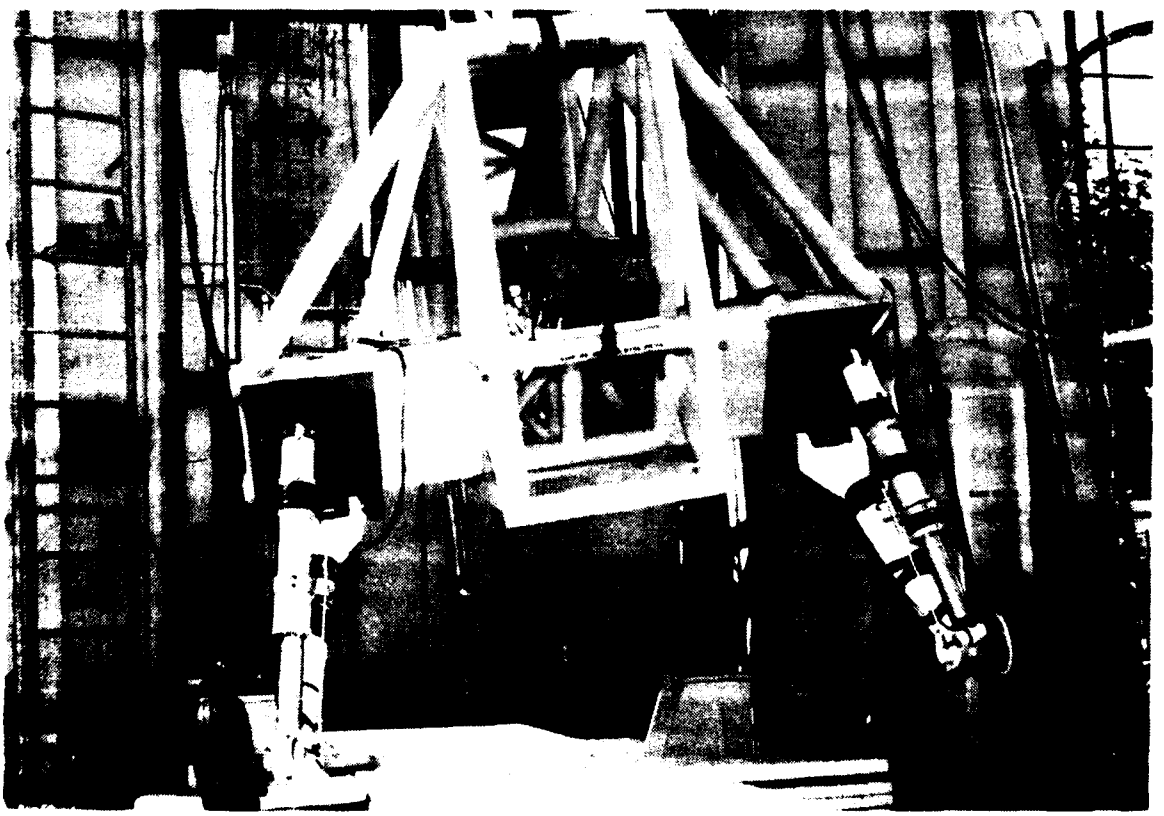

Figure 21. Typical combined 10° roll and +15° pitch attitude of iron-bird fixture in the drop-test tower.

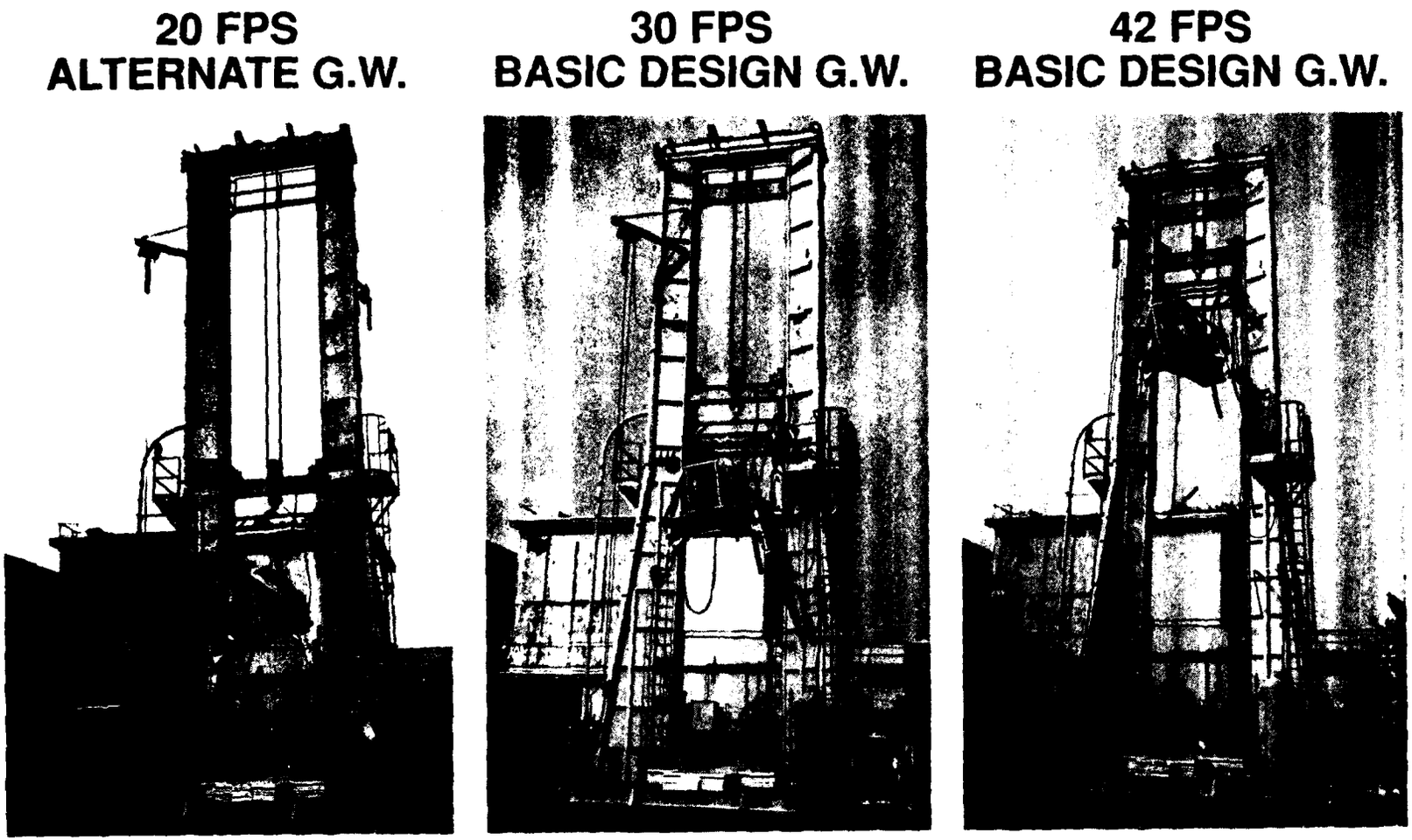

Figure 22. Iron-bird fixture in the drop test tower before the start of test at three impact velocities.

5.2 TEST SPECIMENS

Four landing gear systems were used for the five iron-bird drop tests. The components used were the shock strut, P/N 1252100, the trailing arm, P/N 1252001, and the axle, P/N 1252002. Though four trailing arms and four axles were used for the tests, only three shock struts were used. One shock strut was used on the down-side gear for all the tests. The specific components used are identified by use in the down-side (D) or up-side (U) gear in Table 10.

TABLE 10. TEST SPECIMENS FOR THE IRON-BIRD DROP TESTS

Component	P/N	Tests where components were used					
		Group #1 Impact, fps				Group #2 Impact, fps	
		10	17	20	30	20	42
Shock Strut #1	1252100	U	U	U	U	No	No
Shock Strut #2	1252100	D	D	D	D	D	D
Shock Strut #3	1252100	No	No	No	No	U	U
Trailing Arm & Axle #1	1252001	D	D	D	D	No	No
Trailing Arm & Axle #2	1252001	U	U	U	U	No	No
Trailing Arm & Axle #3	1252001	No	No	No	No	D	D
Trailing Arm & Axle #4	1252001	No	No	No	No	U	U

Note: The down-side gear is designated by 'D' and the up-side gear by 'U.'

As explained in Section 3.4, the R016-0055 pivot crank was not used in any of the tests. Instead, provisions were made in the iron-bird fixture for appropriate clevises to mount the trailing arm and the shock strut correctly. This method of attachment is clearly seen in Figure 21. Since the iron-bird tests were designed to evaluate the crashworthiness behavior of the landing gear, the retraction actuator and linkage system, P/N 1252400 and 1252300, respectively, were not used in these tests.

The tires were pressurized to 113±8 psig under no load. The shock strut gas chambers were precharged with dry nitrogen in the fully extended position. The first stage was precharged to 325+10/-0 psig and the second stage to 2,292+25/-0 psig.

5.3 TEST RESULTS

5.3.1 Tests #1 and #2, 10 and 17 FPS

The results of the tests are presented in Tables 11 and 12. There were no failures during the tests. During teardown examination of the components, all dimensions were checked. There were no deformations or unusual wear.

5.3.2 Test #3, 20 FPS

During this test, the tire on the up-side gear burst on contact with the ground. The redundant lugs of the up-side trailing arm struck the ground, resulting in a bright spark which burnt the striking portion of the lugs. Following this test, the redundant lugs from all the trailing arms were removed and the section blended to the adjacent contours. The test results are presented in Table 13. Damage or unusual wear to the other components was not recorded during teardown inspection. The post-test behavior of the iron-bird fixture is shown in Figure 23. The ground loads are significantly higher than for the test at 17 fps. This is a result of the combination of higher drop weight and velocity.

TABLE 11. IRON-BIRD DROP TEST #1 RESULTS AT 10 FPS

Ambient Temp. (°F)	72
Drop Height (in.)	16.3
Drop Weight (lb), Req'd/Actual	8500/8500
Impact Velocity (fps), Req'd/Actual	10.0/10.1
Fixture Acceleration (g)	+1.1/-2.7
Fixture Displacement (in.)	29.2
Rotor-Lift Force (lb), Req'd/Actual	5667/5900

	Landing Gear		
	Down-Side	Up-Side	Nose
Vert. Grnd. Load (lb)	10,965	13,000	*
Lateral Grnd. Load (lb)	4,230/-3,700	1,100/-500	*
Shock Strut Load (lb)	11,230	17,670	11,700
Shock Strut Stroke (in.)	4.42	3.32	13.15
Gear Acceleration (g)	10.9/-11.1	9.6/-8.7	2.6/-9.8

TABLE 12. IRON-BIRD DROP TEST #2 RESULTS AT 17 FPS

Ambient Temp. (°F)	82
Drop Height (in.)	47.0
Drop Weight (lb), Req'd/Actual	8500/8500
Impact Velocity (fps), Req'd/Actual	17.0/16.6
Fixture Acceleration (g)	+2.22/-3.67
Fixture Displacement (in.)	30.6
Rotor-Lift Force (lb), Req'd/Actual	5667/7650

	Landing Gear		
	Down-Side	Up-Side	Nose
Vert. Grnd. Load (lb)	27,570	30,650	*
Lateral Grnd. Load (lb)	2,470/-2,540	-2,090/2,170	*
Shock Strut Load (lb)	20,550	24,880	15,790
Shock Strut Stroke (in.)	5.40	3.70	14.35
Gear Acceleration (g)	11.0/-10.8	9.75/-10.00	4.32/-4.96

TABLE 13. IRON-BIRD DROP TEST #3 RESULTS AT 20 FPS

Ambient Temp. (°F)	79
Drop Height (in.)	70.0
Drop Weight (lb), Req'd/Actual	10,625/10,625
Impact Velocity (fps), Req'd/Actual	20.0/19.8
Fixture Acceleration (g)	0.7/-3.7
Fixture Displacement (in.)	36.0
Rotor-Lift Force (lb), Req'd/Actual	7083/10,900

	Landing Gear		
	Down-Side	Up-Side	Nose
Vert. Grnd. Load (lb)	40,040	39,020	*
Lateral Grnd. Load (lb)	8,150/-370	1,960/-660	*
Shock Strut Load (lb)	28,180	31,260	19,495
Shock Strut Stroke (in.)	7.72	5.32	13.75
Gear Acceleration (g)	8.8/-11.3	17.5/-18.3	3.1/-18.0

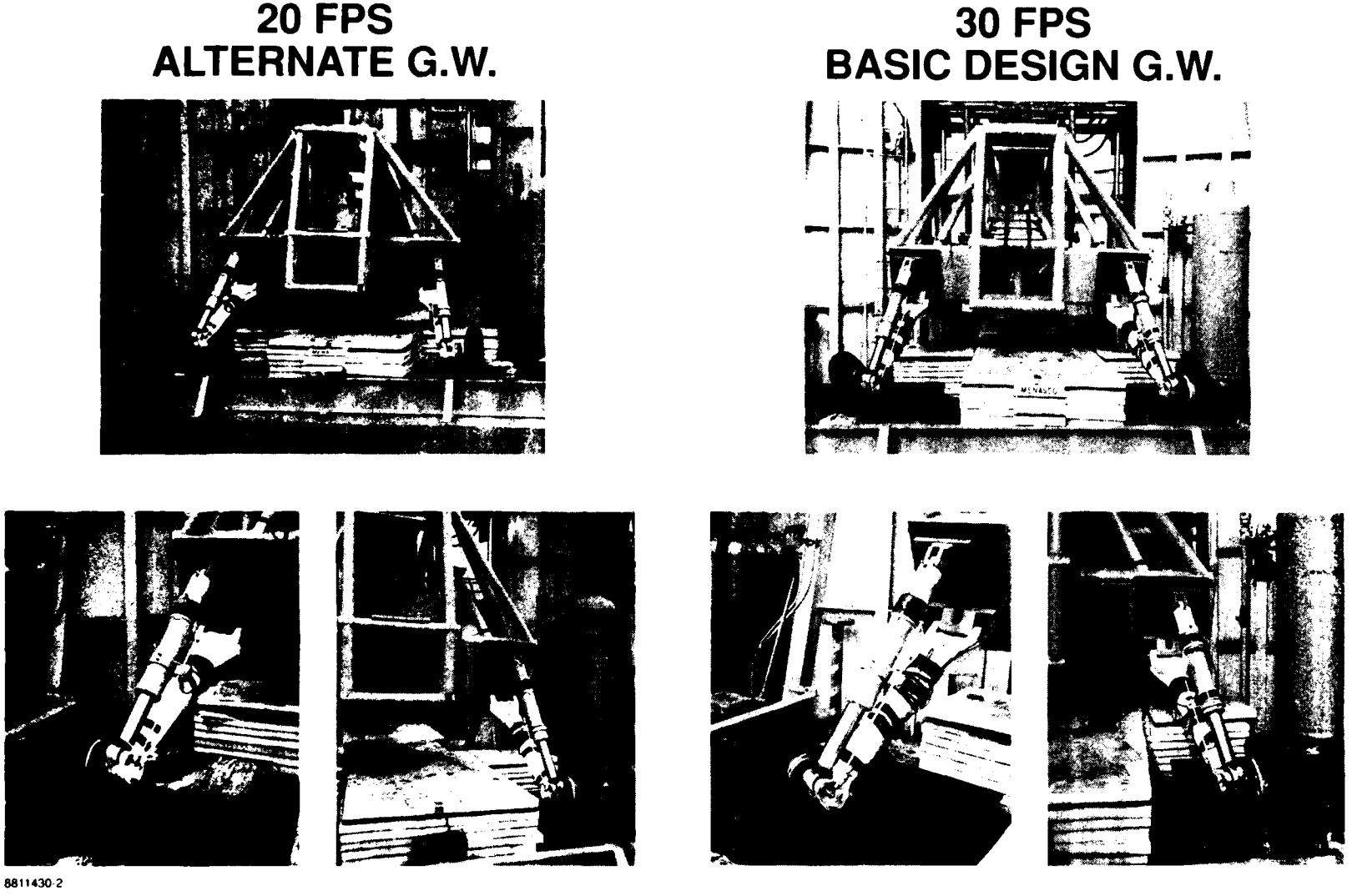

Figure 23. Views of the iron-bird fixture after tests at 20 and 30 fps.

5.3.3 Test #4, 30 FPS

During this test, with the redundant lugs removed the trailing arm did strike the ground. The area of the removed redundant lugs was further machined to reduce as much as possible of the thickness of the boss where it is most likely to strike the ground. The results for this test are given in Table 14. The post-test behavior of the iron-bird fixture is shown in Figure 23. The detail results of the test and inspection of the components follow.

1. Up-Side Gear

   a. The tire burst on contact.

   b. The redundant lugs of the trailing arm contacted the ground, leaving a gash in the steel plate.

   c. The pin in the fused orifice sheared.

   d. The trailing arm was bent, with a large bulge in the upper transition section as seen in Figure 24.

2. Down-Side Gear

   a. The tire burst on contact.

   b. The inboard flange of the wheel sheared off.

   c. The trailing arm and the shock strut were undamaged.

   d. The pin in the fused orifice did not shear.

TABLE 14. IRON-BIRD DROP TEST #4 RESULTS AT 30 FPS

Ambient Temp. (°F)	74
Drop Height (in.)	164.0
Drop Weight (lb), Req'd/Actual	8500/8500
Impact Velocity (fps), Req'd/Actual	30 0/30.4
Fixture Acceleration (g)	1.5/-5.6
Fixture Displacement (in.)	39.3
Rotor-Lift Force (lb), Req'd/Actual	5667/16,500

	Landing Gear		
	Down-Side	Up-Side	Nose
Vert. Grnd. Load (lb)	49,545	56,460	*
Lateral Grnd. Load (lb)	2,258/-2,100	1,730/-540	*
Shock Strut Load (lb)	38,710	44,000	23,510
Shock Strut Stroke (in.)	6.39	7.58	19.75
Gear Acceleration (g)	5.7/-7.3	17.9	4.3

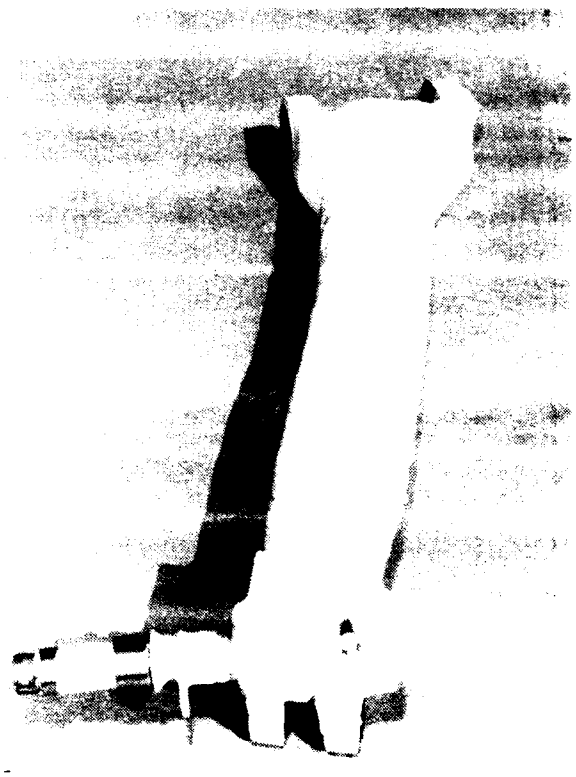

Figure 24. Bent trailing arm after the 30 fps test.

5.3.4 Test #5, 20 FPS

During this test, the tire on the up-side gear burst. The sidewall of the tire on the down-side gear sustained a cut but did not burst. There was no damage to the trailing arms or the shock struts. The results are presented in Table 15.

5.3.5 Test #6, 42 FPS

The test results are given in Table 16. The detail results of the test and the inspection are given below.

1. Up-Side Gear

   a. The tire burst on impact, and the wheel bent where it impacted the ground.

   b. The shock strut and the trailing arm failed at their attachment to the iron-bird fixture and flew approximately 20 feet from the drop test tower. The failed subassembly is shown in Figure 25.

   c. Due to sudden extension of the shock strut during separation from the iron-bird fixture, the fused orifice dislodged in the strut and the shear pin was not activated.

TABLE 15. IRON-BIRD DROP TEST #5 RESULTS AT 20 FPS

Ambient Temp. (°F)	66
Drop Height (in.)	71.0
Drop Weight (lb), Req'd/Actual	10,625/10,625
Impact Velocity (fps), Req'd/Actual	20.0/20.1
Fixture Acceleration (g)	1.3/-3.3
Fixture Displacement (in.)	34.2
Rotor-Lift Force (lb), Req'd/Actual	7083/8780

	Landing Gear		
	Down-Side	Up-Side	Nose
Vert. Grnd. Load (lb)	48,340	34,880	*
Lateral Grnd. Load (lb)	6,687/-980	2,370/-730	*
Shock Strut Load (lb)	31,740	31,830	21,166
Shock Strut Stroke (in.)	7.76	5.29	16.25
Gear Acceleration (g)	15.4/-20.1	15.8/-6.8	5.1/-15.8

TABLE 16. IRON-BIRD DROP TEST #6 RESULTS AT 42 FPS

Ambient Temp. (°F)	80
Drop Height (in.)	325.0
Drop Weight (lb), Req'd/Actual	8500/8500
Impact Velocity (fps), Req'd/Actual	42.0/42.2
Fixture Acceleration (g)	1.1/9.0
Fixture Displacement (in.)	51.95
Rotor-Lift Force (lb), Req'd/Actual	5667/19,540

	Landing Gear		
	Down-Side	Up-Side	Nose
Vert. Grnd. Load (lb)	63,990	67,480	*
Lateral Grnd. Load (lb)	3,212/-300	1,980/-850	*
Shock Strut Load (lb)	97,090	49,100	20,040
Shock Strut Stroke (in.)	8.73	2.28	18.00
Gear Acceleration (g)	11.2/-35.6	10.7/-24.4	6.5/-12.9

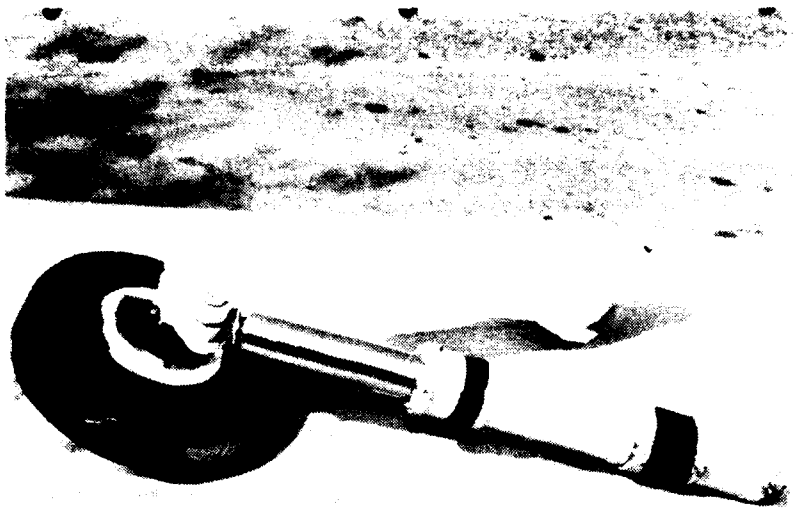

Figure 25. Failed subassembly of the trailing arm and shock strut in the 42 fps test.

d. Post-test examination of the failed up-side shock strut showed the piston had scraped the inside of the strut cylinder. Even though the strut did not exhibit permanent deformation, the bending load was high enough to bend the strut and prevent smooth action of the piston.

2. Down-Side Gear

a. The tire burst on impact, and the wheel fractured.

b. The shear pin in the fused orifice sheared.

c. Visual inspection of the trailing arm and shock strut did not identify any damage.

3. Iron-bird Fixture

The middle brace tube, inboard of the main frame, suffered a dent and a crack in the weld. On reviewing the high-speed films, the cause of the damage was identified as the left-hand rotor-lift support striking the iron-bird fixture.

5.4 DISCUSSION

The iron-bird tests were successfully completed. The results are discussed below. There were several differences between the design and test of the iron-bird fixture and that of the helicopter it represented. The first was encountered in matching the moments of inertia of the iron-bird to that of the

helicopter after matching the gross weight, center of gravity and critical dimensions. The difficulty encountered in the test was in controlling the rotor-lift force at high impact velocity. It was increasingly difficult as the impact velocity increased. The worst condition was in the test at 42 fps when the actual rotor-lift force was 345 percent of that desired.

In evaluating the behavior of the test fixture from the test results, it was evident that the total momentum of the up-side gear will always be higher than that of the down-side gear. This momentum damaged components of the up-side gear more than those of the down-side gear. Furthermore, the tire on the up-side gear always burst at a lower impact velocity than the tire on the down-side gear. A failure of the down-side tire was a signal that the up-side tire would fail immediately on impact. The vertical ground loads in Tables 11 through 16 bear further evidence of this behavior.

The results are graphically summarized and discussed below in terms of the major parameters.

5.4.1 Differences in the Responses of Up- and Down-Side Gears

In studying Tables 10 through 15, the vertical ground load and the shock strut load are greater in the up-side gear than the down-side gear, whereas the stroke is lower in the up-side shock strut. The only exceptions are the loads at 20 fps and the stroke at 30 fps. The high loads in the up-side gear indicate that the impact velocity of the up-side gear is greater than the impact velocity of the down-side gear. Since the down-side gear has already absorbed some of the energy, the stroke of the up-side gear is less because of the lower residual energy and the higher load.

5.4.2 Vertical Ground Loads

The vertical ground loads increased with increasing impact velocity, as seen in Figure 26 for the response of the down-side gear. A distinct spike in the load was evident in all cases. Interestingly, the spike in the load occurred increasingly later after impact with decreasing impact velocity. The same was true for the vertical ground loads of the up-side gear as seen in Figure 27. The loads were higher for the up-side gear as can be seen in comparing Figures 26 and 27.

5.4.3 Lateral Ground Loads

The lateral ground loads of the down-side gears exhibit quite different trends from the vertical ground loads. The lateral ground loads of the down-side gear did not reach a maximum at the first impact but on subsequent rebounds. This is clearly seen in Figure 28. The opportunities for rebound for the up-side gear are fewer, and the maximum generally occurs at the first opportunity (Figure 29).

5.4.4 Shock Strut Loads

The shock strut load for the down-side gear increased with increasing impact velocity. However, the down-side strut load for the 42 fps impact was excessively high at 97,090 pounds. This high load may have occurred when the fused orifice did not operate as designed. It was determined on teardown inspection

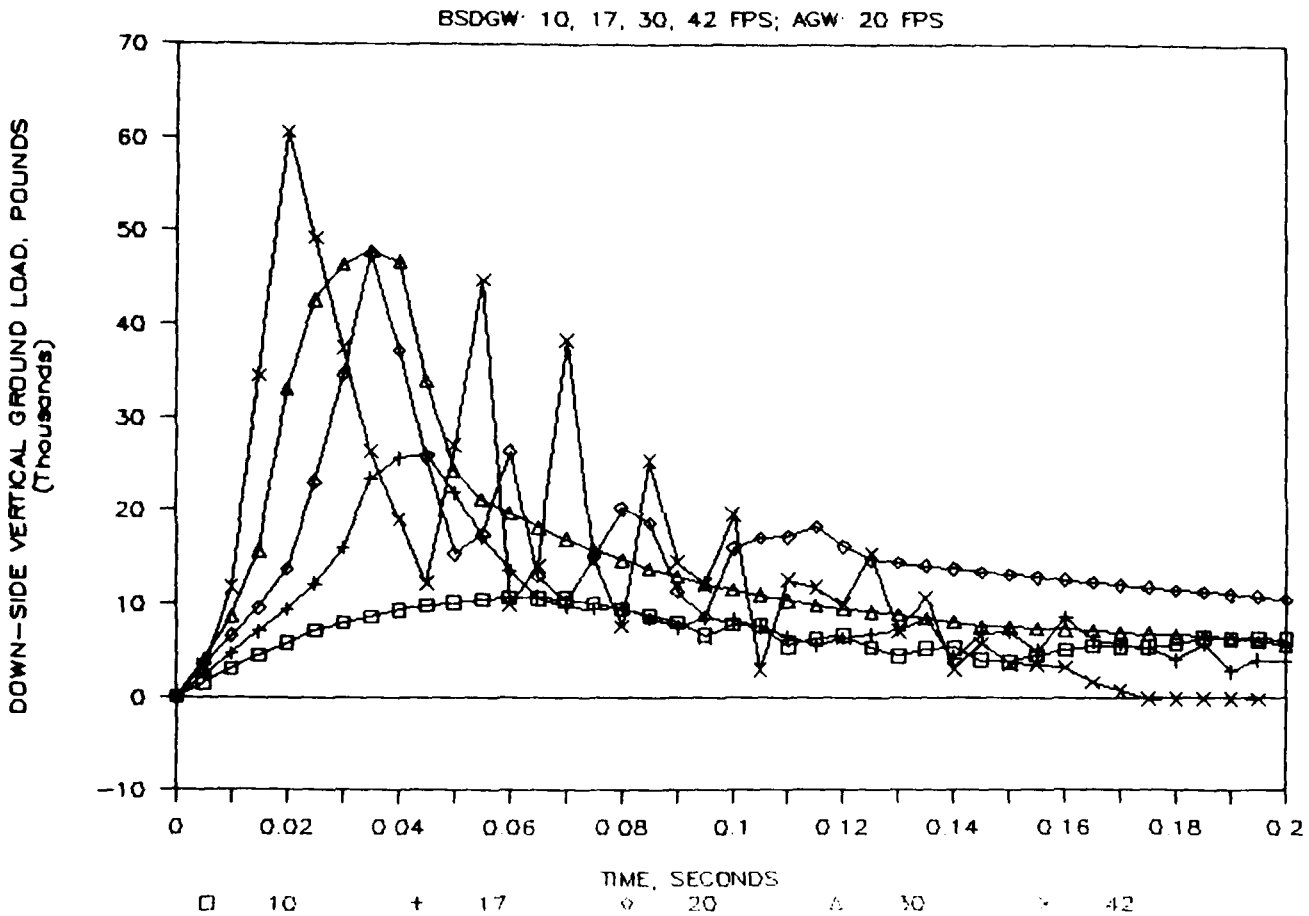

Figure 26. Vertical ground loads in the down-side gear in the iron-bird tests.

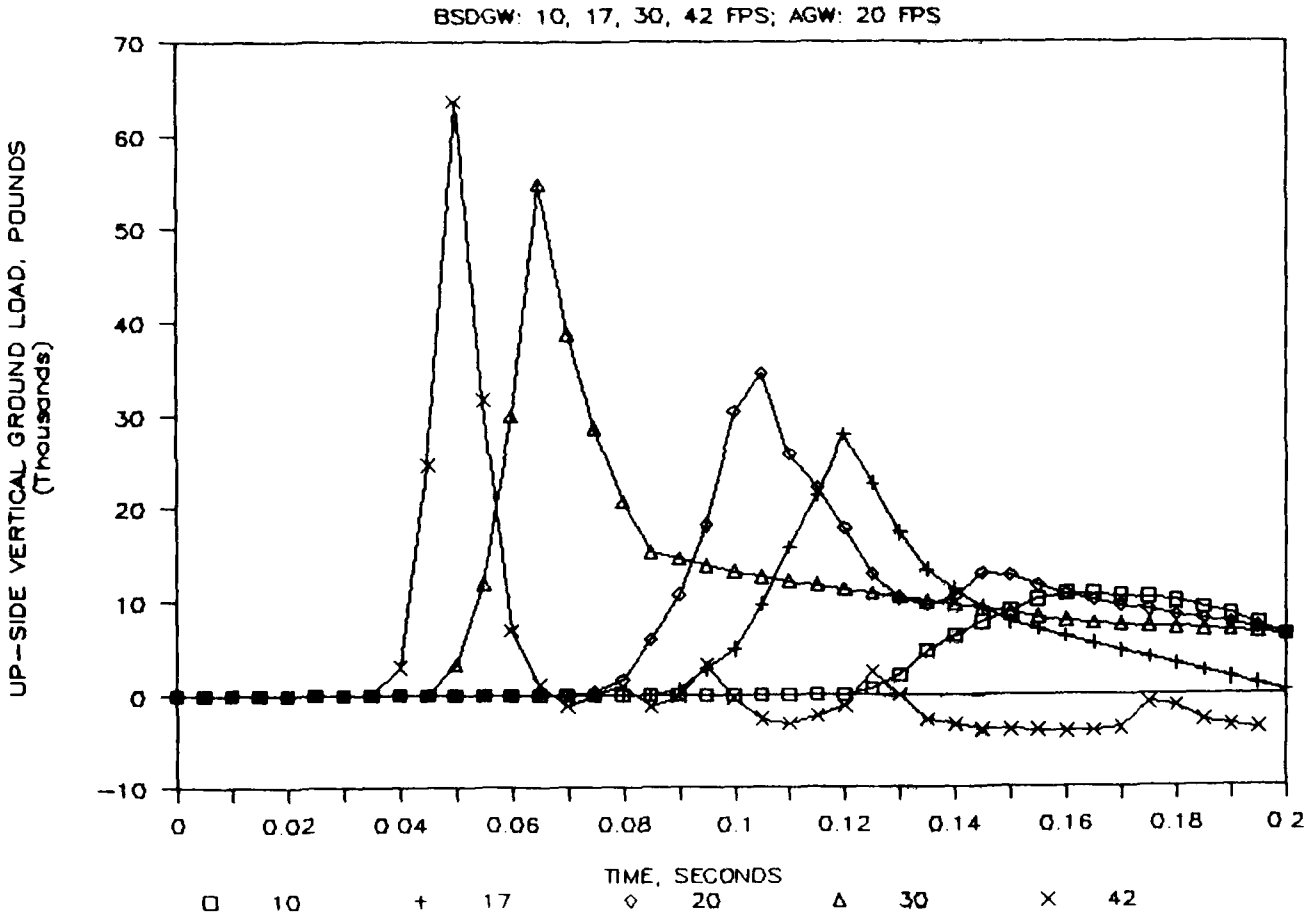

Figure 27. Vertical ground loads in the up-side gear in the iron-bird tests.

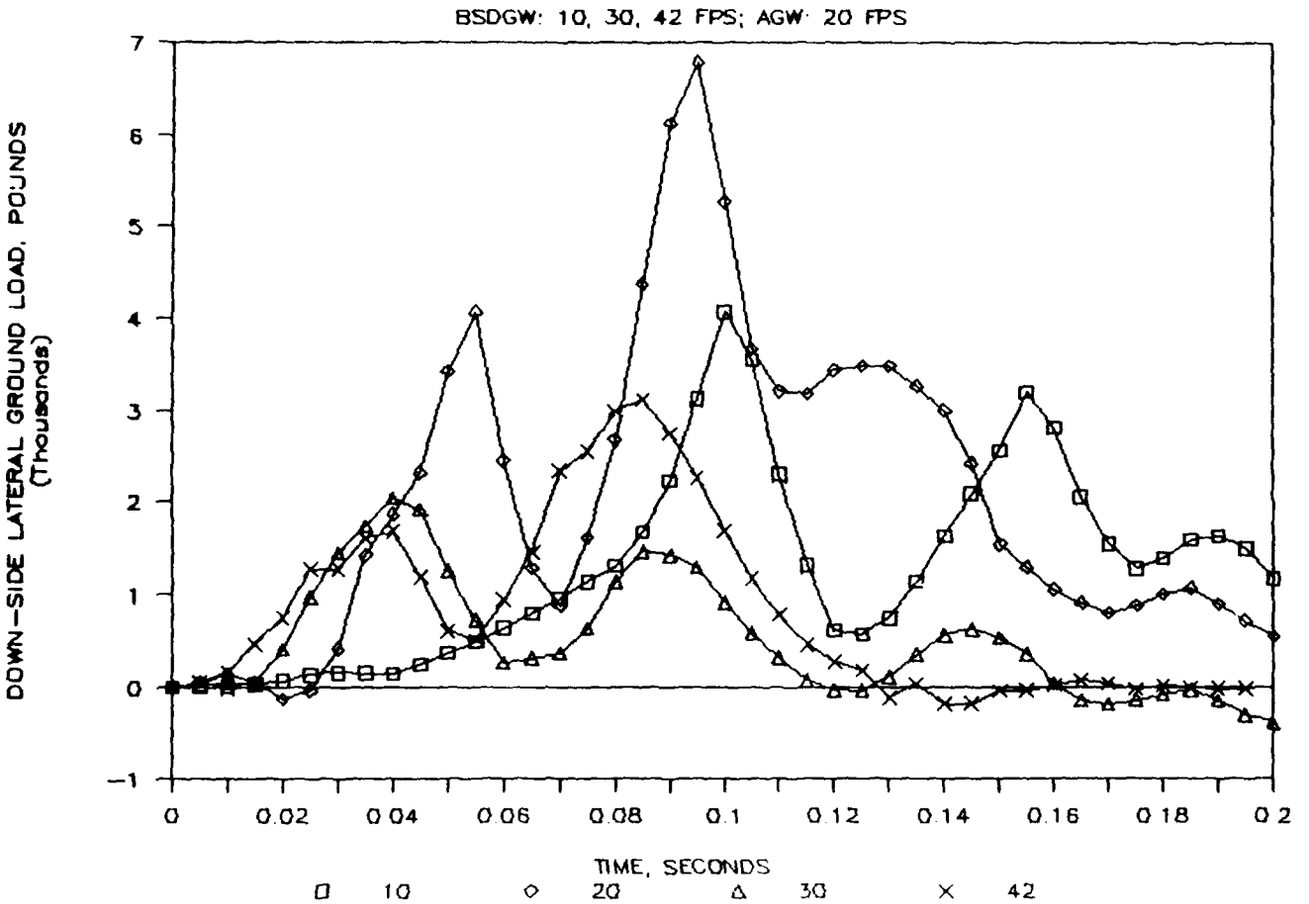

Figure 28. Lateral ground loads in the down-side gear in the iron-bird tests.

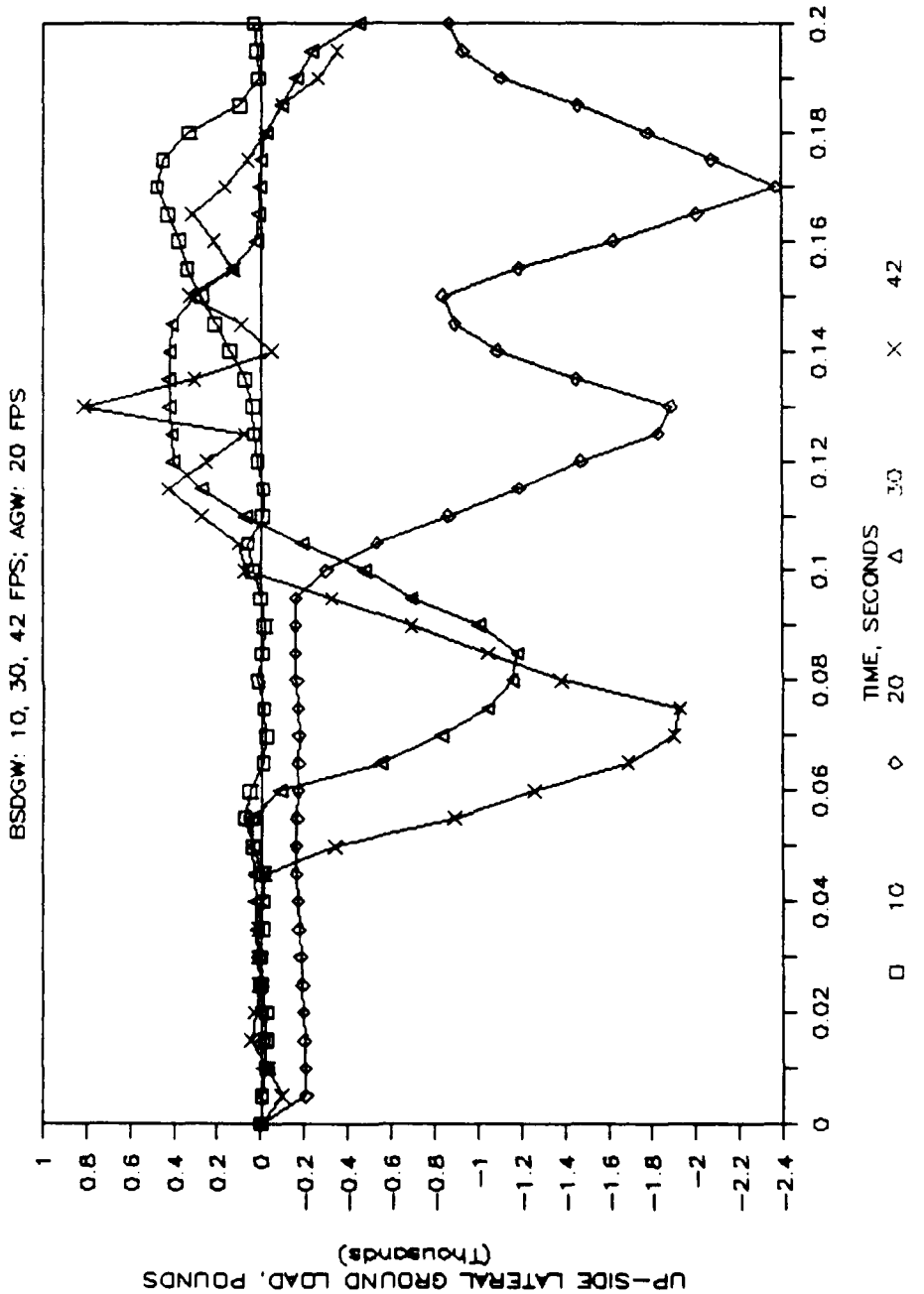

Figure 29. Lateral ground loads in the up-side gear in the iron-bird tests.

that the fused orifice was dislodged without shearing the pin. This indicates that

1. this orifice either malfunctioned because the orifice did operate correctly in the single-gear platform tests, or

2. the behavior of an iron-bird fixture (and, therefore, of a helicopter) under combined roll and pitch impact cannot be predicted by inclined impacts of single-gear platform tests.

The response of the down-side shock strut is shown in Figure 30 and that of the up-side strut in Figure 31, where the plot for the 42 fps test is incomplete because of the failure of the entire up-side landing gear. It is apparent from Figure 30 that the maximum at each of the impact velocities occurs later with respect to initial impact as the impact velocity decreases. The time for the up-side gear to impact the ground, and for the shock strut load to reach a maximum, is increasingly longer with decreasing impact velocity.

5.4.5 Shock Strut Deflection

The axial deflections of the shock strut increase gradually with time and do not exhibit any spikes at their maxima. The gradual increase in the deflection indicates that the deflection lags load, which indicates that the load-stroke curve will approach a flat top. This is apparent in the deflection curves of the down-side and up-side gears shown in Figures 32 and 33, respectively.

5.5 COMPARISON OF SINGLE-GEAR AND IRON-BIRD TESTS

These results show that single-gear drop tests do not accurately reproduce the results from iron-bird drop tests. This is particularly evident in comparing the inclined-impact platform test results with the iron-bird test results. These are discussed below:

1. The equivalent weight for single-gear drop tests can only be accurately calculated for level landing conditions. For roll and pitch impact conditions, the calculated equivalent weight will continue to act throughout the test and will not be unloaded as its pair, in an actual helicopter or in an iron-bird fixture, impacts the ground.

2. In the single-gear tests, the tire burst only in the test at 42 fps and +15° pitch impact condition. In the iron-bird tests, the tire of the up-side gear burst at all impact velocities from and above 20 fps, and the down-side gear tire only from and above 30 fps. This result demonstrates that the single-gear tests do not simulate the severity of the loads that the landing gear is subjected to in the iron-bird tests or in a helicopter under crash.

3. The roll and pitch conditions at impact were not duplicated by the single-gear tests. The redundant lugs of the trailing arm repeatedly struck the ground in the iron-bird tests from and above 20 fps, but only struck the ground in single-gear drop tests at 42 fps and +15° pitch condition.

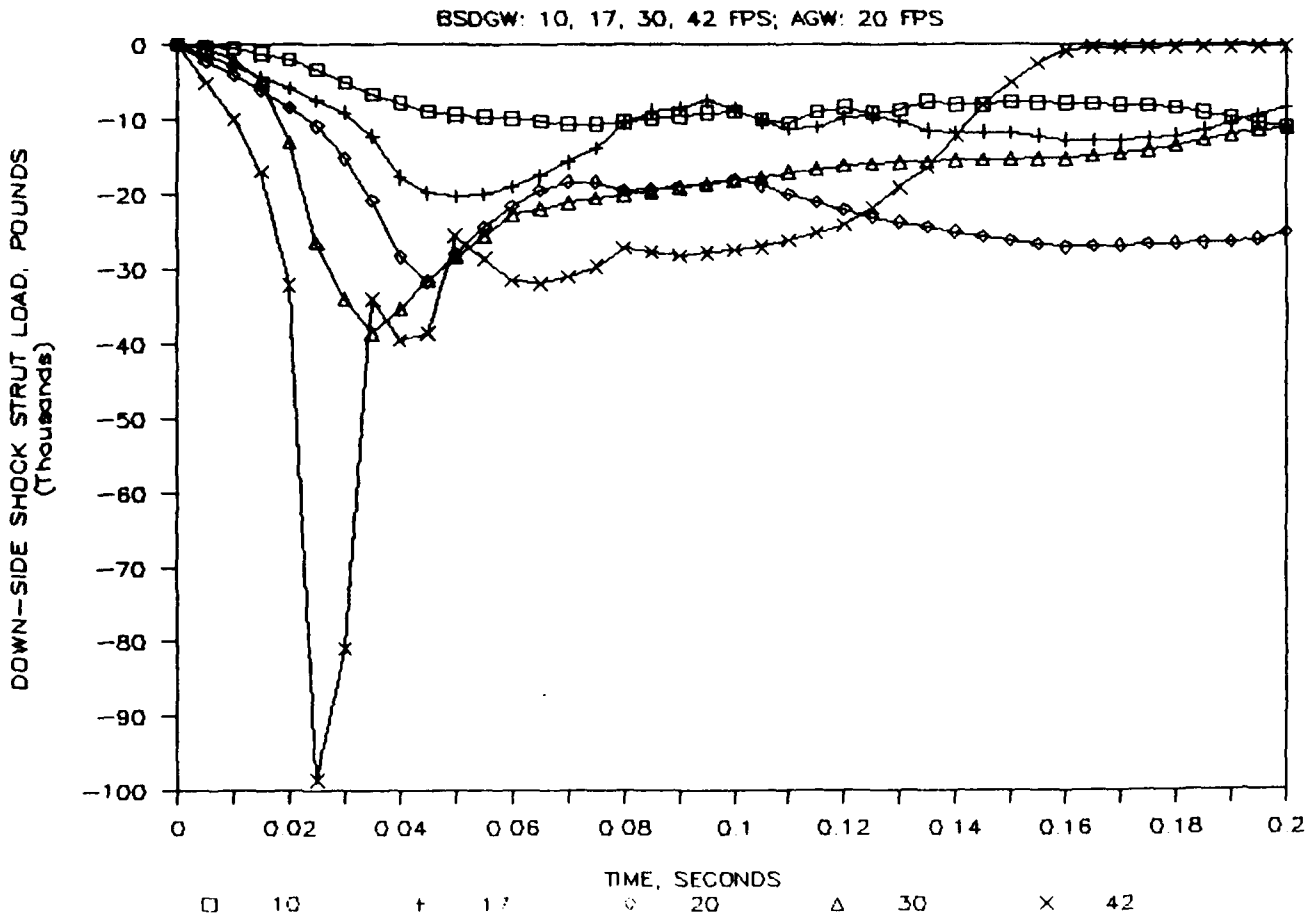

Figure 30. Shock strut loads of the down-side gear in the iron-bird tests.

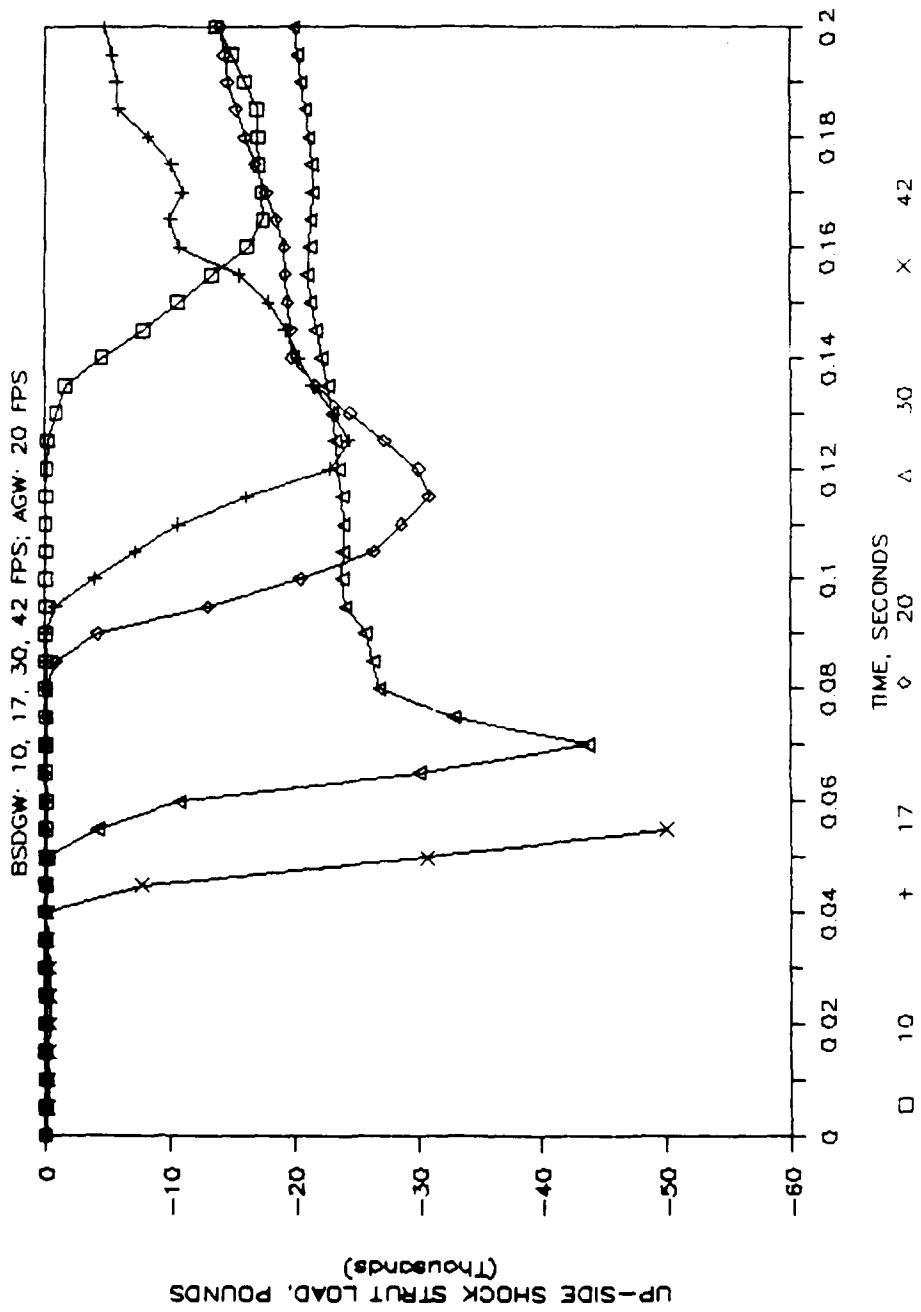

Figure 31. Shock strut loads of the up-side gear in the iron-bird tests.

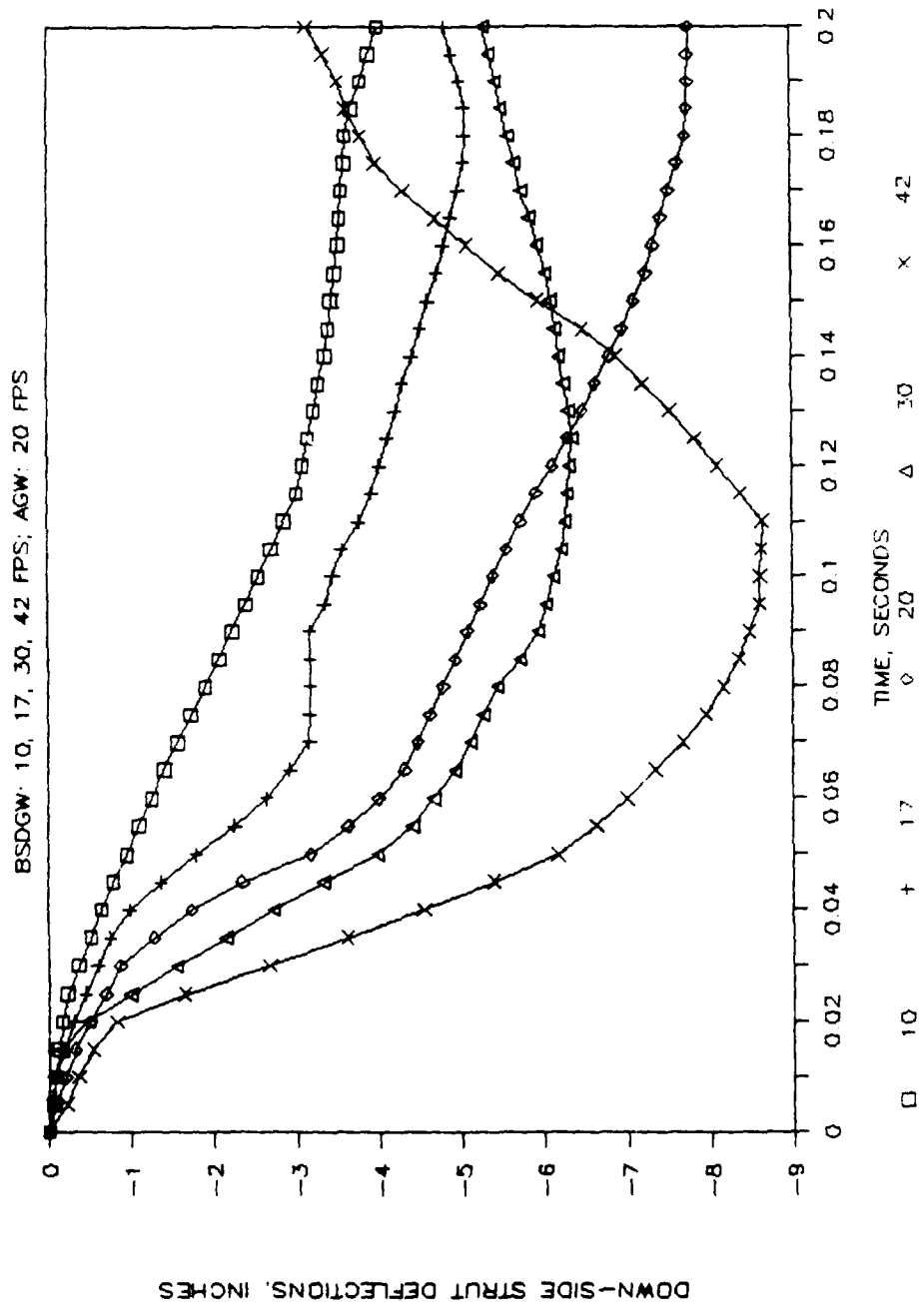

Figure 32. Shock strut deflections of the down-side gear in the iron-bird tests.

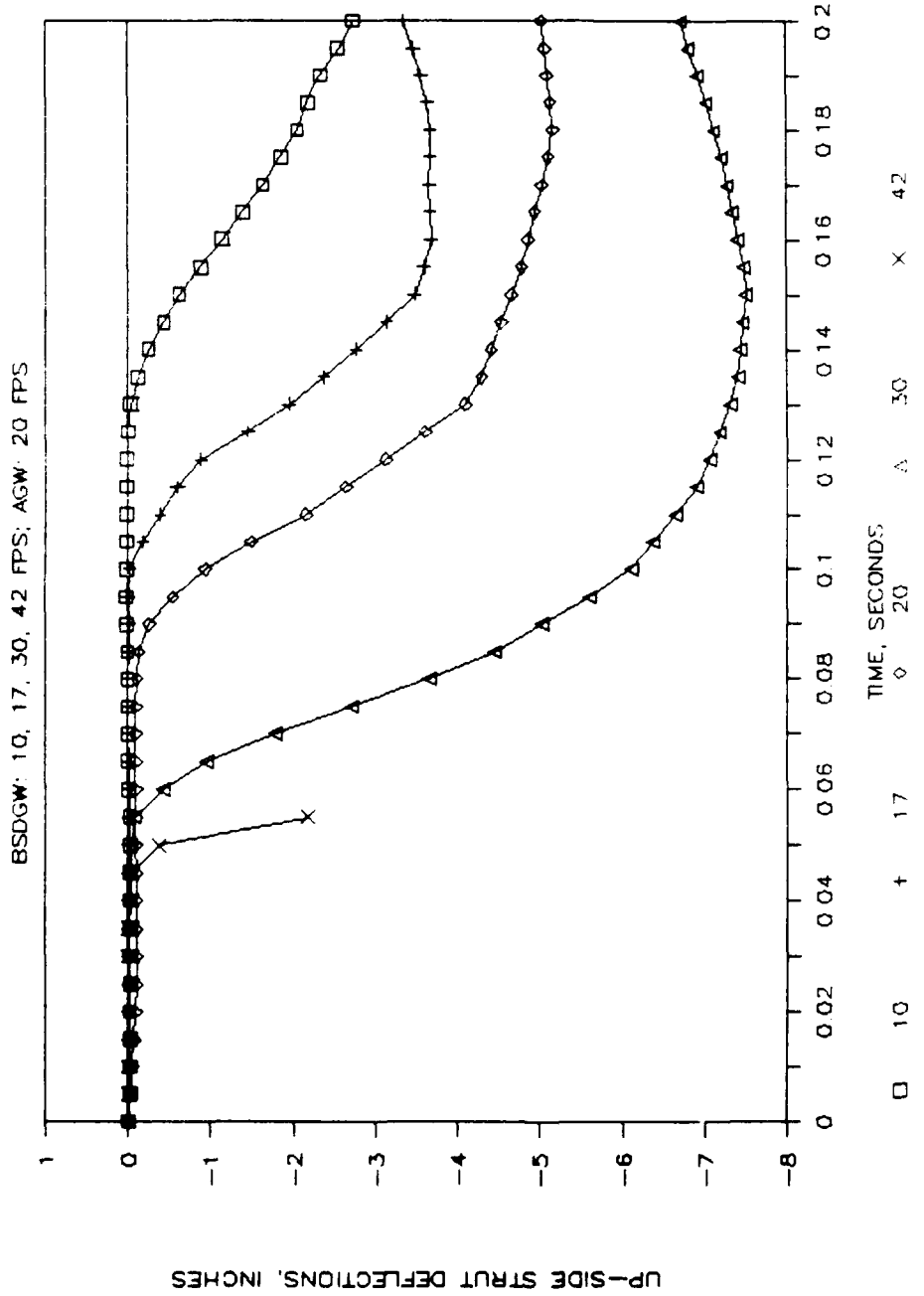

Figure 33. Shock strut deflections of the up-side gear in the iron-bird tests.

4. The severity of the bending in the up-side shock strut, which failed the gear in the 42 fps iron-bird drop test, was not predicted in the single-gear tests.

5. The high load (almost 100 percent above the design load) in the down-side shock strut of the 42 fps iron-bird drop test was not evident in the single-gear tests. This load is a result of impact attitude and velocity which is not simulated in the single-gear tests.

6.0 CORRELATION OF TEST AND KRASH RESULTS

6.1 GENERAL

The method of analysis with program KRASH is described in Volume I of this report. The correlation presented here is for all the tests, i.e., for impact speeds of 10, 17, 20, 30, and 42 fps. The impact attitude for all tests with the iron-bird fixture was combined 10° roll and +15° pitch. The data correlated are the vertical ground loads, and the loads and deflections of the shock struts on the up-side and down-side landing gears.

A brief description of the KRASH models used in the analyses is followed by a detailed discussion of specific loads and deflections, with a graphical summary. Further comparisons of all the parameters, individually by impact velocity, is presented in Graphs A-1 through A-62 in the Appendix.

6.2 CORRELATION WITH DESIGN LOADS

The landing gear was designed on the basis of calculated ground loads presented in Table 14 of Volume I. The ground loads for 25 landing conditions including crash impact were calculated. The vertical ground loads and the shock strut loads for the conditions tested are compared in Table 17. The design shock strut loads were calculated with NASTRAN from the design loads and the landing gear geometry. The table compares the most damaging of the calculated loads with the highest test results from platform or iron-bird drop tests as applicable.

TABLE 17. CORRELATION OF DESIGN AND TEST LOADS

No. From Table 14	Condition	Vert. Grnd. Load (kips)			Shock Strut Load (kips)		
			Test			Test	
		Design	Platform	Iron-Bird	Design	Platform	Iron-Bird
8a	Hard Level	17.00	14.13	-	45.26	35.78	-
10	Hard +15° Pitch 10° Roll	23.30	-	48.34	56.17	-	31.74
19b	Level Crash	30.20	27.60	-	62.06	65.08	-
20	Crash +15° Pitch	30.20	38.98	-	62.06	42.95	-
21	Crash +15° Pitch 10° Roll	30.76	-	63.99	62.06	-	97.09

The calculated design loads for level impact, hard and crash, are within ±20 percent of the test loads from platform drop tests. In the case of crash at +15° pitch, test loads vary up to ±30 percent of the design loads. For the cases of impact at 10° roll and +15° pitch, the conditions for the iron-bird drop tests, the design and test loads vary between -43 and +108 percent.

6.3 KRASH MODEL

The KRASH model of the iron-bird fixture is based on the detail model of the helicopter. The detail KRASH model of the full helicopter with 53 masses and 106 beams is shown in Figure 34. The moments of inertia of the detail model are the same as that of the utility helicopter given in Table 2. The KRASH model of the iron-bird fixture consists of only six masses and eight beams. Five masses at the landing gears are exactly of the same magnitude as in the detail model. The remaining sixth mass, which is the largest of the masses, is at the center of gravity. The sum of the masses equals that of the BSDGW or the AGW. The moments of inertia are assigned the values given in Table 2. The KRASH model, therefore, simulates the iron-bird fixture exactly in mass and moments of inertia.

The KRASH model of the iron-bird fixture is shown in Figure 35. The floor of the fuselage is outlined by broken lines for convenience and does not represent any model parameter. The springs, the landing gear components, and the tires are the same as those of the detail model of Figure 34. The springs and the landing gear components are connected to the center of gravity by rigid, massless beams, not shown in Figure 35 for clarity.

The shock strut designed for the ATLG is velocity-sensitive. Thus, the magnitude of the maximum load reached by the shock strut in a test depends on the impact velocity. Since the shock strut is modeled as a nonlinear beam in the KRASH code, the maximum shock strut load is an input parameter. The correspondence between the maximum shock strut load and the impact velocity, determined from the results of single-gear platform tests, is given in Figure 36. The results for 10° roll-impact and +15° pitch-impact are extrapolated parallel to the case for level-impact for impact velocities beyond 17 fps. The case for combined 10° roll and +15° pitch was not experimentally determined before the iron-bird tests were conducted. Thus, the maximum shock strut load used as input into the KRASH model of the iron-bird fixture was taken conservatively as the case for 10° roll and 0° pitch in all cases except for the impact at 42 fps, where an average of the two extrapolated curves from Figure 36 was taken.

One other unknown parameter in the test was the coefficient of friction between the tires and the ground. In the test the perfectly rigid ground was represented by a steel plate. The coefficient of friction (CoF) during the test varied with the sequence of test events. To estimate the CoF, two values of CoF, 0.25 and 0.50, were analyzed by program KRASH for 42 fps. The effects of CoF on the ground loads and on the response of the shock struts are compared in Graphs A-1 to A-8 of the Appendix. The vertical ground loads for the down-side and up-side gears, Graphs A-1 and A-2, are almost identical except that the up-side gear impacts 0.005 second later when CoF=0.50 than when CoF=0.25. The largest difference is in the lateral ground loads, Graphs A-3 and A-4, with the higher CoF yielding higher load. The phasing of the loads (load direction with respect to time) is identical at the initial stages and similar at the later stages. The loads and deflections of the down-side and up-side shock struts, Graphs A-5 to A-8, are almost identical. For this reason, all the KRASH analyses of the iron-bird were evaluated for a CoF of 0.50.

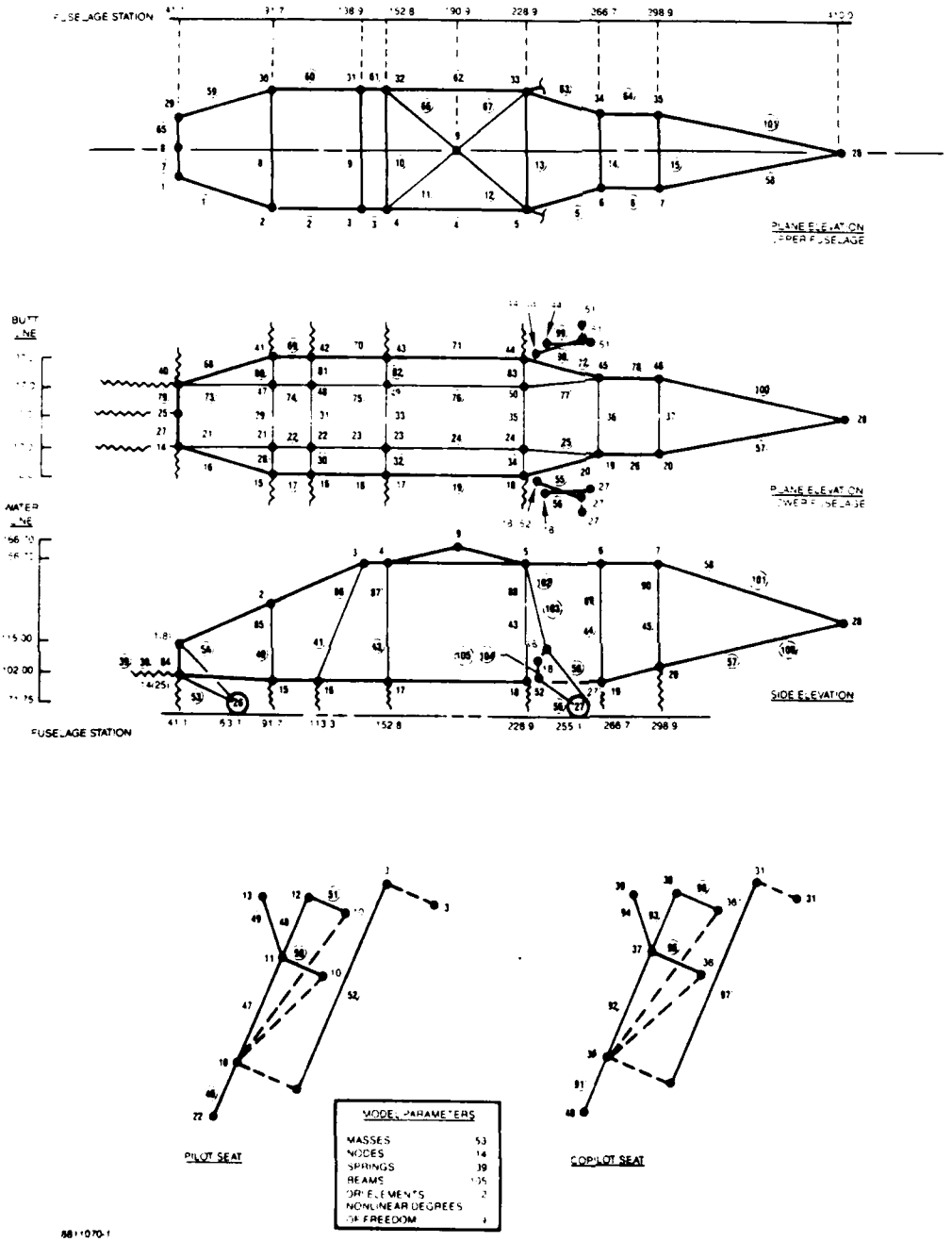

Figure 34. Detail KRASH model of the full helicopter.

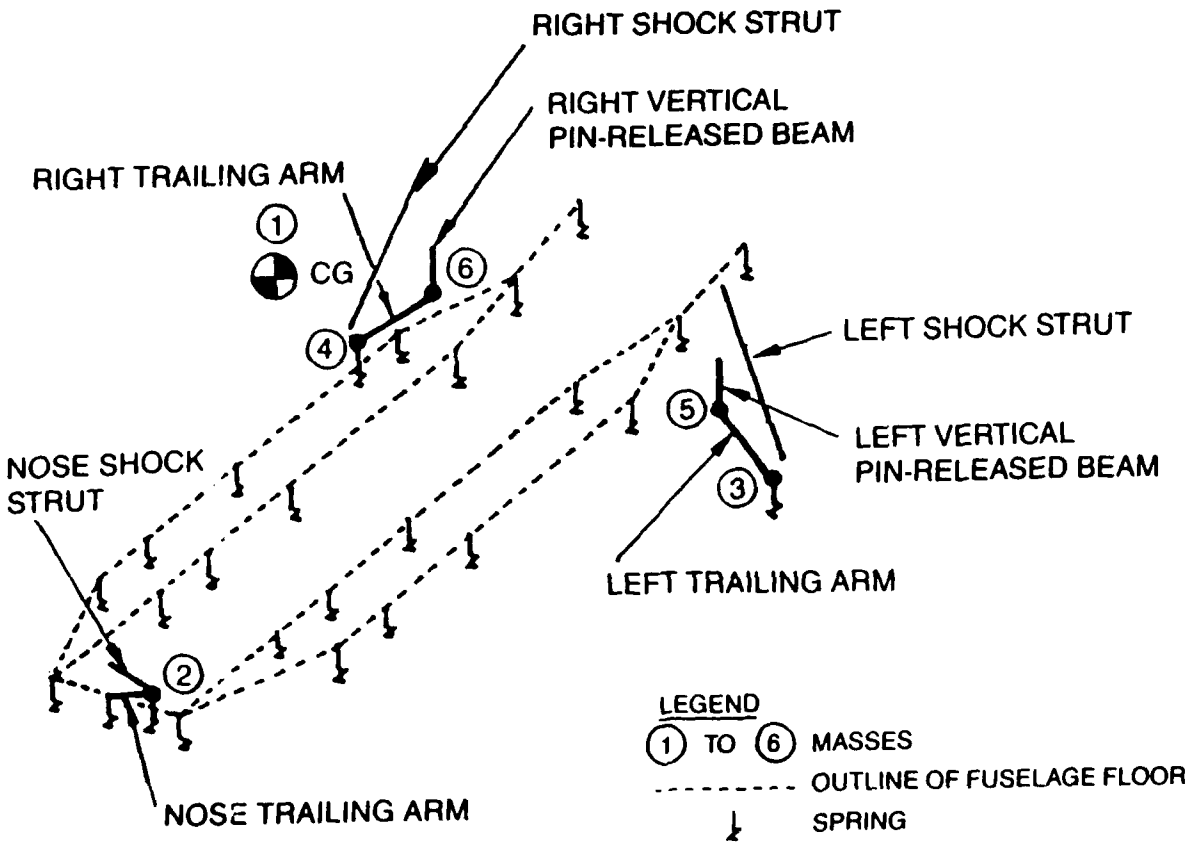

Figure 35. KRASH model of the iron-bird fixture.

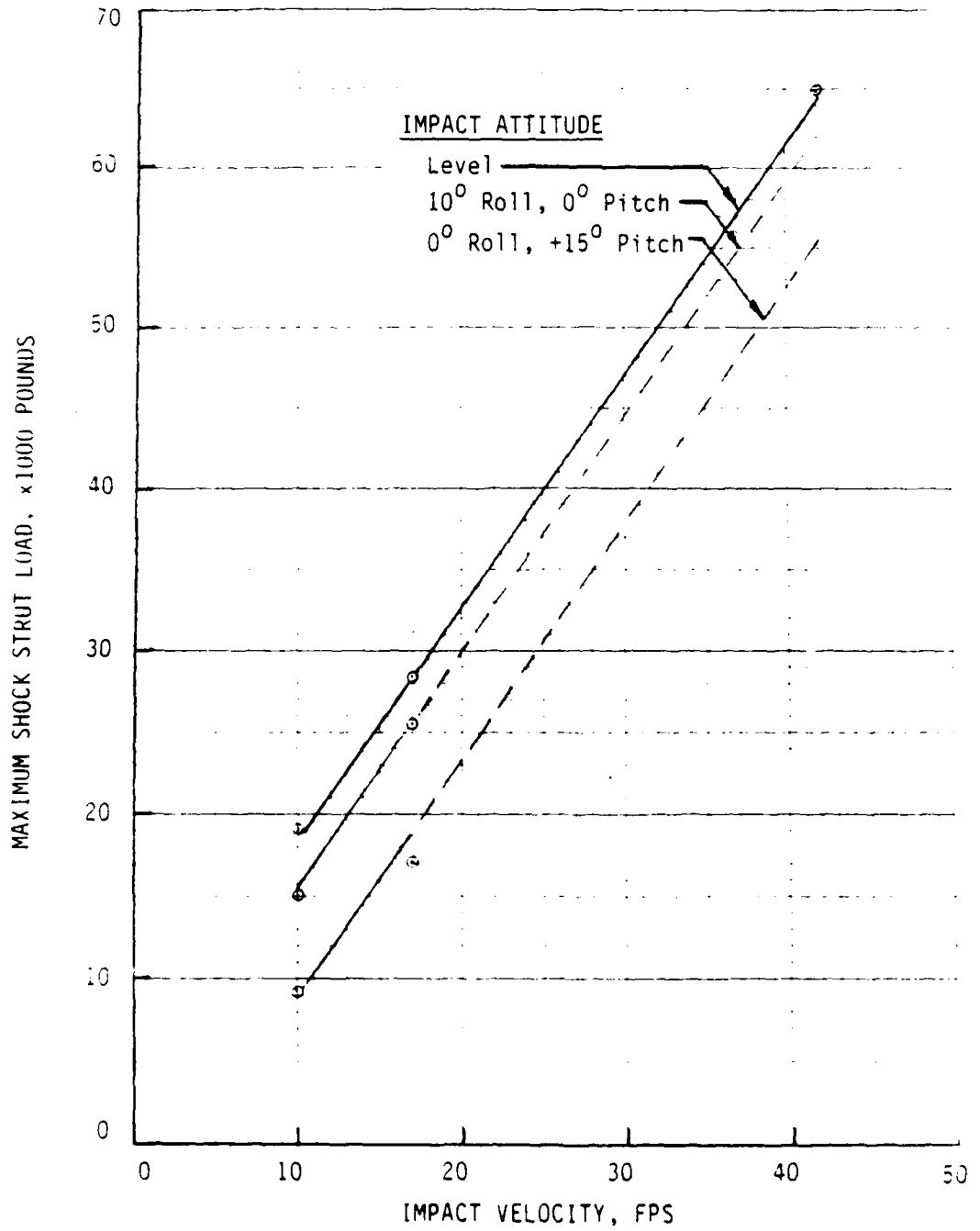

Figure 36. Correspondence between maximum shock strut load and impact velocity.

6.4 CORRELATION WITH KRASH RESULTS

The correlation presented is for 10, 17, 20, 30 and 42 fps. In all cases the impact attitude was combined 10° roll and +15° pitch, with a CoF=0.50. Even though the KRASH analyses were conducted at these precise impact velocities, the test impact velocities varied. The test impact velocities are shown below along with the gross weights at which the KRASH analyses and tests were conducted.

Impact Velocity, fps		
KRASH	Test	Gross Weight, lb
10.0	10.8	8,500
17.0	16.55	8,500
20.00	20.10	10,625
30.00	30.40	8,500
42.00	42.16	8,500

Only in the drop test at 42 fps did the iron-bird fixture (simulating the helicopter fuselage) contact the ground. In all other tests, the total kinetic energy was absorbed by the landing gears. Also during the test at 42 fps, the up-side landing gear failed at the fuselage-attachment clevises 0.055 second after initial ground contact by the down-side gear. All data for the up-side landing gear after 0.055 second into the test are therefore disregarded.

The correlation of the KRASH and test results is summarized in Table 18. The results are discussed below. The correlation of the results is presented in subsequent figures and in Graphs A-9 to A-62 in the Appendix.

6.4.1 Vertical Ground Loads
(Graphs A-9, A-10, A-21, A-22, A-31, A-32, A-41, A-42, A-51, and A-52)

Down-Side Landing Gear. The maximum vertical ground loads correlated very well between the KRASH and test results, except for the lower impact velocities of 10 and 20 fps. The time to reach the peak magnitude correlated exceedingly well within 5 or 10 microseconds. The phasing of the sequence of events was the same in most cases. These are summarized in Figures 37 and 38.

Up-Side Landing Gear. The maximum vertical ground loads did not correlate well except for the impact velocity for 10 fps. In all other cases, the test load had a high peak of very short duration. This high peak load may be due to secondary vibrations not filtered by the 1 KHz filter used. The good correlation of the time when the maximum load occurs and the good similarity in the phasing of the KRASH and test conditions suggest further evaluation of how the data should be filtered. The results are summarized in Figures 39 and 40.

TABLE 18. SUMMARY OF CORRELATION OF KRASH AND TEST RESULTS OF THE IRON-BIRD FIXTURE

	Impact Velocity at 10° Roll and +15° Pitch				
	10 fps	17 fps	20 fps	30 fps	42 fps
Gross Weight, lb	8,500	8,500	10,625	8,500	8,500
VERTICAL GRND LOAD					
Down-side					
Magnitude:KRASH/Test	1.40	0.99	0.64	0.94	0.93
Peak Time:Test-KRASH	0.035	0.010	0.005	0.010	-0.005
Phasing Compared	Same	Same	Similar	Same	Similar
Up-side					
Magnitude:KRASH/Test	0.84	0.63	0.65	0.62	0.69
Peak Time:Test-KRASH	0.000	0.015	0.010	-0.010	-0.005
Phasing Compared	Same	Similar	Same	Similar	(Failure)
STRUT LOAD					
Down-side					
Magnitude:KRASH/Test	1.46	1.33	0.96	1.21	0.55
Peak Time:Test-KRASH	0.045	0.030	0.025	0.015	0.010
Phasing Compared	Same	Same	Similar	Similar	(Failure)
Up-side					
Magnitude:KRASH/Test	0.89	1.10	0.99	1.07	1.08
Peak Time:Test-KRASH	0.000	0.020	0.025	0.005	0.000
Phasing Compared	Same	Same	Similar	Similar	(Failure)
STRUT DEFLECTION					
Down-side					
Magnitude:KRASH/Test	0.72	0.93	0.99	1.18	1.33
Peak Time:Test-KRASH	0.155	0.080	0.060	0.065	-0.010
Phasing Compared	Similar	Similar	Similar	Similar	Similar
Up-side					
Magnitude:KRASH/Test	0.50	0.69	0.92	0.69	(Failure)
Peak Time:Test-KRASH	0.020	0.010	0.015	0.045	(Failure)
Phasing Compared	Similar	Similar	Similar	Similar	(Failure)
TIME LAG FOR GRND, CONTACT OF UP-SIDE GEAR					
KRASH	0.140	0.085	0.075	0.045	0.040
Test	0.125	0.090	0.075	0.045	0.040

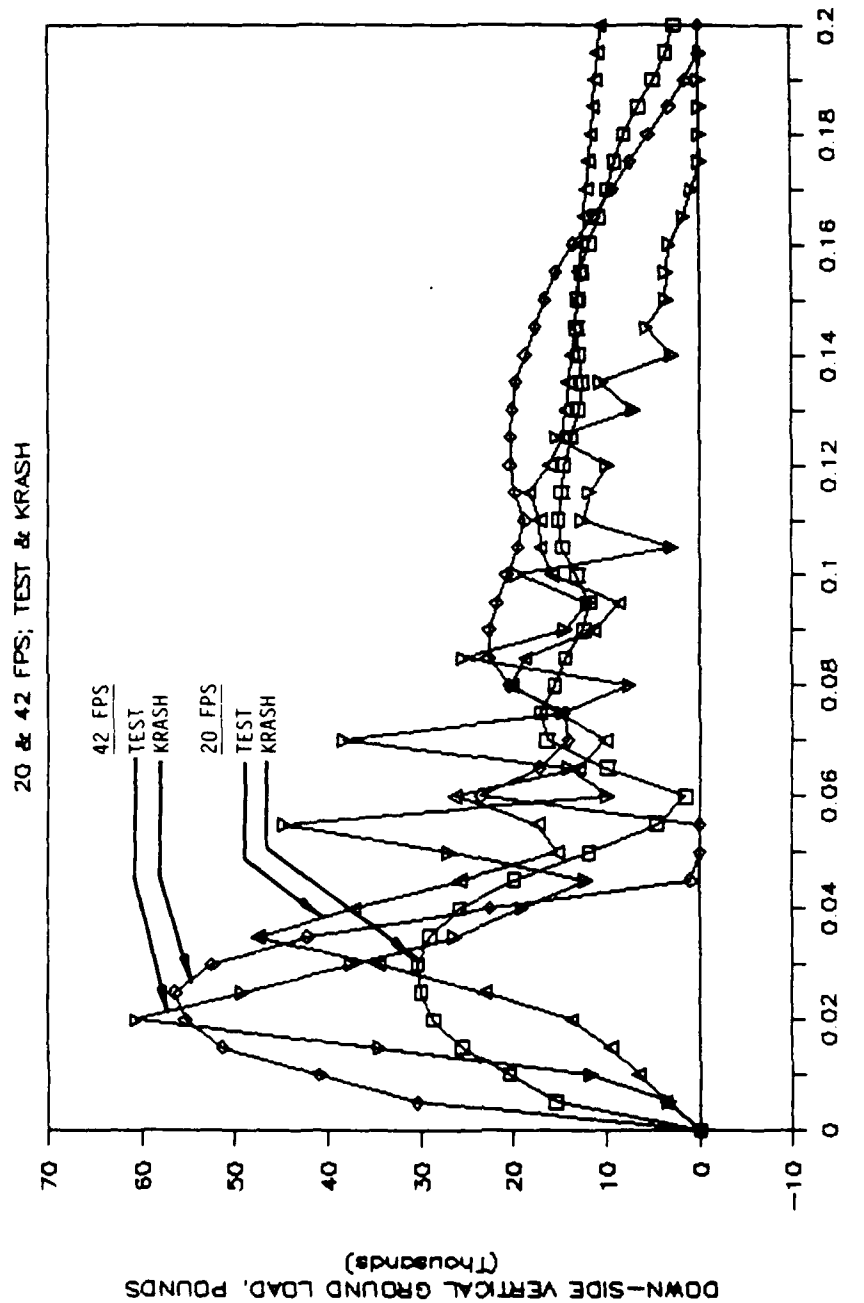

Figure 37. Correlation in the down-side vertical ground loads for 20 and 42 fps.

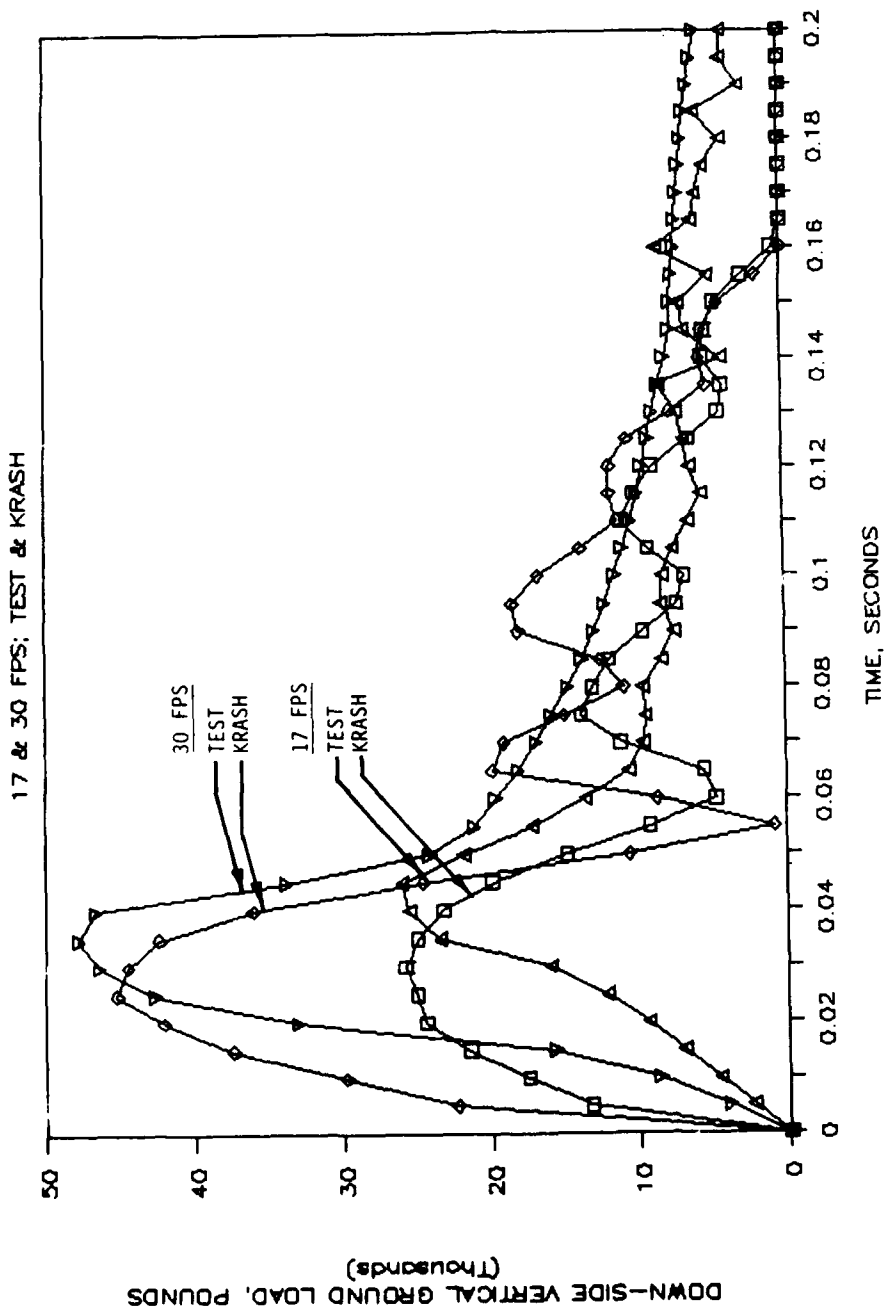

Figure 38. Correlation in the down-side vertical ground loads for 17 and 30 fps.

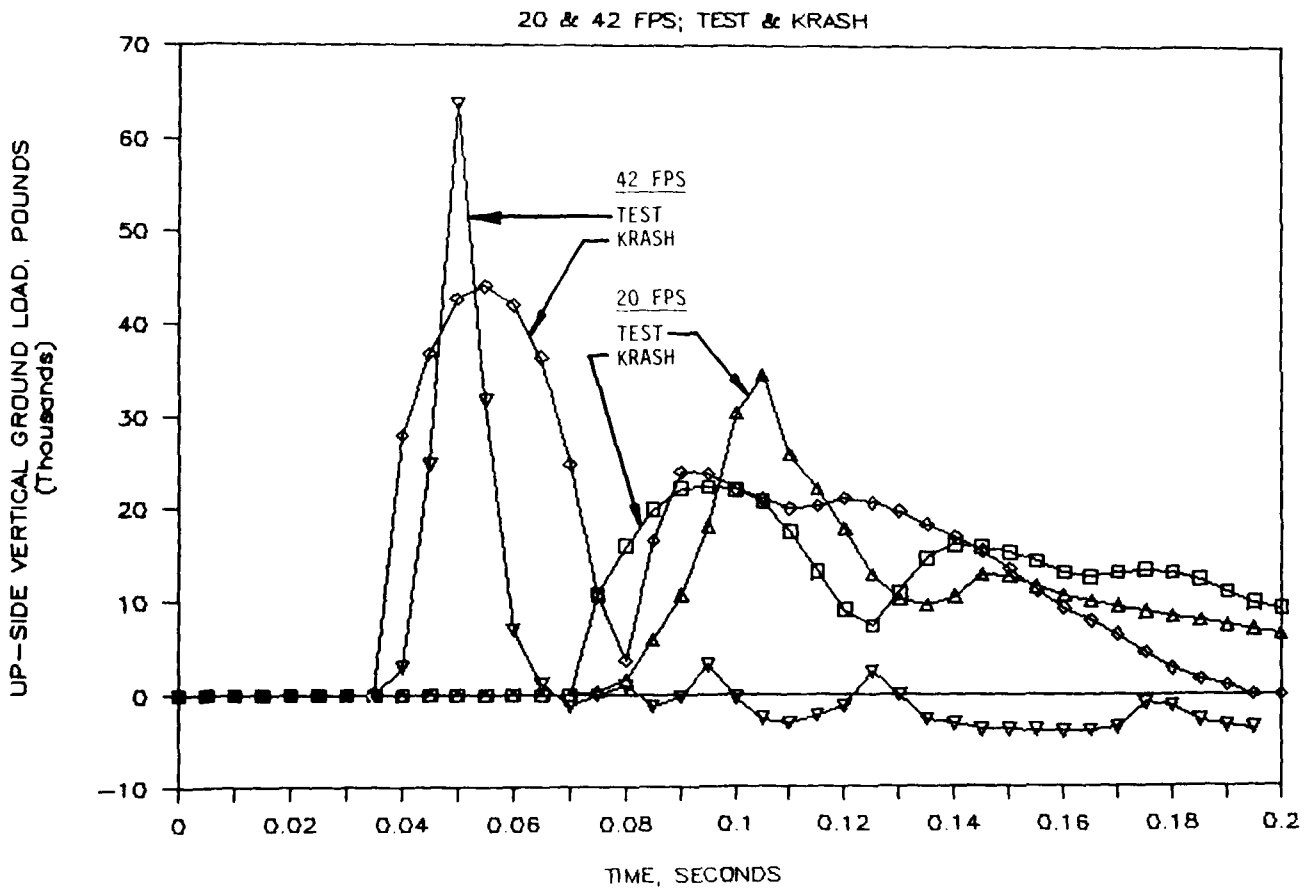

Figure 39. Correlation in the up-side vertical ground loads for 20 and 42 fps.

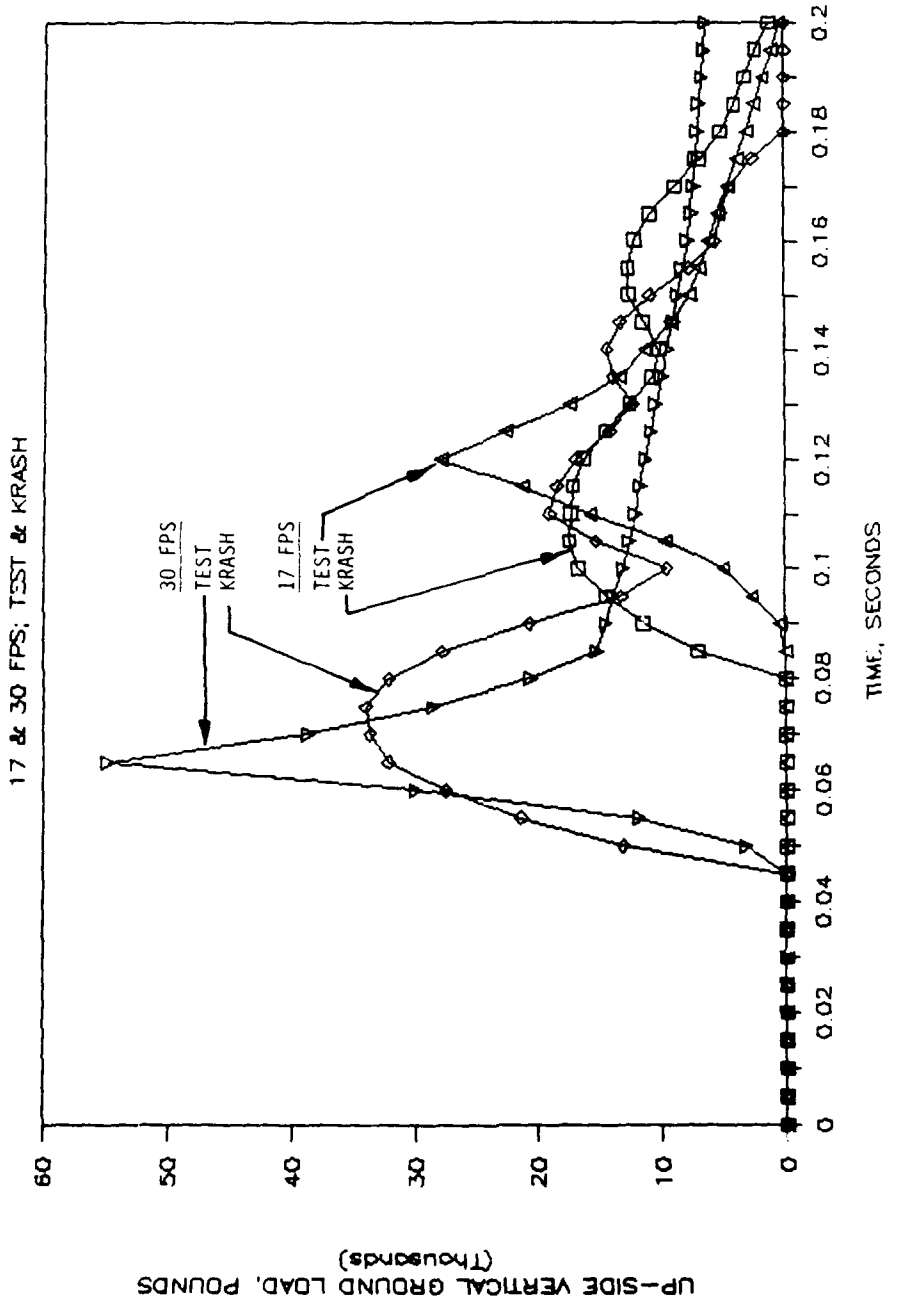

Figure 40. Correlation in the up-side vertical ground loads for 17 and 30 fps.

6.4.2 Lateral Ground Loads
(Graphs A-11, A-12, A-33, A-34, A-43, A-44, A-53, and A-54)

Down-Side Landing Gear. The lateral loads, which depend on the CoF, are higher in KRASH analysis than in test for impact velocities of 10 and 20 fps. The phasings from KRASH and test results for both test conditions are similar. The CoF in both tests is between 0.33 and 0.35 instead of 0.50 used in KRASH analyses. A comparison is not possible for the tests at 30 and 42 fps because the tires burst on impact, a condition which cannot be simulated in KRASH analysis.

Up-Side Landing Gear. The lateral load for the up-side landing gear can be evaluated only for the test condition of 10 fps. For the other tests at 20, 30 and 42 fps, the up-side tires burst on impact. For the test condition of 10 fps, the maximum test load was so small that the CoF is estimated as 0.12. The difference in the CoF of the down- and up-side gears indicates the difference in the severity of the two impacts and in the condition of the tires.

6.4.3 Shock Strut Loads
(Graphs A-13, A-14, A-23, A-24, A-35, A-36, A-45, A-46, A-55, and A-56)

Down-Side Landing Gear. The maximum shock strut loads in KRASH analyses were assigned from the single-gear platform tests. The shock strut, modeled as a nonlinear beam, therefore showed a flat maximum load when the assigned magnitude was reached. This is explained in Section 5.5. The sensitivity to the impact velocity with 10° roll and +15° pitch, however, was different from the assigned magnitude, and the variation from the test loads ranged from -4 to +46 percent. For the condition at 42 fps impact, however, the maximum strut load was 97,090 pounds, which is 52 percent higher than the design load. The probable reasons for this high load were discussed in Section 5.0. The phasings of the loads for the KRASH and test results were similar.

Up-Side Landing Gear. The KRASH correlation with the up-side shock strut load was much better, even though the assigned maximum shock strut loads in KRASH analyses were the same as those for the down-side shock strut. The range of variation was from -11 to +10 percent. This indicates that the up-side gear experienced a higher impact velocity due to rotation than the down-side gear. The phasing of the loads for the KRASH and test results can be categorized as same to similar.

6.4.4 Shock Strut Deflection
(Graphs A-15, A-16, A-25, A-26, A-37, A-38, A-47, A-48, A-57, and A-58)

The deflections of the down-side and up-side shock struts were lower in KRASH analyses than in tests, except for the test at 20 fps. The lower deflections can be partly explained by the higher shock strut load for tests at 10 and 17 fps. At the higher impact conditions of 20 and 30 fps, fuselage contact with the ground reduced the energy absorbed by the landing gear in KRASH analyses because the iron-bird fixture did not contact the ground in the tests. The results at 42 fps cannot be compared because of the failure of the up-side landing gear.

6.4.5 Shock Strut Load-Deflection Curves (Graphs A-17 to A-20, A-27 to A-30, and A-59 to A-62)

The results presented here show the differences in the response of the shock strut in tests and in KRASH analyses. In KRASH analyses, the curve becomes flat once the assigned maximum magnitude is reached. In tests, such a phenomenon is not exhibited in any of the impact conditions.

6.5 CONCLUSIONS

The correlation with and the prediction from KRASH analyses are good. The differences in the results between KRASH and test can be attributed to:

1. the KRASH analyses being for a free-fall of the iron-bird fixture, whereas in tests the iron-bird fixture was guided between vertical rails and restrained in the yaw direction.

2. the shock strut being modeled as a nonlinear beam with an assigned maximum load in KRASH analyses.

3. the coefficient of friction being estimated and assumed constant throughout KRASH analyses, thus the bursting of the tires and fracture of the wheel rims could not be accurately modeled.

4. the rotor lift force, which was designed to be 67 percent of the gross weight, varying between 104 percent for 10 fps and 345 percent for 42 fps.

7.0 CONCLUSIONS AND RECOMMENDATIONS

7.1 SUMMARY

An advanced technology landing gear which is crashworthy and retractable was designed, analyzed and tested. The landing gear designed was for an LHX-size utility helicopter of 8,500 pounds of design gross weight, and an alternate gross weight of 10,625 pounds. The testing included platform drop tests of the landing gear, the standard tests to which landing gears are subjected, and drop tests with an iron-bird fixture simulating a helicopter. The iron-bird fixture tests simulated roll and pitch impact conditions. Extensive crashworthiness analysis with program KRASH correlated the iron-bird test results and predicted the crash-impact response of the full helicopter.

The specific requirements of the program to design, build and test a crashworthy, retractable landing gear were satisfied through test and KRASH analyses. The approach taken to absorb the kinetic energy from a crash was a systems approach where the system of the landing gear, fuselage and seat work in concert to share the kinetic energy and make the impact survivable. The energy distribution between the landing gear and the fuselage for a 42 fps level impact was 60 percent to 40 percent.

The design is very compact. The key to the design is the pivot crank, which acts as the interface between the landing gear and the fuselage, and permits the entire landing gear to retract and stow within the space allocated. The crank also makes the landing gear highly reliable and maintainable. With the removal of only two bolts or pins, the entire landing gear or any one of the major components can be removed from service.

The landing gear also demonstrated the capability of emergency extension. The entire landing gear is deployed under all conditions in less than 2.5 seconds. This capability satisfies the emergency deployment requirement. Tests have demonstrated that the landing gear actually deploys in less than 1.5 seconds. In an emergency, the landing gear is designed to deploy of its own accord from signals emanating from the onboard cockpit computer. In the case of a failure of the onboard hydraulic and electrical systems, the landing gear can be deployed by operating one valve to the helicopter's accumulator unit and letting the gear descend of its own weight.

7.2 CONCLUSIONS

The program has demonstrated the differences in the behavior of the landing gear in platform and iron-bird drop tests. The close correlation achieved between test and crashworthiness analysis using program KRASH has demonstrated the validity of innovative modeling techniques. The specific conclusions are summarized below:

1. Single-gear drop tests simulating roll and pitch conditions with wedge-like ground platforms do not produce results meaningful to the qualification of landing gears.

2. The inclusion of the crank, an improvement over existing landing gear designs, provides the interface with the fuselage that permits the landing gear to be stowed in a very limited volume and results in a design which is highly maintainable.

3. The crashworthiness requirements are generally based on cumulative frequency of accident occurrence, rather than their influence on helicopter weight. In a previous study (Figure 86 in Reference 1), a vertical crash impact requirement of 42 fps at 10° roll and -5°/+15° pitch, which is equivalent to a cumulative frequency of accident occurrence of 80.75 percent whereas the 42 fps crash impact corresponds to the 95th percentile, resulted in an estimated 5.7 percent increase in weight over a noncrashworthy standard helicopter. This estimate has been improved in this study where the increase in weight of the ATLG over a standard landing gear is 5.3 percent (Table 30 of Volume I) provided each link in the crashworthiness system contributes equally to the increase in weight of the helicopter. It was recommended in Reference 1 that a weight-effective design of a retractable landing gear would be to the following crashworthiness criteria:

Velocity	Maximum Roll Angle	Pitch Angle	Wt. Increase (Ref. 1)	Cum. Freq. of Occurrence
42 fps	±5 deg	-5 to +15 deg	5.4%	67.5%
36 fps	±10 deg	-5 to +15 deg	5.4%	75.5%

If the same ratios of weight increases hold true in the ATLG study, the estimates of 5.4 percent shown in the above table would decrease to 5.0 percent. The estimate of these ratios must be carefully taken because the crashworthiness behavior is configuration-sensitive. In the case of landing gears, the configuration parameters are the wheel base, ground clearance and the ratio of the energy split between the landing gear and the fuselage.

4. The crashworthiness requirement in the ATLG program of "no structural yield and no fuselage contact" for impacts at vertical velocities less than 20 fps at 10° roll and -5°/+15° pitch at maximum gross weight is considered to be a severe condition from the point of view of weight increase. The severity is in the inclusion of the impact attitude of roll and pitch conditions. The roll and pitch requirements will result in landing gear design that, depending on the helicopter configuration, will exceed the energy-absorbing capability at level impact for 20 fps by as much as 50 percent. The associated high landing gear load factors and stroke requirements will result not only in heavier landing gears but also in heavier fuselage structures due to increased fuselage bending and landing gear attachment fitting loads.

5. The modeling with enhanced KRASH analysis closely predicted the results from the iron-bird drop tests. It was also shown that the results from level platform tests matched the results from KRASH analysis, whereas the results of inclined-impact platform tests did not correlate with iron-bird tests or KRASH results. The modeling methodology, together with enhancement of KRASH, provides a tool that can be correlated with simple platform tests before predicting the behavior of a full helicopter under crash impact conditions.

6. The method used in the ATLG program to simulate rotor lift was inadequate at vertical velocities in excess of 20 fps. The rotor lift should not be simulated by trying to arrest the descending iron-bird fixture with pistons acting in simple hydraulic cylinders because the momentum of the iron-bird fixture is too large for the cylinders to respond adequately. The alternate method of reducing the drop mass to reflect the rotor lift effect, as was done on the ACAP dynamic tests, would be more appropriate (References 2 and 3).

7. The failure of the up-side landing gear in the iron-bird test at 42 fps highlights the severity of the load and the velocity with which the flow of fluids in hydraulic cylinders and actuators are required under this test condition.

7.3 RECOMMENDATIONS

The extensive test and analyses completed in this program lend themselves to extending the data base on the response of landing gears and of helicopters under crash impact. Extension of the data base will increase an understanding of the crash-impact behavior, provide data for the analysis of future systems, and result in future systems which are optimized for crashworthiness, weight and cost. Tasks recommended for future work are tabulated below:

1. Program KRASH models the shock strut as a nonlinear beam. As such, the response of a velocity-sensitive shock strut cannot be modeled accurately. A modification to the code will permit shock struts to be accurately modeled, which will yield accurate results of load and stroke of the struts.

2. The test data correlates very well with KRASH results except for the occasional "peak load" in the test data. It is believed that the peak load is the result of inadequate filtering, since the load data was filtered with single-pole Butterworth filters with non-optimized filtering frequencies. An analysis of filtering the test and KRASH data, and determination of their correlation will provide direction for future test and analysis. It will also result in greater accuracy in predicting crash-impact response of helicopters and helicopter systems.

3. The data generated in this program lends itself to determining the incremental weight of each element of the crashworthiness system for each crash-impact condition. This task would enhance the data base on crashworthiness.

4. The data presented here is for a tricycle configuration of a utility helicopter. The study in Reference 1 was also of a utility helicopter but with a tailwheel. Since the crash-impact response is very configuration sensitive, a detailed analytical comparison of the two configurations will further the data base on crashworthiness.

5. Program KRASH has limited capability in modeling ground frictional effects and tire-spring damping rates. Additional modeling techniques need to be developed to correctly model these effects.

6. The iron-bird fixture was restrained in the drop test tower during tests. A free-fall test with the iron-bird fixture, together with a crashworthiness analysis, should provide further data to demonstrate how analyses with minimum testing can be used to qualify future landing gear systems.

REFERENCES

1. J. K. Sen, M.V. Votaw and D.C. Weber, "Advanced Technology Helicopter Landing Gear Preliminary Design Investigation," McDonnell Douglas Helicopter Company, USAAVSCOM-TR-84-D-20, Applied Technology Laboratory, U.S. Army Research and Technology Laboratory (AVSCOM), Fort Eustis, Virginia, May 1985.

2. J.P. Perschbacher and N. Chase, "ACAP Airframe Crashworthiness Demonstration," Proceedings, AHS National Specialists' Meeting on Rotary Wing Test Technology, Bridgeport, Connecticut, 15-16 March 1988.

3. J. D. Cronkhite and L. T. Mazza, "KRASH Analysis Correlation with the Bell ACAP Full-Scale Aircraft Crash Test," Proceedings, AHS National Specialists' Meeting on Advanced Rotorcraft Structures, Williamsburg, Virginia 25-27 October 1988.

APPENDIX
DETAIL CORRELATION OF TEST AND KRASH RESULTS

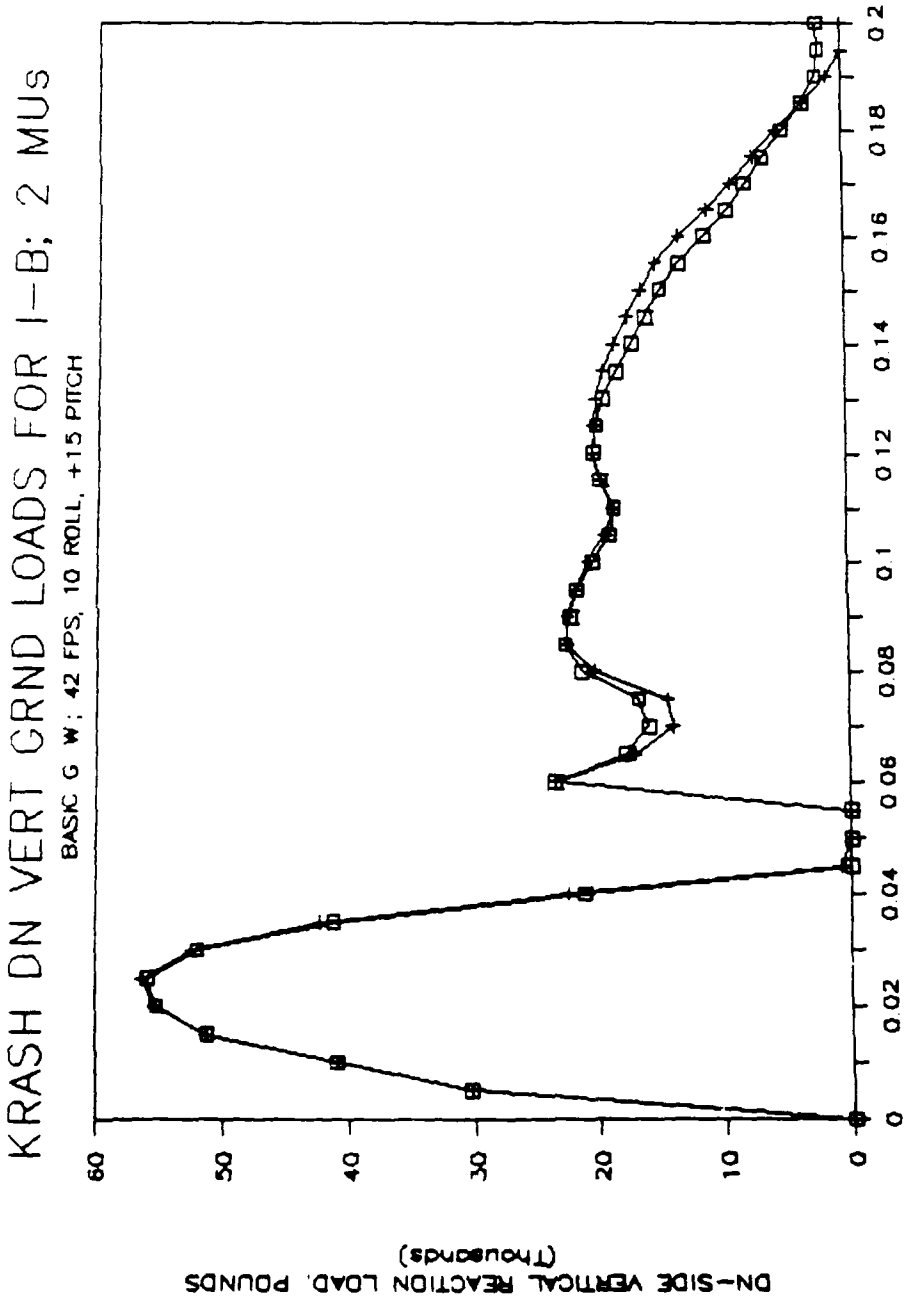

Graph A-1. KRASH down-side vertical ground loads.

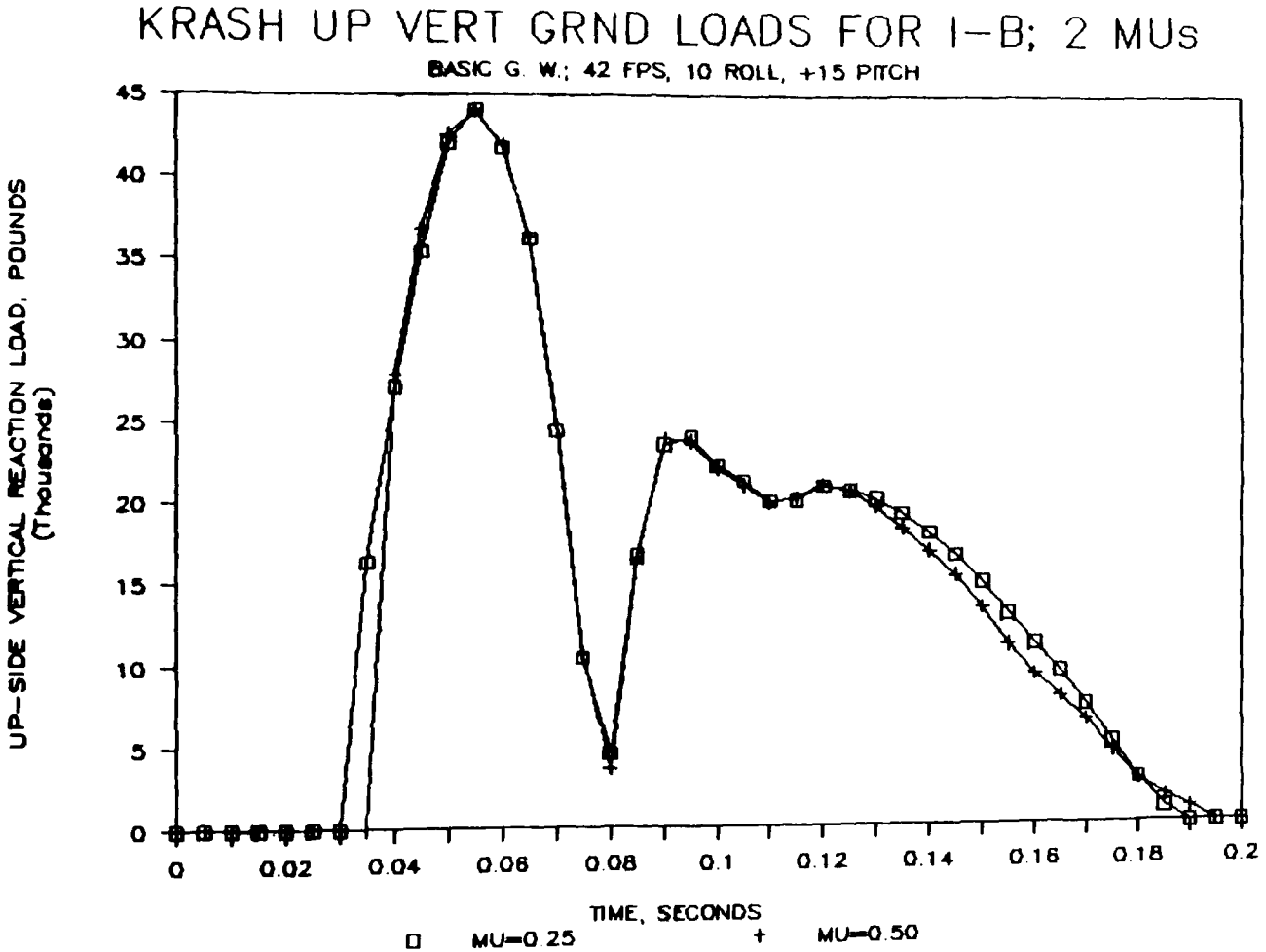

Graph A-2. KRASH up-side vertical ground loads.

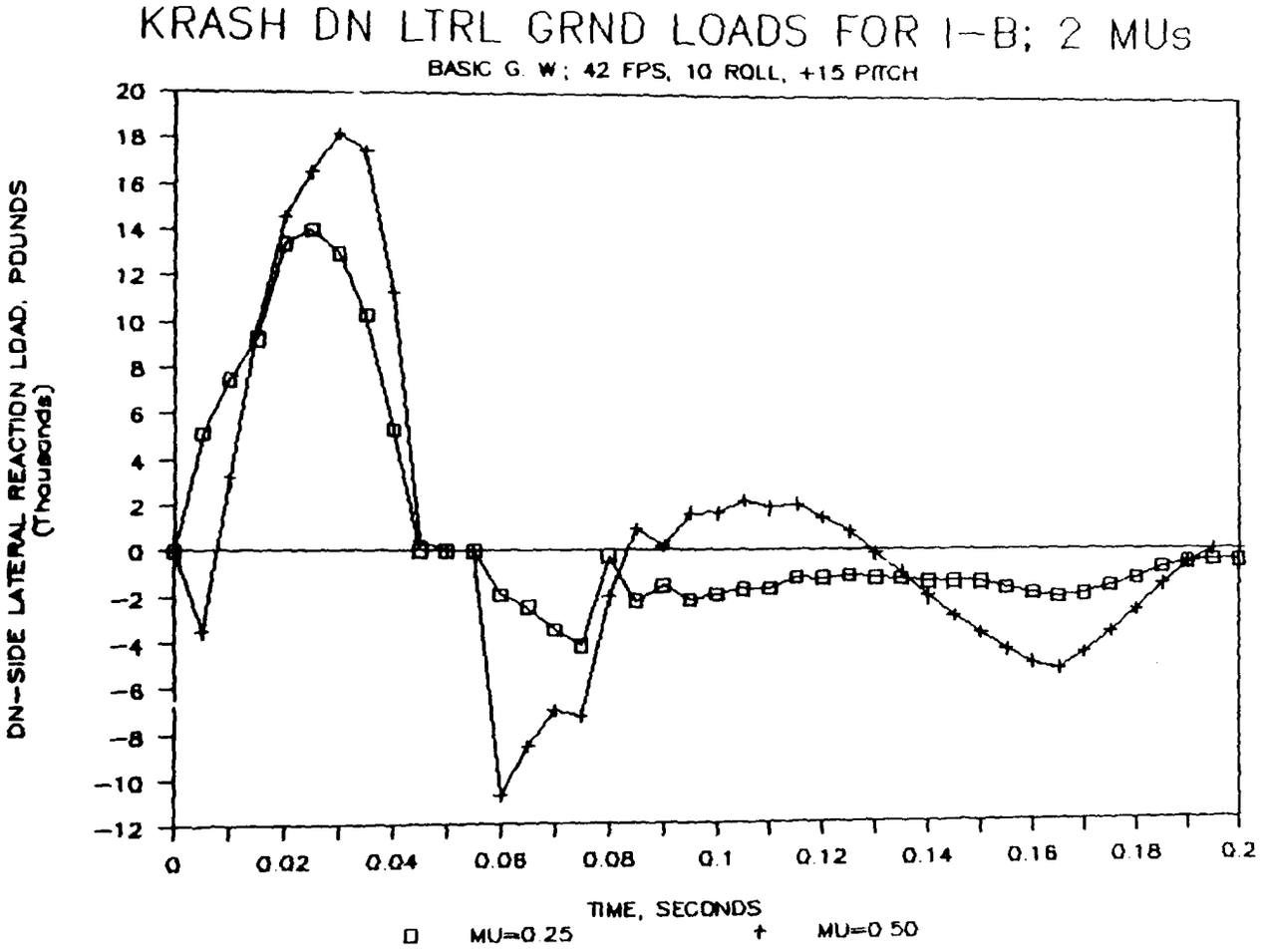

Graph A-3. KRASH down-side lateral ground loads.

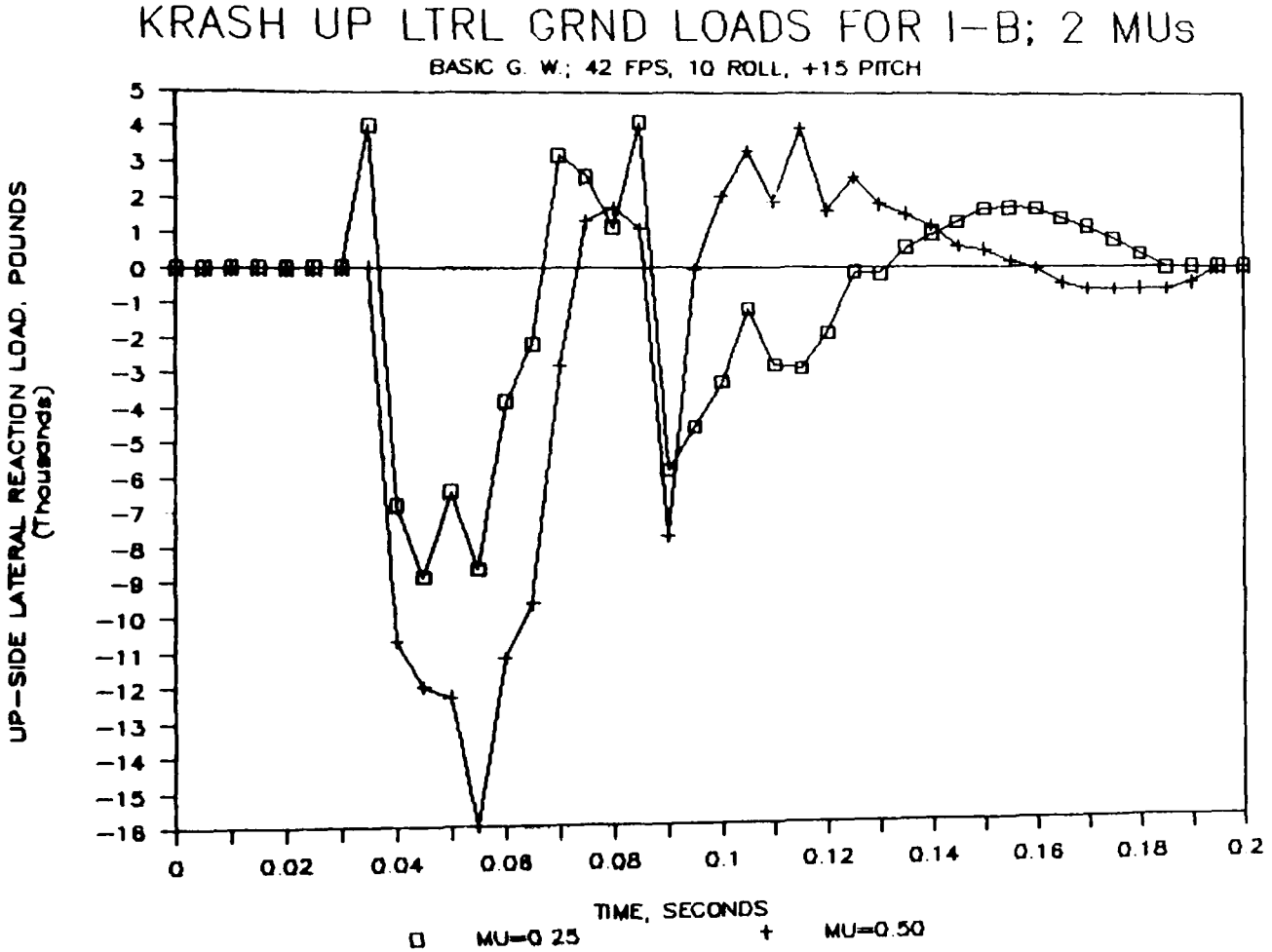

Graph A-4. KRASH up-side lateral ground loads.

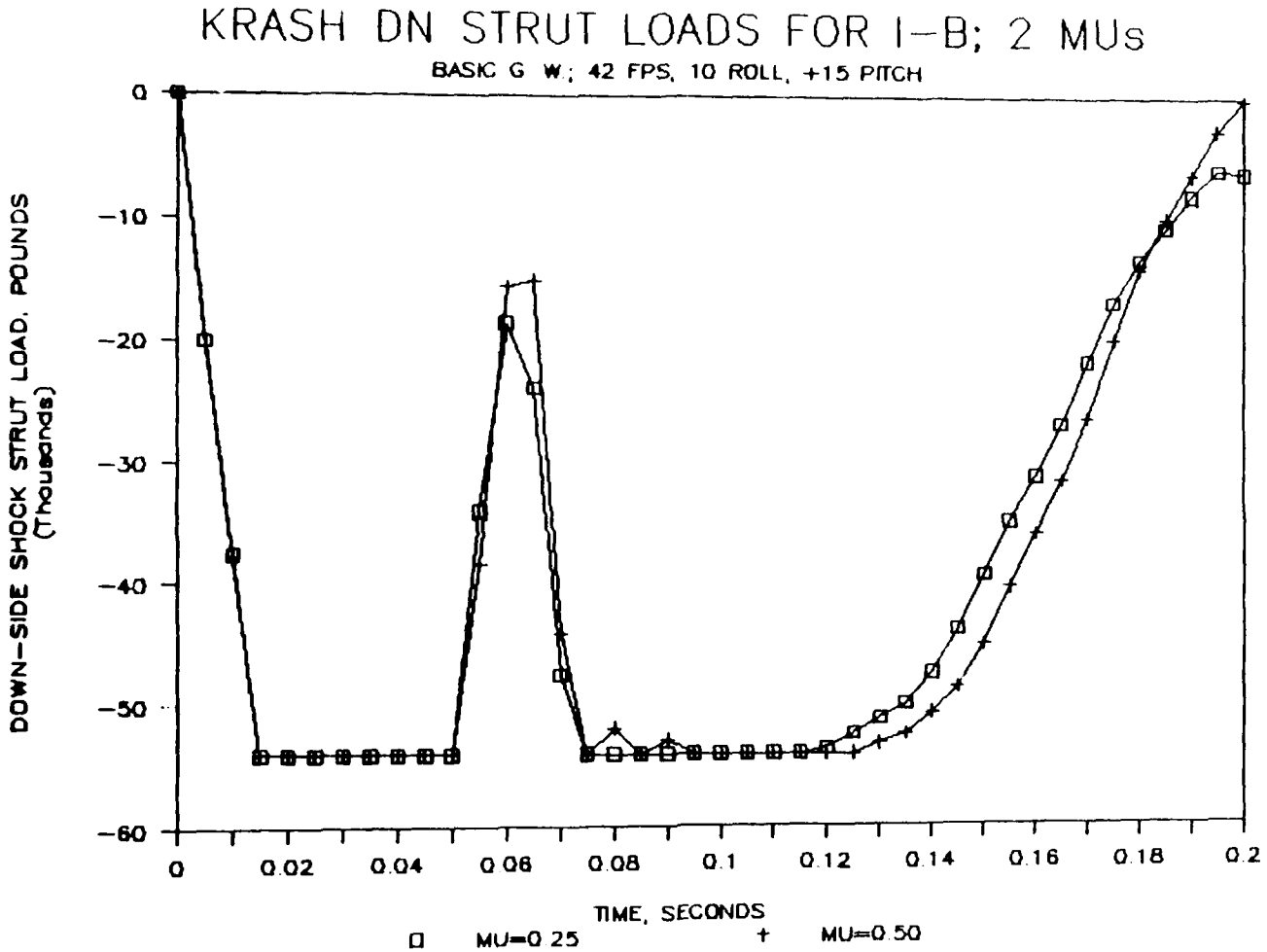

Graph A-5. KRASH down-side strut loads.

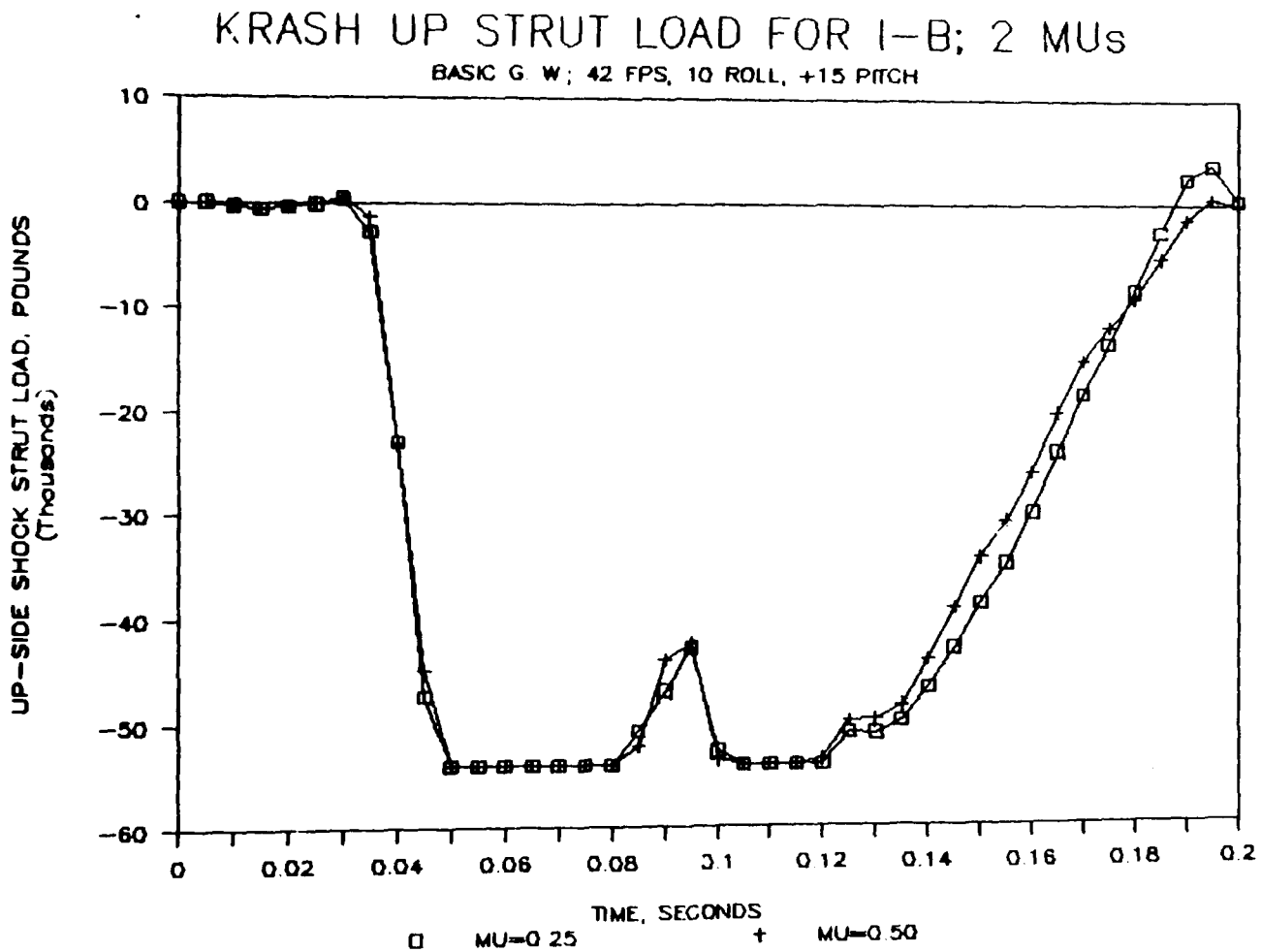

Graph A-6. KRASH up-side strut loads.

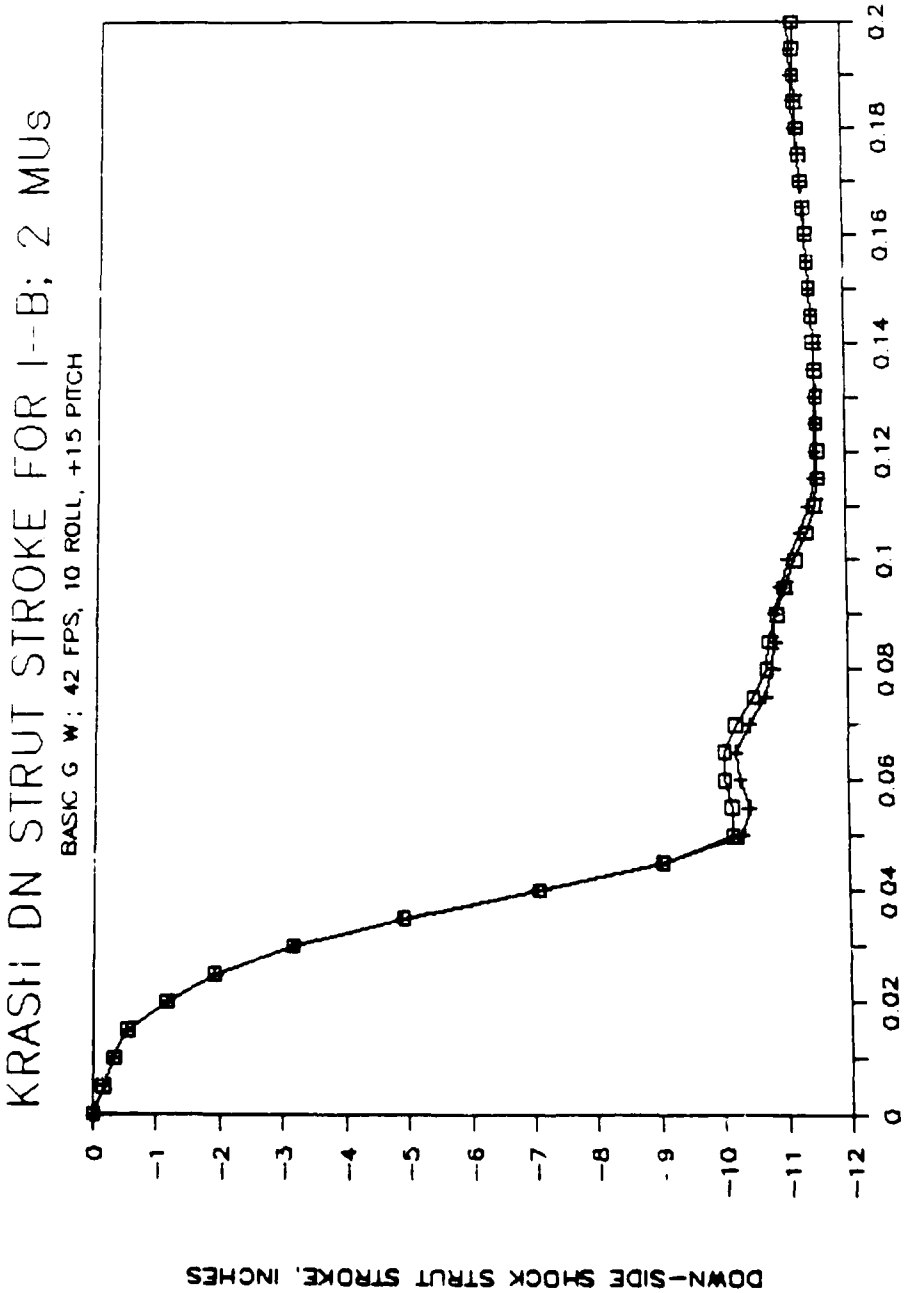

Graph A-7. KRASH down-side strut stroke.

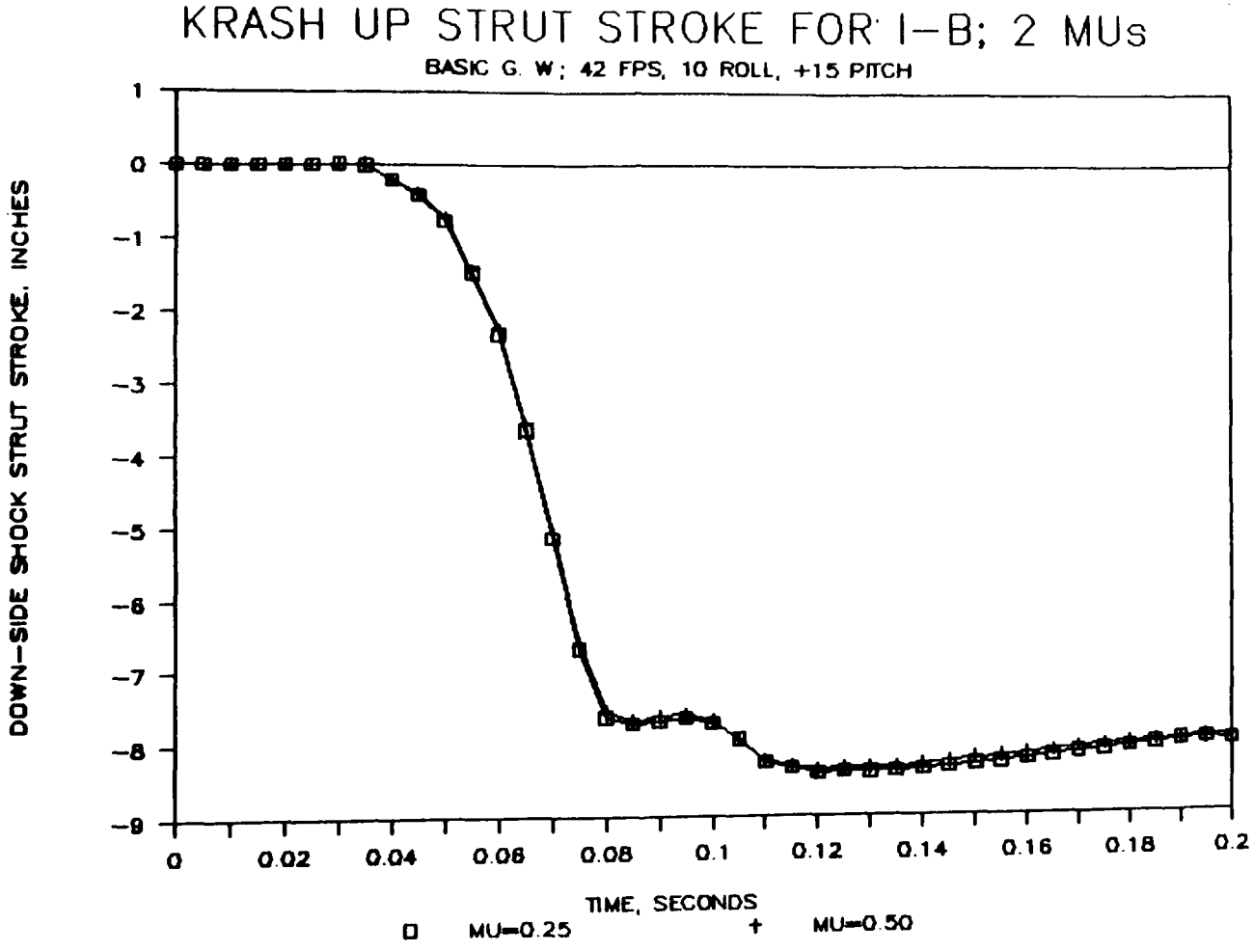

Graph A-8. KRASH up-side strut stroke.

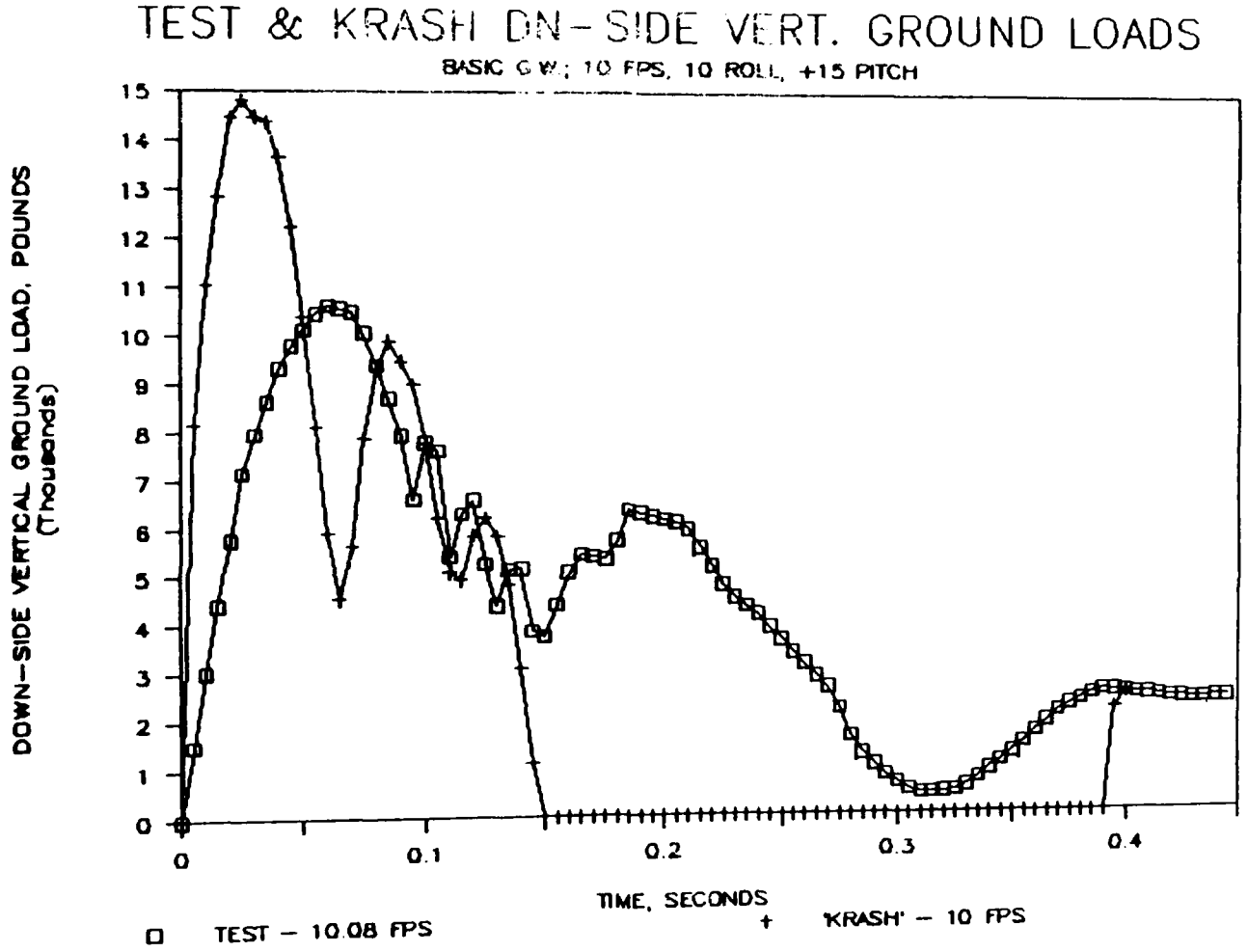

Graph A-9. Test and KRASH down-side vertical ground loads.

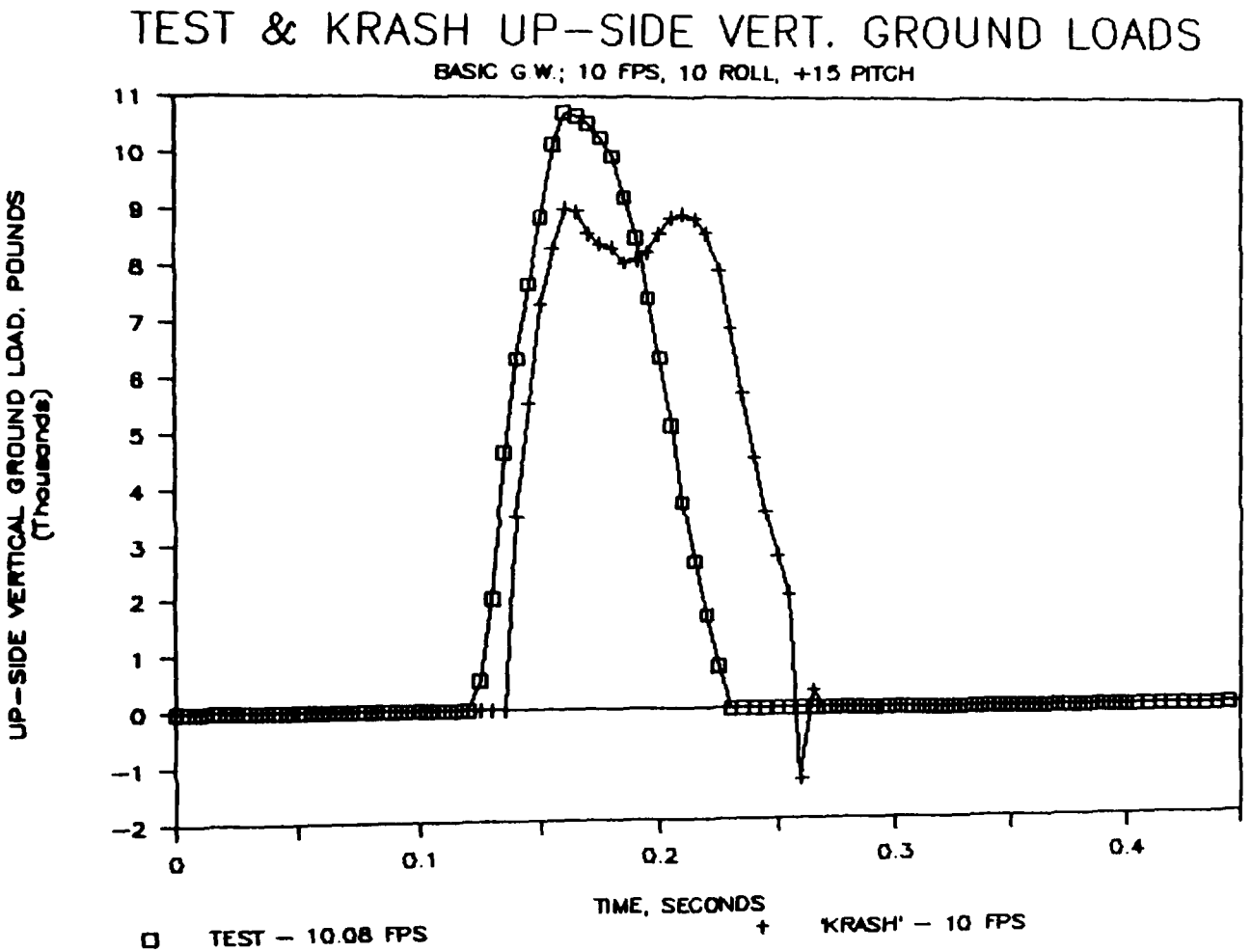

Graph A-10. Test and KRASH up-side vertical ground loads.

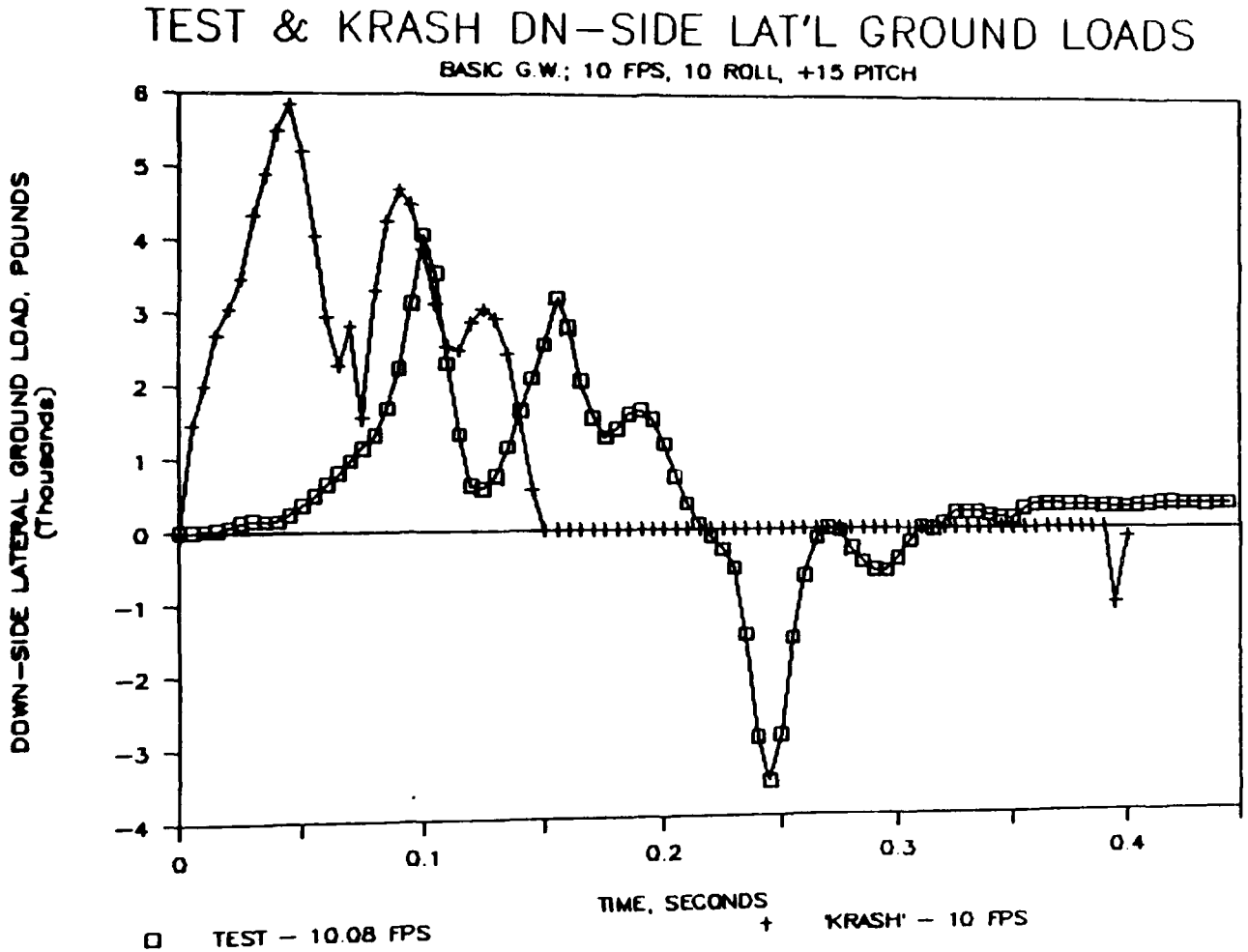

Graph A-11. Test and KRASH down-side lateral ground loads.

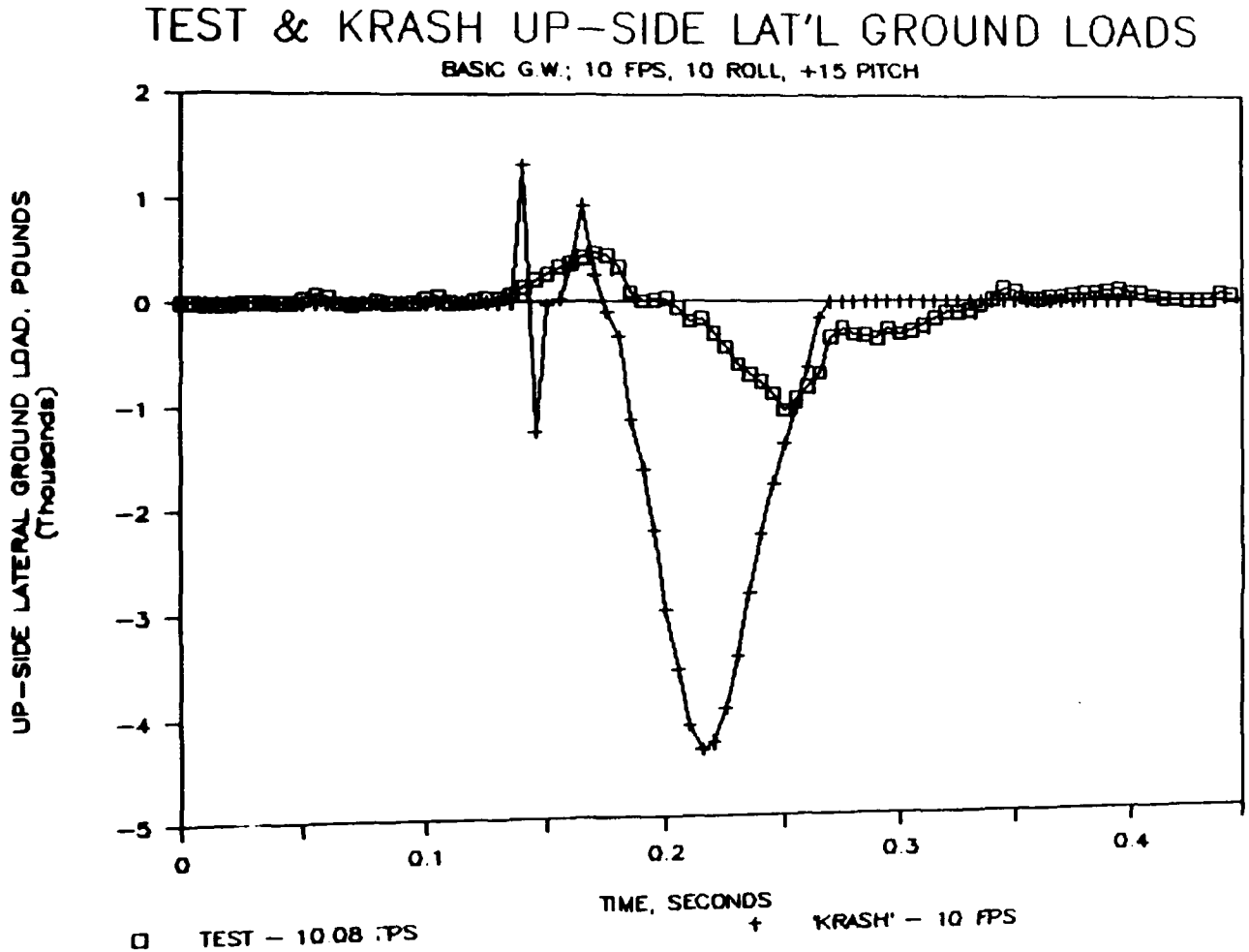

Graph A-12. Test and KRASH up-side lateral ground loads.

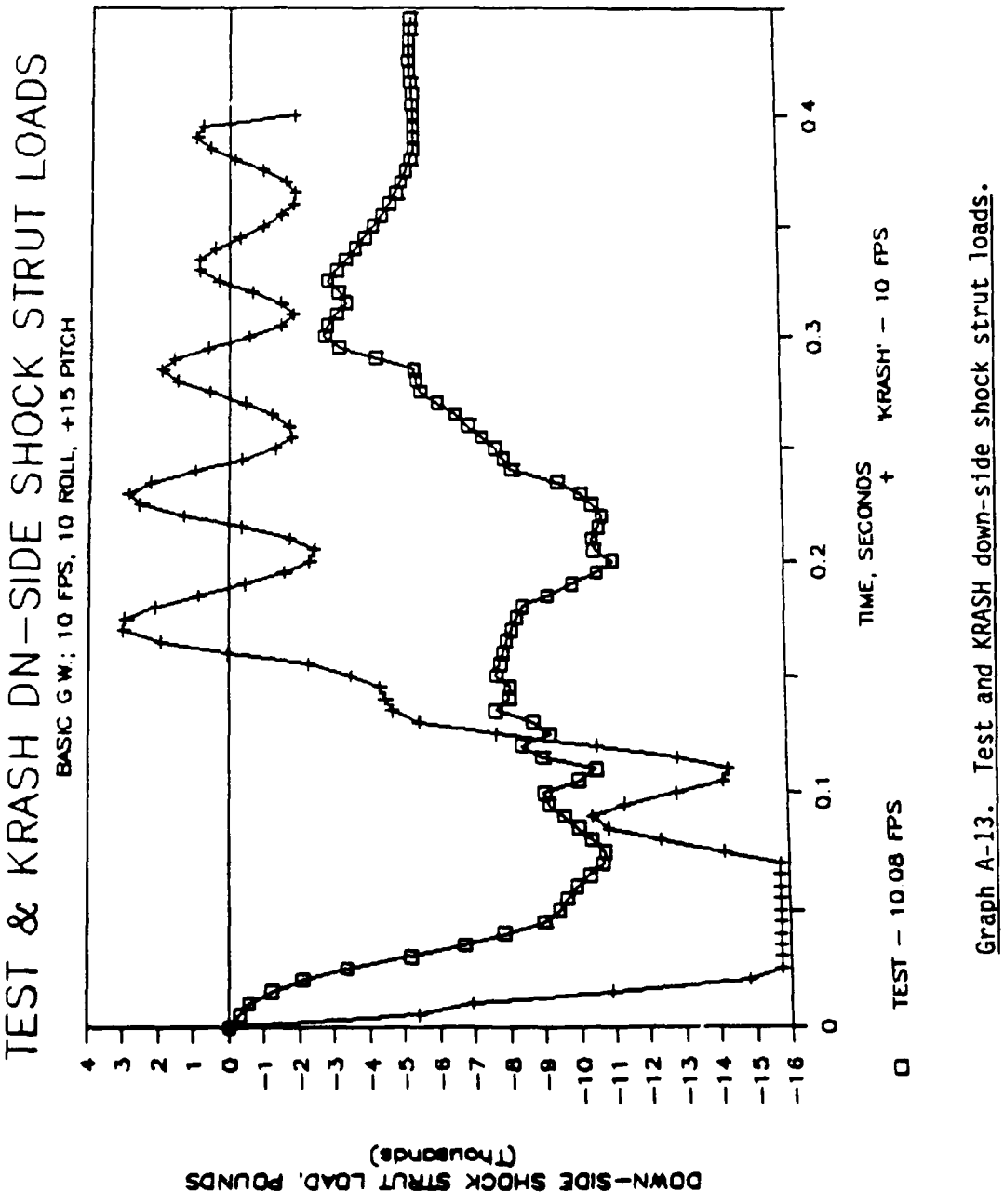

Graph A-13. Test and KRASH down-side shock strut loads.

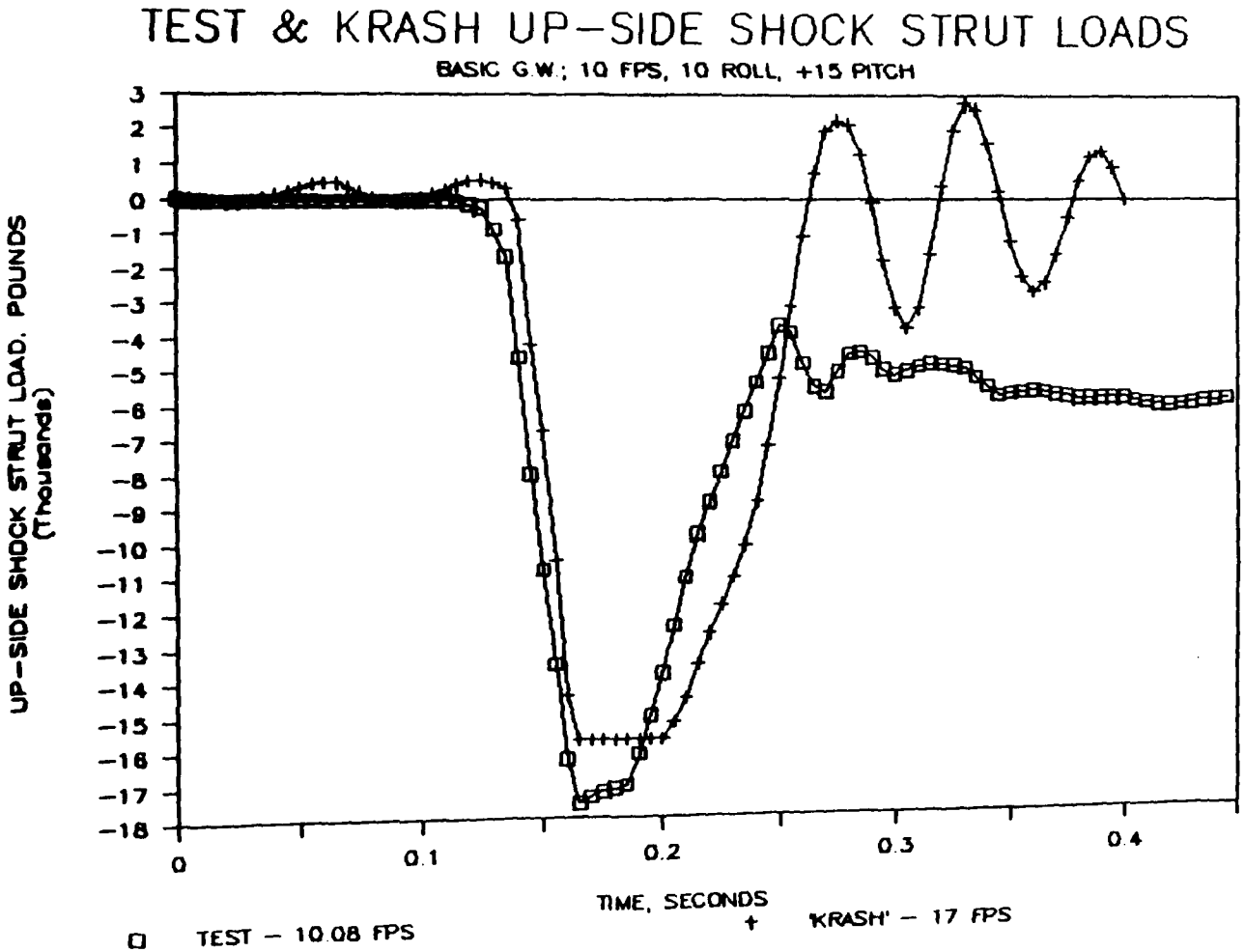

Graph A-14. Test and KRASH up-side shock strut loads.

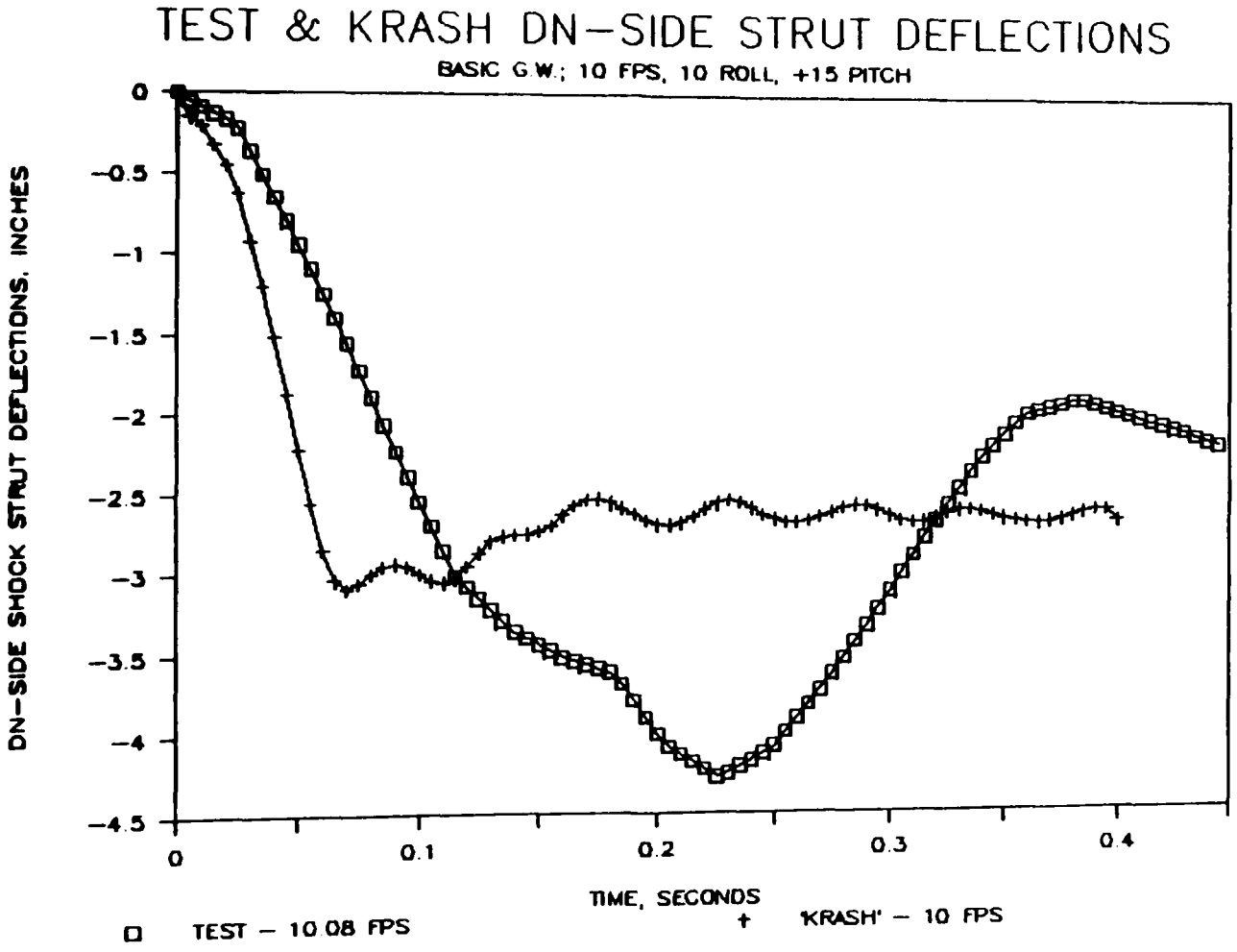

Graph A-15. Test and KRASH down-side strut deflections.

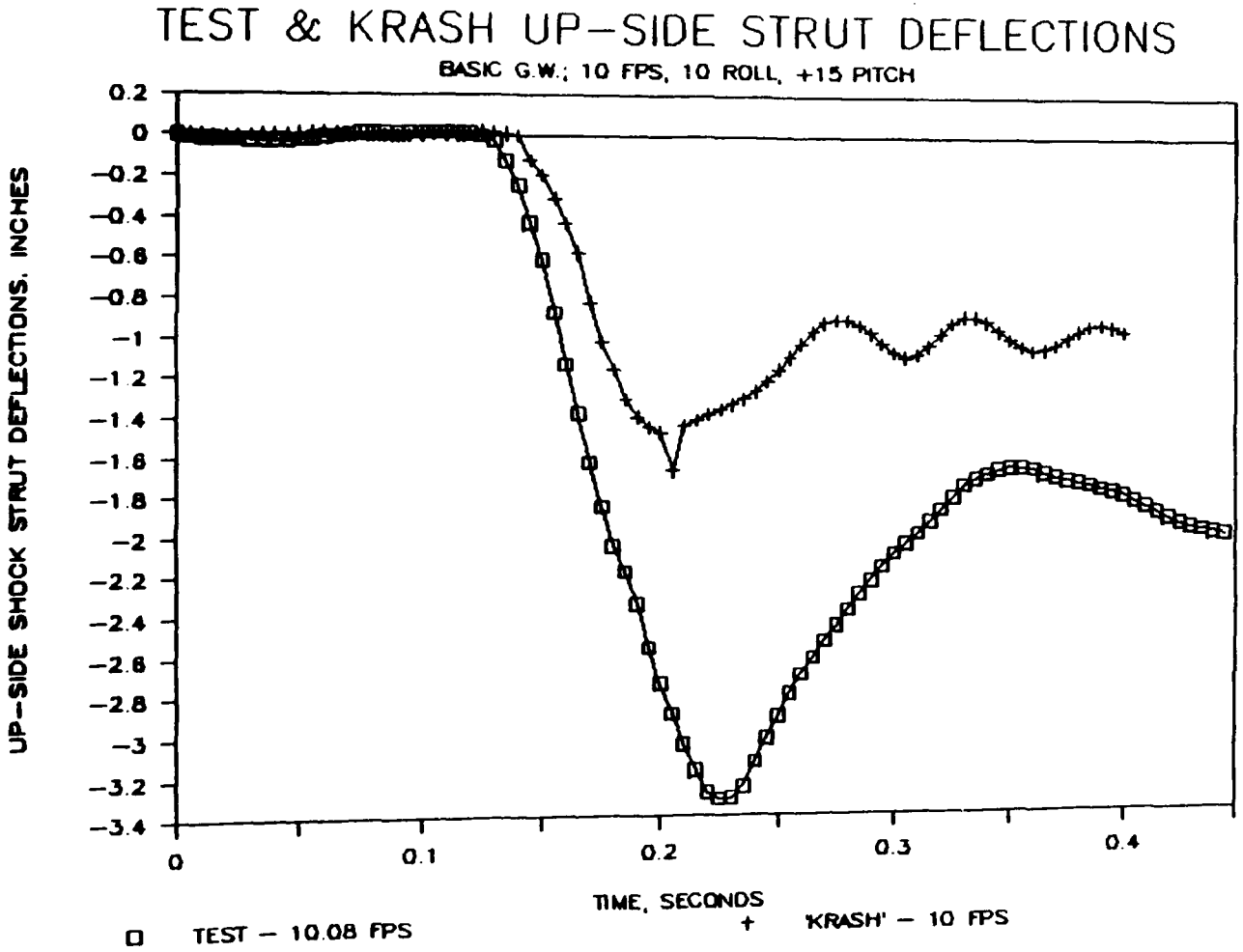

Graph A-16. Test and KRASH up-side strut deflections.

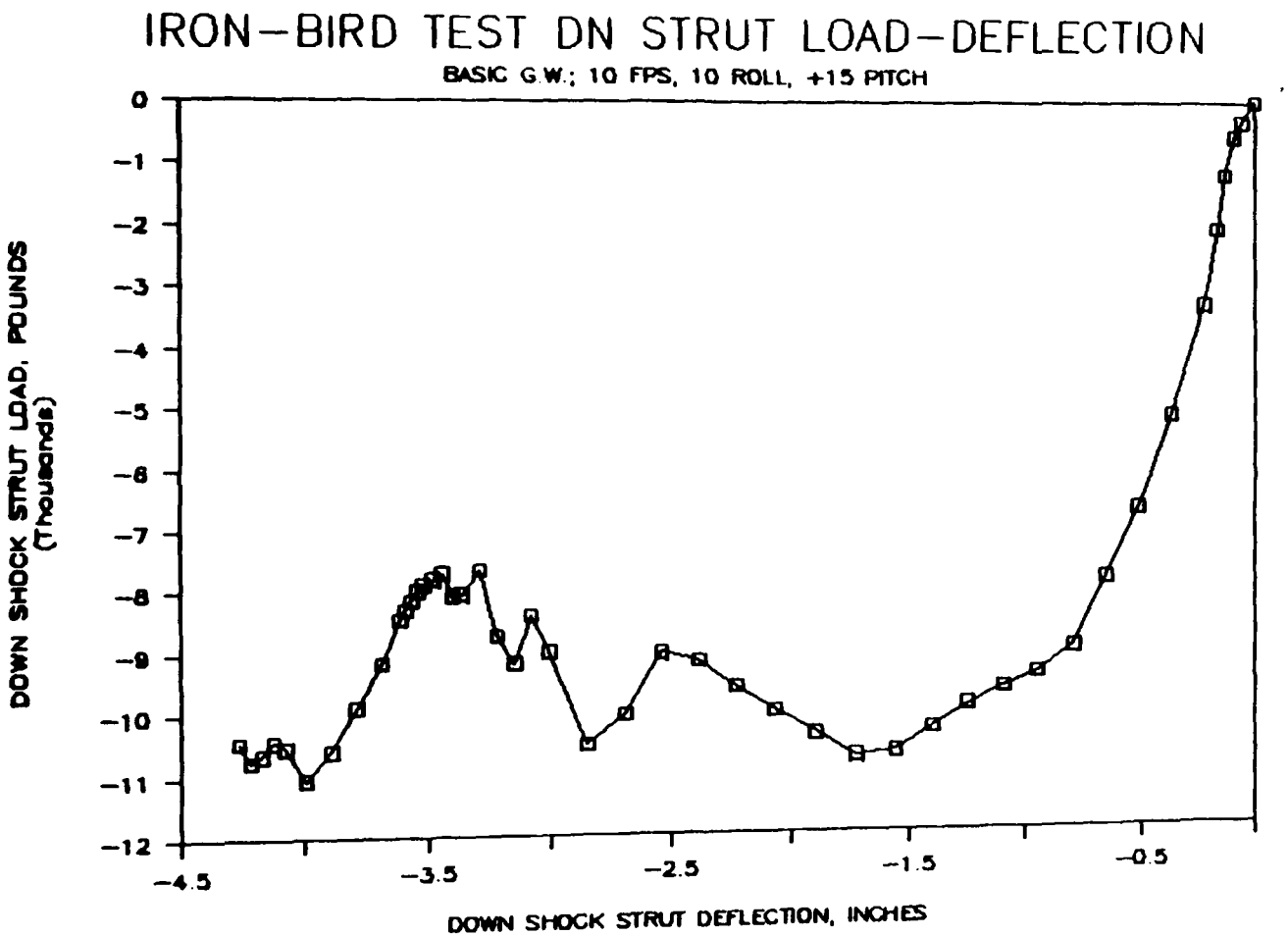

Graph A-17. Iron-bird test down-side strut load-deflection curve.

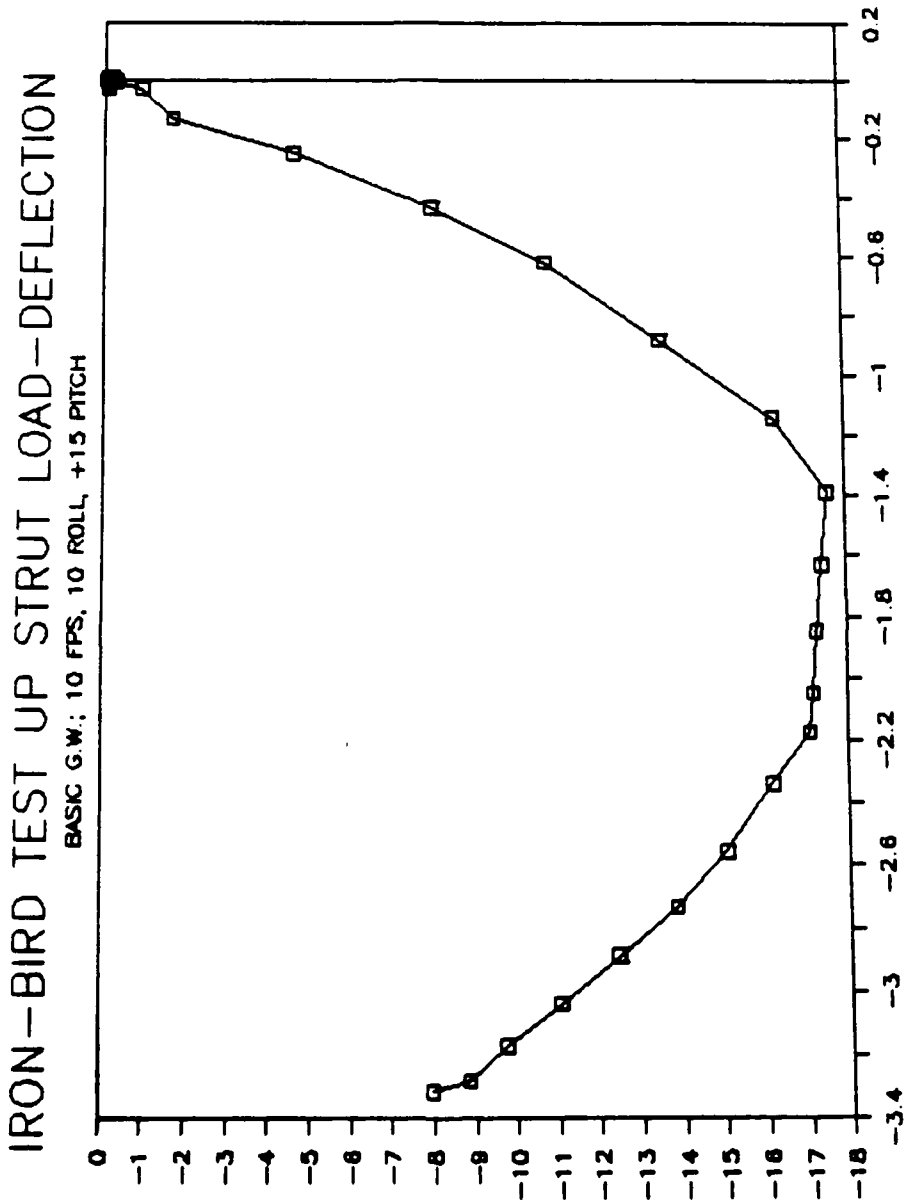

Graph A-18. Iron-bird test up-side strut load-deflection curve.

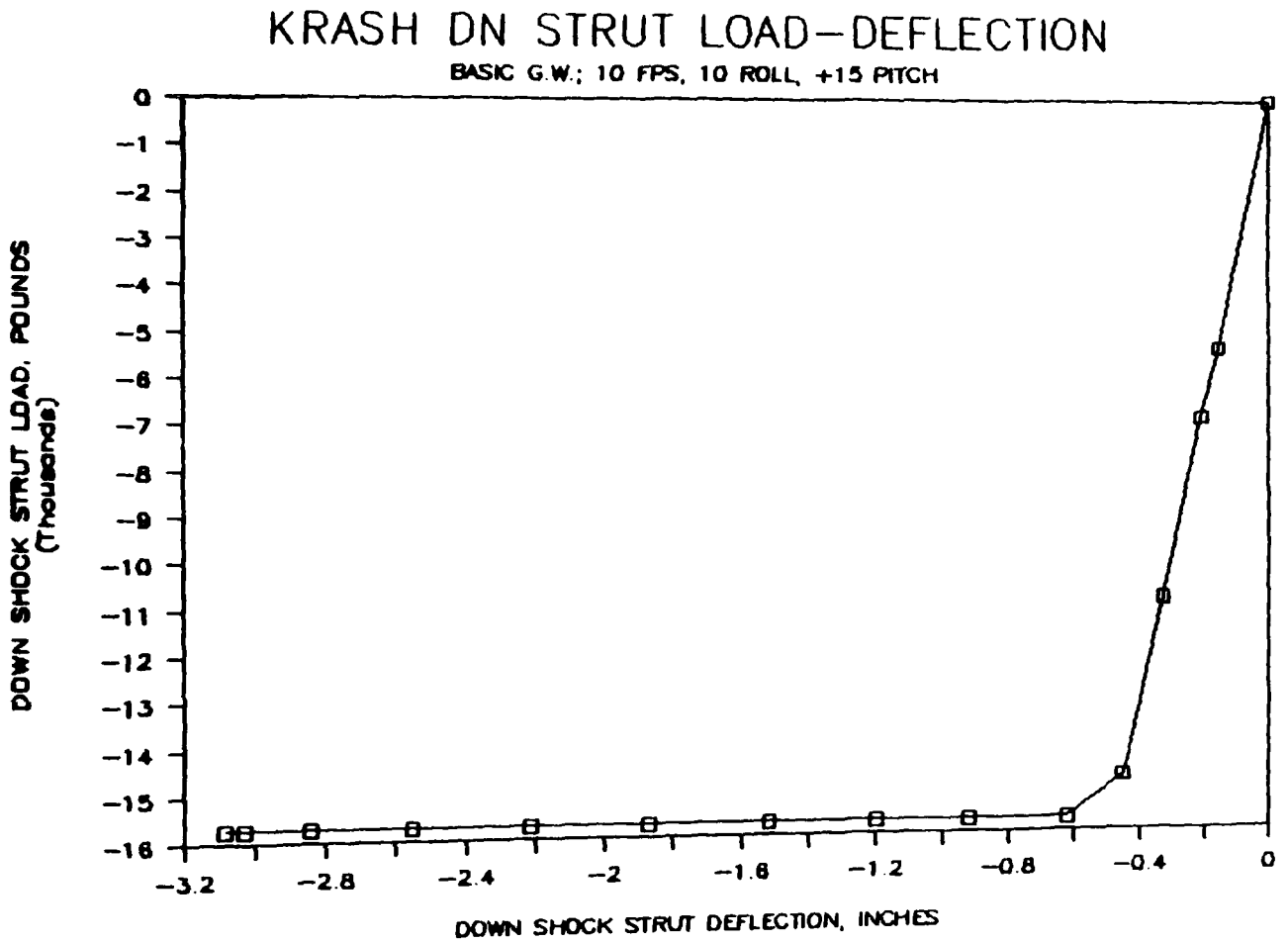

Graph A-19. KRASH down-side strut load-deflection curve.

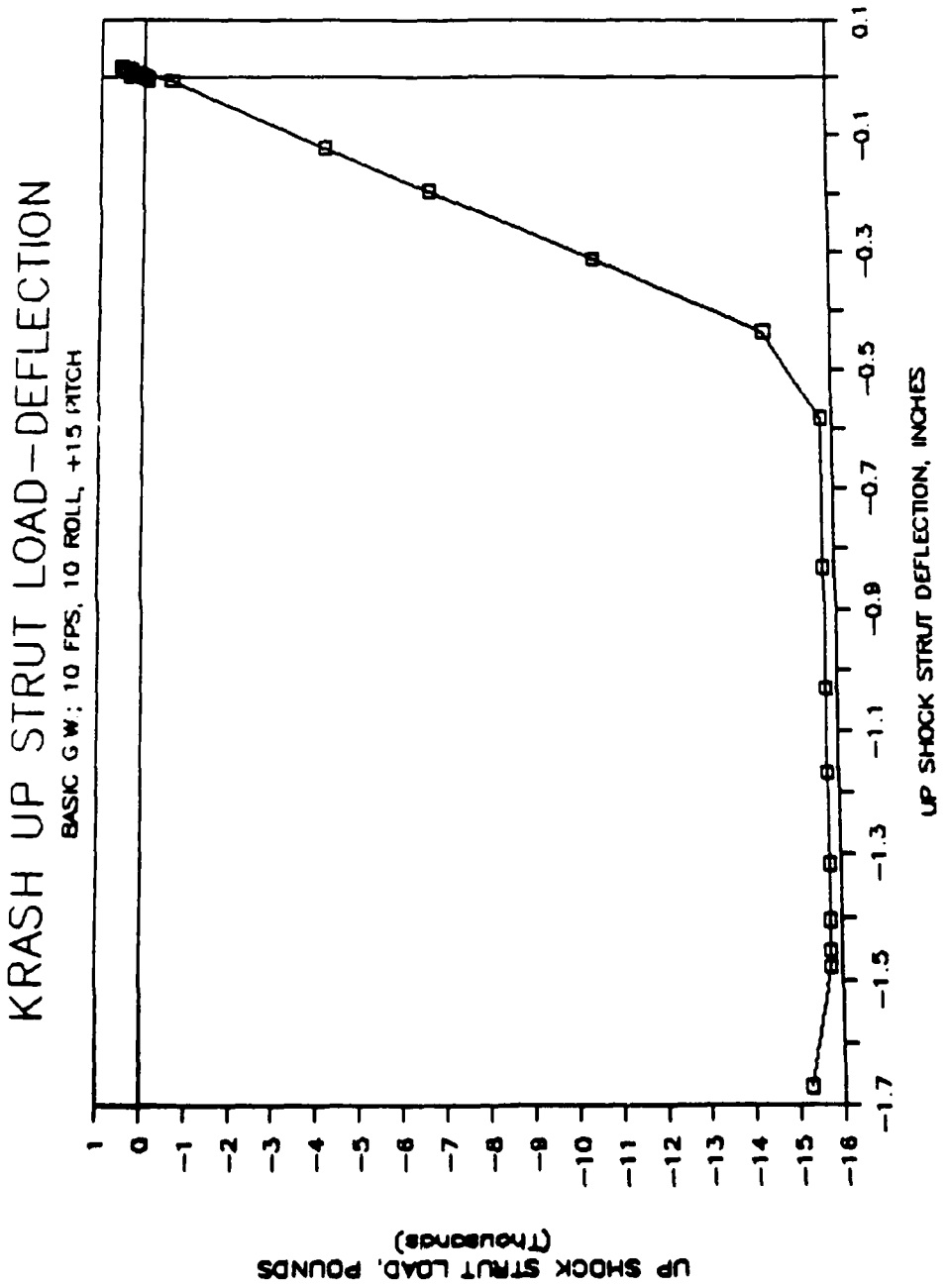

Graph A-20. KRASH up-side strut load-deflection curve.

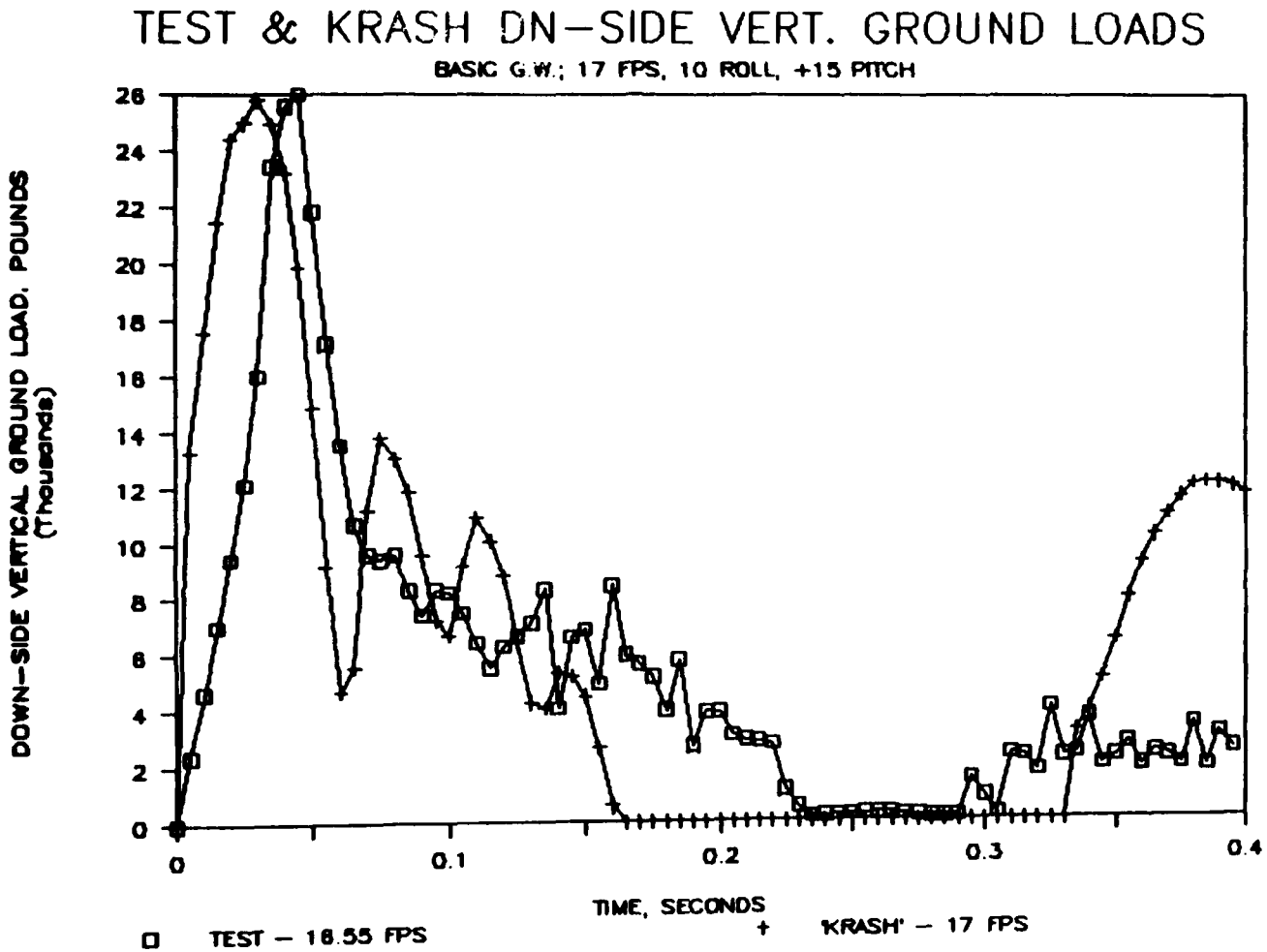

Graph A-21. Test and KRASH down-side vertical ground loads.

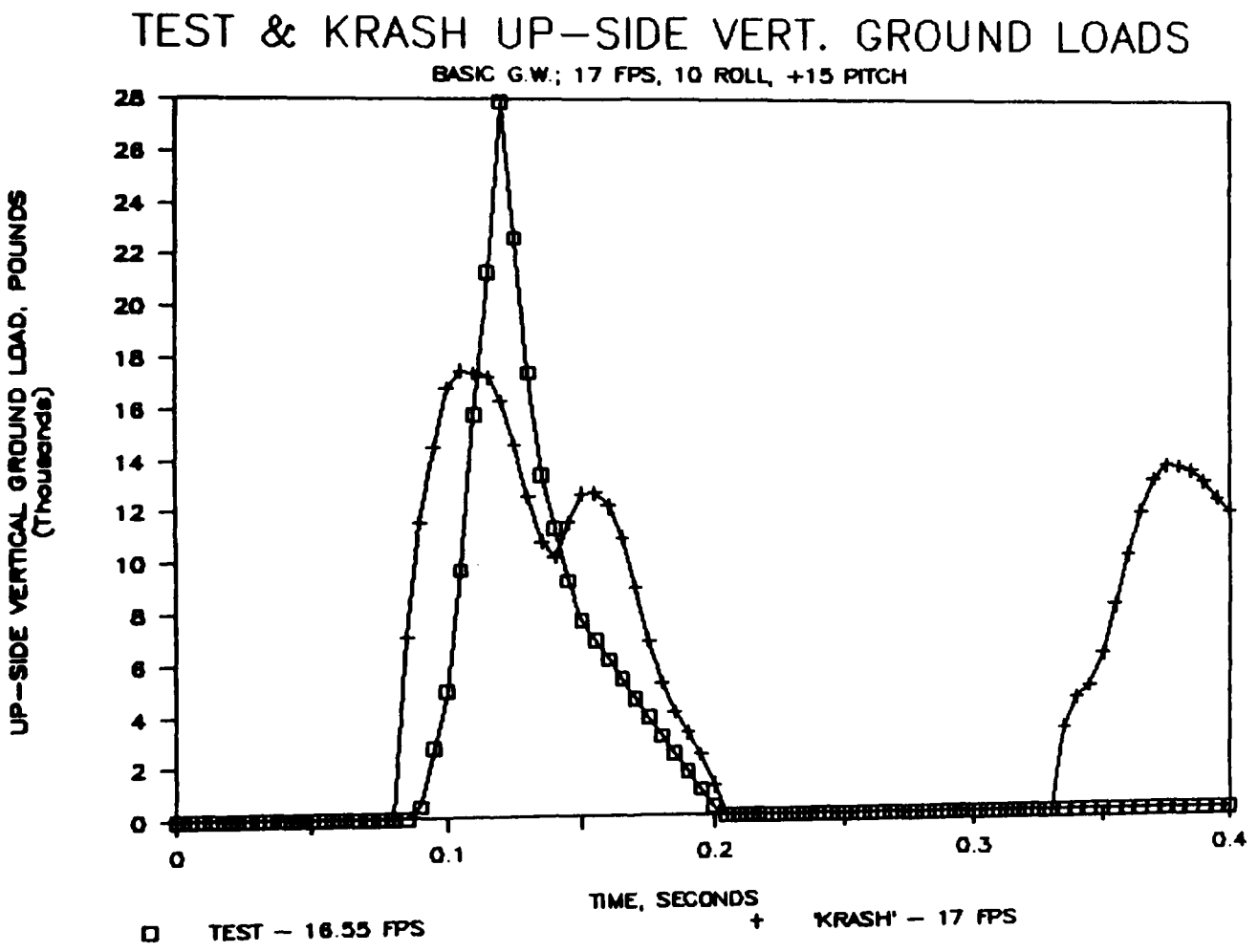

Graph A-22. Test and KRASH up-side vertical ground loads.

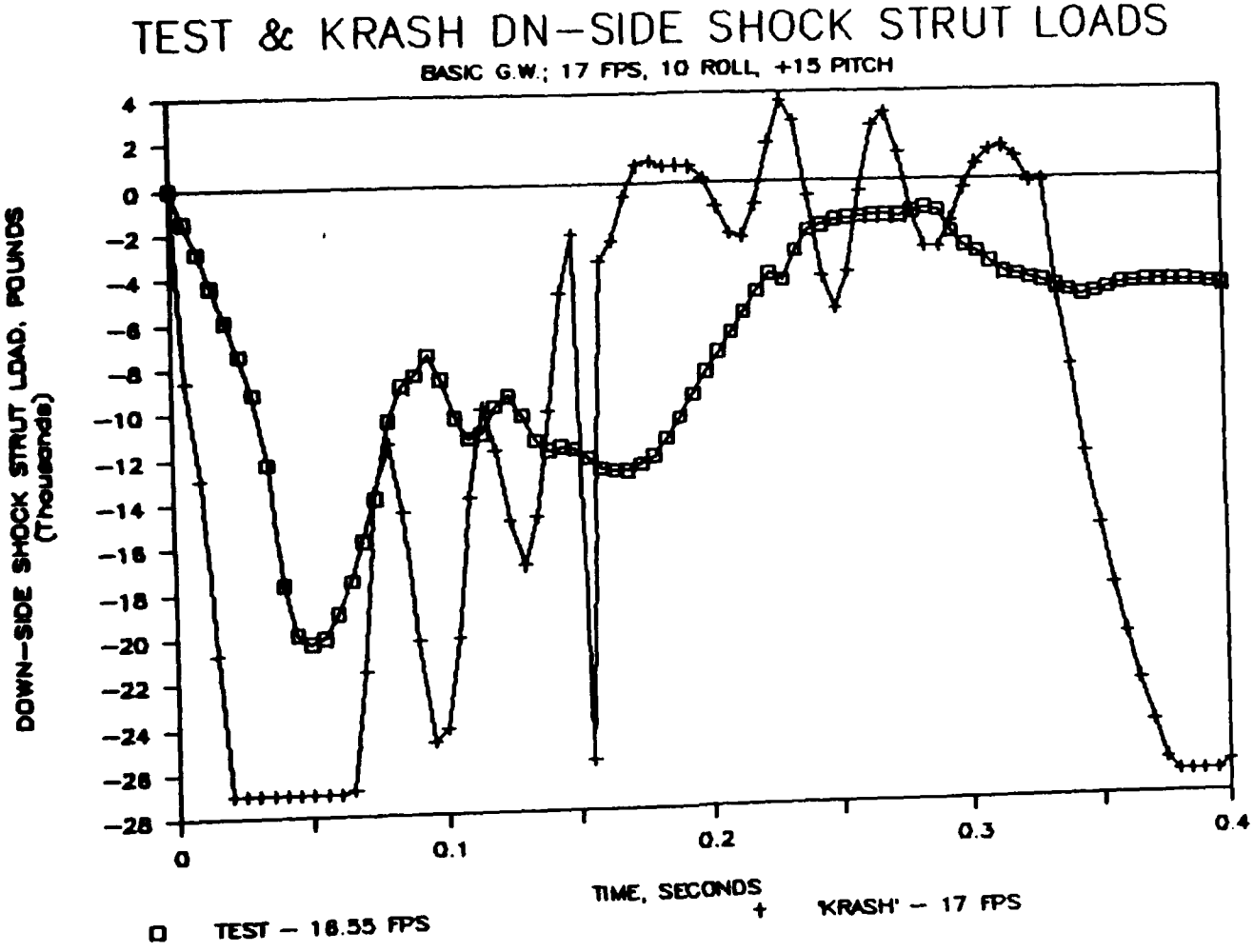

Graph A-23. Test and KRASH down-side shock strut loads.

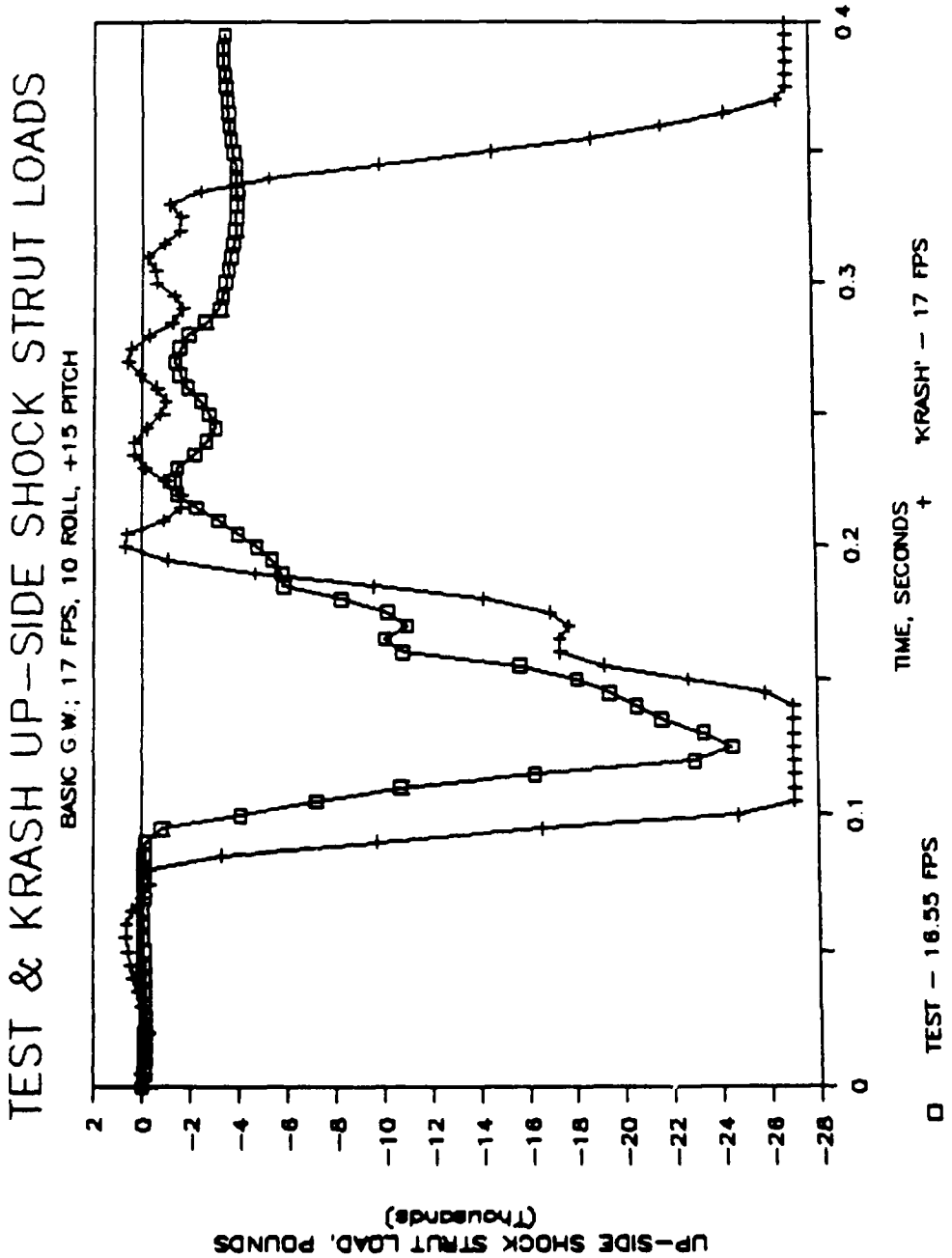

Graph A-24. Test and KRASH up-side shock strut loads.

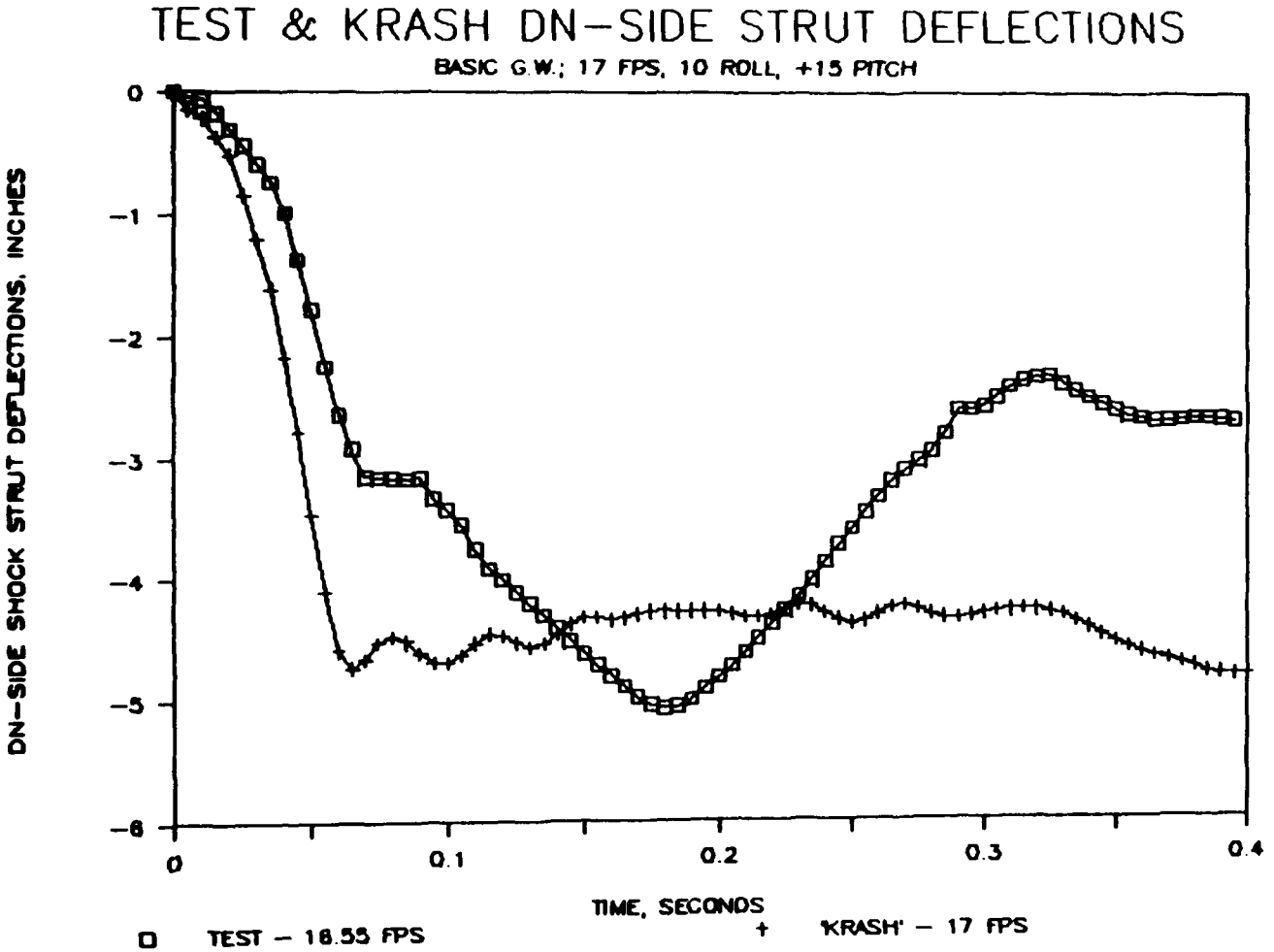

Graph A-25. Test and KRASH down-side strut deflections.

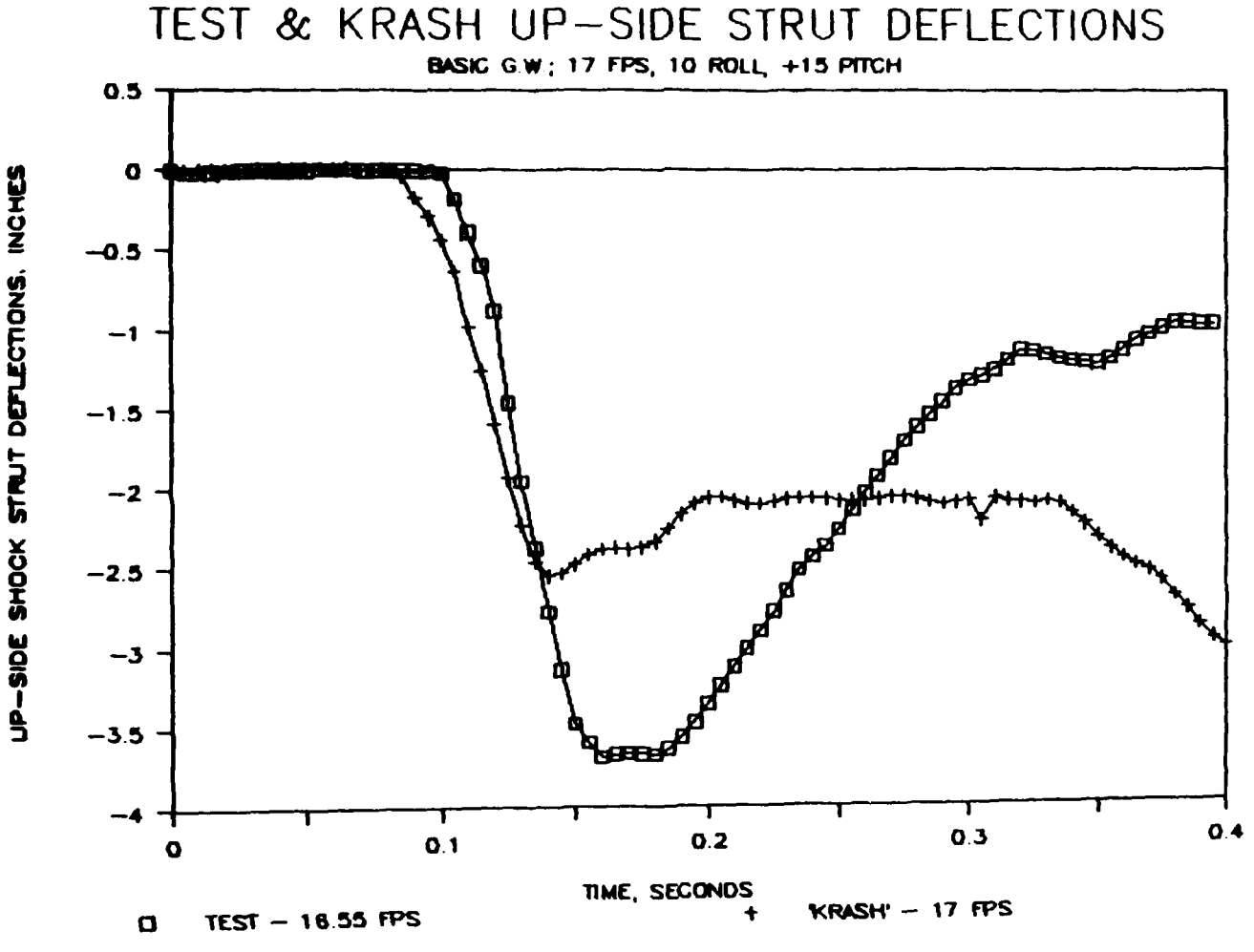

Graph A-26. Test and KRASH up-side strut deflections.

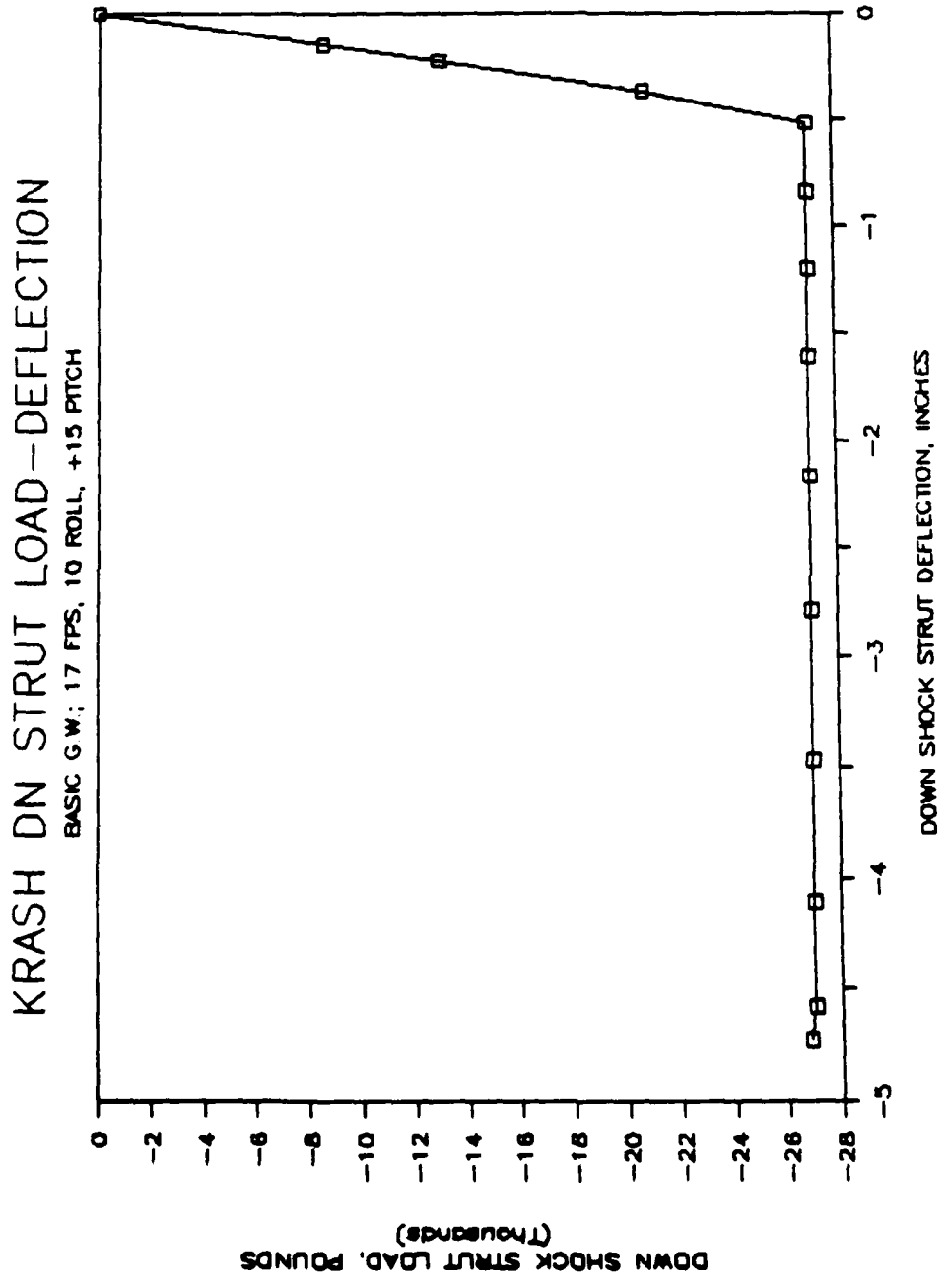

Graph A-27. KRASH down-side strut load-deflection curve.

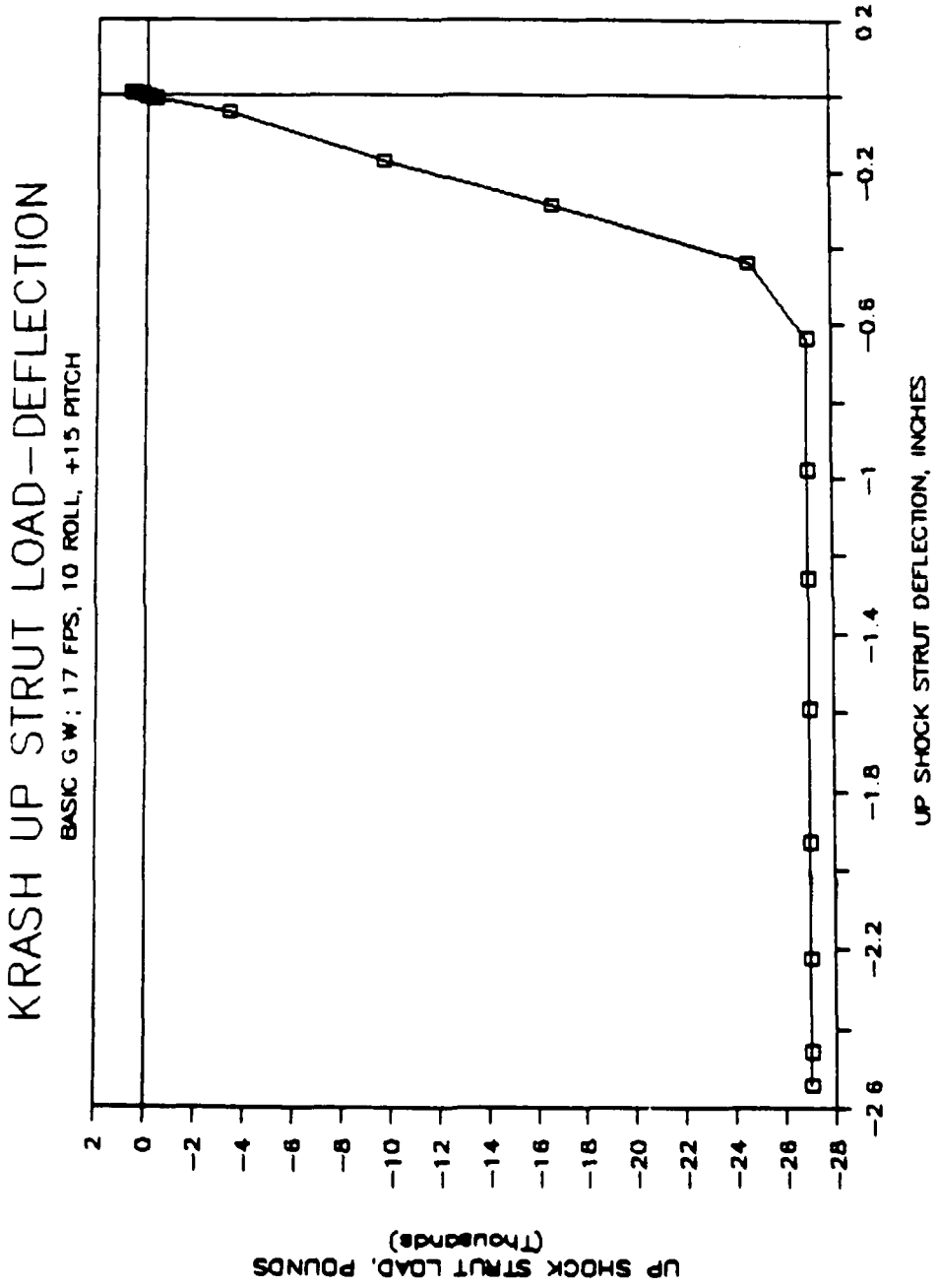

Graph A-28. KRASH up-side strut load-deflection curve.

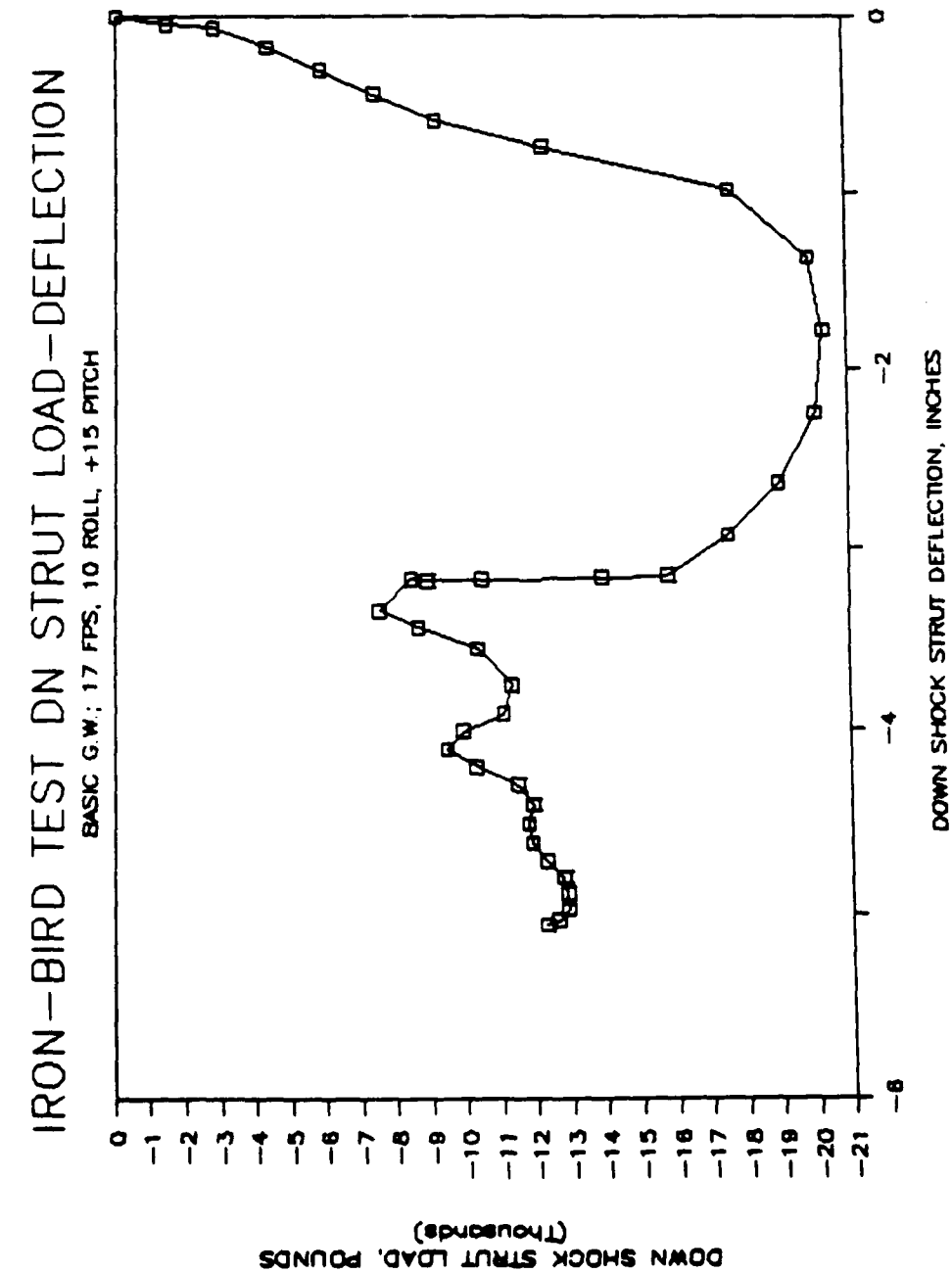

Graph A-29. Iron-bird test down-side strut load-deflection curve.

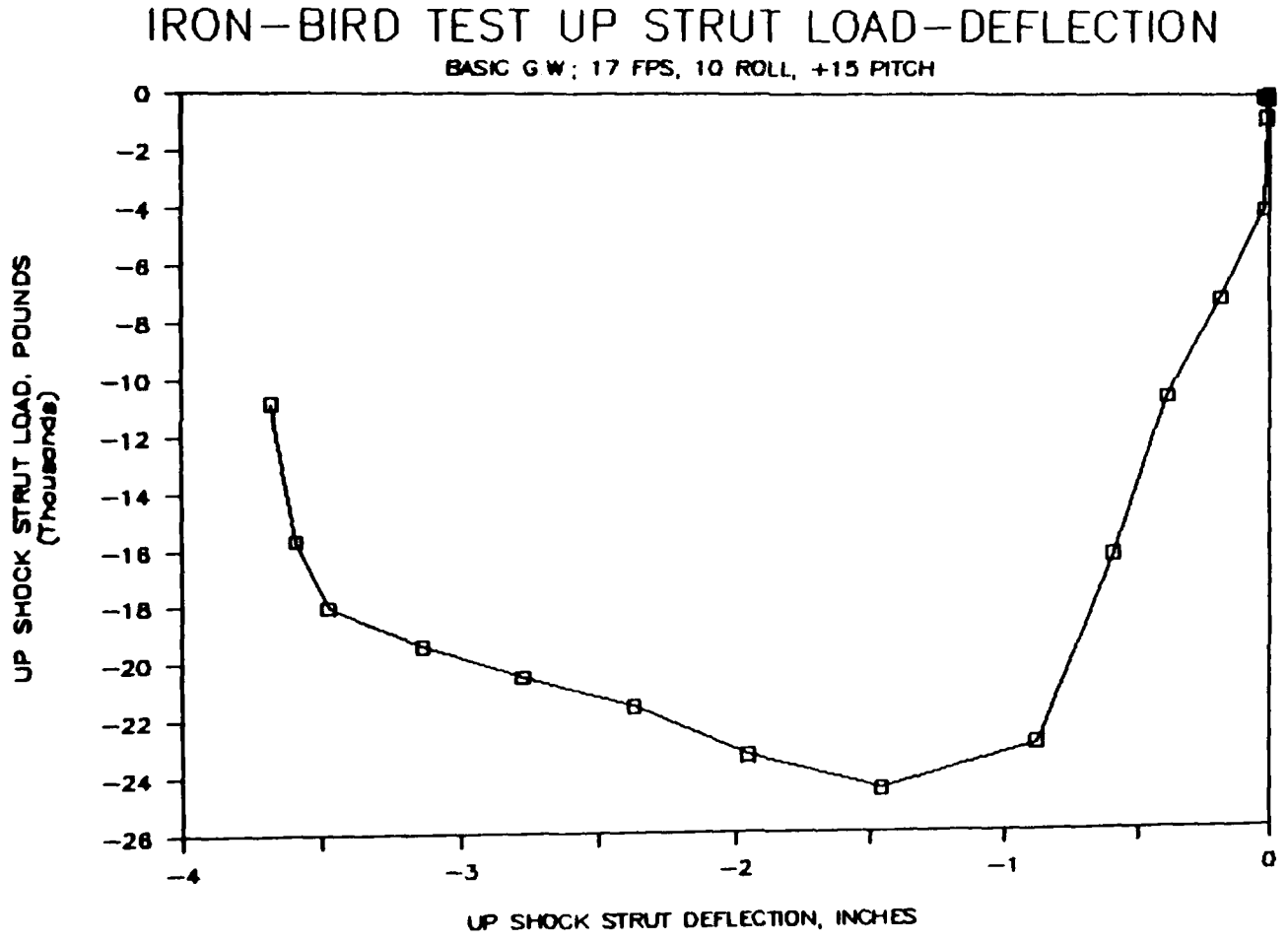

Graph A-30. Iron-bird test up-side strut load-deflection curve.

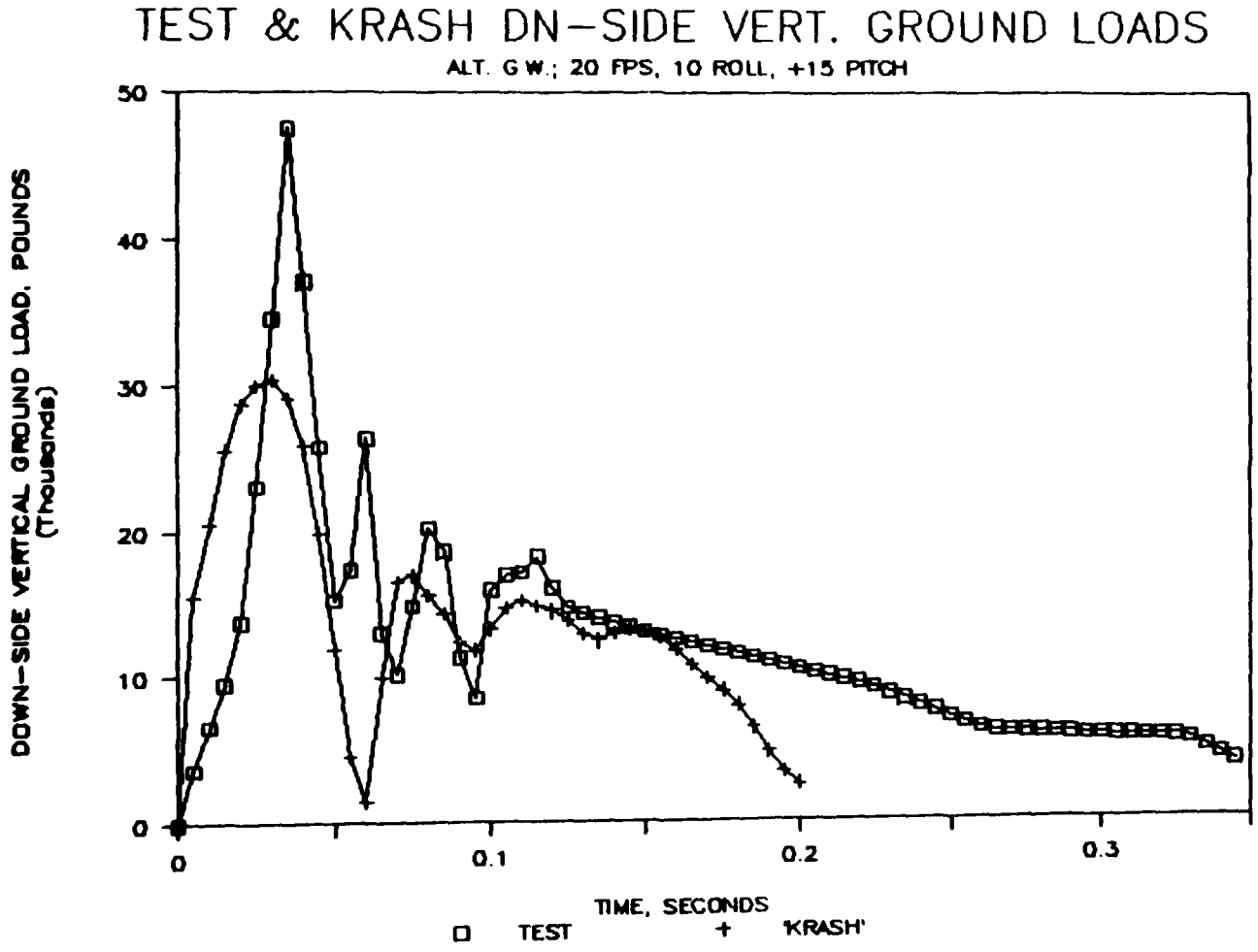

Graph A-31. Test and KRASH down-side vertical ground loads.

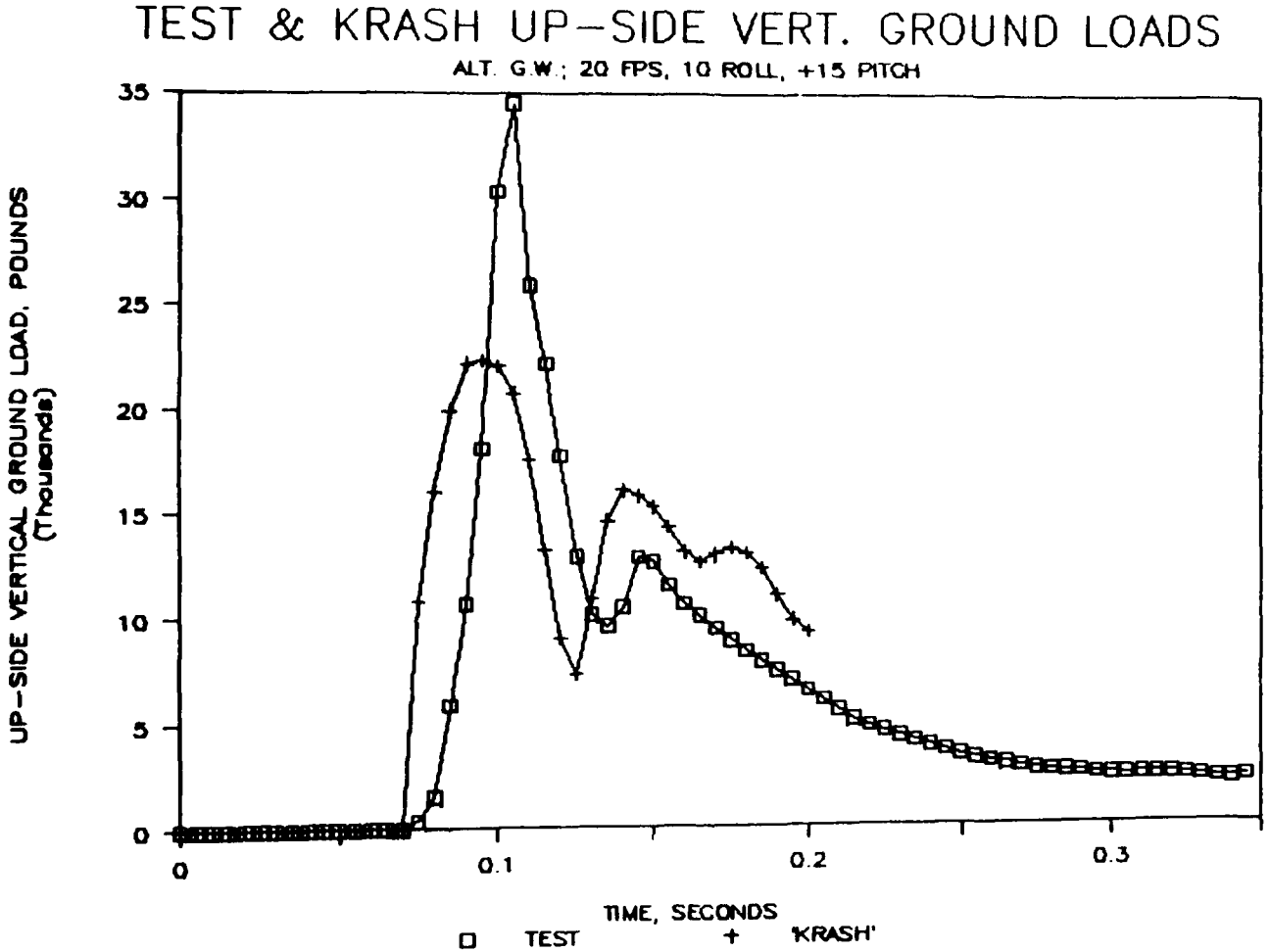

Graph A-32. Test and KRASH up-side vertical ground loads.

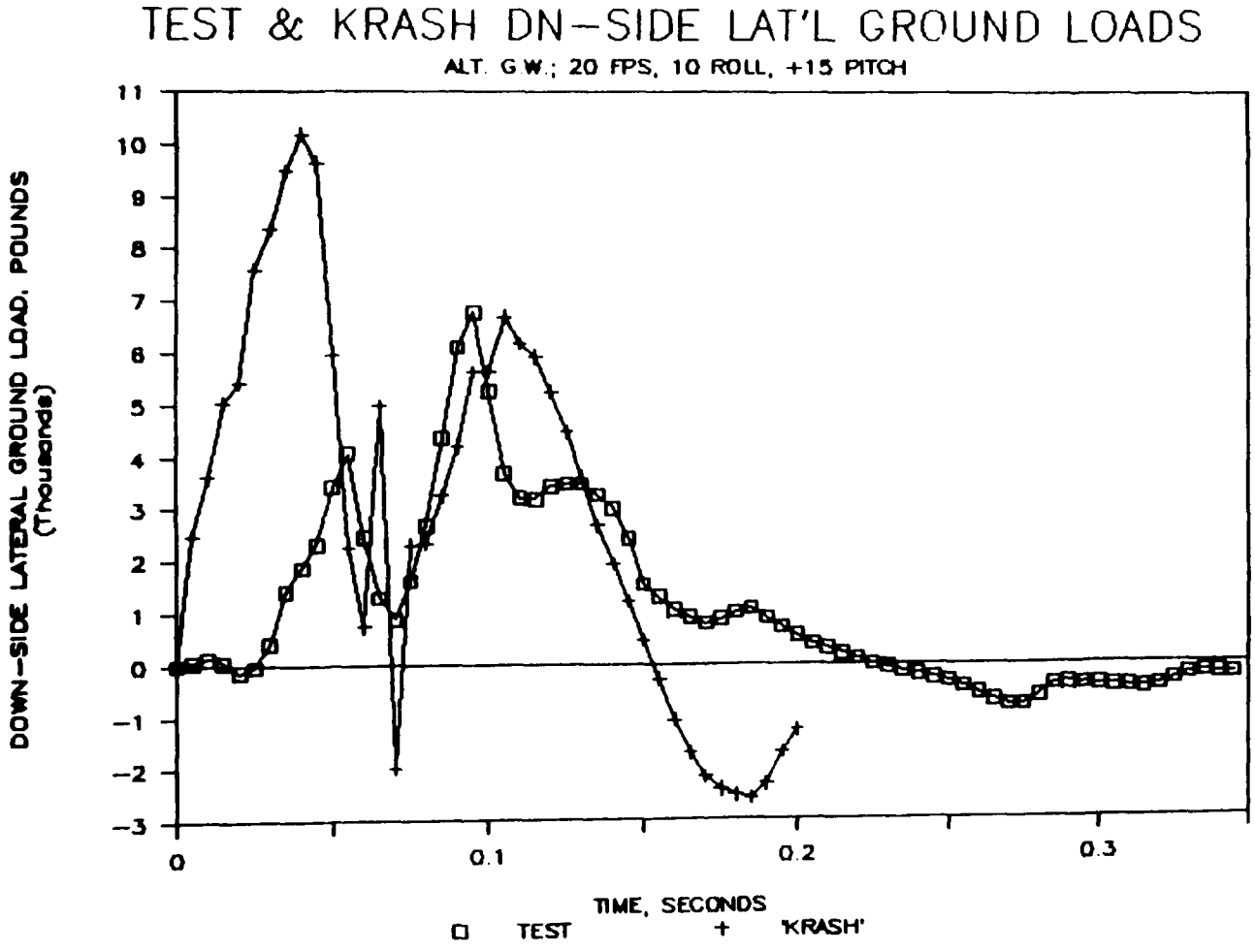

Graph A-33. Test and KRASH down-side lateral ground loads.

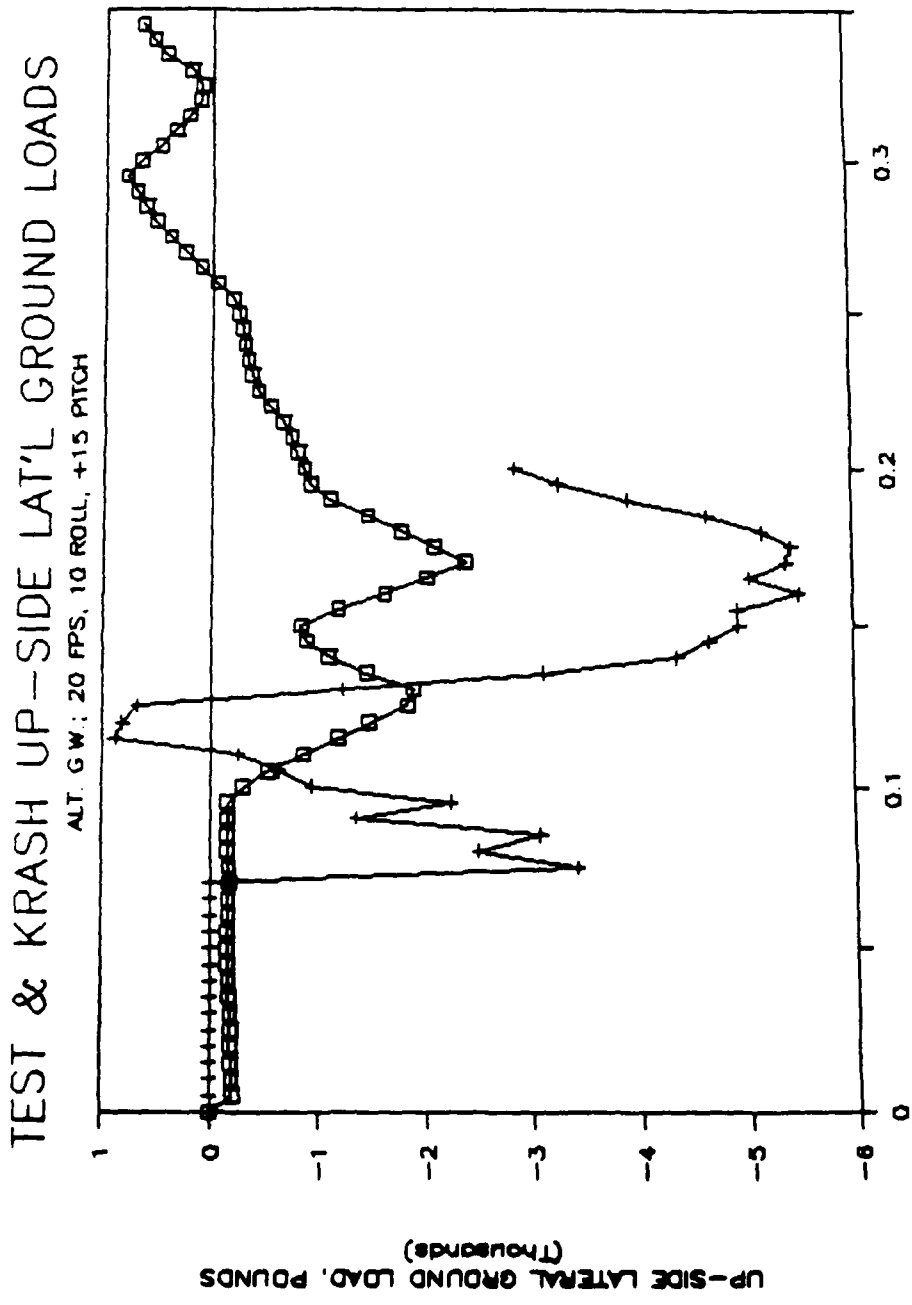

Graph A-34. Test and KRASH up-side lateral ground loads.

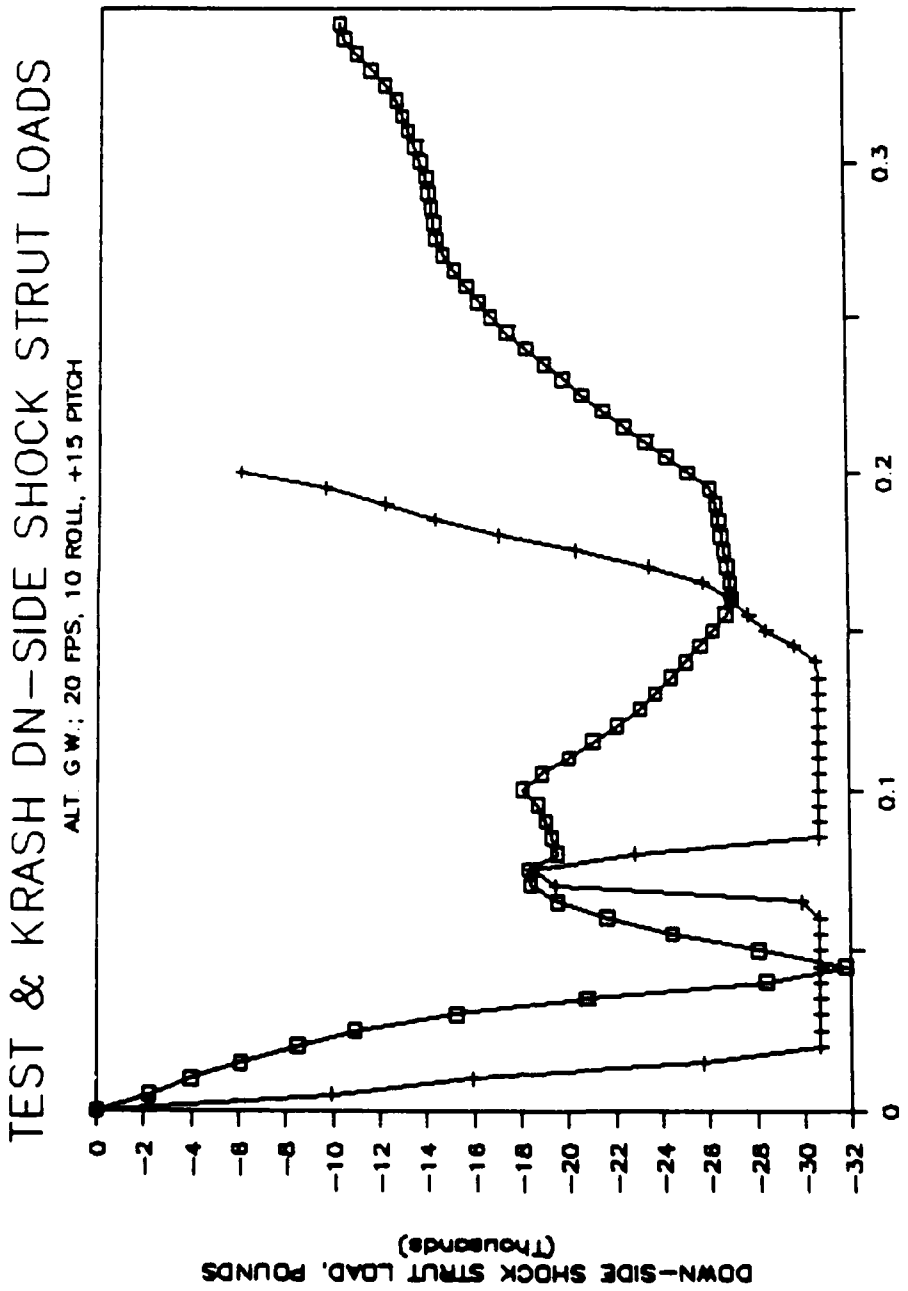

Graph A-35. Test and KRASH down-side shock strut loads.

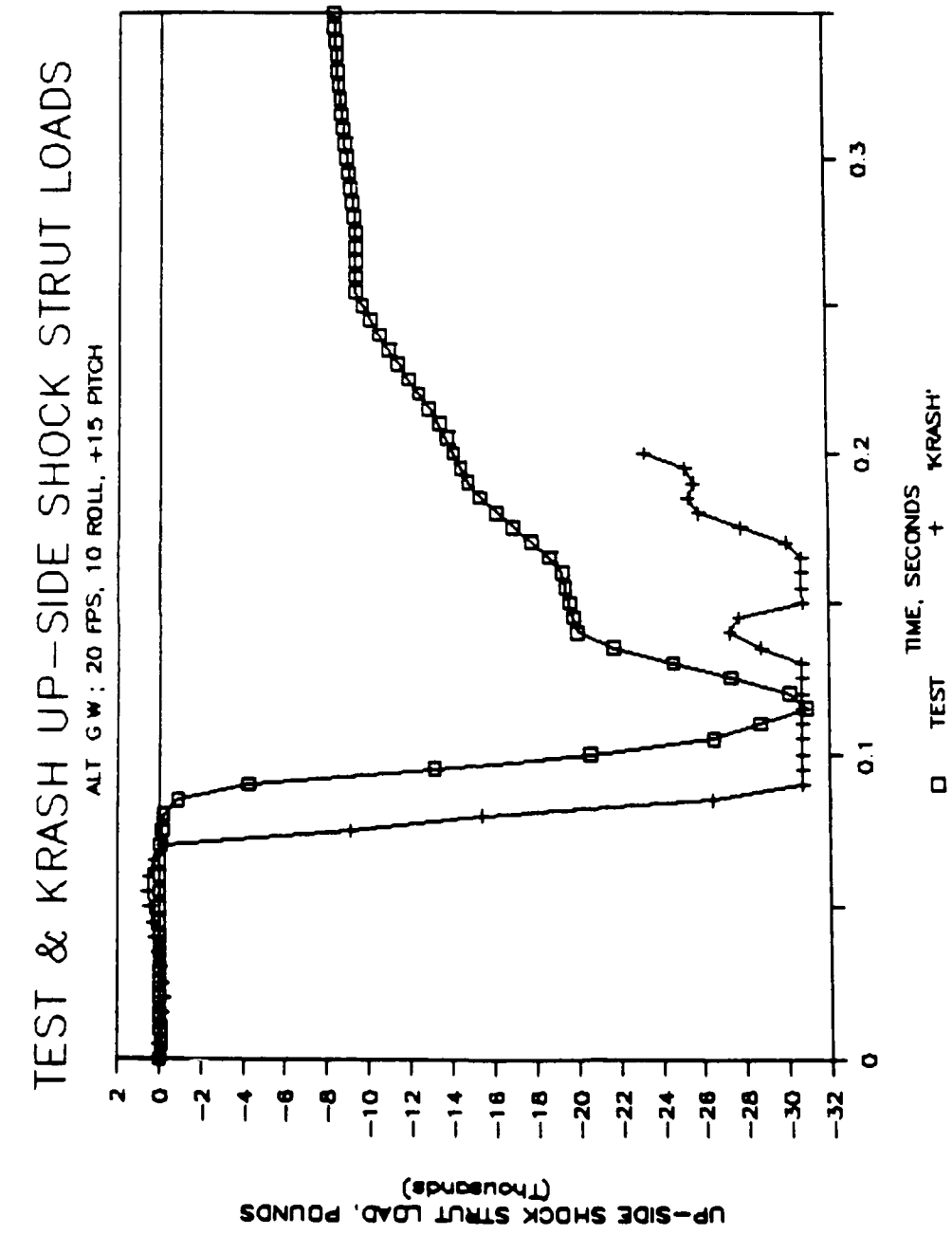

Graph A-36. Test and KRASH up-side shock strut loads.

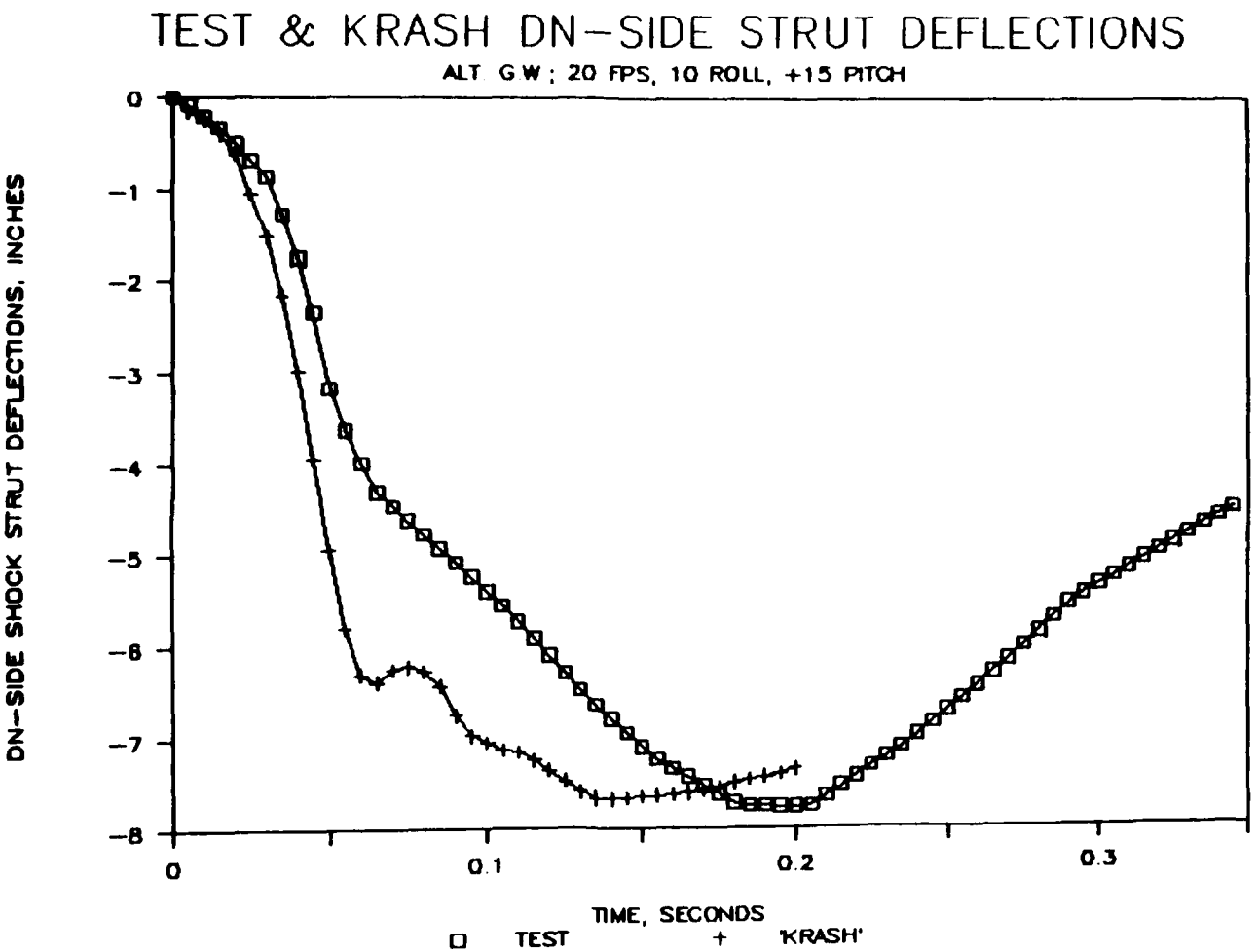

Graph A-37. Test and KRASH down-side strut deflections.

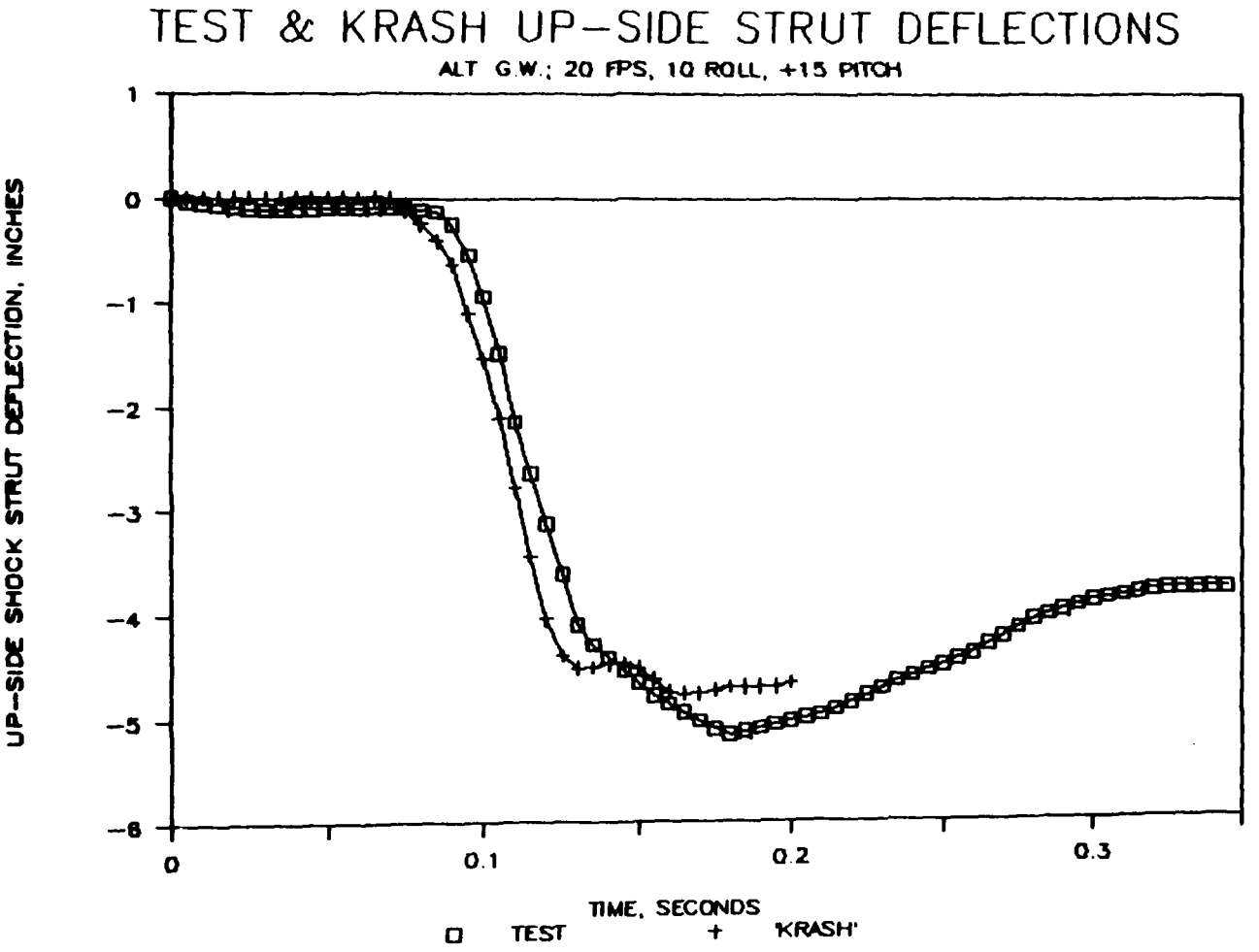

Graph A-38. Test and KRASH up-side strut deflections.

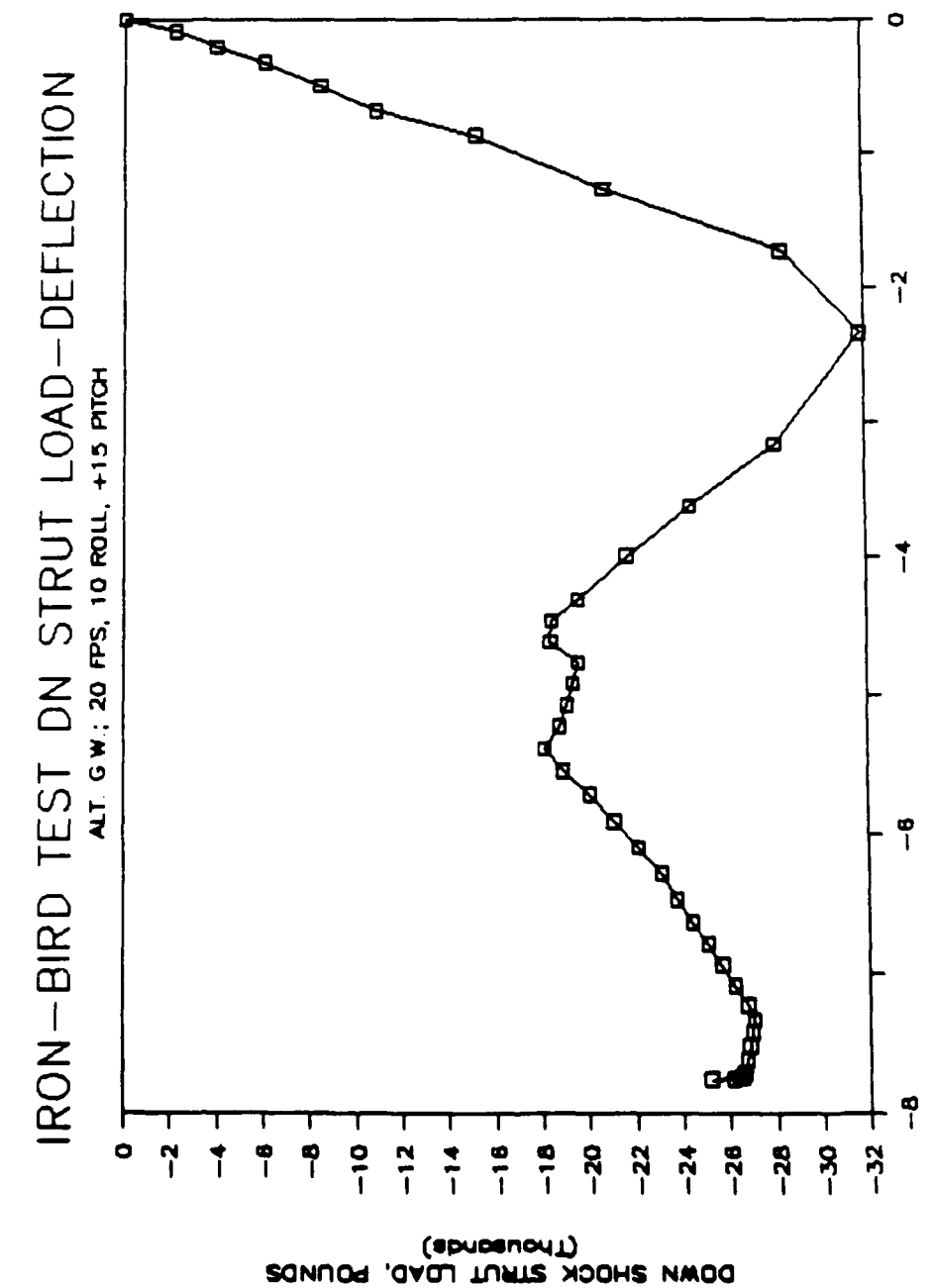

Graph A-39. Iron-bird test down-side strut load-deflection curve.

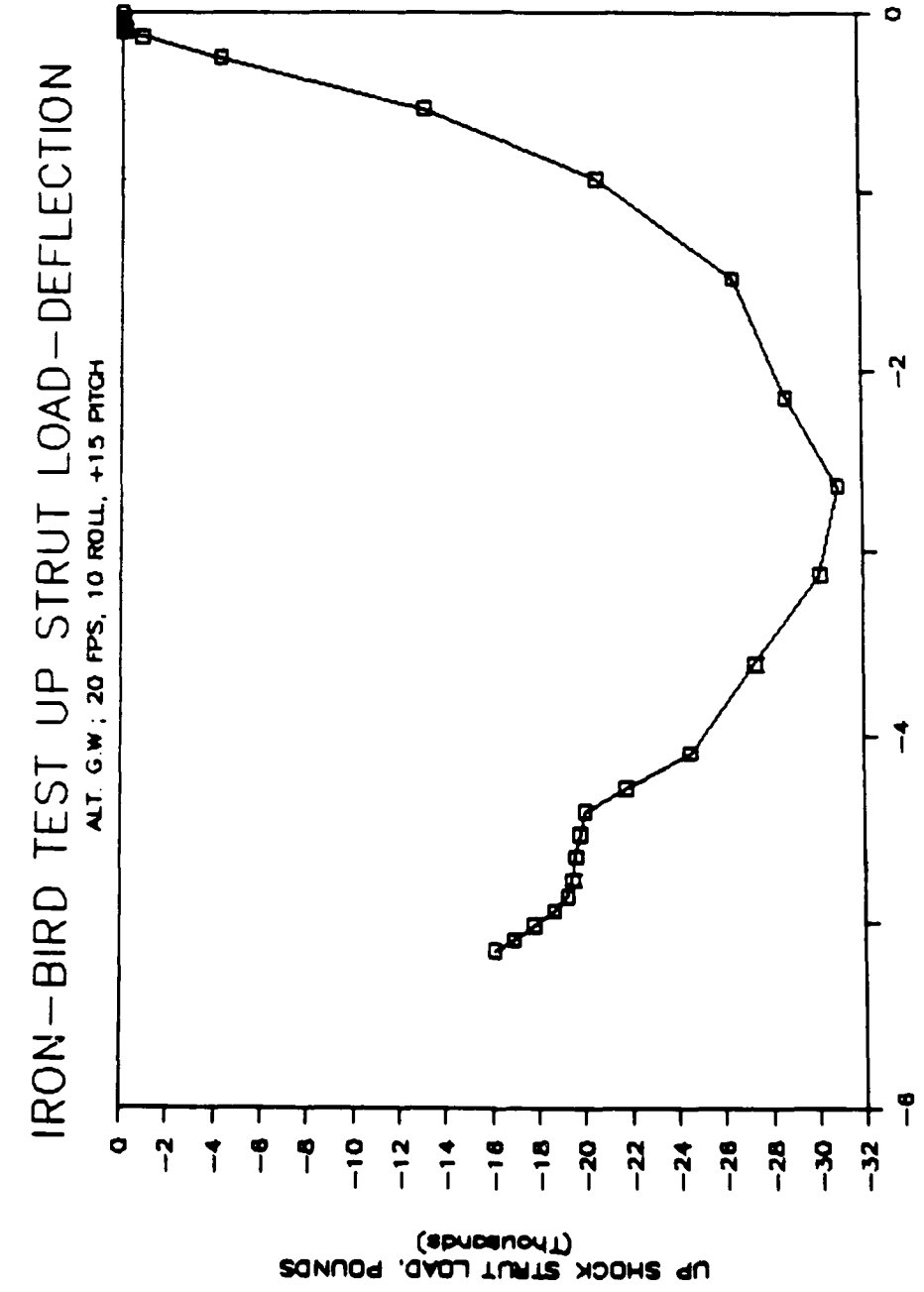

Graph A-40. Iron-bird test up-side strut load-deflection curve.

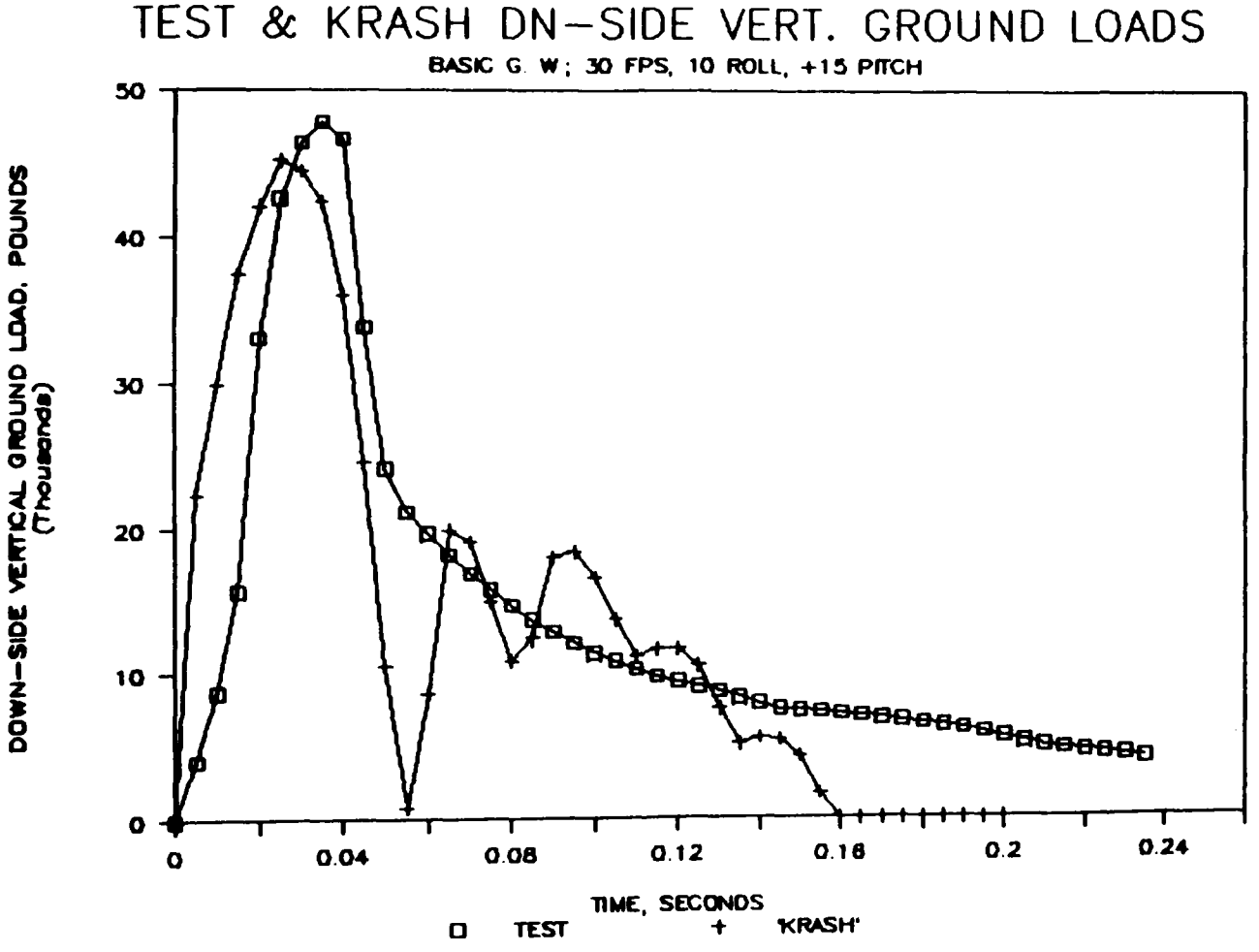

Graph A-41. Test and KRASH down-side vertical ground loads.

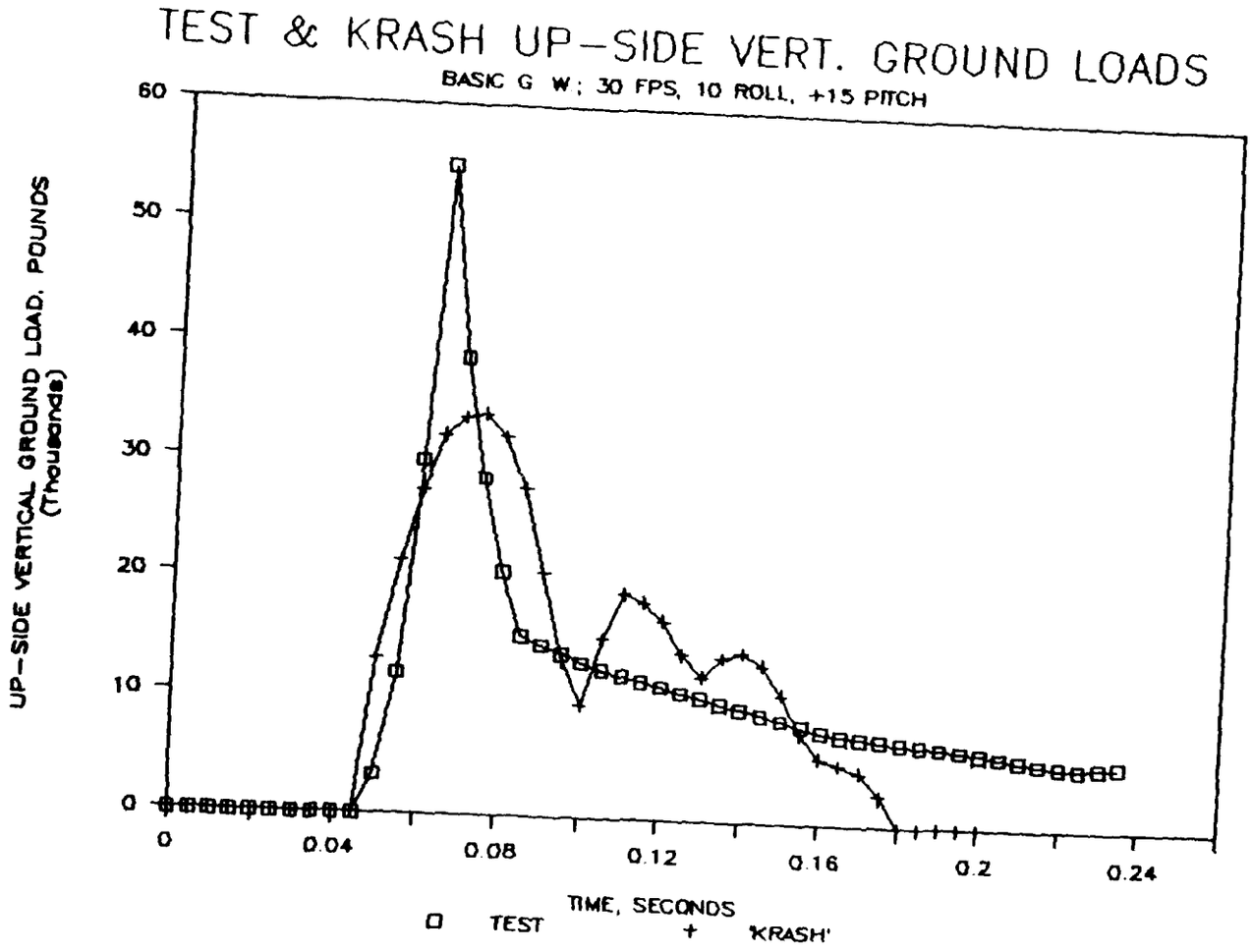

Graph A-42. Test and KRASH up-side vertical ground loads.

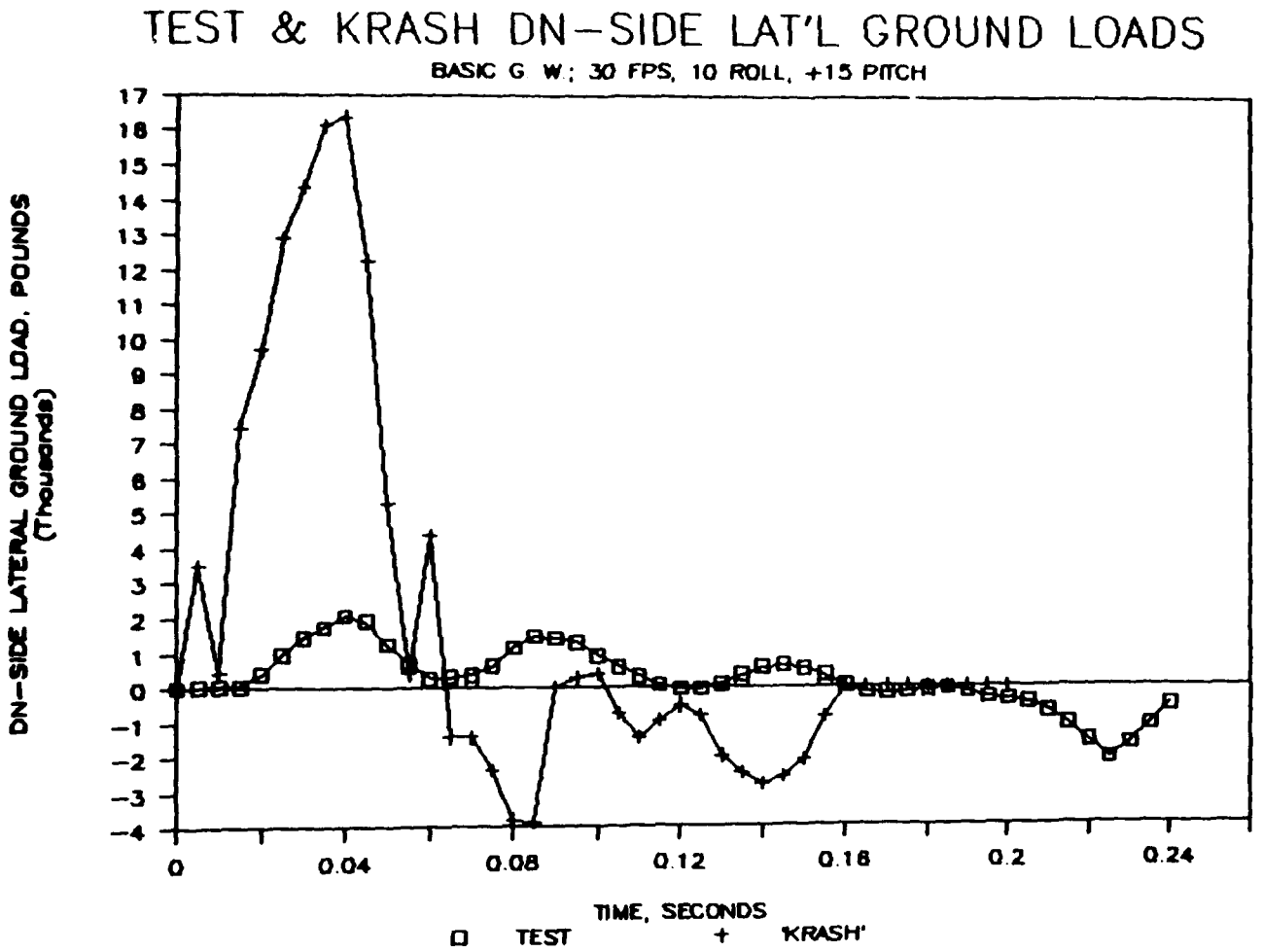

Graph A-43. Test and KRASH down-side lateral ground loads.

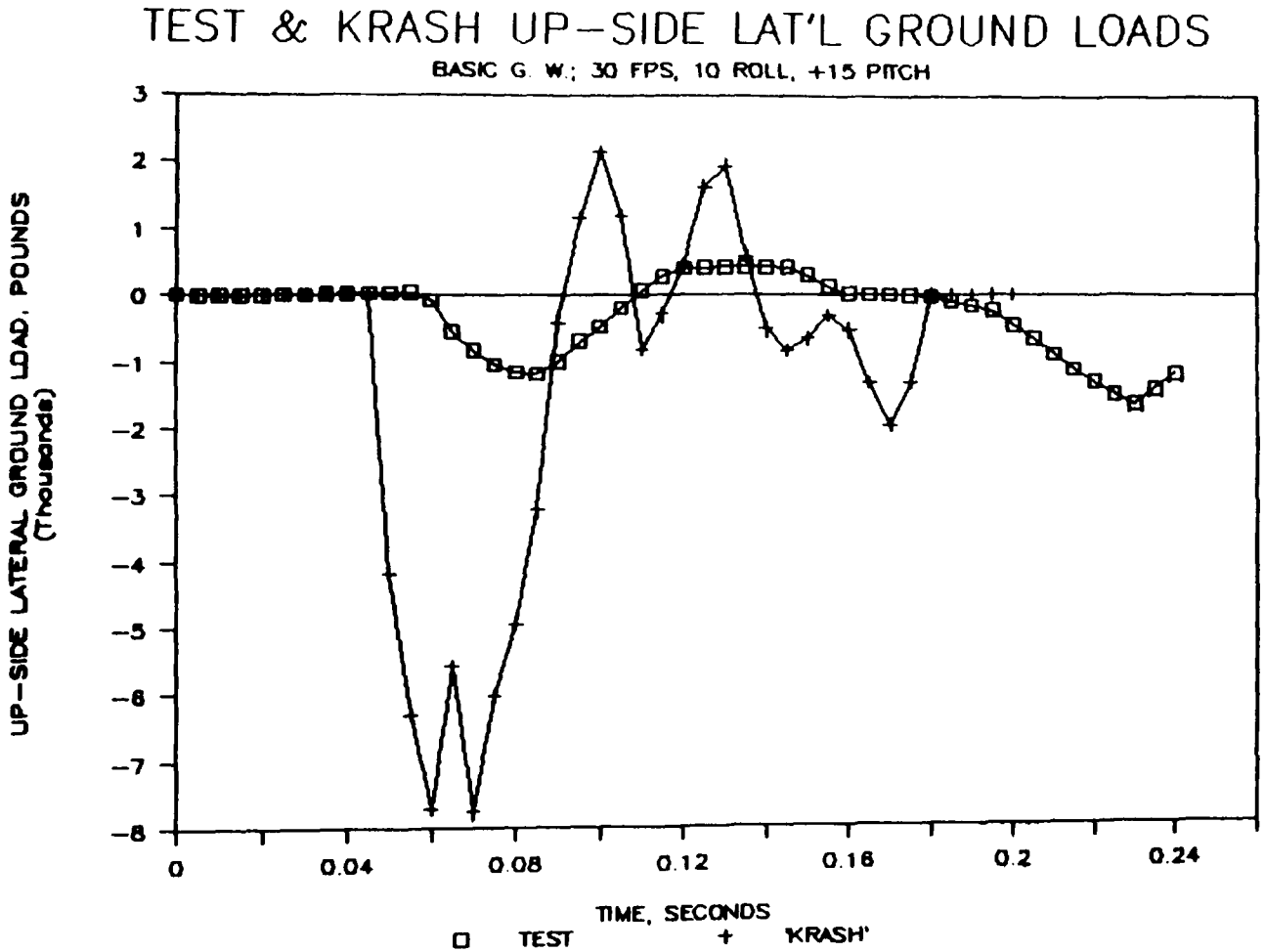

Graph A-44. Test and KRASH up-side lateral ground loads.

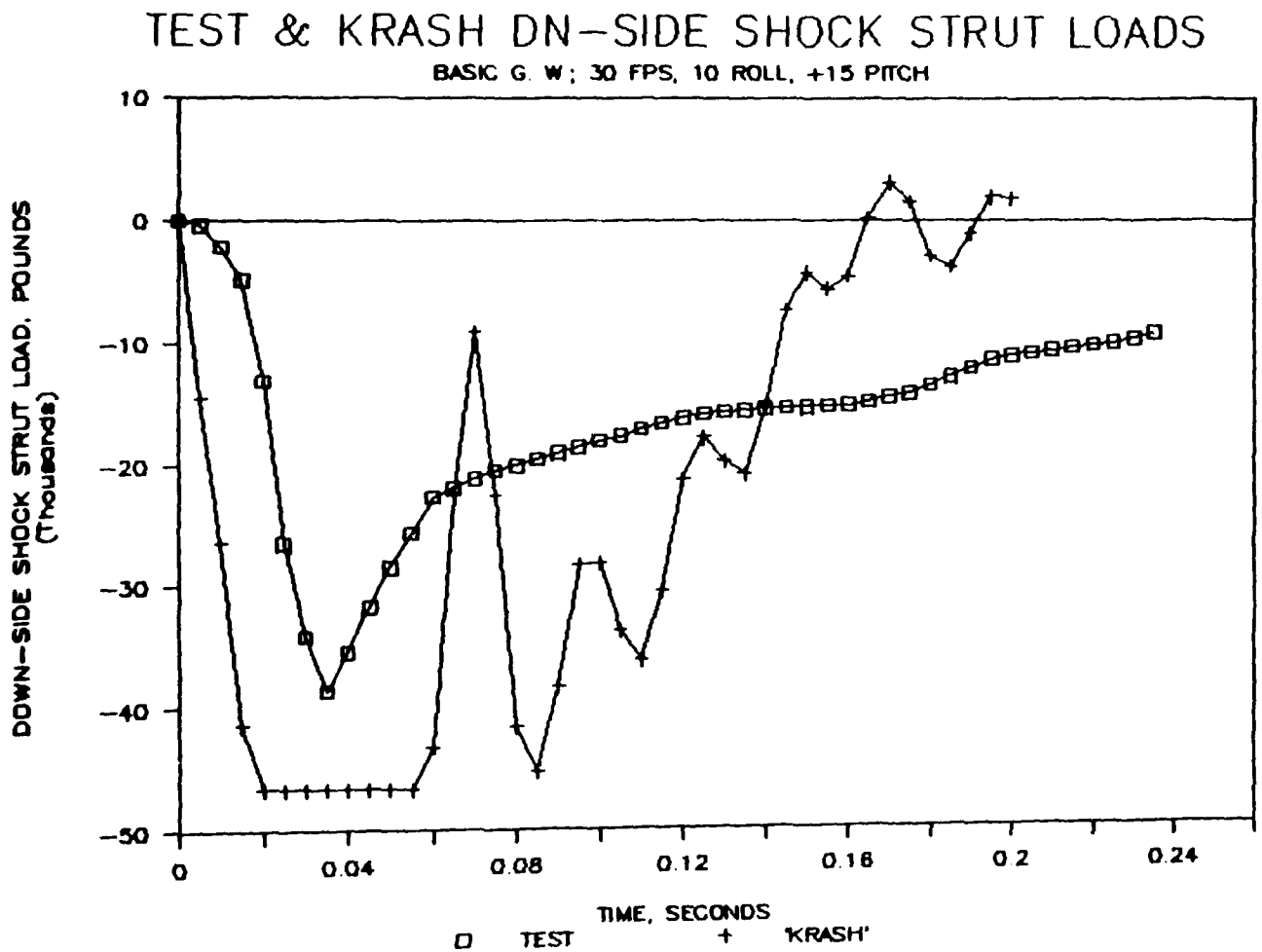

Graph A-45. Test and KRASH down-side shock strut loads.

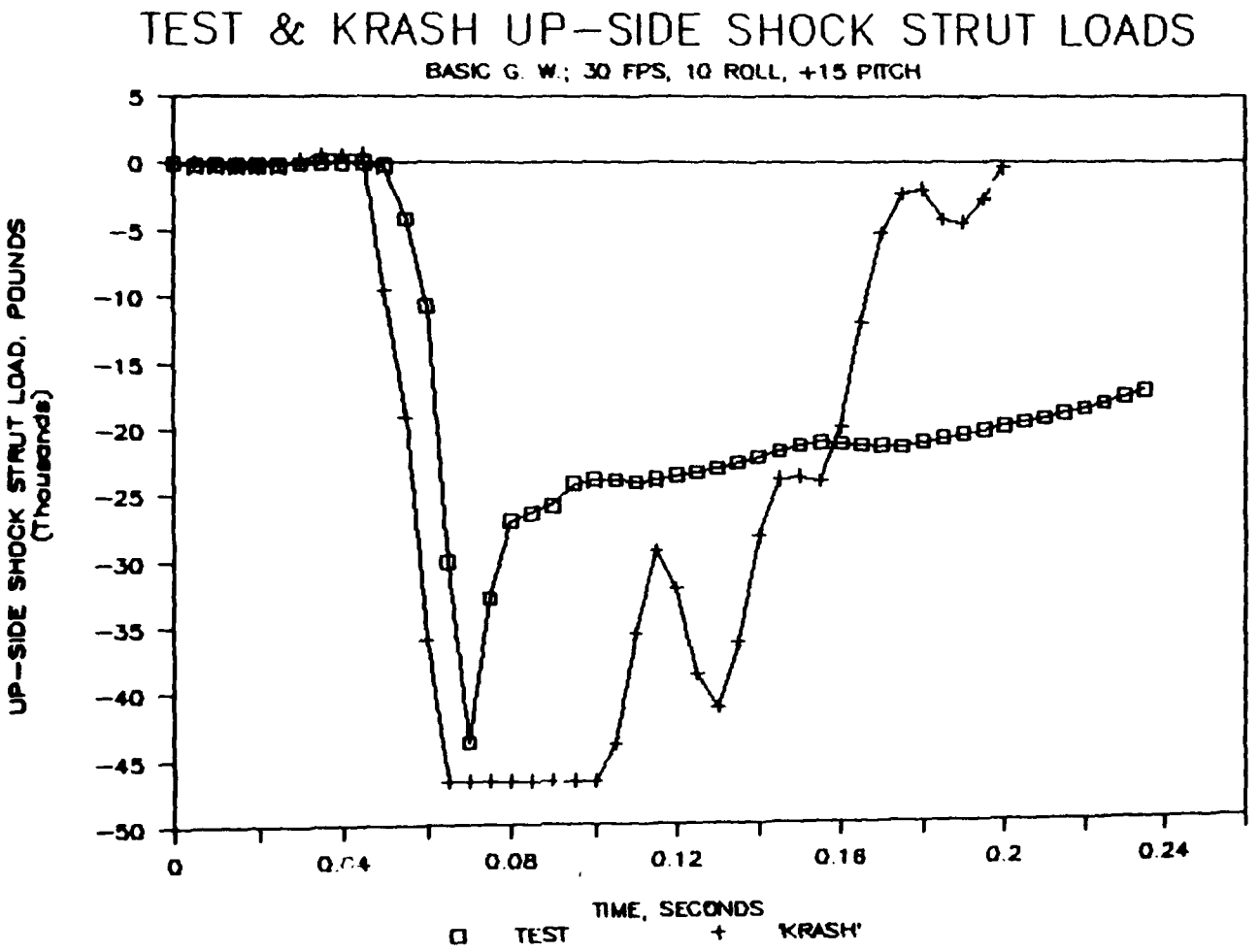

Graph A-46. Test and KRASH up-side shock strut loads.

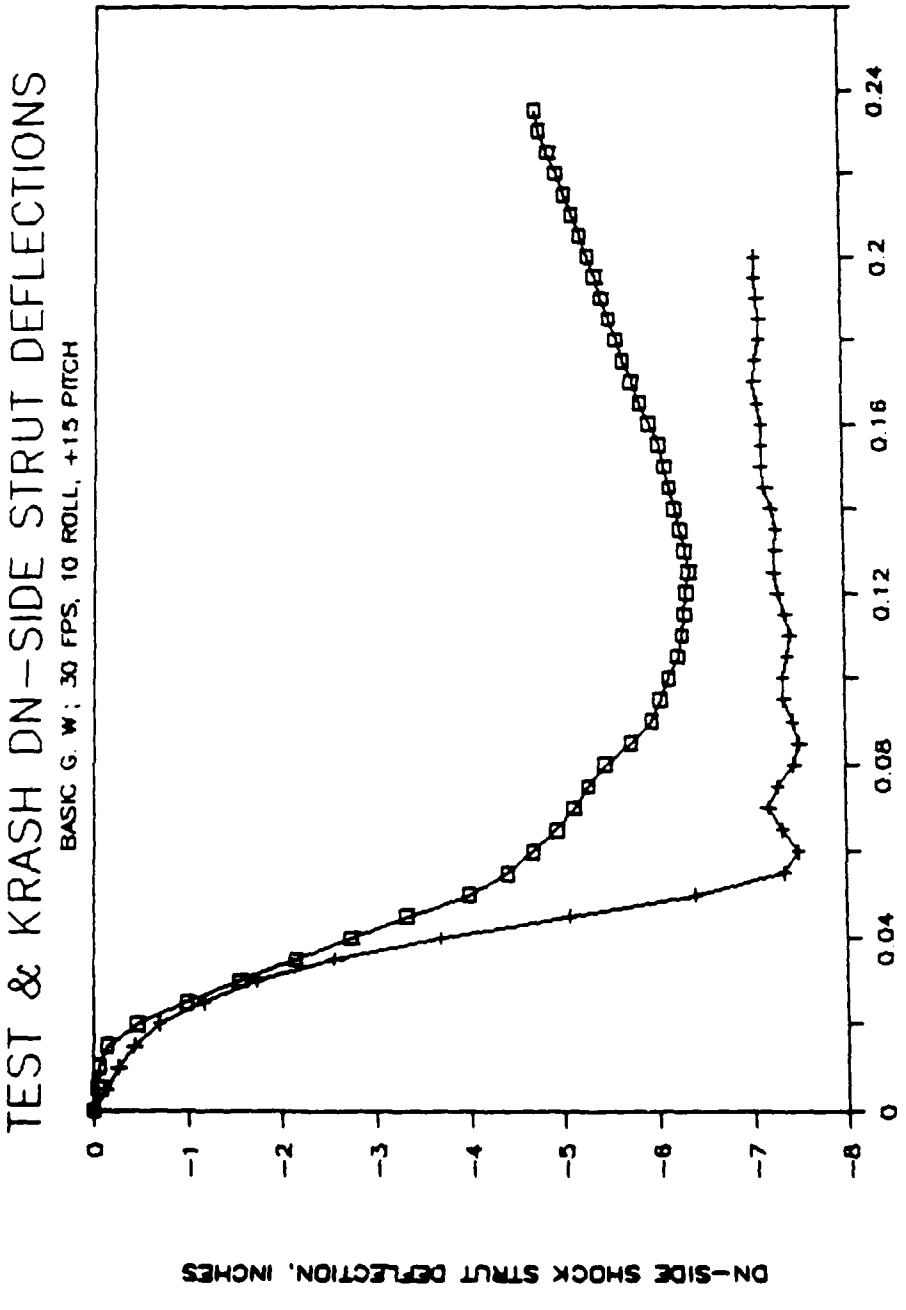

Graph A-47. Test and KRASH down-side strut deflections.

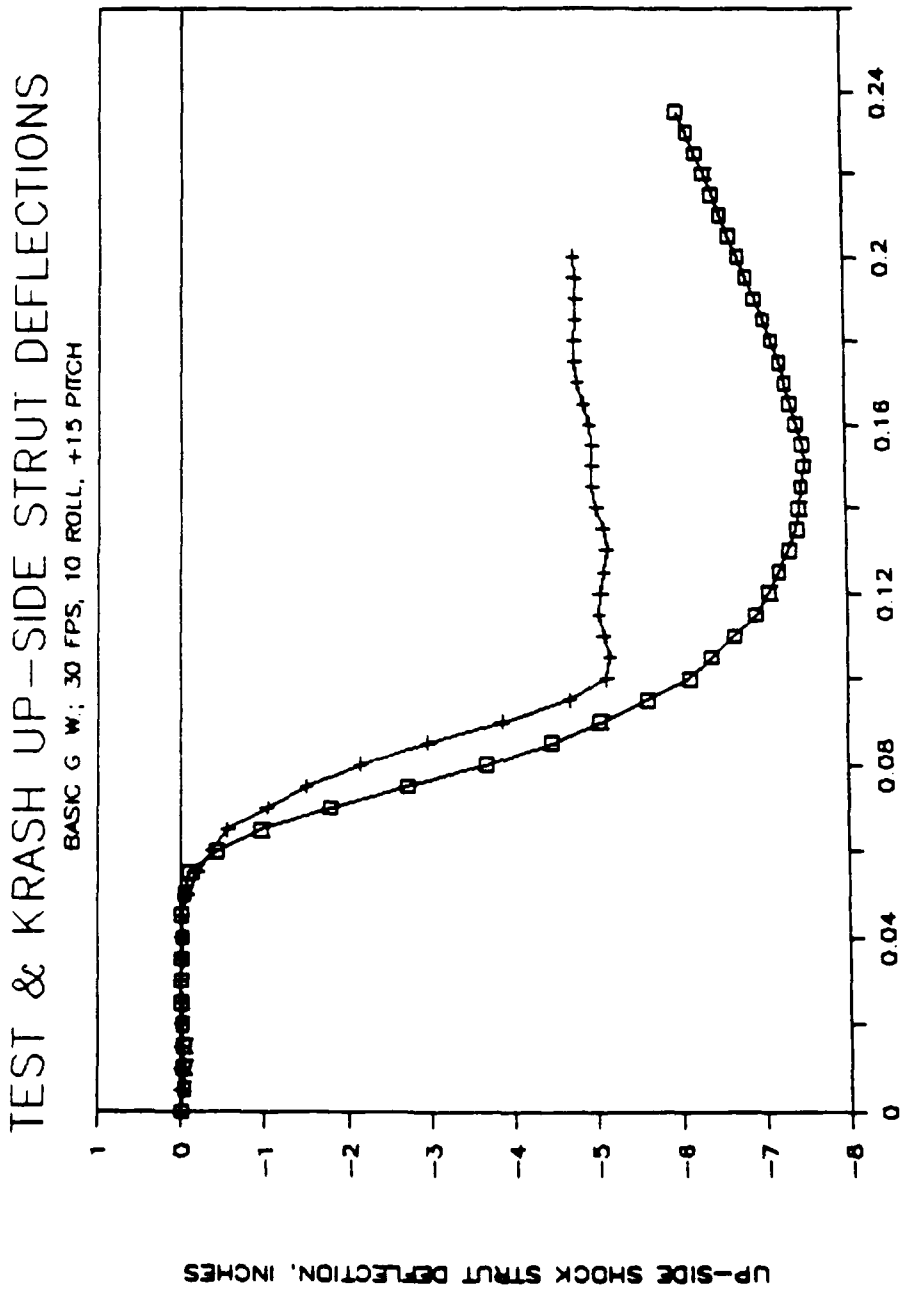

Graph A-48. Test and KRASH up-side strut deflections.

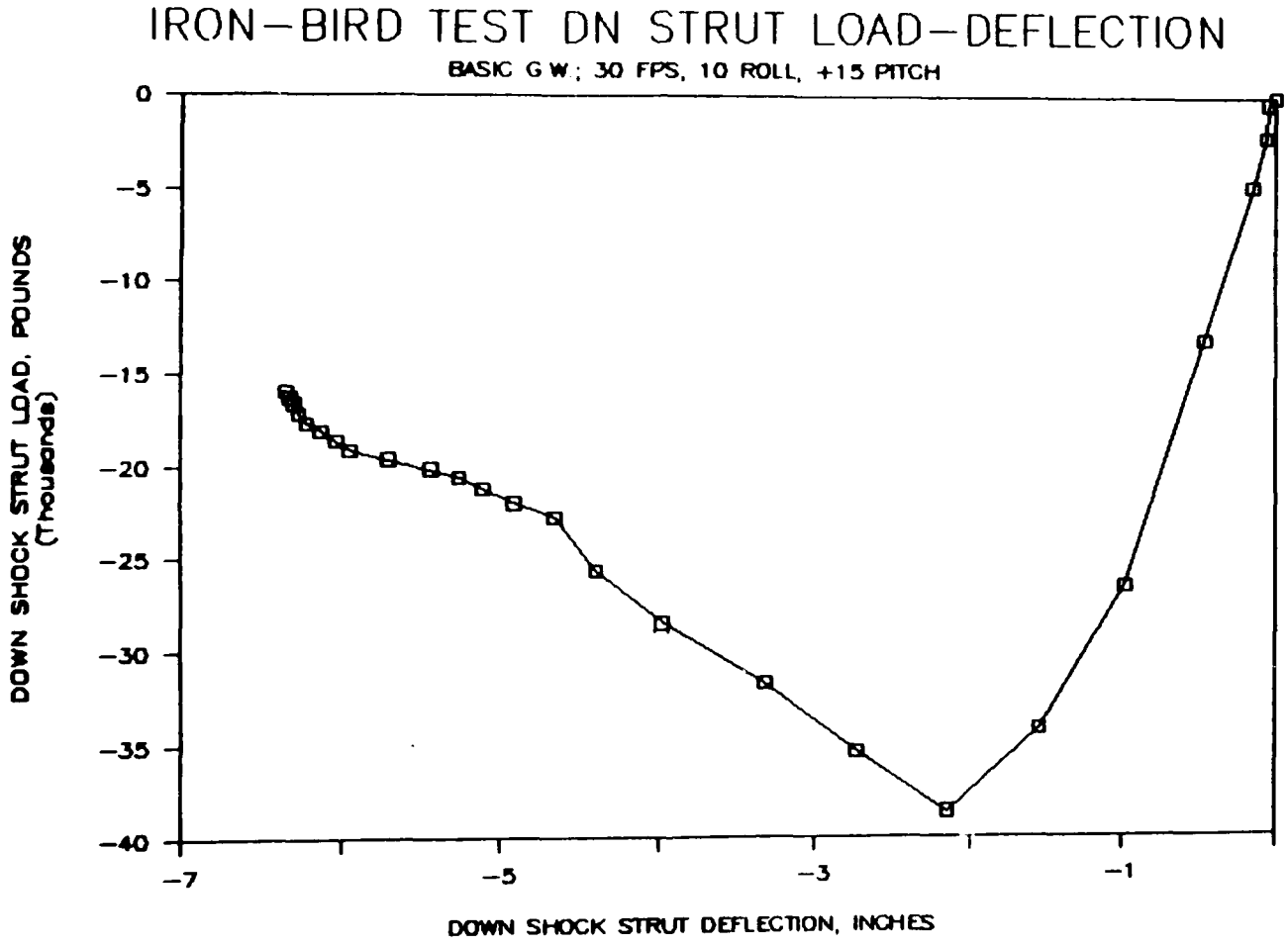

Graph A-49. Iron-bird test down-side strut load-deflection curve.

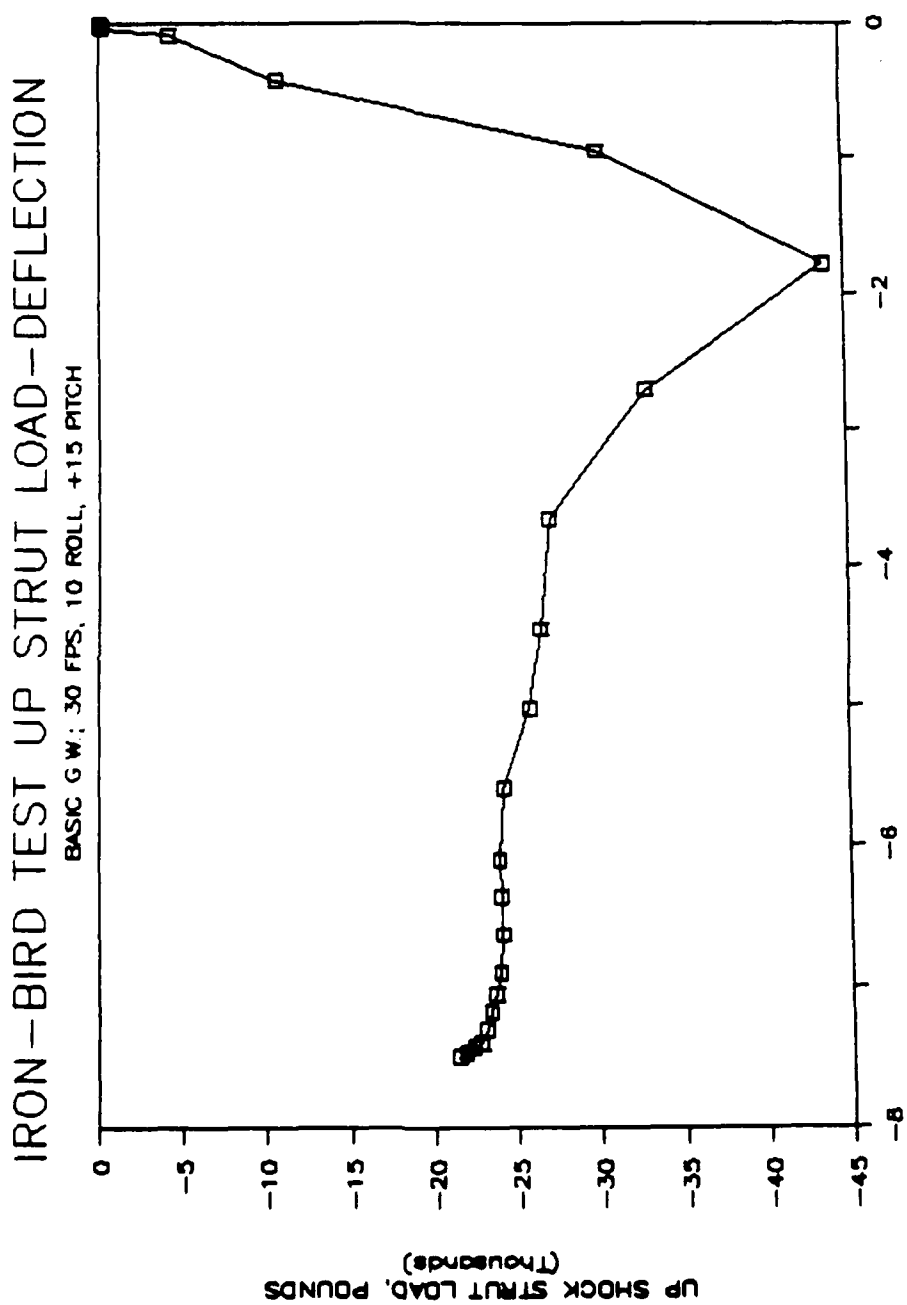

Graph A-50. Iron-bird test up-side strut load-deflection curve.

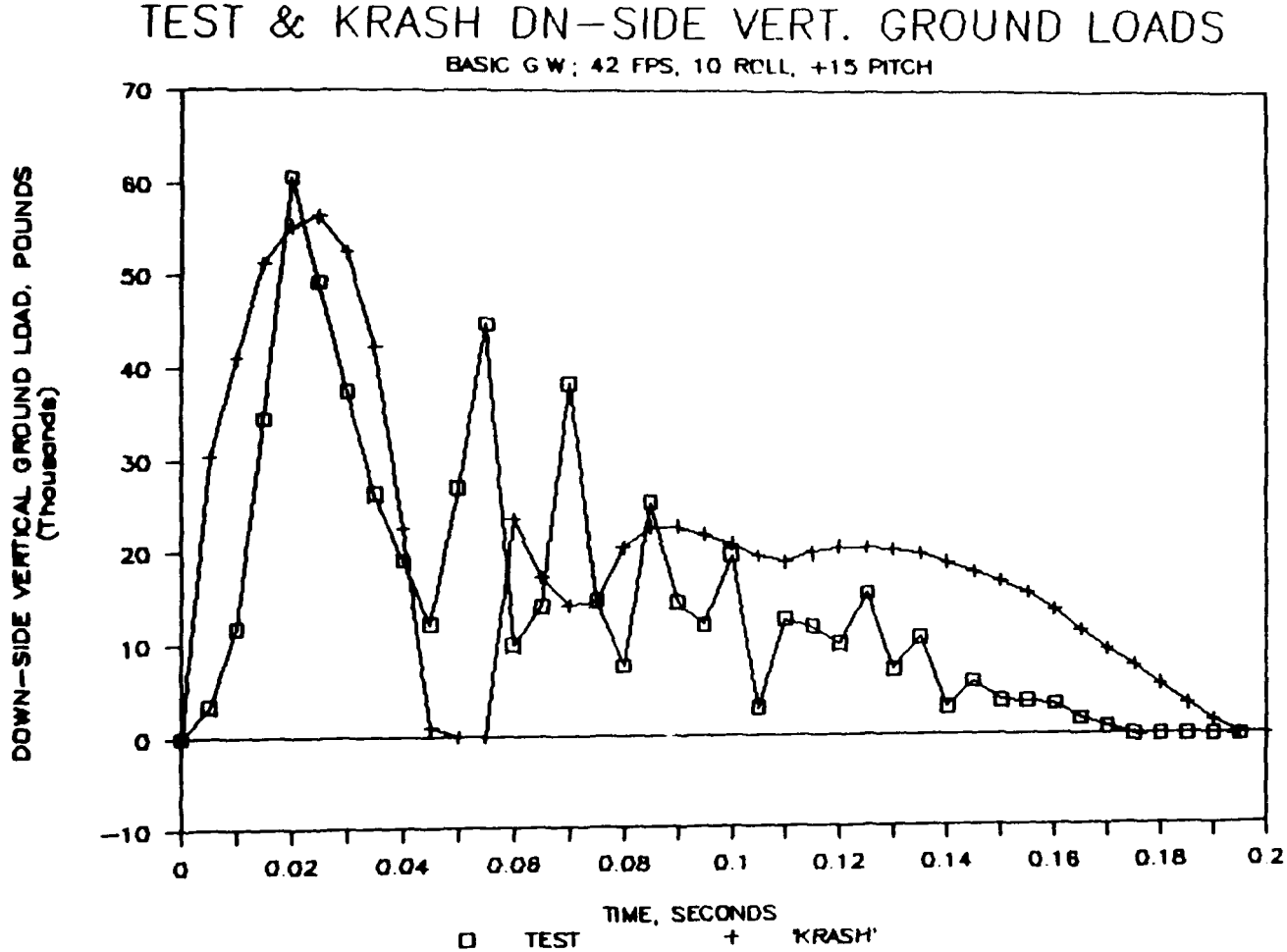

Graph A-51. Test and KRASH down-side vertical ground loads.

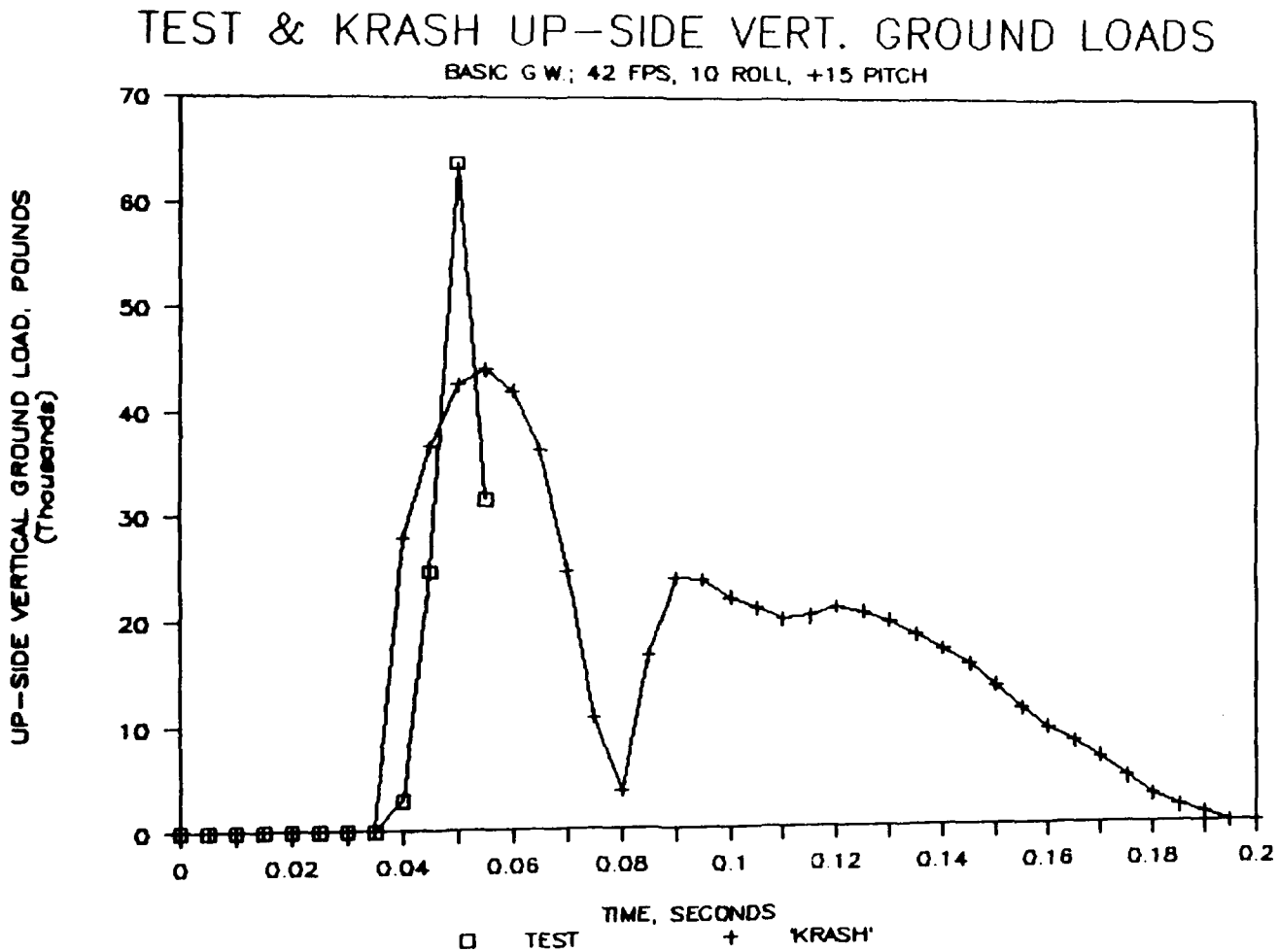

Graph A-52. Test and KRASH up-side vertical ground loads.

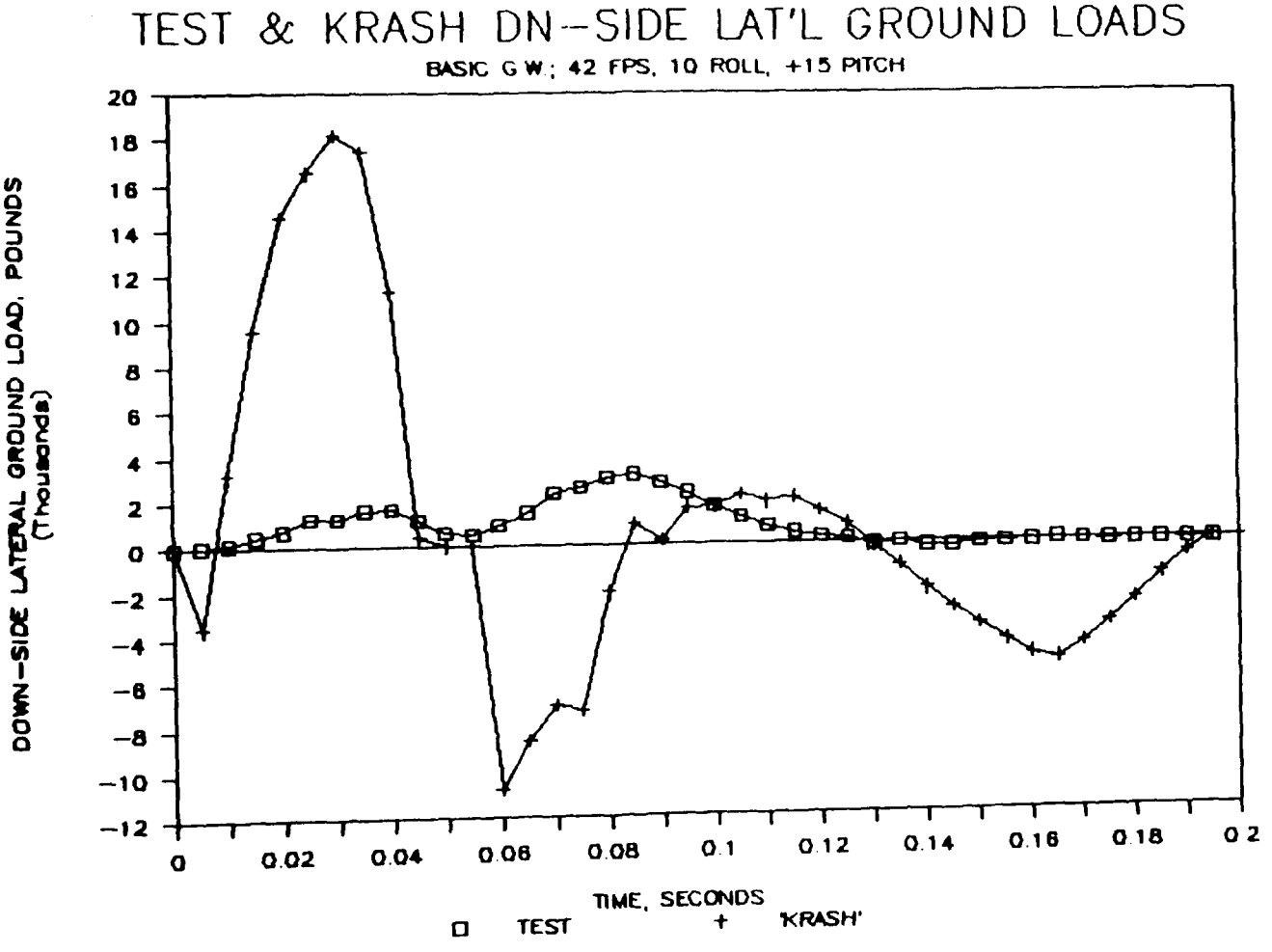

Graph A-53. Test and KRASH down-side lateral ground loads.

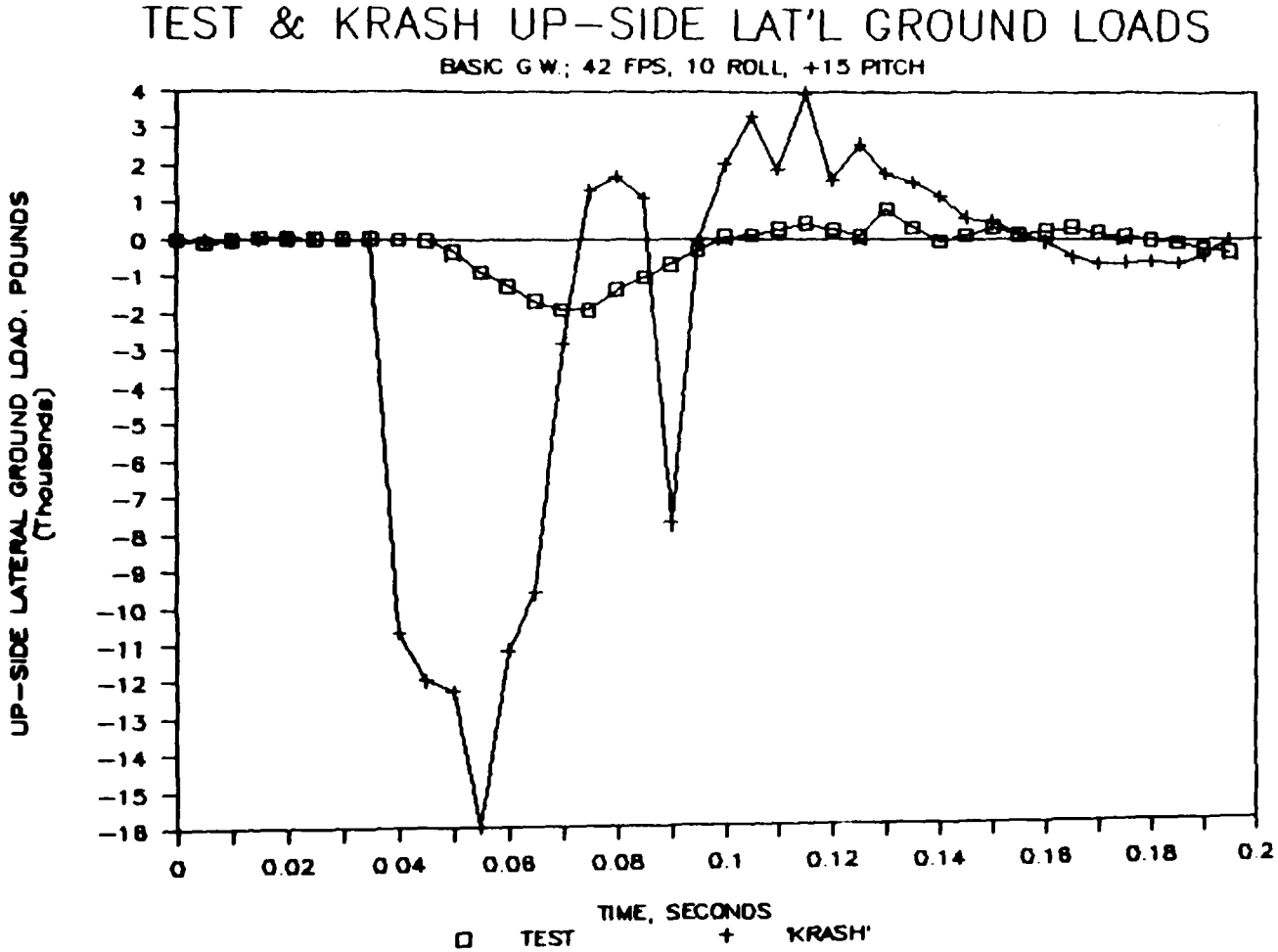

Graph A-54. Test and KRASH up-side lateral ground loads.

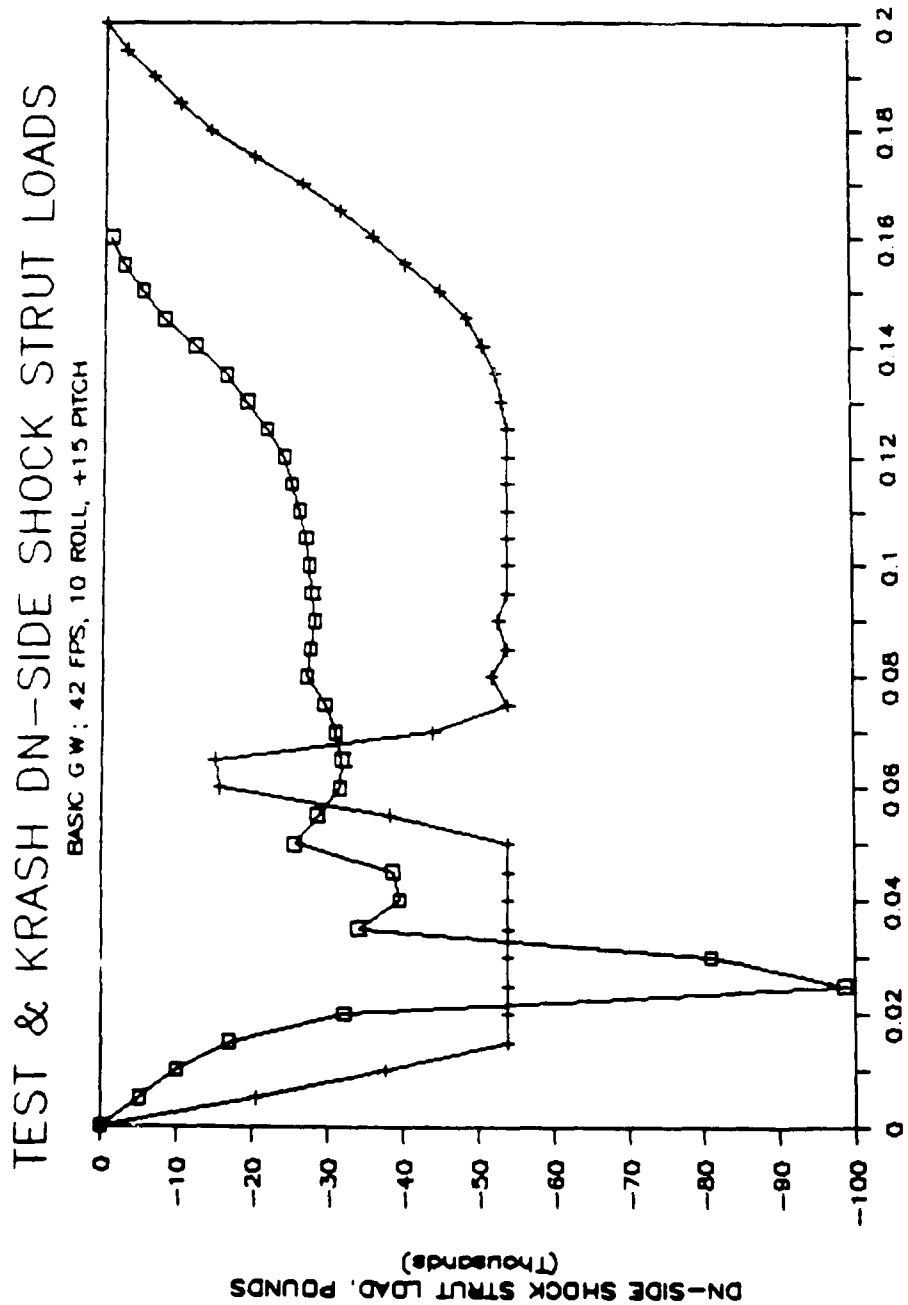

Graph A-55. Test and KRASH down-side shock strut loads.

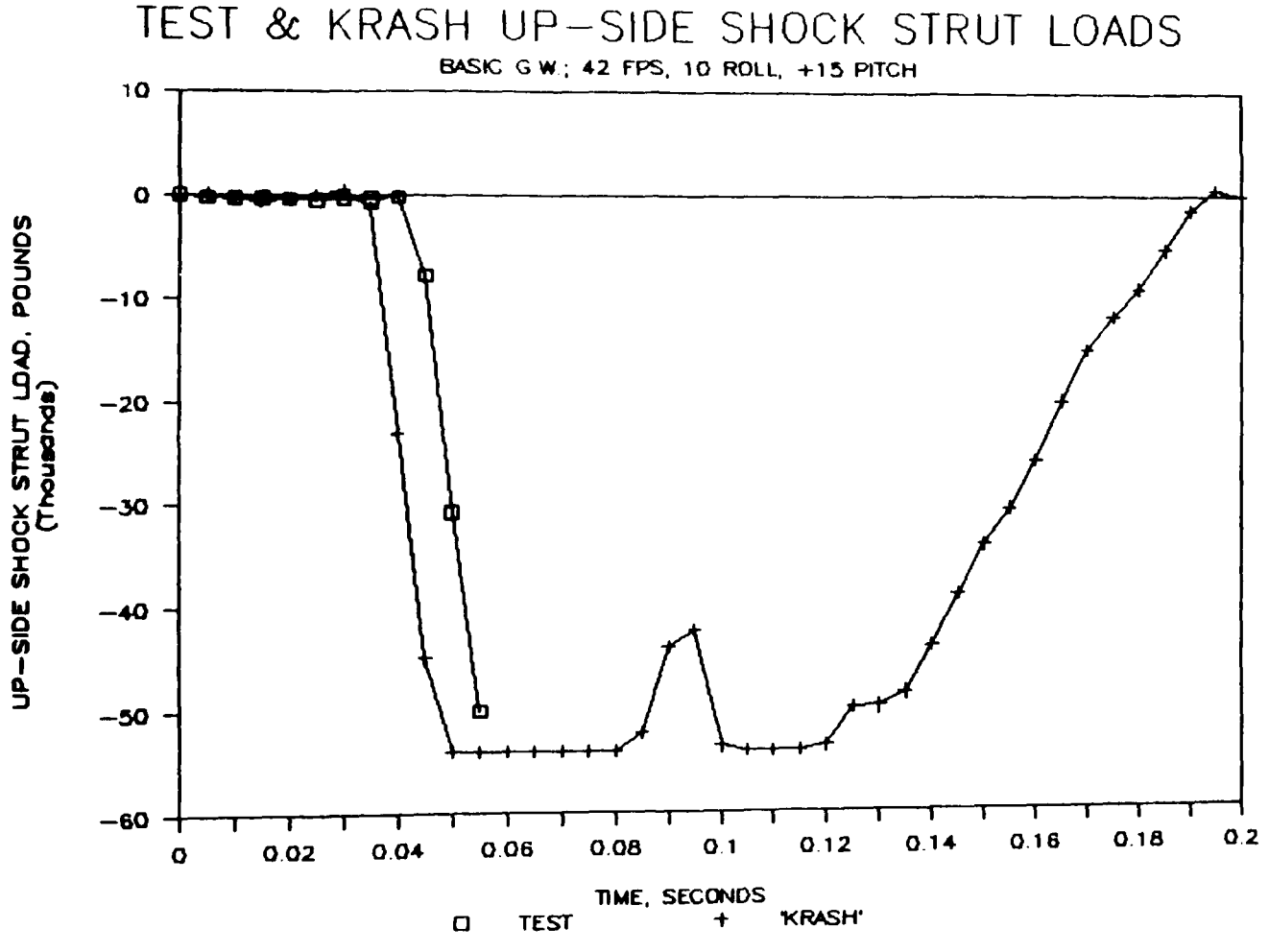

Graph A-56. Test and KRASH up-side shock strut loads.

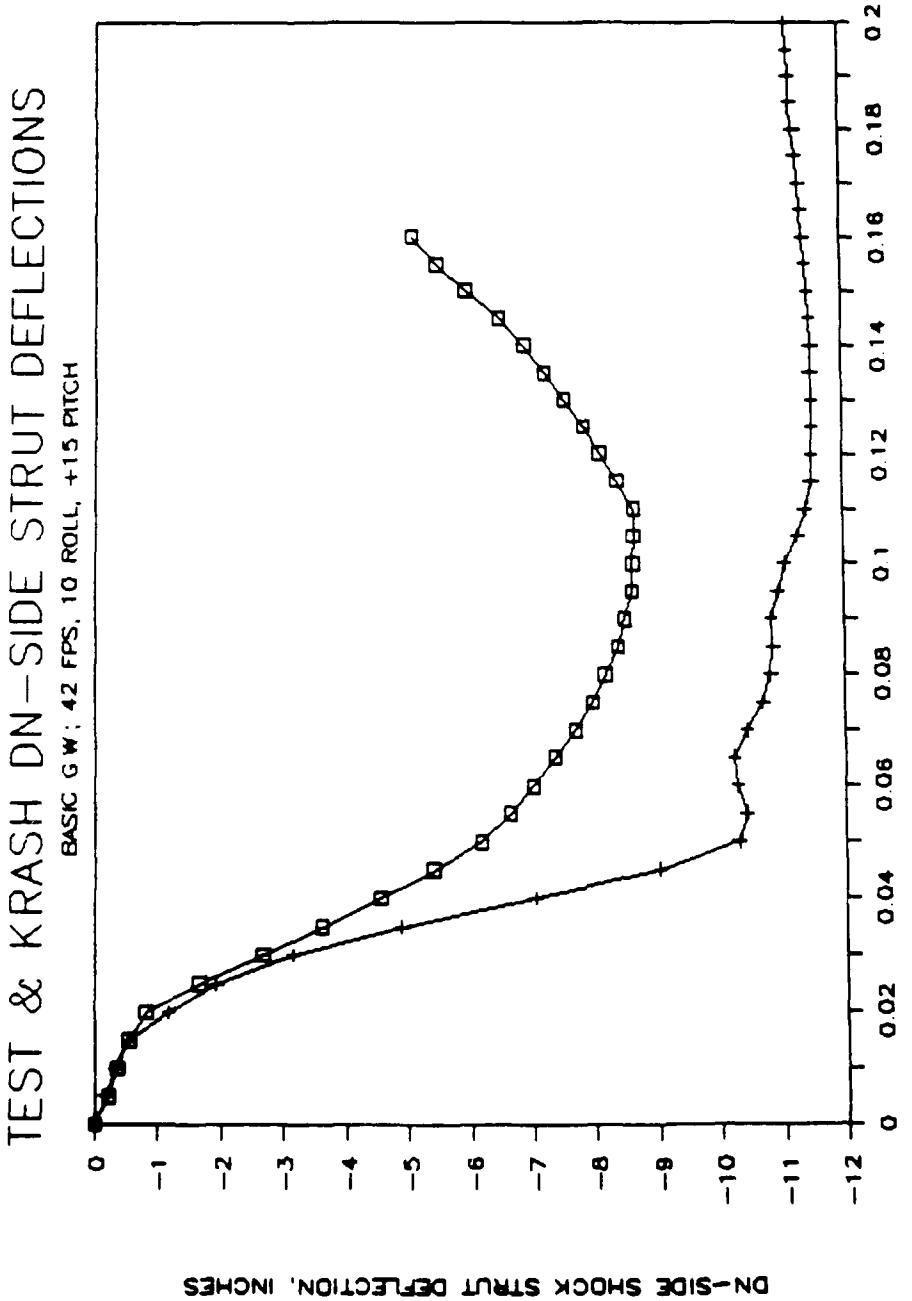

Graph A-57. Test and KRASH down-side strut deflections.

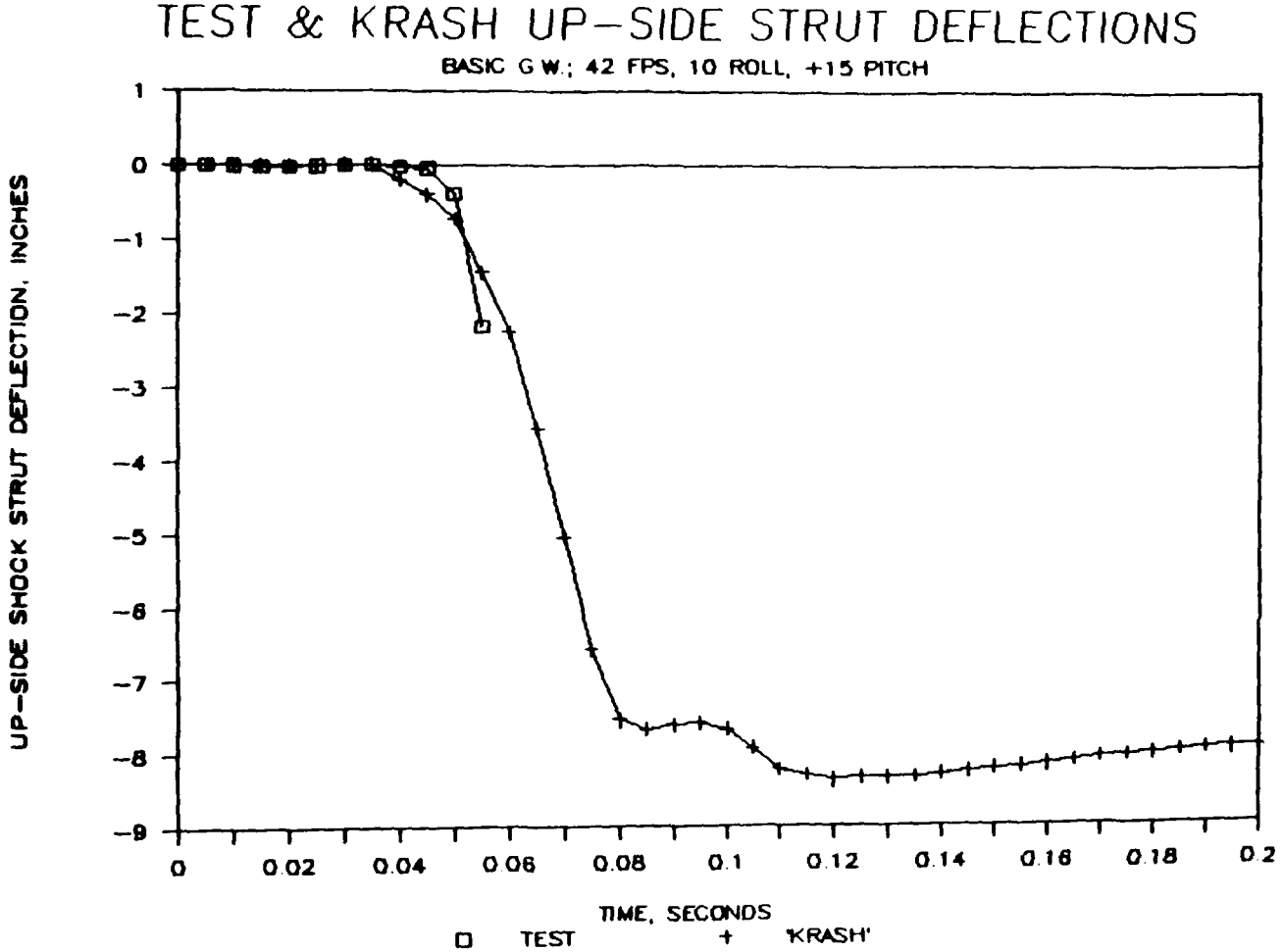

Graph A-58. Test and KRASH up-side strut deflections.

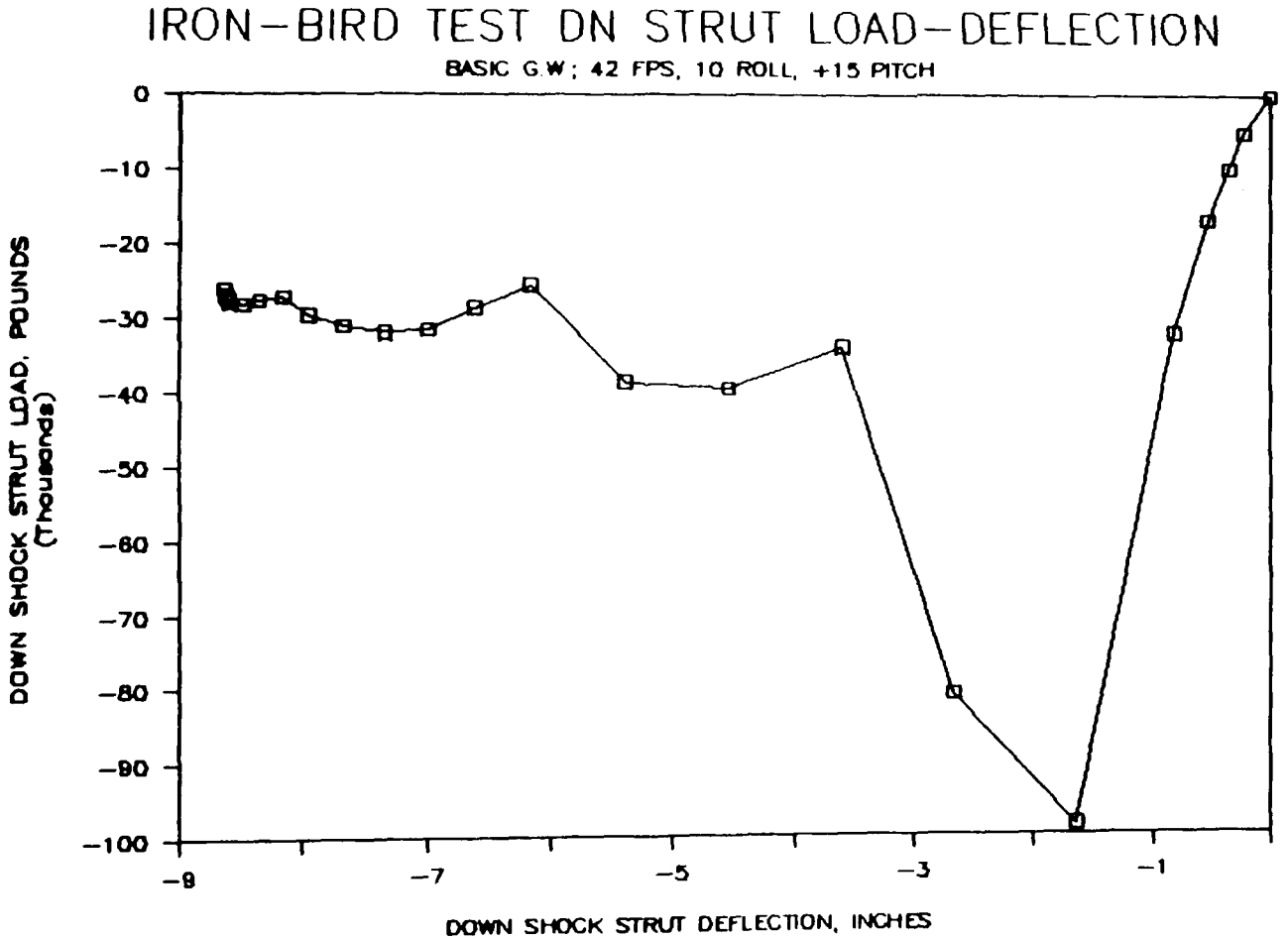

Graph A-59. Iron-bird test down-side strut load-deflection curve.

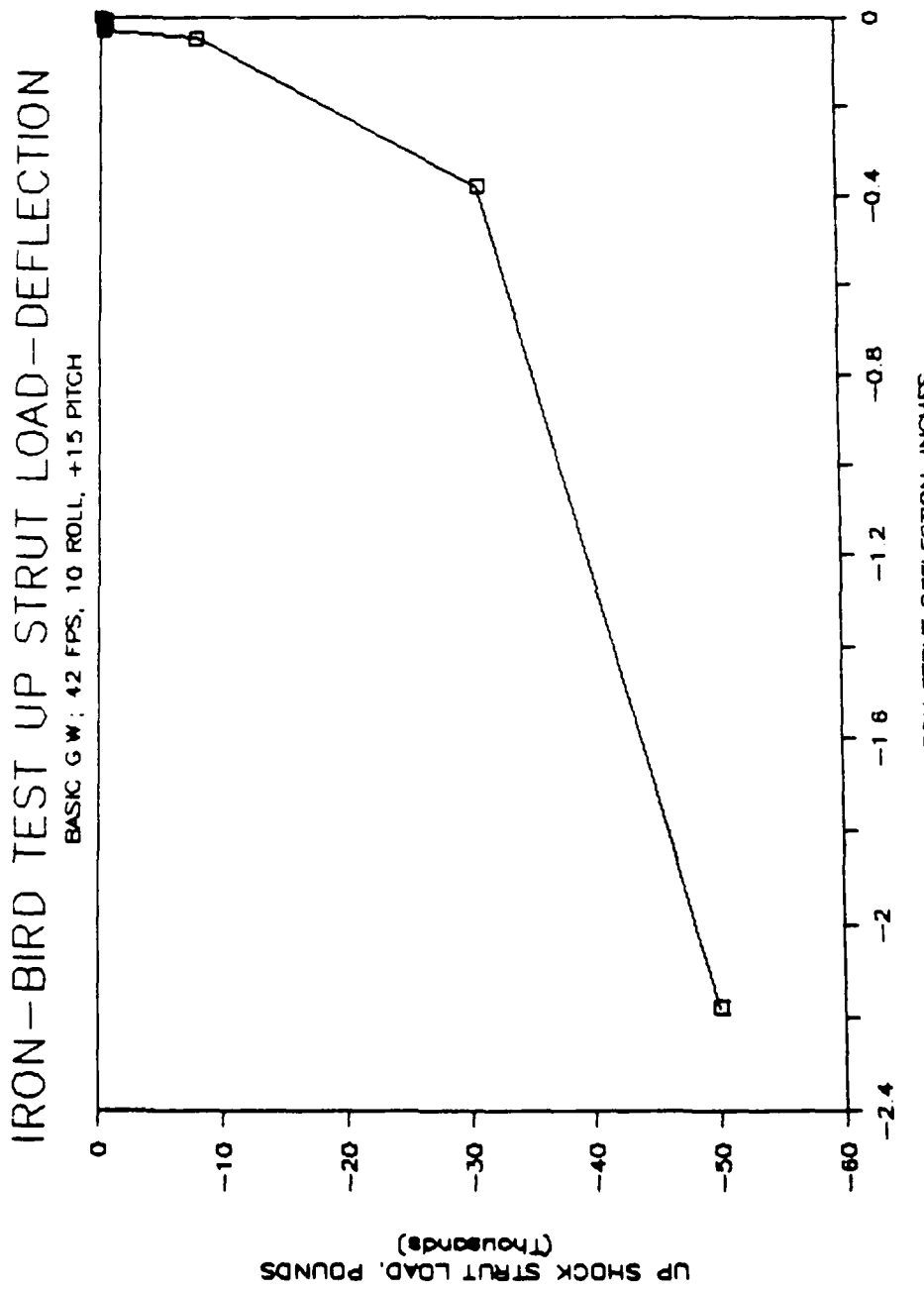

Graph A-60. Iron-bird test up-side strut load-deflection curve.

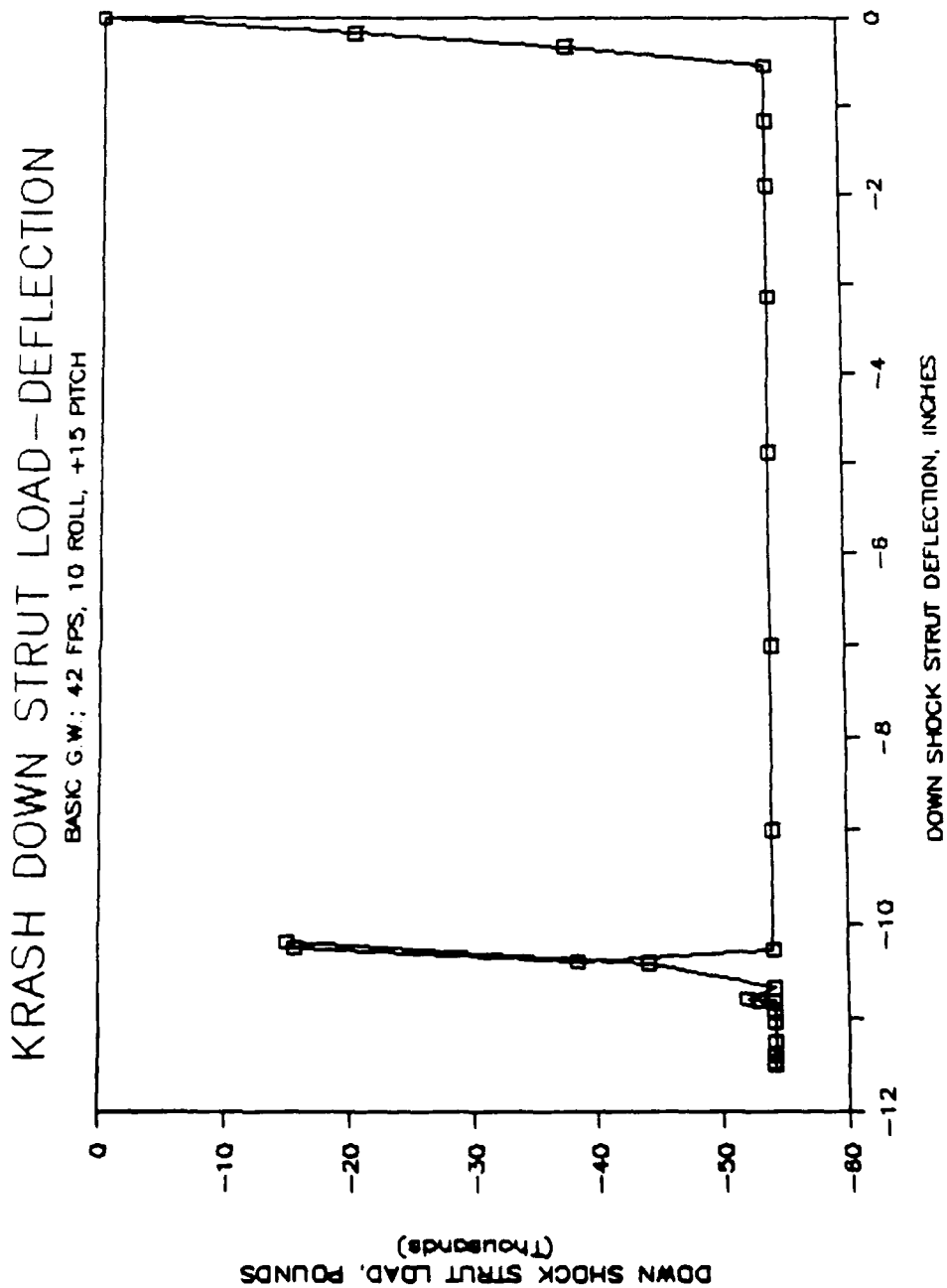

Graph A-61. KRASH down-side strut load-deflection curve.

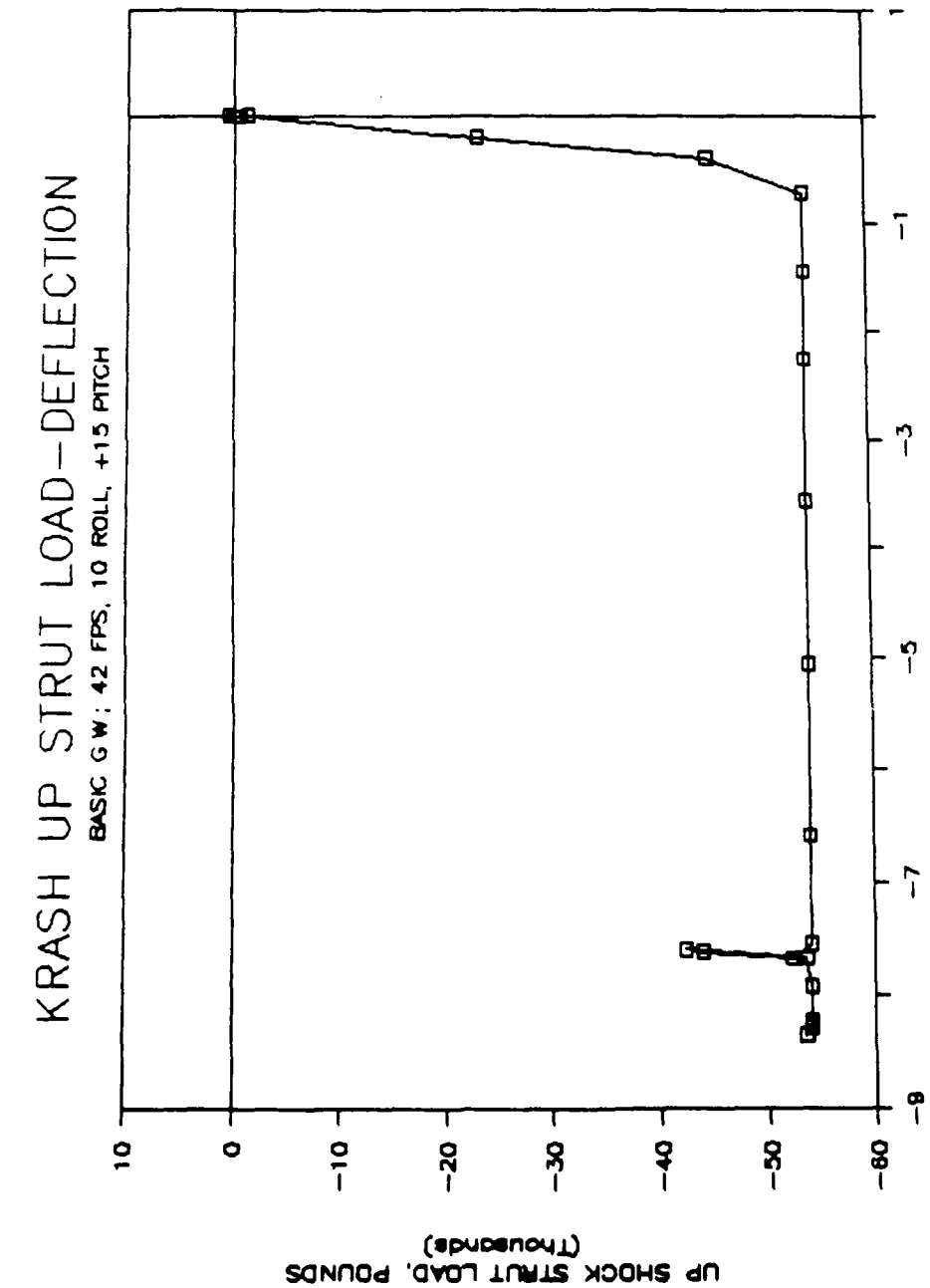

Graph A-62. KRASH up-side strut load-deflection curve.